Prediction, validation and functional analysis of miRNA targets in *Arabidopsis thaliana*

Dissertation

to obtain the academic title
Doctor of Natural Sciences
(Dr. rer. nat.)

at the Faculty of Biology
in the Bielefeld University

presented by

Leonardo Alves Junior
from Itajaí (Brazil)

MAY, 2007

Acknowledgments

First of all I thank Thomas Merkle for being such a nice supervisor and a friend during my time in Bielefeld, and Prof. Bernd Weisshaar for giving me the opportunity to come to Germany and work at the Chair of Genome Research to pursue my PhD. I would also like to thank Marc Rehmsmeier, without who the analysis of miRNA targets would have been much harder.

Special thanks also go to Prof. Robert Giegerich and all my colleagues from the Graduate College in Bioinformatics, especially Sergio A. de Carvalho Junior, for his friendship and for helping me using Linux commands to handle the prediction data.

I would like to thank all the past and present members of the Chair of Genome Research, especially Melani Kuhlmann, Sandra Niemeier, Julia Starmann, Ute Bürstenbinder, Katja Schmied, Ralf Palmisano, Hirofumi Ishihara, Gunnar Huep, Martin Sagasser, Betina Kah, Agnes Bohne, Moritz Shön, Rashmi Prasad and Prisca Viehoever for support and a pleasant time.

I would like to thank all my Brazilians friends in Bielefeld, for those who had already returned, for those who are still here, for friendship, support and help.

I would like to thank to my family in Brazil, my parents, my sisters and my niece, who never let me alone, in spite of the distance.

Finally, to my wife Gisele, who has accepted to leave her dreams aside and supported me to allow my dream to come true.

Para Gisele e meus pais, Leonardo e Elcina

Table of Contents

Abstract

MicroRNAs (miRNAs) are small noncoding RNAs whose function as modulators of gene expression is crucial for many aspects of plant and animal development. A major challenge in understanding the regulatory role of miRNAs is to accurately predict regulated targets. In this work, 281 novel miRNA targets in Arabidopsis were predicted employing the program RNAhybrid with additional assumptions based on already validated miRNA:target interactions. Comparing gene ontology (GO) annotation of both previously predicted/validated targets and novel predicted targets found in this work with the GO categorization for the whole genome revealed that, contrary to previously predicted/validated miRNA targets, there is no over-represented protein class among the novel predicted targets. Some GO annotation classes that were over-represented (e.g. transcription factors) or under-represented, now show distributions close to their representation in the whole genome. Nine putative miRNA targets were subjected to experimental validation, five of them were validated, including *MYB101*, *MYB125*, *MRG1* and *ACS8*, which are targets of miR159, and *GAE1*, which is a target of miR161. The validation of four candidate targets failed.

Among the novel validated miRNA targets, two were further analyzed: *MYB101* and *MRG1*. Overexpression of *MYB101* containing silent mutations in the miR159 binding site (*MYB101mutBS*) resulted in accumulation of *MYB101* in tissues where the transcript is normally absent. The overexpression of wild-type *MYB101* did not show this effect. Adult plants overexpressing *MYB101mutBS* were smaller than wild-type, whereas *MYB101* overexpressors showed no difference to wild-type plants. Contrasting with the *MYB101* transcript levels that are highest in pollen, the expression pattern of *MYB101* analyzed by promoter-GUS lines revealed that the *MYB101* promoter is active in seedlings (cotyledons, leaves and roots) and flowers, again showing a strong signal in pollen. These findings confirm the regulatory role of miR159 for proper *MYB101* expression. *MRG1* is found only in Arabidopsis and contains no conserved protein motif. The expression pattern of *MRG1* analyzed by promoter-GUS lines revealed that the *MRG1* promoter is active in many different tissues whereas the *MRG1* transcript can be detected at

very low levels only. The overexpression of *MRG1* was only effective when silent mutations in the miR159 binding site had been introduced. In *MRG1mutBS* overexpressing plants several defects in leaf morphology were observed and the number of leaves was altered drastically. Nevertheless, plants overexpressing wild-type *MYB101* showed similar, but weaker phenotypes. *MRG1* protein, expressed as fusion protein with GFP, was localized in the nucleus of BY-2 protoplasts Therefore, *MRG1* may represent a novel regulator that affects leaf development, and miR159 controls the precise expression of *MRG1.*

The expression patterns of *MIR159A*, *MIR159B* and *MIR161* were analyzed by promoter-GUS lines. Although the promoters of both *MIR159* genes show an overlapping expression pattern, promoter-GUS lines confirmed previous indications that *MIR159A* is the gene responsible for the majority of mature miR159 accumulation. Deletion analysis of the *MIR159A* promoter identified regions that have regulatory properties. The promoter activity of *MIR161* confirmed that miR161 is a broadly expressed miRNA. This conclusion is also supported by the analysis of serial deletions of the *MIR161* promoter. Even the smallest promoter fragment conferred high activity of the reporter protein. In addition, two regulatory regions where found within the miR161 promoter. The regulatory regions found within these two *MIRNA* promoters can now be used to identify proteins that drive the expression of these genes.

List of Figures

List of Tables

List of Abreviations

4MU	4-methylumbelliferyl
4MUG	4-methylumbelliferyl-beta-D-glucuronide
ABA	abscisic acid
ACS	1-aminocyclopropane-1-carboxylic acid synthase
AGO1	ARGONAUT1
AP2	APETELA2
APS	ATP sulfurylase
ARF	AUXIN RESPONSE FACTORS
ATP	adenosine 5'-triphosphate
bp	base pair
BRX	*BREVIS RADIX*
BSA	bovine serum albumin
CaMV	Cauliflower Mosaic Virus
cDNA	complementary DNA
CDS	coding sequence
CoA	Coenzyme A
CSD	Cu/Zn superoxide dismutase
CUC	CUP-SHAPED COTYLEDON
DCL	DICER-LIKE
DEPC	Diethylpyrocarbonate
DNA	Deoxyribonucleic acid
dNTP	deoxyribonucleotide triphosphate
DPA	Dimerization partner A
dsRNA	double-stranded RNA
DTT	dithiotreitol
EDTA	ethylenediaminetetraacetic acid
ELF	Early Flowering
F3H	flavone-3-hydroxilase
FLC	Flowering Locus C
g	relative centrifugal field unit
GA	gibberellin
GAE	UDP-4-epimerase
GFP	green fluorescent protein
GO	gene ontology
HEN1	HUA ENHANCER1
HST	HASTY
HYL1	HYPONASTIC LEAVES1
kb	kilobase

LFY	LEAFY
MFE	minimum free energy
miRNA	microRNA
MRG1	*MICRORNA-REGULATED GENE1*
mRNA	messenger RNA
MS	Murashige Skoog
NASC	The European Arabidopsis Stock Centre
nt	nucleotide
OD	optical density
ORF	open read frame
P bodies	processing bodies
PCR	polymerase chain reaction
PEG	polyethylene glycol
PHB	PHABULOSA
PHV	PHAVOLUTA
Pi	inorganic phosphate
pol II	RNA polymerase II
PPR	Pentatricopeptide repeat
pre-miRNA	precursor microRNA
pri-miRNA	primary microRNA
RACE	rapid amplification of cDNA ends
RDR	RNA-DEPENDENT RNA polymerase
RISC	RNA-induced silencing complex
RLU	relative light units
RNA	ribonucleic acid
rpm	revolution per minute
RT-PCR	reverse transcriptase-PCR
SAM	shoot apical meristem
SDS	sodium dodecylsulfate
SE	SERATE
siRNA	small interfering RNA
SPL	Squamosa promoter-binding protein-like
TBE	Tris/Borate/EDTA
TE	Tris.HCl EDTA
TEMED	N,N,N',N' tetramethylenethylendiamine
Tnos	nopaline synthase terminator
TPQ	transcripts per quarter million
Tris	Tris(hydroxymethyl) aminomethane
UBC	ubiquitin-conjugating E2 enzyme
uidA	beta-glucoronidase gene
UTR	untranslated region
X-Gal	5-bromo-4-chloro-3-indolyl-â-D-galactopyranoside
X-Gluc	5-bromo-4-chloro-3-indolyl-â-D-glucuronic acid

1. Introduction

A novel class of noncoding small RNAs emerged as new player in one of the most important networks in eukaryotic cells, namely the regulation of gene expression. These so-called microRNAs (miRNAs) are between 21-24 nucleotides long small RNAs that post-transcriptionally regulate gene expression, share similar biogenesis and mechanism of action with previously known small interfering RNAs (siRNAs), but have distinct roles. The first miRNA gene was described in *C. elegans*. *LIN-4*, a gene known as an important regulator of developmental timing in *C. elegans*, did not produce a protein but instead two small RNAs, 22 and 61 nucleotides (nt) in length, respectively. Interestingly, the 22 nt long RNA showed sequence complementarity to another gene involved in developmental timing in *C. elegans*, *LIN-14*. The level of LIN-14 protein was decreased because of the 22 nt *LIN-4* RNA bound to the 3'UTR of *LIN-14* transcripts (Lee *et al*., 1993). The binding of *LIN-4* RNA to *LIN-14* 3'UTR revealed to be essential for proper development of *C. elegans*, and mutations in the binding site affected the accumulation LIN-14 protein (Wightman *et al*., 1993). At that time, no homologous gene was found in any other organism and a gene that produced an RNA that was able to affect the production of a protein of an unrelated gene was considered an exception (Lee *et al*., 1993).

Seven years later, a second miRNA gene was described, again in *C. elegans*. However, homologues of this gene were found in human and fly genomes, and this finding highlighted the possibility that miRNAs could be a common regulatory mechanism (Reinhart *et al*., 2000). Soon thereafter, several miRNA genes were described in *Homo sapiens*, *Mus musculus*, *Drosophila melanogaster* (Pasquinelli *et al*., 2000; Lagos-Quintana *et al*., 2001; Lau *et al*., 2001; Lee and Ambros, 2001), *Arabidopsis thaliana* (Arabidopsis; Llave *et al*., 2002b; Reinhardt *et al*., 2002) and in virus (Pfeffer *et al*., 2004).

1.1. MicroRNAs in plants

The first miRNAs described in plants were isolated through cloning of RNA samples enriched with small RNAs (Llave *et al*., 2002b). There were four miRNAs

among dozens of cloned small RNAs sequences. Using a more elaborated protocol, designed to clone small RNAs produced by DICER-LIKE 1 (DCL1), which is an RNaseIII endonuclase involved in the biogenesis of small RNAs, 37 miRNA genes were described, including those previously isolated (Reinhart *et al*., 2002). Direct isolation and cloning of small RNAs from biological samples proved to be a powerful method to discover miRNAs in plants. Consequently, many miRNAs were described using this approach (Llave *et al*., 2002b; Mette *et al*., 2002; Park *et al*., 2002; Reinhart *et al*., 2002; Xie *et al*., 2003; Sunkar and Zhu, 2004). To find novel expressed miRNA genes, the small RNA transcriptome of samples from plant lines carrying mutations in genes encoding essential enzymes for the biogenesis of other classes of small RNAs were analysed. Thus, miRNAs were enriched in these samples; therefore, miRNAs expressed at a low level could also be cloned and identified. However, even after isolation of 5521 small RNA clones, only one new miRNA family was identified. Most miRNA sequences matched to previously described genes (Xie *et al*., 2003). The cloning and sequencing strategy used in the beginning to identify miRNA genes resulted in a bias towards miRNA genes that were highly expressed or present in many tissues or both. Moreover, miRNA genes that are conserved in other plant species were also easily identified (Bartel, 2004). To solve this problem, two distinct approaches were applied: bioinformatics and deep sequencing of small RNA transcriptomes.

Although bioinformatic tools applied for discovery of miRNA genes resulted in more success in animals than in plants, many miRNA genes were isolated after predictions with bioinformatic pipelines (Bonnet *et al*., 2004; Jones-Rhoades and Bartel, 2004; Wang *et al*., 2004b; Adai *et al*., 2005; Xie *et al*., 2005). Jones-Rhoades and Bartel (2004) were the first to apply computational methods to identify novel miRNA genes in plants. They used a comparative genomic approach to identify conserved miRNA genes in Arabidopsis and *Orysa sativa* (rice), resulting in seven experimentally confirmed new miRNA families and many novel miRNA genes of existing miRNA families. Wang *et al*. (2004) analyzed the attributes of previously confirmed miRNAs and used them for defining features for the prediction of novel miRNA genes. Intergenic regions of the Arabidopsis genome were used to search for sequences that could fold into a hairpin structure, and then filters derived from previously validated miRNAs were applied. Filters

were based on precursor-miRNA length (pre-miRNA; an intermediary product of the miRNA biogenesis; see Figure 2), GC content of the mature miRNA, and a minimum identity of 90% with any rice sequence. This pipeline was able to predict 83 new miRNA candidates. A few of them were detected by northern blotting, resulting in eight novel miRNA families in Arabidopsis (Wang *et al*., 2004b). No attempt was made to validate any of the predicted miRNAs in rice (Wang *et al*., 2004b). Even though this approach considered the identity of new miRNA genes with sequences from rice, there is no strong evidence that these miRNAs are also present in any other genome (Jones-Rhoades *et al*., 2006). Two other bioinformatic approaches resulted in prediction of many novel miRNA genes (Bonnet *et al*., 2004; Adai *et al*., 2005). They also predicted many previously validated ones. However, no experimental evidence was obtained for those newly predicted miRNA genes, and therefore, these miRNA genes were not included in the miRBASE (Griffiths-Jones, 2004). The miRBASE (http://microrna.sanger.ac.uk/) is a database that contains miRNA sequences from all species that were experimentally validated and provides specific guidelines for miRNA annotation and nomenclature (Ambros *et al*., 2003).

With the advance of novel powerful sequencing technologies, small RNA cloning techniques were adapted for massive parallel signature sequencing (Lu *et al*., 2005a) and, more recently, for high-throughput pyrosequencing (Rajagopalan *et al*., 2006; Fahlgren *et al*., 2007). This so-called deep sequencing of small RNA samples allowed the characterization of miRNAs that were expressed at low levels or showed gene expression that was limited to specific cells. Together, these approaches contributed 59 novel miRNAs, all of them present only in the genome of Arabidopsis.

Genetic screens contributed to the discovery of only one novel miRNA family in Arabidopsis (Palatnik *et al*., 2003). In an activation tagging screen, a phenotype with similarity to the *cincinnata* mutant of snapdragon was selected for further analysis. The T-DNA was inserted in an intergenic region and the protein-coding genes surrounding the integration locus were not overexpressed. A global profile of gene expression revealed that the phenotype was caused by the downregulation of several *TCP* transcription factor genes. The intergenic region at the T-DNA insertion showed sequence similarity of 21 nucleotides to *TCP* genes.

Table 1. Conserved microRNA genes in plants.
MicroRNA families present in Arabidopsis with homologous in other plant species that are listed in the miRBASE (http://microrna.sanger.ac.uk/), are presented with the number of genes per species for each family. Ath-*Aradidopsis thaliana*, Gma-*Glycine max*, Mtr-*Medicago truncatula*, Osa-*Oryiza sativa*, Ppt-*Physcomitrella patens*, Ptc-*Populus trichocarpa*, Sbi-*Sorghum bicolor*, Sof-*Saccharum officinarum* and Zma-*Zea mays*. The total number of miRNAs per species is shown.

miRNA family	Ath	Gma	Mtr	Osa	Ppt	Ptc	Sbi	Sof	Zma
miR156	12	4	1	12	1	11	5	1	11
miR159	3	1	0	6	0	6	2	5	4
miR160	3	1	1	6	0	8	5	0	6
miR162	2	0	1	2	0	3	0	0	1
miR164	3	0	0	6	0	6	3	0	4
miR166	9	2	1	14	0	17	7	0	13
miR167	4	2	0	10	0	8	7	2	9
miR168	2	1	0	1	0	2	1	2	2
miR169	14	1	2	15	0	27	9	0	9
miR171	4	0	1	9	0	10	6	0	11
miR172	5	2	0	4	0	8	5	0	5
miR319	3	3	1	2	4	9	1	0	3
miR390	2	0	0	1	3	4	0	0	0
miR393	2	0	1	2	0	4	1	0	1
miR394	2	0	0	1	0	2	2	0	2
miR395	6	0	16	23	0	10	6	0	3
miR396	2	2	0	5	0	7	3	1	2
miR397	2	0	0	2	0	2	0	0	0
miR398	3	2	0	2	0	3	0	0	0
miR399	6	0	5	11	0	12	9	0	6
miR403	1	0	0	0	0	3	0	0	0
miR408	1	0	0	1	0	1	0	5	1
Total number of miRNA genes	184	22	30	242	39	215	16	72	96

Moreover, a fold-back structure was predicted, and the product of this intergenic region was confirmed as a miRNA, called miR319 (Palatnik *et al*., 2003). Three other genes that belong to already known miRNA families were also isolated by gain-of-function mutants (Aukerman and Sakai, 2003; Kim *et al*., 2005; Williams *et*

al., 2005). Only one loss-of-function mutant was described in Arabidopsis. The *early extra petal1* mutation is caused by an insertional mutation (transposon) in a region upstream of the predicted pre-miRNA of *MIR164C* (Baker *et al*., 2005).

Characterization of miRNAs was also carried out in other plant species, both with direct cloning and bioinformatic approaches (Reinhart *et al*., 2002; Jones-Rhoades and Bartel, 2004; Juarez *et al*., 2004; Wang *et al*., 2004a; Arazi *et al*., 2005; Bedell *et al*., 2005; Guddeti *et al*., 2005; Li *et al*., 2005b; Liu *et al*., 2005a; Lu *et al*., 2005b; Sunkar *et al*., 2005; Zhang *et al*., 2005; Dezulian *et al*., 2006; Luo *et al*., 2006; Talmor-Neiman *et al*., 2006; Tuskan *et al*., 2006). So far, 916 miRNA genes in nine plant species were catalogued in the miRBASE. In Arabidopsis, 184 miRNA genes were described, comprising 22 families sharing homologues in other plant species, and 84 miRNA families that seem to be specific for Arabidopsis (Table 1). For most of the nonconserved miRNA families there was only one gene described. In four families of nonconserved miRNAs, more than one gene was described.

The classification of miRNAs into gene families takes into account the sequence of the mature miRNA only, because the sequence and the stem-loops of members a family do not resemble each other. Thus, are classified in the same family miRNAs that differ at most at four positions (Griffiths-Jones *et al*., 2006; Jones-Rhoades *et al*., 2006). Although highly different in the pre-miRNA and stem-loop structure, most of members of a miRNA family produce identical miRNAs. For example, *MIR166/165* and *MIR156/157* families, each family consist of 8 and 12 genes, respectively, corresponding to distinct stem loops, however there are only three and five different mature miRNAs in the miR166/165 and miR156/157 families, respectively (Figure 1A, Band C). The stem-loop structure, rather than the sequence, is more important for production of mature miRNA, and this feature was exploited to create an artificial miRNA, by changing only the sequence of the mature miRNA and the miRNA* in a pre-miRNA, without changing its stem-loop structure. Artificial miRNAs can be applied for simultaneously knockout several members of a target gene family (Parizotto *et al*., 2004; Alvarez *et al*., 2006; Schwab *et al*., 2006).

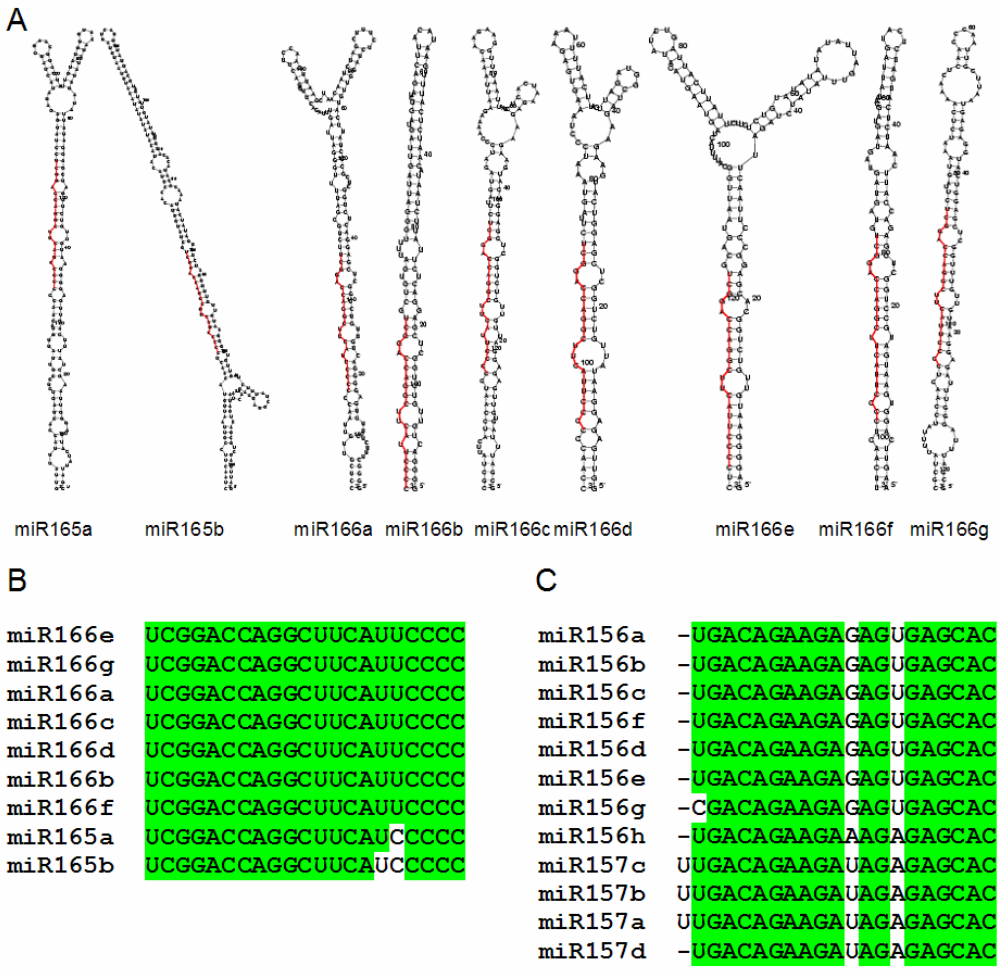

Figure 1. Examples of miRNA stem loops and mature miRNA.
A Stem loop structures of the Arabidopsis *MIR166/165* family. Mature miRNAs are labeled in red. Stem-loop structures were predicted by RNAfold (Hofacker, 2003). Multiple alignments of mature miRNA sequences of Arabidopsis are shown. B *MIR156/157* and C *MIR166/165* families.

All miRNAs described above are specific to the plant kingdom. There is no miRNA species that is found in both plant and animals. Recently, Arteaga-Vazquez *et al*. (2006) described the existence of a miRNA family that has homologous sequences in animals genomes. Combining miRNA prediction with target prediction, a database of experimentally confirmed 3'UTR sequences was used for sequence comparison search against a dataset of all Arabidopsis intergenic regions. Several filters were applied, including limits for the size of candidate miRNA sequences to 21 or 22 nucleotides and for double hits in the intergenic region, one hit in the sense and one in the antisense orientation. The other filters were based on the characteristics of miRNA interactions with theirs targets as

observed in animals. The 3'UTR of the target must have at least two potential binding sites for a candidate miRNA. Bulged nucleotides were allowed at positions 8 to 12 from the 5'-end of the candidate miRNA sequence, and G:U base pairing was allowed. At the end, nine miRNA candidates were described and the expression of three of them was confirmed. The efficient target regulation was shown for two miRNAs whose binding sites were predicted to be in the 3'UTR of the same gene. The presence of a target 3'UTR in a transgene carrying *35S$_{pro}$:GUS* reduced the expression of the transgene, compared to a *35S$_{pro}$:GUS* construct without the 3'UTR of the target. However, the most interesting finding is that one of these miRNA families, *MIR854*, is conserved beyond the plant kingdom, as homologous sequences were found in *C. elegans*, *M. musculus*, *Pan troglodytes* and *H. sapiens*. In addition, the predicted targets of miR854 found in *C. elegans*, *M. musculus* and *H. sapiens* belong to the same family as the target in Arabidopsis (Arteaga-Vazquez *et al*., 2006).

1.2. miRNA biogenesis in plants

The biogenesis of miRNAs is not elucidated completely. There is a great deal of evidence that RNA polymerase II (Pol II) is the polymerase involved in the transcription of miRNA genes. The primary transcript (pri-miRNA), which can be more than one kb in length, is longer than the sequence necessary to form the stem-loop structure. In addition, some pri-miRNAs are spliced, polyadenylated and CAP structures were also observed (Aukerman and Sakai, 2003; Xie *et al*., 2005). In many miRNA genes, a TATA box motif was found upstream to the transcription start site (Xie *et al*., 2005).

In animals, two enzymes are responsible for cleavage of the pri-miRNAs. The first cleavage is done by DROSHA inside the nuclear compartment. The second cleavage takes place in the cytoplasm and it is done by DICER. Both, DROSHA and DICER are RNase III endonucleases. The intermediate of the first cleavage is called precursor miRNA (pre-miRNA), and can be detected with northern blots or amplified by PCR (Lee *et al*., 2003). Plants do not have a homologue of DROSHA. Moreover, pre-miRNA is seldom detected by northern blot and does not accumulate in *dcl1* mutants (Jones-Rhoades *et al*., 2006). The pri-miRNA is processed by Dicer-like1 (DCL1), which cleaves the stem-loop formed by the pri-

miRNA twice to release the miRNA:miRNA* duplex that contains two-nucleotide overhangs at the 3'ends (Park *et al*., 2002; Papp *et al*., 2003). The miRNA* species derives from the complementary arm of the hairpin and pairs imperfectly to the miRNA (Reinhart *et al*., 2002). Two other proteins are also required for proper cleavage of pri-miRNAs in plants: SERRATE (SE) and HYPONASTIC LEAVES1 (HYL). In *hyl1* or *se* mutants, mature miRNAs are not produced, but pri-miRNAs can be detected by northern blots instead (Han *et al*., 2004; Vazquez *et al*., 2004a; Grigg *et al*., 2005; Kurihara *et al*., 2006; Lobbes *et al*., 2006; Yang *et al*., 2006). Both proteins clearly play role in miRNA biogenesis, thought not well defined yet. Methylation is also a crucial step in miRNA biogenesis. HUA ENHANCER1 (HEN1) adds methyl groups to the ribose of the last nucleotide in either strand of the miRNA:miRNA* duplex. The methyl group is thought to protect the duplex against degradation by endonucleases (Li *et al*., 2005a). The transport of the duplex may be done by HASTY (HST; Park*et al*., 2005), a plant homolog of animal EXPORTIN 5. *hst* null mutants are viable, which indicates that miRNAs find their way to the cytoplasm without HST as well or that there is another export pathway. In the cytoplasm, the mature miRNA is incorporated into the RNA-induced silencing complex (RISC), the most important protein of which is ARGONAUT1 (AGO1). However, the *hst* mutation does not affect the accumulation of all miRNAs and the evidence the mature miRNAs accumulate in the cytoplasm and in the nucleus suggest that the incorporation of the mature miRNA into the RISC may also happen inside the nucleus. Consequently, the transport of the RISC to the cytoplasm could be done by HST or by other transporters that may interact directly with the RISC (Chen, 2005; Park *et al*., 2005). The miRNA serve as a guide for the RISC to downregulate gene expression by three mechanisms: cleavage of target mRNA, chromatin methylation and translational repression (Figure 2; Bartel, 2004).

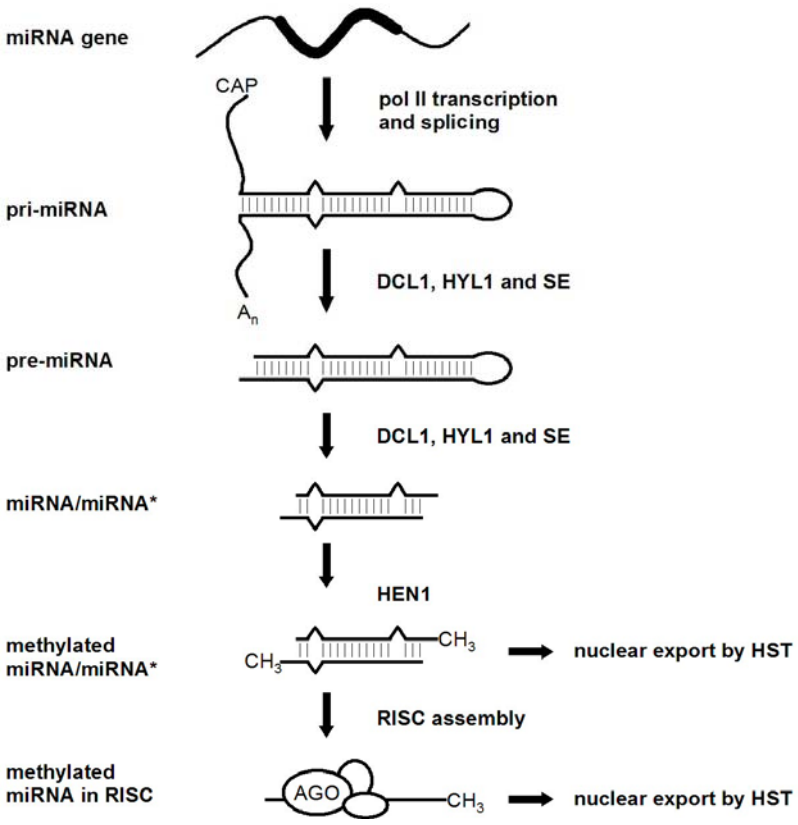

Figure 2. Schematic view of miRNA biogenesis in plants.
The-miRNA is produced by RNA polymerase II (pol II), capped, and has a poly A tail. After splicing, the pri-miRNA is cleaved by DCL1 with the help of HYL1 and SE, releasing a pre-miRNA that is cleaved in the same way by DCL1. The cleavage product is a duplex consisting of miRNA/miRNA*. Methyl groups are added to the ribose of the last nucleotide in either strand by HEN1. Then, the duplex is transported to the cytoplasm and the mature miRNA is incorporated into the RISC. Alternatively, some miRNAs appear to be incorporated into the RISC in the nucleus and are then transported to the cytoplasm. Modified from Chen (2005). DICER-LIKE1 (DCL1), HYPONASTIC LEAVES1 (HYL), SERRATES (SE) and HUA ENHANCER1 (HEN1).

The incorporation of the mature miRNA in to the RISC complex seems to follow the same rules as in animals. The 5'end of the miRNA* displays less stability than the 5'end of the mature miRNA. This asymmetry is a key feature for strand selection and incorporation into the RISC complex (Khvorova *et al*., 2003; Schwarz *et al*., 2003).

Deep sequencing of small RNA samples also revealed that not all miRNAs are produced by DCL1. The accumulation of two miRNAs, which are found only in Arabidopsis, was not affected in *dcl1* mutants, and mature miRNAs were not detected in *dcl*4 mutants instead. In addition, the accumulation of these miRNAs

was not affected by mutations in genes whose products participate in the biogenesis of siRNAs (Rajagopalan *et al*., 2006).

1.3. Mechanism of action

miRNAs regulate gene expression at the post-transcriptional level by two mechanisms: repression of translation (Aukerman and Sakai, 2003; Chen, 2004; Arteaga-Vazquez *et al*., 2006; Gandikota *et al*., 2007) or cleavage of mRNA (Llave *et al*., 2002b). In addition, specific miRNAs can silence genes at the transcriptional level by chromatin methylation (Bao *et al*., 2004; Mallory *et al*., 2004b). In plants, examples of all three mechanisms could be observed, however, because of the high complementarity of miRNAs to their target mRNAs, the expression of most plant miRNA targets is regulated by cleavage of target mRNAs by the RISC guided by a miRNA (Jones-Rhoades *et al*., 2006).

1.3.1. Cleavage of target mRNA

Cleavage of target mRNAs is the main mechanism of action of plant miRNAs, due to the high sequence complementarity of plant miRNAs with their target mRNA. In most cases, the binding sites are located in the ORF of their target transcripts. This means that the mechanism of action of most plant miRNAs does not differ from other classes of small RNAs found in plants: small interfering RNAs (siRNAs), trans-acting siRNAs (ta-siRNAs) and natural antisense transcript siRNAs (nat-siRNA; Hamilton and Baulcombe, 1999; Peragine *et al*., 2004; Vazquez *et al*., 2004b; Borsani *et al*., 2005). The RISC contains several proteins, but the most characterized so far is AGO1, which contains the slicer activity necessary to cleave the target mRNA (Baumberger and Baulcombe, 2005). The miRNA guides the RISC to bind the mRNA target at the miRNA binding site and AGO1 cleaves the mRNA, usually at the position that corresponds to the tenth nucleotide of the miRNA binding site (Figure 3A). The cleavage fragments are released and the RISC can target another mRNA (Bartel, 2004). mRNA cleavage is not limited to plants. Indeed, miR196 guides the cleavage of *HoxB8* mRNA in mice, presumably due to the unusually high degree of complementarity between the miRNA and its target (Yekta *et al*., 2004).

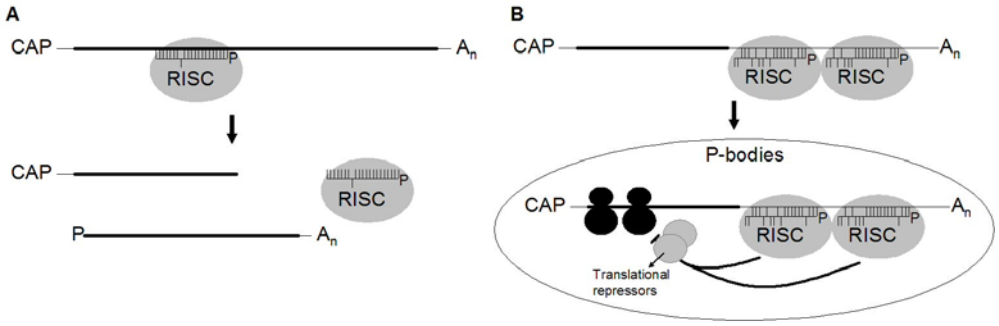

Figure 3. Post-transcriptional silencing by miRNAs.
A. Messenger RNA cleavage is specified by a miRNA. The RISC is guided to the miRNA binding site on target mRNA by the miRNA and AGO1 slices the mRNA, in most cases after the tenth nucleotide of the miRNA:mRNA hybrid. After cleavage, RISC releases the cleaved products and can target another mRNA. B. Translational repression, a mechanism of action that is more common in animals. However, there are a few examples in plants. RISC redirects the bound mRNA to P-bodies, where global translational repressors are recruited that may interact with RISC, resulting in a decrease of the protein but not of the mRNA level.

1.3.2. Repression of translation

Instead of driving the RISC to bind and cleave target mRNAs, miRNA-RISC complexes also regulate gene expression by a not well characterized mechanism that results in more or less unchanged levels of target mRNAs, but in decreased levels of encoded proteins. This mechanism, often called repression of translation, is more common in metazoa than in plants (Bartel, 2004). In animals, the complementarity of miRNAs and with their targets is not as high as in plants. As a consequence of the imperfect base pairing between a miRNA and its miRNA binding site, the RISC does not cleave the target mRNA. Moreover, in animals, miRNA binding sites are more frequent in 3'UTRs of the transcripts and often there is more than one miRNA binding site for the same miRNA on the 3'UTR of the target gene. The RISCs repress translation by an unclear mechanism, but localization of RISCs and target mRNA in the processing bodies (P bodies) raised some clues about the mechanism. In the P bodies, mRNAs are stored and degraded (Figure 3B). Thus, miRNA-guided binding of RISC to mRNAs leads to redirection of mRNAs to P bodies where translation is repressed by global translational repressors (Liu *et al*., 2005b; Sen and Blau, 2005; Chu and Rana, 2006). In plants, four different miRNAs have been implicated in regulation of gene

expression by translational repression (Aukerman and Sakai, 2003; Chen, 2004; Arteaga-Vazquez *et al*., 2006; Gandikota *et al*., 2007).

1.3.3. DNA methylation

DNA methylation mediated by miRNAs is the least known mechanism of miRNA actions, with only one example. Dominant mutations in the *PHABULOSA* (*PHB*) and *PHAVOLUTA* (*PHV*) loci lead to abnormal leaf development. The observation that these mutations are located in the miR166/165 binding site and that the levels of these mRNAs are higher in *phb* and *phv* mutants than in wild-type confirmed the regulation of these genes by miR166. Interestingly, the observed leaf morphogenesis defects correlate with mutations that lead to reduced DNA methylation in these loci. Indeed, it was found that in these dominant mutants the methylation is reduced in these loci. The miRNA binding site in *PHB* and *PHV* mRNA span an exon junction, therefore miR166/165 interacts with spliced mRNAs and not with genomic DNA or unspliced mRNAs. Moreover, in heterozygous *phb* plants, the only allele that showed reduced methylation was the mutant allele. Thus, miR166/165 interacts with *PHD* and *PHV* mRNA leading to cleavage and degradation and, in addition, chromatin modification factors may be recruited and the locus is repressed through DNA methylation (Bao *et al*., 2004; Mallory *et al*., 2004b). Even though this is an intriguing finding, the functional significance is still unclear.

1.4. Prediction of miRNA targets

Plant miRNAs display a high sequence complemetarity to target mRNAs, and this is a crucial characteristic for target prediction and validation. Indeed, many predicted miRNA targets in plants have been validated, whereas in animals, only a few targets were experimentally validated (Bartel, 2004).

Based on the high sequence complemetarity, Rhoades *et al*. (2002) applied a pattern search algorithm to predict Arabidopsis miRNA targets. Their approach searched for miRNA complemetarity in the Arabidopsis genome with less than four mismatches, considering G:U base pairing as a mismatch. Insertions or deletions, which could lead to bulged nucleotides or gaps in either strand, were not allowed. This approach predicted 49 miRNA targets, and many of them were successfully

validated. The high sequence complementarity of miRNAs with their target mRNAs was employed to predict additional targets in Arabidopsis as well as in other plant species (Park *et al*., 2002; Reinhart *et al*., 2002; Sunkar and Zhu, 2004; Adai *et al*., 2005).

Initial efforts to predict miRNA targets missed possible candidates because of the presence of more than three mismatches or bulged nucleotides in the miRNA binding site. Moreover, evidence that plant miRNAs can actually target mRNA sequences with more than three mismatches was provided by Palatnik *et al*. (2003), whose work described that the overexpression of miR-JAW, later renamed miR319, resulted in the decrease of mRNA levels of five members of the *TCP* transcription factor family. Cleavage products induced by miR319 could be detected for all down-regulated *TCP* genes. The binding site for miR319 in these *TCP* mRNAs show up to five mismatches, considering G:U base pairing as a mismatch.

In a more sophisticated approach that allowed more mismatches and bulged nucleotides, the conservation of the miRNA binding site in homologous sequences of two different species was considered. As consequence, the miRNA binding site must be present in homologous sequences of Arabidopsis and rice, in this approach. In addition, the miRNA binding site was scored according to the presence of mismatches. Each matching nucleotide in the miRNA:mRNA duplex was given the value zero. A mismatch was assigned the value one, bulged nucleotides received 1.5. Base pairing between G and U was assigned 0.5. In a miRNA target, the sum of all values in a given miRNA binding site should not be higher than 3.5 and the miRNA binding site must be found in at least one homologous mRNA in rice (Jones-Rhoades and Bartel, 2004).

A similar approach was used by Wang *et al*. (2004) using a nucleotide alignment algorithm in which mismatches were given a lower penalty than a bulge. In addition, a penalty for gap opening and gap extension was included. The top 500 hits in Arabidopsis and rice were compared and a hit was considered as true miRNA target when the miRNA binding site could be found in homologous mRNAs of both species.

A microarray analysis of plants overexpressing specific miRNAs, together with structure analysis of validated miRNA:binding-site hybrids resulted in a set of rules that could be used for evaluation of a putative miRNA target (Schwab *et al*., 2006). Generally, the pairing in the 5' part of the miRNA is more important, and only one mismatch would be allowed in the regions corresponding the nucleotides 2 to 12, which includes the presumptive cleavage site between positions 10 and 11. In the 3'end of the miRNA, a mismatch loop could be tolerated up to maximal two nucleotides, and a perfect match in this part would compensate the presence of up to two mismatches in the 5'end (Figure 4). The minimum free energy of the duplex should be at least 72% of a perfect match with the same miRNA and the value should be about -30 kcal/mol or below (Schwab *et al*., 2006).

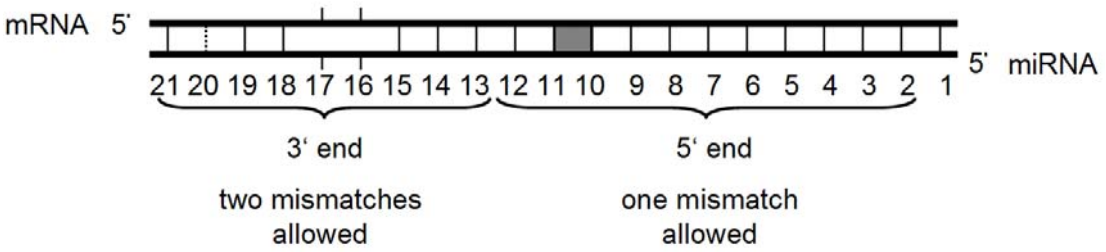

Figure 4. Characteristic miRNA binding site structure.
Schematic view of the interaction (hybrid) between miRNA and mRNA in plants according to Schwab *et al*., (2005). The proposed model was based on empirically validated miRNA targets. In this model, no mismatch is allowed in the presumptive cleavage site (gray box). Mismatches are shown in the nucleotide positions 16th and 17th, G:U base pairing is shown in the 20th nucleotide.

An approach based on minimum free energy comparison was developed by Rusinov *et al*. (2005). In this implementation, the first six nucleotides of the miRNA were used for an initial sliding-window search for six Watson-Crick matches or five Watson-Crick matches and one G:U base pairing in all Arabidopsis annotated genes. When a hit was found, a portion of 32 nucleotides was extracted and a hybridization structure of the miRNA and the putative binding site was predicted with a folding program for RNA. Based on known previous miRNA:binding site duplexes, filters were implemented, considering the size of the bulge and the size of the mismatch loop.

1.5. Validation of miRNA targets

Many predicted miRNA targets have been validated in Arabidopsis. The validation of miRNAs in plants is more straightforward than in animals because most plant miRNAs act like siRNAs, inducing the cleavage of the mRNA target. The phosphodiester bond between two nucleotides is broken, resulting in a 3' cleavage product that contains a phosphate group at its 5'end. This feature was intensively used for validation of miRNA targets. A modified version of 5' rapid amplification of cDNA ends (5'RACE) could be used for mapping the precise point of the cleavage by the RISC. In this approach, an RNA adaptor is ligated to the 5'end of the cleavage product and the adaptor-ligated RNA is used as template for reverse transcriptase followed by PCR with gene specific nested primes. The PCR product is then cloned and many clones are sequenced revealing the position of the miRNA-guided RISC-mediated cleavage (Llave *et al*., 2002a). In this way, many miRNA targets were validated (Llave *et al*., 2002a; Kasschau *et al*., 2003; Palatnik *et al*., 2003; Allen *et al*., 2004; Chen *et al*., 2004; Jones-Rhoades and Bartel, 2004; Mallory *et al*., 2004a; Mallory *et al*., 2004b; Allen *et al*., 2005; Lu *et al*., 2005a; Mallory *et al*., 2005; Rajagopalan *et al*., 2006; Reyes and Chua, 2007).

Transient *A. tumefaciens* infiltration can be also used as a means for miRNA target validation (Llave *et al*., 2002a; Kasschau *et al*., 2003). The cDNA of a target and the corresponding pre-miRNA are cloned into a binary vector and transiently expressed in Arabidopsis or *Nicotiana benthamiama* leaves, and the cleavage products are analyzed by northern blotting experiments (Llave *et al*., 2002a; Kasschau *et al*., 2003; Palatnik *et al*., 2003; Achard *et al*., 2004; Wang *et al*., 2005). Alternatively, RNA extracted from infiltrated leaves can be used for 5'RACE as described above (Llave *et al*., 2002a; Kasschau *et al*., 2003; Palatnik *et al*., 2003).

An *in vitro* assay for detection of cleavage products of miRNA targets was also developed (Tang *et al*., 2003). In this experiment, a cDNA of a miRNA target was cloned and used for *in vitro* transcription. The transcript was then mixed with standard wheat germ extracts that contain all the components of the miRNA silencing pathway. After incubation, the RNA was isolated and analyzed by northern blotting. The result were similar to those observed in the infiltration assay

(Tang *et al*., 2003; Mallory *et al*., 2004a; Mallory *et al*., 2004b; Kim *et al*., 2005; Reyes and Chua, 2007).

All the methods for target validation described above demonstrate miRNA-dependent cleavage of mRNA targets, but lack evidence for the functional role of miRNAs *in planta*. To analyze the effects of miRNA regulation *in planta*, thereby also contributing to miRNA target validation, the disruption of miRNA binding site was successfully employed. By using site-directed mutagenesis, nucleotides in a miRNA binding site can be mutated by introducing silent mutations that do not result in changes in the amino acid sequence of the encoded protein. This cDNA can be expressed *in planta* under the control of an endogenous or constitutive promoter, leading to the expression of a miRNA-resistant mRNA. The effects observed *in planta* not only provide confidence for target validation, but also help to understand the functions of a miRNA and its target (Palatnik *et al*., 2003; Bartel, 2004; Kidner and Martienssen, 2004; Mallory *et al*., 2004a; Mallory *et al*., 2004b; Parizotto *et al*., 2004).

1.6. Expression of miRNA genes

The expression of miRNA genes is a topic not well investigated to date. It is clear that miRNA genes are also subjected to regulation at the transcriptional level. In addition, all steps of the miRNA biogenesis may be regulated. However, there are a few data addressing what precisely drives miRNA gene expression. Much of the miRNA expression data available derives from northern blots that detect the mature miRNA. The tissue-specific accumulation of a many miRNAs could be described using this approach (Reinhart *et al*., 2002; Achard *et al*., 2004; Sunkar and Zhu, 2004; Wang *et al*., 2004b; Arteaga-Vazquez *et al*., 2006). Many plant miRNAs come in gene families and detection of specific mature miRNA species does not tell anything about which miRNA gene is actually expressed.

The tissue-specific expression of miRNAs was also demonstrated by *in situ* hybridizations. For example, the expression of miR172 was observed in the floral whorls of stage 1 flowers and in inner whorls of stage 7 flowers (Chen, 2004). In another example, miR165 expression was detected at the abaxial side of leaf primordia. The expression of its target, *PHB*, was detected at the adaxial side.

Interestingly, in a mutant that does not accumulate miR165, *PHB* transcripts were detected on both sides of leaf primordia (Kidner and Martienssen, 2004). DNA microarrays were also applied for a rapid survey of miRNA expression (Axtell and Bartel, 2005).

Reporter constructs were employed to determine precisely the expression pattern among members of miRNA gene families. The cell specific pattern of miR171 expression was analyzed using a promoter fragment of miR171 to drive expression of the reporter gene that encodes the green fluorescent protein (GFP; Parizotto *et al*. 2004). In a similar way, the *uidA* gene encoding GUS was also employed for analysis of miRNA gene expression (Baker *et al*., 2005; Wang *et al*., 2005; Aung *et al*., 2006; Wu *et al*., 2006). The differential expression of each member of the miR167 (Wu *et al*., 2006) and the miR399 (Aung *et al*., 2006) families was described using promoter-GUS lines.

A quantitative analysis of miRNA expression was possible when deep sequencing techniques like MPSS or 454-pyrosequencing were adapted for cloning and sequencing of small RNAs, resulting in a gene expression pattern for several miRNA genes (Lu *et al*., 2005a; Rajagopalan *et al*., 2006).

The expression of miRNA genes is affected by plant hormones and growth conditions. The level of miR164 was demonstrated to be affected by a phytohormone. Supplying plants with 10 mM 1-naphthalene acetic acid (NAA), a synthetic auxin, resulted in an increased level of miR164 accumulation (Guo *et al*., 2005). In addition, the presence of miR395 in plants grown under standard growth conditions was hardly detected. Moreover, its amount was increased several times in plants growing in medium lacking sulfate (Jones-Rhoades and Bartel, 2004). Phosphate is a key regulator of gene expression of members of the miR399 family. Phosphate starvation induced the expression of miR399 (Fujii *et al*., 2005) and each member of the gene family was affected to a different extent, leading to a gene-specific expression pattern that as a whole makes up the expression pattern of miR399 (Aung *et al*., 2006). The expression of miR398 decreased after three different kinds of oxidative stress: high light and high concentration of copper or iron (Sunkar *et al*., 2006).

1.7. Role of Arabidopsis miRNAs

Observations that mutants with impaired biogenesis of miRNAs showed abnormalities during development highlighted the importance of miRNAs in plant biology. Many of these mutants were described prior to the discovery of miRNAs in plants. Consequently, these genes were classified according to the specific pathways they belong to, for example, shoot apical meristem (SAM) maintenance, leaf morphogenesis, hormone response (Jacobsen *et al*., 1999, Lu and Fedoroff, 2000). Later, the observed phenotypes were explained by the fact that specific miRNAs were not produced and their miRNA targets were up-regulated in these mutants (Han *et al*., 2004; Vaucheret *et al*., 2004; Vazquez *et al*., 2004a; Kurihara *et al*., 2006; Lobbes *et al*., 2006; Yang *et al*., 2006).

Defining specific functions for a miRNA includes not only to show the cleavage of the target by RISC, but also to show the functionality of the regulation for proper plant growth and development. Unfortunately, many miRNAs are present in gene families. This characteristic makes the use of knock-out mutants to understand the function of a miRNA difficult. In addition, the size of the stem-loop sequence that is necessary for DCL1 cleavage is very small and thus difficult to be target of an insertional mutant (Jones-Rhoades *et al*., 2006). A simple way to overcome this problem is to overexpress a miRNA gene. However, this may lead to the complication that many targets could be downregulated at the same time. Nonetheless, by using this approach the functions or the involvement of a few miRNAs in specific biological processes was described (Palatnik *et al*., 2003; Achard *et al*., 2004; Laufs *et al*., 2004; Mallory *et al*., 2004a; Vaucheret *et al*., 2004; Guo *et al*., 2005; Kim *et al*., 2005; Mallory *et al*., 2005; Sunkar *et al*., 2006).

A different approach that allows the analysis target by target, is the analysis of the effects of disrupting the miRNA regulation in a given target. This led not only to the study of target functions, but also to the elucidation of the role of the presence or absence of miRNA regulation.

With combinations of different approaches, several groups have demonstrated that many miRNAs regulate various plant developmental processes, including leaf morphogenesis and polarity (Palatnik *et al*., 2003), floral differentiation and development (Aukerman and Sakai, 2003; Chen, 2004) root initiation and

development (Laufs *et al*., 2004; Mallory *et al*., 2004a; Guo *et al*., 2005), vascular development (Kim *et al*., 2005), transition of plant growth from the vegetative to the reproductive phase (Achard *et al*., 2004; Lauter *et al*., 2005), phosphate homeostasis (Fujii *et al*., 2005; Aung *et al*., 2006; Chiou *et al*., 2006), and even small RNA biogenesis and function (Xie *et al*., 2003; Vaucheret *et al*., 2004). Some specific examples of miRNA function are further discussed below.

1.7.1. Leaf morphogenesis

At least two miRNA families are involved in the regulation of leaf development, miR166 and miR319. The role of miR319 in leaf development is caused by the fact that this miRNA has a subset of *TCP* transcription factor genes among its target (Palatnik *et al*., 2003). Overexpression of miR319 resulted in low levels of some *TCP* mRNAs and caused jaw-D phenotypes, including uneven leaf shape and curvature. In contrast, overexpression of miR139-resistant *TCP* mutants indicated that miR319-guided mRNA cleavage was sufficient to restrict TCP function (Palatnik *et al*., 2003).

The abaxial and adaxial pattern in Arabidopsis leaves is also controlled by miRNAs. This pattern is controlled by the polar expression of class-III homeodomain leucine zipper (*HD-ZIP*) transcription factor genes in the SAM (Emery *et al*., 2003). *PHB*, *PHV* and *REV* are three closely related Arabidopsis HD-ZIP transcription factors and mutations in any of these genes resulted in severe modifications of leaf development. Several experiments have demonstrated that all of these transcription factors are targets of miR166/165 (Emery *et al*., 2003; Bao *et al*., 2004; Mallory *et al*., 2004b).

The regulation of the *HD-ZIP* gene family by the miR166/165 family is a conserved mechanism that was also observed in all lineages of land plants, including mosses, ferns, gymnosperms, and angiosperms (Floyd and Bowman, 2004). Moreover, the same developmental abnormalities caused by disruption of miRNA regulation and loss of function of *HD-ZIP* genes in Arabidopsis were observed in *Z. mays* (Juarez *et al*., 2004).

1.7.2. Vascular development

Another role of miR166 and HD-ZIP proteins is the regulation of vascular development. ATHB15, a member of the HD-ZIP family, is predominantly expressed in vascular tissues, suggesting that it may play some role in plant vascular development. *ATHB15* is also one target of miR166/165 (Rhoades *et al*., 2002). Overexpression of miR166a resulted in decrease of *ATHB15* mRNA levels, which in turn caused accelerated vascular cell differentiation of cambial/procambial cells. Consequently, an altered vascular system with expanded xylem tissue and an interfascicular region was produced (Kim *et al*., 2005). This regulatory mechanism may exist in all vascular plant species as well (Floyd and Bowman, 2004; Kim *et al*., 2005).

1.7.3. Small RNA biogenesis and function

The biogenesis and function of miRNAs and ta-siRNAs in general is affected by several miRNAs. The major enzyme of miRNA biosynthesis, DCL1, is itself regulated by miR162 (Xie *et al*., 2003). In addition, another very important protein, AGO1, the major protein of RISC, shows regulation of mRNA accumulation by miR168. The expression of an AGO1 mutant that is not subject to miR168 regulation resulted in developmental defects similar to other miRNA biogenesis mutants (Vaucheret *et al*., 2004). At least three miRNAs are involved in the biogenesis of ta-siRNA: miR173, miR390, and miR828. Together, they mediate the biogenesis of four ta-siRNAs (Peragine *et al*., 2004; Vazquez *et al*., 2004b; Allen *et al*., 2005; Rajagopalan *et al*., 2006).

1.7.4. Flower development

The flower development is regulated by at least four miRNAs: miR156, miR159, miR164 and miR172. The APETELA 2 (AP2) and AP2-like proteins are required for proper floral organ identity and flowering. Overexpression of miR172 resulted in the complete absence of AP2 and other AP2-like proteins. As a consequence, plants set flowers early with disrupted specification of floral organ identity, a very similar phenotype as displayed by *ap2* null mutants (Aukerman and Sakai, 2003; Chen, 2004). An early flowering phenotype was also observed in plants overexpressing a mutant form of *SPL3* mRNA leading to a lack of regulation of

SPL3 by miR156. In flowers of *35S$_{pro}$:SPL3-UTR∆4* plants with developmental abnormalities were also observed (Gandikota *et al*., 2007).

LEAFY (LFY) is an important factor in floral development. LFY itself is not a miRNA target, but a group of MYB transcription factors, whose members act as positive regulators of *LFY* expression, are target of miR159. Overexpression of miR159 resulted in downregulation of *LFY*, which in turn lead to a delay in flowering in short-day photoperiods and to defects in anther development (Achard *et al*., 2004; Schwab *et al*., 2005).

The involvement of miR164 in flower development was uncovered when the transposon insertion in the mutant *early extra petal1* was characterized. The position of the insertion was mapped to the promoter of *MIR164C*. As the mutant name says, it was observed an early-flowering phenotype and the presence of extra petal (Baker *et al*., 2005).

1.7.5. Shoot and root development

Five members of a family of genes encoding NAM/ATAF/CUC (NAC)-domain transcription factors are targets of miR164 (Rhoades *et al*., 2002; Laufs *et al*., 2004; Mallory *et al*., 2004a; Guo *et al*., 2005). Cup-shaped cotyledon 1 (CUC1) and CUC2 regulate meristem development and separation of aerial organs (Aida *et al*., 1997), and NAC1 is involved in root development (Xie *et al*., 2002). Both, gain-of-function and loss-of-function mutants of miR164 caused several developmental defects, which were associated with misexpression of *NAC1*, *CUC1* and *CUC2* (Laufs *et al*., 2004; Mallory *et al*., 2004a; Guo *et al*., 2005). The phenotypes observed in miR164 overexpressing plants were very similar to those observed in *cuc1 cuc2* double mutants (Laufs *et al*., 2004; Mallory *et al*., 2004a).

1.7.6. Auxin signaling

Several miRNAs are involved in hormone signaling pathways. At least four miRNAs are involved in the signal transduction of auxin. *TIR1*, which encodes an auxin receptor, is a predicted target of miR393. Auxin Response Factors (ARFs) are transcription factors that bind to auxin response elements in promoters of early auxin response genes. *ARF10*, *ARF16* and *ARF17* were validated as miR160 targets in 5'RACE experiments (Kasschau *et al*., 2003; Mallory *et al*., 2005).

Moreover, the mutation of the miR160 binding site in *ARF17* resulted in elevated levels of *ARF17* mRNA and dramatic developmental defects, including embryo symmetry anomalies, premature inflorescence development, leaf shape defects and root growth defects (Mallory *et al*., 2005). Cleavage of *ARF8* mRNA regulated by miR167 was demonstrated (Kasschau *et al*., 2003). Two ARFs are affected indirectly by miR390. For both *ARF3* and *ARF4* mRNA cleavage is mediated by TAS3-siRNAs. The miR390 participate in TAS3-siRNAs biogenesis (Allen *et al*., 2005).

1.7.7. Sensing nutrient stress

miRNAs are also involved in regulating plant responses to nutrient stresses (Jones-Rhoades and Bartel, 2004; Allen *et al*., 2005; Fujii *et al*., 2005; Aung *et al*., 2006; Chiou *et al*., 2006). MiR395 seems to regulate two different groups of genes that function coordinately in the sulfate pathway, three out of four ATP sulfurylase (APS) in Arabidopsis have a miR395 binding site on their mRNAs, and 5'RACE fragments were recovered from *APS1* and *APS4*, but not from *APS3* mRNAs (Jones-Rhoades and Bartel, 2004). Interestingly, *APS* mRNAs that contain a miR395 binding site encode proteins that are localized in the plastid, whereas *APS2* encodes a protein that is a cytosolic isoform. This may reflect the role of miR395 in the regulation of sulfate assimilation in plastids (Chiou, 2007). In seedlings of Arabidopsis growing under low sulfate conditions, miR395 accumulated to higher amounts and the level of *APS1* mRNA was decreased. On the other hand, in media with higher sulfate concentration, miR395 was not detected and *APS1* accumulated to higher levels (Jones-Rhoades and Bartel, 2004).

In addition to targeting *APS* genes, miR395 also targets *AST68*, which encodes a sulfate transporter that was experimentally validated as miR395 by 5′-RACE analysis (Jones-Rhoades and Bartel, 2004).

MiRNA399 controls inorganic phosphate (Pi) homeostasis by regulating the expression of *UBC24* encoding an ubiquitin-conjugating E2 enzyme in Arabidopsis. Transgenic plants overexpressing miR399 accumulated excessive Pi in the shoots and displayed phosphate toxicity symptoms (Fujii *et al*., 2005).

Moreover, miR399 was up-regulated by Pi deprivation and, consequently, *UBC24* is downregulated (Fujii *et al*., 2005; Aung *et al*., 2006; Chiou *et al*., 2006).

1.7.8. Oxidative stress tolerance

The involvement of miRNAs in oxidative stress tolerance was first taken into account when two Cu/Zn superoxide dismutase genes, *CSD1* and *CSD2* were predicted and subsequently validated using 5'RACE as miR398 targets (Jones-Rhoades and Bartel, 2004). The accumulation of miR398 was shown to be down-regulated by oxidative stresses and the down-regulation of miR398 interrupts the suppression over *CSD1* and *CSD2*. Overexpression of *CDS2* harboring silent mutations in the miR398 binding site elevated the *CDS2* expression and consequently, plants were much more tolerant to high light, heavy metals, and other oxidative stresses (Sunkar *et al*., 2006).

1.8. *MIR159/319* family

Six genes in Arabidopsis make up the *MIR159/319* family of miRNA genes. The miR159/319 family is conserved in other plant genomes (Rhoades *et al*., 2002; Zhang *et al*., 2005; Dezulian *et al*., 2006; Tuskan *et al*., 2006). This family can be further classified into two subfamilies in Arabidopsis, *MIR159* and *MIR319*. The difference between miR159 and miR319 species is not greater than four nucleotides (Figure 5B; Reinhart *et al*., 2002; Rhoades *et al*., 2002; Palatnik *et al*., 2003). In fact, five different miRNA species are produced from the six members of the *MIR159/319* family. Nonetheless, they are still classified as belonging to the same miRNA family (Griffiths-Jones *et al*., 2006; Jones-Rhoades *et al*., 2006). The overexpression of members of each subgroup led to downregulation of different targets. Most of the miR319 targets belong to the *TCP* gene family of transcription factors (Palatnik *et al*., 2003). In contrast, most of the miR159 targets belong to the MYB transcription factor family (Rhoades *et al*., 2002; Jones-Rhoades and Bartel, 2004). Unlike in other miRNA families, in which the difference between members is situated at the 3'end of the mature miRNA, one of the diferences observed in the mature sequence of miR159 and miR319 is found at the 5'end. Experimental analyses of animal targets and mutational analyses of plant targets demonstrated that the region pairing with the 5'end of the miRNA is specifically sensitive to

mismatches (Lewis *et al*., 2003; Doench and Sharp, 2004; Laufs *et al*., 2004; Mallory *et al*., 2004b; Parizotto *et al*., 2004; Vaucheret *et al*., 2004; Brennecke *et al*., 2005). Althought similar, *MIR159* and *MIR319* could also be regarded as two different families, since the six *MIR159/319* genes have different pre-miRNAs, but rather similar stem-loop structures (Figure 5A).

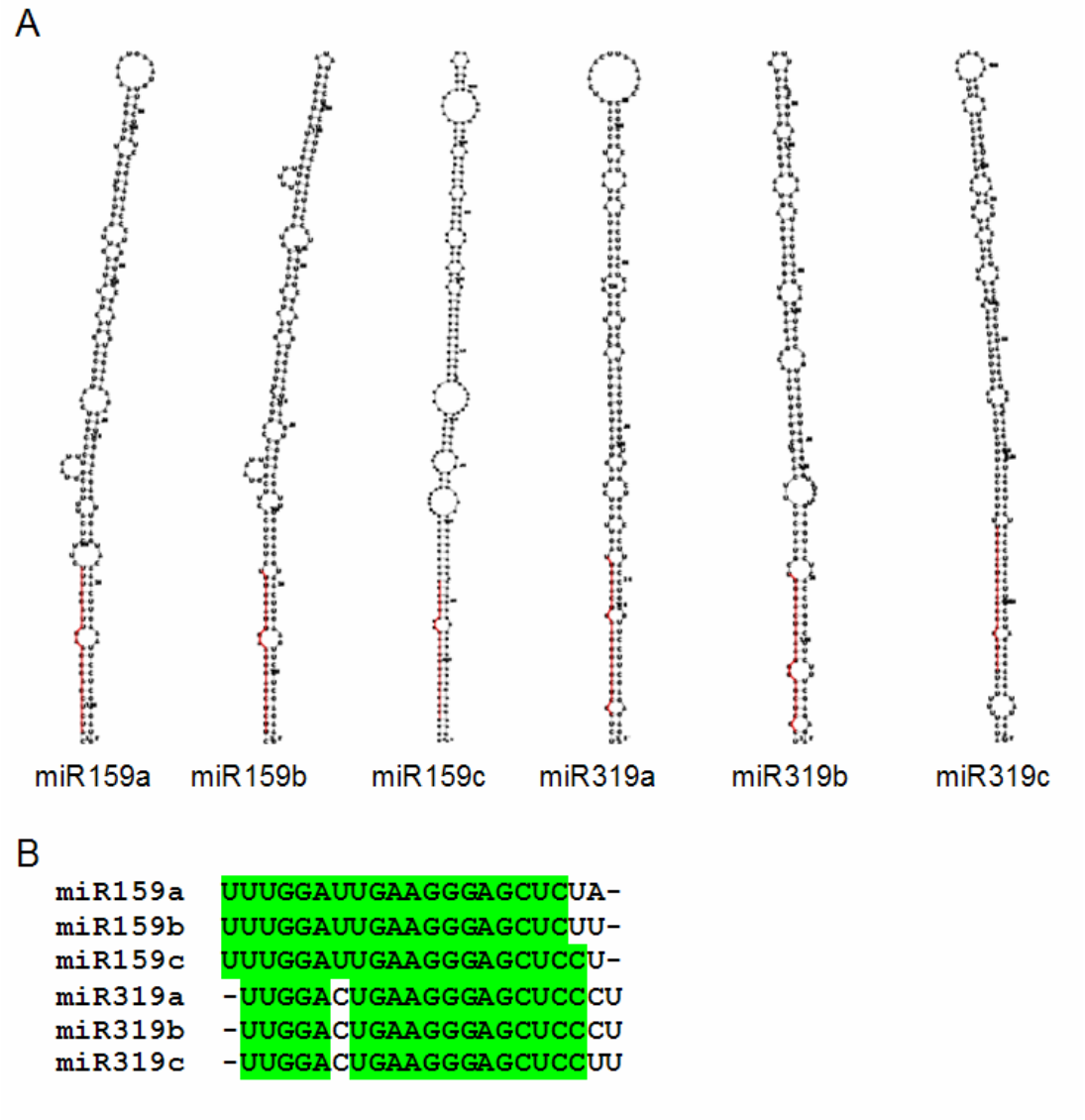

Figure 5. The miR159/319 gene family in Arabidopsis.
A. Stem loop structures of the Arabidopsis *MIR159/319* family. Mature miRNAs are labeled in red. B. Alignment of mature sequences of miR159/319 species.

Expression of miR159 species, analyzed by detection of mature miRNAs in northern blots, accumulated predominantly in young seedlings and flowers, and was less abundant in rosette leaves, cauline leaves or siliques. Expression was undetectable in roots. In addition, the accumulation of miR159 was enhanced by exogenous gibberellin GA_3 (Achard *et al*., 2004). Using promoter-GUS lines, Niemeier (2006), demonstrated that promoter activity of *MIR159A*, and not *MIR159B*, was increased by application of exogenous gibberellin in Arabidopsis seedlings. Analysis of the number of reads that match to members of the miR159 subfamily sequenced by 454-pyrosequencing (Lu *et al*., 2006) also clearly demonstrated that *MIR159A* is the member with the highest expression, with 205 transcripts per quarter million (TPQ). This is markedly higher than *MIR159B*, with a value of 48 TPQ. *MIR159C* is the least active gene under normal conditions with as few as four TPQ (Lu *et al*., 2006).

Targets of miR159 were predicted and some of them validated. A subfamily of genes encoding MYB transcription factors were predicted as target of miR159, including *MYB33*, *MYB65*, *MYB81*, *MYB97*, *MYB101*, *MYB104* and *MYB120* (Rhoades *et al*., 2002; Jones-Rhoades and Bartel, 2004). In addition, many other genes were predicted as miR159 targets, namely *MYB125*, At1g29010, At5g55930 (*OPT1*) and At4g37770 (*ACS8*) (Jones-Rhoades and Bartel, 2004; Schwab *et al*., 2005). Moreover, using 5'RACE, cleavage products of *MYB33*, *MYB65*, *MYB101* and *OPT1* were detected (Palatnik *et al*., 2003; Schwab *et al*., 2005; Reyes and Chua, 2007) and constitutive expression of miR159 led to reduced levels of *ACS8*, *MYB120*, *MYB101* and *OPT1* (Schwab *et al*., 2005).

The expression of *MYB33* is constrained by the presence of the miR159 binding site on its mRNA. A fusion protein of MYB33:GUS accumulates in many plant tissues, like whole seedlings, roots, leaves and flower organs. In a similar construct containing silent mutations in the miR159 binding site, mMYB33:GUS accumulates only in the anthers, which were the only organ where were observed phenotypic abnormalities in *myb33 myb65* double mutant plants (Millar and Gubler, 2005). In mMYB33:GUS plants the expression of the fusion protein was under the control of the *MYB33* promoter. Expression of mMYB33:GUS caused up-curling in leaves, as well as shorting in the petiole length (Millar and Gubler, 2005). In $35S_{pro}$*:mMYB33* plants, also show upwardly curled leaves, but do not

show decreasing in petiole length. However, theses plants displayed a dramatically reduction in size (Palatnik *et al*., 2003).

The overexpression of miR159 caused male sterility and a delay in the flowering time (Achard *et al*., 2004; Schwab *et al*., 2005). In miR159 overexpressing lines, the levels of *LEAFY*, an important floral meristem identity gene, and its activator *MYB33* were reduced. The effects observed as a result of miR159 overexpression could be an effect of decreased levels of *LEAFY*, indirectly caused by reduced accumulation of the miR159 target, *MYB33* (Achard *et al*., 2004).

1.9. GAMYB transcription factors in Arabidopsis

In Arabidopsis, the R2R3 MYB transcription factors comprise a super gene family with 125 members that are characterized by the presence of two MYB repeats. MYB transcriptions factors take part in many diverse functions in Arabidopsis. For example, they are involved in leaf morphogenesis, plant responses to environmental signals, and in the regulation of the phenylpropanoid metabolism (for a review, see Stracke *et al*., 2001). Further classification of MYBs into subfamilies was achieved by analysis of conserved domains apart from the MYB domain, resulting in the definition of functional groups. One of them is composed of seven proteins that share similarity to *Hordeum vulgare* (barley) GAMYB (Stracke *et al*., 2001). Barley *GAMYB* encodes a transcriptional activator that binds specifically to a GA-response element in the α-amylase promoter (Gubler *et al*., 1995).

Among seven Arabidopsis *GAMYB* genes, only *MYB33*, *MYB65* and *MYB101*, were experimentally verified as being able to bind and activate the transcription of GA-response element present in the α-amylase promoter from barley (Blazquez and Weigel, 2000). In Arabidopsis, the function of GAMYB is more related to signal transduction of the plant hormone gibberellin with respect to flowering control through LFY, a potent inducer of flowering in Arabidopsis. The *LFY* gene is activated by application of gibberellin (Blazquez *et al*., 1997; Blazquez *et al*., 1998). The activation probably occurs via gibberellin activation of *GAMYB* genes, which in turn act as a transcriptional activators of LFY, whose promoter contains a

GA-response element. MYB33 can bind to this GA-response element (Blazquez and Weigel, 2000).

1.10.miR161

miR161 is produced by a single miRNA gene characterized only in Arabidopsis, and its targets encode members of the pentatricopeptide repeat (PPR) protein family (Rhoades *et al*., 2002). An interesting observation was made by Allen *et al*. (2004), when they noticed high sequence similarity of pre-miR161 to its targets, and a possible explanation of the evolutionary origin of *MIR161* was proposed. In the proposed model, *MIR161* originated after recent inverted duplication events associated with active expansion of target gene family (Allen *et al*., 2004).

miR161 is differentially expressed in Arabidopsis tissues. Northern blots detected a higher accumulation of miR161 in seedlings, a moderate accumulation in stem, and flowers. In leaves and siliques, the lowest miR161 accumulation was detected (Reinhart *et al*., 2002). According to Rajagopalan *et al*. (2006), miR161 is one of the most highly expressed miRNA gene.

1.11. Aims of the present study

The present work aims to study different aspects of miRNAs and their targets in *Arabidopsis thaliana*. One of the major goals was to predict novel miRNA targets employing a software tool called RNAhybrid and based on assumptions derived from validated miRNA targets, and to experimentally validate selected miRNA target candidates.

The second main objective was to study two genes that were validated as miR159 targets in this work, *MYB101* and *MRG1*, using promoter-GUS lines, T-DNA lines and overexpressor lines in order to understand to which extend miR159 regulates the expression of these two targets based on an analysis of the effects caused by disrupting miR159 regulation on these genes.

Finally, the last objective was to investigate the expression of specific miRNA genes by characterizing their spatial and temporal expression pattern using promoter-GUS lines of *MIR159A*, *MIR159B* and *MIR161.* In addition, regulatory regions within the promoter of *MIR159A* and *MIR161* should be identified.

2. Material and Methods

2.1. Material

2.1.1. Plant Material

Arabidopsis thaliana ecotype Col-0 was used as wild-type in all experiments and transformations in this work. T-DNA lines were ordered from The European Arabidopsis Stock Centre (NASC) (http://arabidopsis.info/). Two T-DNA lines were purchased from Salk T-DNA population (Alonso *et al*., 2003) and one was from the Syngenta Arabidopsis Insertion Library (Sessions *et al*., 2002).

2.1.2. Bacterial Strains

For general cloning techniques, *Escherichia coli* strains XL1Blue (Stratagene) and TOP10 (Invitrogen) were used. Transformation of *E. coli* was done according to Sambrook and Russel (2001) . A special strain, K12 ER2925 (New England Biolabs), was used for plasmid DNA extraction when constructs were employed for promoter analysis in At7 protoplasts. K12 ER2925 has a deficiency in the methylation of adenine and cytosine DNA residues DNA by methyltransferases,

For stable transformation of Arabidopsis, *Agrobacterium tumefaciens* strains GV3101 pMP90, with rifampicin and gentamicin resistance, and GV3101 pMP90RK with rifampicin, gentamicin and kanamycin resistance (Koncz and Schell, 1986) were used.

2.1.3. Vectors

Different vectors were used according to specific purpose. For cloning cDNAs in translational fusion with the Green Fluorescent Protein (GFP), the pMAV5-‘3GFP vector (Thomas Merkle, unpublished) was used. This vector contains a multiple cloning site flanked by the Cauliflower Mosaic Virus 35S promoter and the GFP gene. The latter is followed by nopaline syntase terminator (nosT). A great advantage of this vector is that the cassette containing the *35Spro:GFP:nosT* is situated between HindIII and EcoRI restriction sites, and it can be easily sub-cloned into pGPTV-BAR (Becker *et al*., 1992) or into another vector, provided that

the insert does not have any HindIII and EcoRI restriction sites. The binary vector pGPTV-BAR was used for stable transformation into Arabidopsis. This vector confers kanamycin resistance to *E.coli* and *A. tumefaciens*. The T-DNA portion of pGPTV possesses the BAR gene that confers BASTA resistance to the plant.

The vectors pANGUS (Jakoby and Weisshaar, unpublished) and pTB10 (Sprenger-Haussels and Weisshaar, 2000) were used for promoter analysis. The first is a binary vector with an ampicilin resistance gene for selection in bacteria and kanamycin resistance gene for selection in planta. The multiple cloning site is just upstream to the *BETA-GLUCORONIDASE* (*uidA*) gene. Transcriptional fusions were created with promoters of interest and uidA for analysis of promoter activity in planta. The second vector was used for analysis of serial deletions on miRNA promoters, employing the AT7 protoplast system. In this vector, the cloning strategy is essentially the same as in pANGUS. However, pBT10 is not a binary vector, and it contains the ampicilin resistance gene for selection in bacteria.

When it was necessary to clone DNA fragments amplified by Polymerase Chain Reaction (PCR), the TOPO-TA cloning kit (Invitrogen) was employed. This kit contains the vector pCR2.1, which allows direct cloning of PCR fragments amplified by Taq DNA polymerase.

2.1.4. Chemicals and Enzymes

The enzymes used in this study were purchased form New England Biolabs, Roche Diagnostics, Ambiom, Invitrogen and Fermentas. Chemicals were obtained from Roth, Merck, Sigma, Difco, Duchefa, Molecular Research Center and Bio-Rad, and were of analytical grade. Radioactively labeled ^{32}P was obtained from Hartmann Analytic GMBH (Braunschweig, Germany).

2.1.5. Oligonucleotides

DNA oligonucleotides were purchased from Invitrogen, Metabion (Martinsried, Germany) and Operon (Cologne, Germany). RNA oligonucleotides and adaptors were purchased from Invitrogen. A list with the oligonucleotides used in this work is presented in the Appendix I.

2.1.6. cDNA library

All cDNAs cloned in this work were amplified via PCR from the MatchMaker Arabidopsis cDNA library (Clontech) prepared from whole plant with inflorescence from ecotype Col-0.

2.1.7. Medium for bacteria culture

Luria-Bertani (LB)-Medium

10 g/L Bacto-Tryptone
5 g/L Bacto-Yest Extract
5 g/L NaCl
deionized water up to 1 liter

YEP-Medium (for Agrobacteria)

10 g/L Bacto-Tryptone
10 g/L Bacto Yest Extract
5 g/L NaCl
deionized water up to 1 liter

LB-plates: LB medium with 1.6% of Bacto Agar
YEP-plates: YEP medium with 1.6% of Bacto Agar

For selective medium, appropriated antibiotics were added to the medium after autoclavation in the following concentration:

Ampicillin	100 µg/ml
Carbenicillin	100 µg/ml
Kanamycin	50 µg/ml
Gentamicin	40 µg/ml
Rifampicin	25 µg/ml

For blue/white selection of TOP10 colonies transformed with the pCR2.1 vector, 32 µl of X-GAL (50 µg/ml) were spread over LB-plates.

2.1.8. MS plates

MS plates contained 0.5x Murashige Skoog medium (Sigma), 0.5x vitamins (Sigma) and 0.8% agar. When necessary, kanamycin was added in the same concentration as mentioned above.

2.1.9. Bioinformatic Softwares and Databases

- Bioedit Sequence Alignment Editor version 4.8.10
- Clone Manager 6 version 6.0
- CLUSTAL W Multiple Sequence Alignment Program version 1.83 (Feb 2003)

- EMBOSS package
- RNAfold, Vienna RNA Package
- T-DNA Primer Design tool (http://signal.salk.edu/tdnaprimers.2.html)
- T-DNAexpress, T-DNA insertion lines database . (http://signal.salk.edu/cgi-bin/tdnaexpress)
- miRBASE, miRNA sequence database (http://microrna.sanger.ac.uk/)
- Arabidopsis thaliana massive parallel signature sequencing and 454 reads database (http://mpss.udel.edu/at/)
- The Arabidopsis Information Resource (TAIR) (http://www.arabidopsis.org/)
- Arabidopsis Small RNA Project database (http://asrp.cgrb.oregonstate.edu/db/)
- The European Arabidopsis Stock Centre (NASC) (http://arabidopsis.info/)
- AtGenexpress (http://jsp.weigelworld.org/expviz/expviz.jsp)
- RNAhybrid (http://bibiserv.techfak.uni-bielefeld.de/rnahybrid/)
- Genevestigator (https://www.genevestigator.ethz.ch/at/)

2.2. Predictions of novel miRNA target genes

For predictions of miRNA targets, the program RNAhybrid (Rehmsmeier *et al*., 2004) was employed. The dataset of candidate targets of Arabidopsis corresponds to the dataset TAIR6_cds_20060907 that include all coding sequences (CDS) from Arabidopsis according to the annotation release TAIR 6.0. In this dataset only sequences from the start-codon to the stop-codon are included. Thus, this dataset does not include intron sequence or untranslated regios (UTRs). Searching for miRNA targets included also 3'UTR and 5'UTR regions. Therefore, two additional datasets were used: TAIR6_3_UTR_20060907 and TAIR6_5_UTR_20060907, that correspond to processed 3' UTR or 5'UTR sequences from all Arabidopsis genes, with full-length cDNAs or EST sequence matches. All datasets were downloaded from ftp://ftp.arabidopsis.org/Sequences/blast_datasets.

The miRNA dataset was downloaded from miRBASE. The version used was miRBASE Release 9.0 (http://microrna.sanger.ac.uk/). This release contains 131

Arabidopsis thaliana miRNA genes. The mature sequence of all miRNA genes were used in this work.

RNAhybrid is a software that performs in silico hybridization between a miRNA and a possible target RNA in a way that optimizes the free energy of the hybridization. In the search for miRNA targets, four basic assumptions were made. First, concerning the hybridization pattern between the miRNA and the miRNA binding site, the duplex of the miRNA and the miRNA binding site must have perfect base pairing from nucleotide 8 to 12 (counting from the 5´end of the miRNA). This pattern will be referred to as “seed”. Second, internal loops (mismatch between nucleotides in different strands) were allowed only with a maximum of two nucleotides in each strand. Third, bulges with no more than one nucleotide were permitted (Figure 6). Lastly, an additional filter was used to increase the specificity of the prediction. It consists of eliminating candidates with the calculated MFE between putative target and miRNA smaller that 70% of the MFE calculated for a hybrid between the same miRNA and its perfect counter-part (Schwab *et al*., 2005; Schwab *et al*., 2006), following DNA-DNA base pairing.

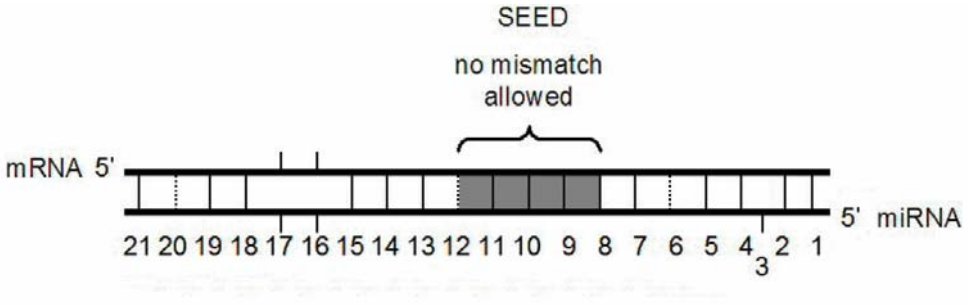

Figure 6. Diagrammatic representation of a miRNA:target hybrid according to the assumptions used in this work.
Proposed model for miRNA binding sites in plants based on the assumptions proposed in this work. Bulges containing only one nucleotide are permitted (3rd nucleotide). Mismatch loops are permitted with no more than two nucleotides (as in the 16th and 17th nucleotide). No mismatch in the presumptive cleavage site is allowed (between the 10th and 11th nucleotide), as well as in the surrounding nucleotides (gray background). G:U base pairings (6th, 12th and 20th nucleotides) are not considered as mismatch.

In this work, the percentage of MFE of a perfect match was used as a cutoff. It was defined after the analysis of the signal-to-noise ratio of the prediction. To estimate the ratio of false positive in this prediction, for each miRNA, 10 randomized sequences were created. Random sequences have the same di-

nucleotide frequency of the authentic miRNAs. Then, the RNAhybrid was used to search for miRNA targets with all random sequences with the same dataset and the four assumptions described above. The set of authentic miRNA used in this analysis contain one member of each miRNA family. The numbers of miRNA targets were counted upon six MFE cutoffs: 70, 72, 75, 77, 80 and 85%. To calculate the signal-to-noise ratio, averages of the number of targets per miRNA (combining data from all miRNAs) were calculated for both authentic miRNA dataset and random miRNA set. The false positive ratio was calculated by dividing the number of miRNA targets per miRNA of the authentic dataset by the number of miRNA targets per miRNA of the random dataset. The sensitivity of this prediction was estimated by the percentage of experimentally validated miRNA targets found among predicted targets in each of MFE percentage cutoff.

2.3. Plant growth

2.3.1. Plants grown in soil

Seeds of Arabidopsis, ecotype Columbia-0, were grown in soil. Seeds were maintained at 4 °C for 3 days to synchronize germination and then transferred to a phytochamber or greenhouse operating at 22 °C under either short-day (8 h light and 16 h darkness) or long-day (14 h light and 10 h darkness) photoperiod conditions.

2.3.2. Plants grown on MS medium plates

Seeds of Arabidopsis were sterilized by rinsing them in a 70% (v/v) ethanol 0.05% (v/v) Triton X-100 for 2 minutes followed by a rinse in 100% ethanol for 5 minutes. Before plating, seeds were washed 5 times with autoclaved water. MS plates with seeds were maintained at 4 °C for 3 days in the dark to synchronize germination. After this incubation, they were transferred to a growth chamber operating at 22 °C in short or long day cycles (2.3).

2.4. DNA Methods

Plasmid DNA isolations were purified with the JETSTAR Plasmid Purification Kit (Genomed, Bad Oeynhausen) following the instructions of the manufacturers.

PCR fragment purification was done with GFX PCR DNA and Gel Band Purification Kit (GE Biosciences) according to the manual's instructions. DNA sequences were determined by the Sequence Core Facility at the Chair of Genome Research, Bielefeld University on the Applied Biosystems Abi Prism 3100 and 3730 sequencers using the BigDye-terminator v3.1 chemistry. Routine techniques, such as DNA agarose gel, DNA precipitation, DNA ligation, DNA cleavage with restriction endonucleases and DNA concentration measurement were done according to Sambrook and Russel, (2001).

2.4.1. Isolation of Genomic DNA

Genomic DNA was isolated according to Edwards (1991). A piece of rosette leaves, about 2 mm^2, harvested from 2 to 4-weeks old Arabidopsis plants, was transferred to a 1.5ml micro centrifuge tube containing 200 µl of DNA extraction buffer. The plant sample was disrupted using a Qiagen TissueLyser. Debris was removed by centrifugation at 16000g for 8 minutes. About 150 µl of the supernatant was transferred to a new 1.5 ml micro centrifuge tube containing one volume of isopropanol. The tubes were inverted several times and incubated at room temperature for 20 minutes. The pellet was collected by centrifugation at 16000g for 5 minutes. The supernatant was discarded and the DNA was washed with 70% ethanol. The DNA pellet was air dried for 20 minutes and dissolved in 100 µl of TE buffer. This DNA was used as a template for PCR with the aim of genotyping transgenic lines.

DNA extraction buffer	TE buffer
200 mM Tris/HCl pH 7,5	10 mM Tris-Cl pH 7.5
250 mM NaCl	1 mM EDTA
25 mM EDTA	
0,5 % SDS	

2.4.2. Polymerase Chain Reaction

Polymerase Chain Reaction (PCR) was employed to amplify DNA fragments for cloning, for genotyping of transgenic Arabidopsis plants, and for screening of transformed bacterial colonies, as well as performing site-directed mutagenic by overlap extension and 5' rapid amplification of cDNA ends (5'RACE) used in microRNA target validation (Sambrook and Russel, 2001). General cycling

conditions were: 94°C to 98°C for 2 minutes, 30 cycles of 94°C for 30 seconds, 55°C to 65°C for 30 seconds and 72°C (1kb/minute), and a final extension step of 72°C for 1 minute. In this section, three protocols employed for PCR are described and another PCR-protocol variant is described in 2.5.5.2.

2.4.2.1. PCR: fragment subject to cloning

When a fragment was going to be cloned, a proof reading DNA polymerase was used. A normal reaction of 50μl contained 1X enzyme buffer, 0.2mM of each dNTP, 10 pmol of forward primer, 10 pmol of reverse primer, 1 unit of DNA polymerase, DNA template (1 μg of Matchmaker cDNA library) and water. The enzymes used were PWO DNA polymerase (Roche) and Phusion High-Fidelity DNA polymerase (Finnzymes, Finland).

2.4.2.2. Colony PCR

Colony PCR was applied whenever it was necessary to screen bacterial colonies for the presence of a desired insert. Colony PCR was done with a gene specific primer and a vector specific primer. A typical 25 μl reaction consisted of 1X Taq DNA polymerase buffer, 0.2mM of each dNTP, 10 pmol of forward primer, 10 pmol of reverse primer, 0.25 μl of Taq DNA polymerase and water. The PCR mix was distributed into reaction tubes but no template DNA was added. Instead a sterilized toothpick was used to touch a bacterial colony on a plate and then the colony was mixed with the PCR mix in each tube. Cycling conditions were almost the same the general cycling conditions, the only change was in the first step, that ws established as 95°C for 5 minutes.

2.4.2.3. Overlapping PCR

To obtain miRNA binding site mutants of MYB101 and MRG1, a PCR-based site directed mutagenesis was used (Figure 7). In the first step, two separate PCRs were performed for each mutant with primers that overlap at the position (s) of the desired mutations. One pair of primers was used to amplify the DNA that contains the mutation site together with its upstream sequence. The second pair of primers was used in a separate PCR to amplify the DNA that contains the mutation site together with its downstream sequence. A third PCR was performed using the

amplicons from the previous reactions as template and a pair of primers to amplify the whole cDNA. For both genes, cDNAs previously cloned into the pMAV5-3´GFP vector were used as template.

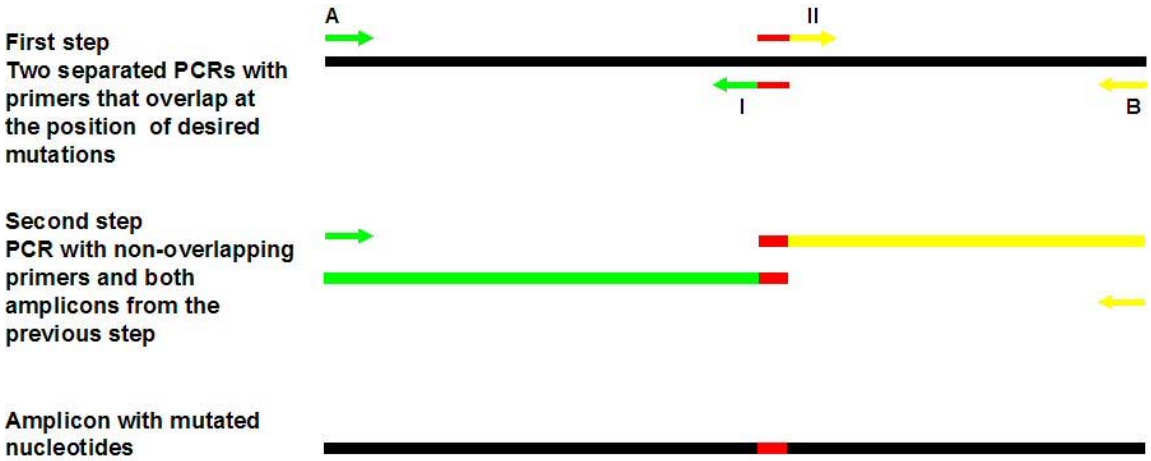

Figure 7. Site-directed mutagenesis via overlapping PCR
Primers I to II were used to introduce point mutations at miRNA binding site region (red). Primers A and B were based on template sequence. Recovery of functional mutated amplicon was achieved by combining PCR products A-I and II-B in a single reaction with primers A and B.

2.4.2.4. Hot Stat PCR: for genotyping

In order to achieve the best results when genotyping T-DNA or transgenic lines, two parameters were changed in the basic PCR setup. ExTaq DNA polymerase (Takara, Japan) and Hot Start PCR were employed. The first reaction mix was set up in a 20 μl reaction consisting of: 1X ExTaq Buffer, 0.2mM of each dNTP, 10 pmol of forward primer, 10 pmol of reverse primer, water and 1 μl of template DNA. Tubes were placed in the thermocycler and the program was initiated. At the end of the initial denaturating step, the reaction was paused and 10 μl of the hot start mix was added (0.25 units of ExTaq DNA polymerase, 1x ExTaq buffer, water), then the cycling conditions continuined without further changes.

2.5. RNA Methods

2.5.1. RNA Isolation for northern blot and RT-PCR

Total RNA was extracted from Arabidopsis AT7 and tobacco BY-2 protoplasts, as well as from different tissues of Arabidopsis transgenic and wild-type plants using TriReagent (Molecular Research Center) according to the protocol suggested by the manufacturer. For 100 mg of plant tissue, 1 ml of Tri Reagent was added into a 2.0 ml screw-cap micro centrifuge tube. The sample was disrupted using a Tissue Lyser (Qiagen). The homogenized sample was incubated for 10 minutes at room temperature and then, 200 µl of chloroform were added followed 30 seconds of homogenization. After 10 minutes of incubation at room temperature, the sample was centrifuged at 12000g at 4°C for 10 minutes. The clear upper phase containing total RNA was collected to a new micro centrifuge tube containing 600 µl of isopropanol. The sample was incubated at room temperature for 5 minutes and centrifuged at 12000g at 4^{o}C for 10 minutes. The supernatant was discarded and the pellet was washed with 70% ethanol. The RNA pellet was air dried for 10 minutes at room temperature and dissolved in DEPC-treated water. The total RNA was treated with DNase I according to the manufacturer's protocol (Ambion), before any reverse transcription and northern blot experiments were performed. The RNA quality was analyzed by gel electrophoresis.

2.5.2. Formamide Gel

RNA samples (5µg of total RNA per lane) were mixed with 1 volume of sample buffer, which was previously denatured for 5 minutes at 65°C. Prior to loading the gel, 1/6 volume of loading buffer was added to each sample. RNA was separated on 1% agarose gel in MOPS-buffer with 2.2 M formaldehyde.

Sample buffer	MOPS buffer	Loading buffer
66% formamide	0.2M MOPS (pH 7.0)	50% Glycerol
8.6% formaldehyde	0.05M sodium acetate	1mM EDTA
1X MOPS buffer	0.005M EDTA (pH 8.0)	0.4 g bromophenol blue

2.5.3. cDNA synthesis

For reverse transcriptase reactions, Superscript reverse transcriptase II (Invitrogen) was used according to the manufacturer's protocol. Reactions were done in 20 µl final volume with 2µg of RNA, 1mM oligo dT (dN-18T), 500µM of each dNTP, 1x First Strand Buffer (Invitrogen), 10µM of dithiothreitol and 20 units of reverse transcriptase II. For 5'RACE libraries (2.5.5), 10µg of adaptor ligated RNA (2.5.5.1) were used.

2.5.4. Small RNA northern blot

Northern blots to detect miRNAs were prepared from RNA samples of protoplasts transfected with a construct containing the precursor miRNA. The protocol for RNA polyacrylamide gel electrophoresis, transfer, probe labeling with radiochemical and hybridization were done following Llave *et al*., (2002).

2.5.4.1. RNA electrophoresis- polyacrilymide gel

RNA samples (20 µg of total RNA per lane) were mixed with one volume of urea loading buffer denatured for 4 minutes at 95°C and cooled down on ice for 5 minutes. The RNA was separated on 17% denaturating polyacrylamide gels in TBE buffer. Before loading the samples, a pre-run was done at 150 volts for 1 hour. After loading, the run was performed at 350 volts for 5 hours. An RNA oligonucleotide of 21 nt was used as a size marker. RNA was transferred to a nylon membrane (Hybond-N+, GE Biosciences) with Trans-blot SD Semi-dry Transfer Cell (Bio-Rad), at 400 mA, for one hour. The RNA was fixed in the membrane by UV crosslinking, with 1200µJ, followed by baking the membrane at 80^{o}C for 30 minutes.

Polyacrylamide gel (DEPC water)

7 M Urea
0.5X TBE buffer
0.5 mM TEMED
2 mM Ammonium Persulfate
17% (v/v) Rotiphorese® Gel 30 (Roth)

Urea loading buffer (DEPC water)

8 M Urea
0.05 % (w/v) Bromophenol blue
0.05 % (w/v) Xylencyanol
0.5 mM EDTA

10x TBE buffer (DEPC water)

0.9 M Tris
0.9 M Boric Acid
0.02 M EDTA

2.5.4.2. Preparation of Radiolabelled DNA probe

Hybridization probes were prepared with 20 μM oligonuclotides, whose sequences were complementary to investigated miRNAs. Probes were labeled with [^{32}P] γ-ATP (5000ci/mmol; 10 mCi/ml, from Hartmann Analytic GmBH, Germany) using polynucleotide kinase (New England Biolabs). The labeled probes were purified with Sephadex G25 spin columns (GE Biosciences).

2.5.4.3. Hybridization

RNA blots were pre-hybridized for 30 minutes at 42°C in PerfectHyb™Plus (Sigma) hybridization buffer. After adding the probe, hybridization was carried out overnight at 42°C. After hybridization, membranes were washed with decreasing concentrations of SSC solution containing SDS (2X SSC, 0.2% SDS; 1X SSC, 0.2% SDS; 1X SSC, 0.1% SDS for 20 minutes each wash with rotation at 50°C). Dried membranes were exposed to Phosphoimaging plates (Kodak), which were read out in a Typhoon scanner (Amersham- GE Biosciences).

2.5.5. 5'RACE

2.5.5.1. RNA adaptor ligation

The validation of miRNA targets takes advantage of a modified RNA ligase-mediated Rapid Amplification of cDNAs Ends (5´RACE) approach, which can be used to precisely map the position of the cleavage induced by the RISC complex (Llave *et al*., 2002a). To construct a 5´RACE library for every target, total RNA was isolated from AT7 protoplasts co-transfected with plasmids that enables the protoplasts to express both the miRNA precursor and the target cDNA in translational fusion with GFP. An RNA adaptor (300ng) was ligated to 10 μg of total RNA using T4 RNA ligase (New England Biolabs) in 1x ligation buffer at 37^{o}C for 1 hour. The synthesis of cDNA was described in 2.5.3.

2.5.5.2. Nested PCR

The RNA adaptor provides an anchoring sequence for PCR primers. A nested PCR with the outer 5RACE primer and a gene specific primer 1 (GSP1) was performed. The nesting reaction was performed with the Inner 5RACE primer and a GSP2 primer. PCR products were gel analyzed and cloned with TOPO-TA cloning kit (Invitrogen). Alternatively, PCR fragments were gel purified with Qiaquick Gel Purification Kit (Qiagen) and then cloned with TOPO-TA cloning kit (Invitrogen). Positive clones were screened using colony PCR (2.4.2.2). In this case another gene specific primer (GSP3) was used with the Inner 5RACE primer. Between 5 and 10 were sequenced clones for each target. Cycling conditions for nested and nesting PCR were done in such a way to optimize the yield and specificity. Therefore, for these reactions, the Hot Start PCR approach was applied. In addition, the touchdown PCR (TD-PCR) approach was also implemented in these reactions. In TD-PCR, the annealing temperature is set 10 degrees higher than in normal PCR and, after each cycle (denaturation, annealing and extension), the annealing temperature decreases by one degree per cycle (ten cycles). Then, the annealing temperature of the tenth cycle is maintained through the rest of 25 cycles. The set up of these PCRs is the same as presented for the Hot Start PCR (2.4.2.4). However, for the nested reaction, 1μl of cDNA was added and in the nesting reactions, between 0.5 to 5μl of nested PCR was added.

2.6. Cloning putative miRNA targets and miRNA precursor sequences

Sequences of nine putative miRNA targets were cloned for the experimental validation of predicted miRNA binding sites. Precursor sequences of four miRNAs were also cloned for the same purpose. Putative miRNA targets were amplified from the Matchmaker cDNA library and cloned into pMAV5-3'GFP in translational fusion with GFP. PCRs were performed with a high fidelity DNA polymerase and the sequence of each clone was confirmed by sequencing. The primers used, as well as their cleavage sites appended to it, are listed in 0. The inserts were cloned in the vector pMAV5-3'GFP, which was cleaved with the same enzymes as the

insert. Positive clones were identified by colony PCR (2.4.2.2) and the sequence of the insert was confirmed by sequencing.

Table 2. Putative miRNA targets cloned in this work.
All miRNA putative targets were cloned into pMAV5-3'GFP in translational fusion with GFP.

Target	*AGI number*	*Primers*	*Clone designation*
MYB94	At3g47600	L081 (XbaI) - L092 (XmaI)	MYB94-GFP
MRG1	At2g34010	At2g34010-51 (BamHI) - At2g34010-32 (SmaI)	MRG1-GFP
ACS8	At4g37770	L126 (BamHI) - L127 (XmaI)	ACS8-GFP
MYB101	At2g32460	MYB101-056 (BamHI) – MYB101-39 (SmaI)	MYB101-GFP
MYB125	At3g60460	L077 (XbaI) - L078 (XmaI)	MYB125-GFP
CKL6	At4g28540	L128 (BamHI) - L129 (XmaI)	CKL6-GFP
GAE1	At4g30440	L143 (BamHI) - L144 (XmaI)	GAE1-GFP
Profilin2	At4g29350	PFL-51 (BamHI) - PFL-31 (XmaI)	Profilin2-GFP
MYB58	At1g16490	L079 (XbaI) - L080 (XmaI)	MYB58-GFP

Precursor sequences of miR156h, miR159a, miR161, miR172, miR395b and miR414 were cloned into pMAV5-3'GFP replacing the GFP gene. Primers were designed to amplify a fragment that surrounds the miRNA precursor sequence. Precursor sequences were amplified from genomic DNA of Arabidopsis Col-0 ecotype. The primers used, as well as theirs cleavage sites, are listed in the Appencix I. In all cases, the cloning sites were XbaI and SacI, but for miR159a, in which the reverse primer has no appended restriction sites, so the SacI site in the vector was filled in with the Klenow fragment of DNA polymerase.

Table 3. Precursor sequences of miRNAs cloned in this work

miRNA	*Primers*	*Clone designation*
miR156h	L073 (XbaI) - L074 (SacI)	$35S_{pro}$:miR156h
miR159a	159a-01-F (XbaI) - 159a-02-R	$35S_{pro}$:miR159a
miR161	mir161-51 (XbaI) - mir161-31 (SacI)	$35S_{pro}$:miR161
miR172a	miR172-51 (XbaI) - miR172-31 (SacI)	$35S_{pro}$:miR172
miR395b	L075 (XbaI) - L076 (SacI)	$35S_{pro}$:miR395b
miR414	L051 (XbaI) - L032 (SacI)	$35S_{pro}$:miR414

2.7. T-DNA insertion lines

The Arabidopsis knockout mutant database, T-DNAexpress (http://signal.salk.edu/cgi-bin/tdnaexpress) was searched for lines containing a T-DNA insertion in the genes of interest. Seeds of the chosen lines were ordered and plants were grown, followed by DNA analysis for the determining the presence of the T-DNA in the gene of interest. Two T-DNA lines were found for the *MYB101* locus. Both were generated by transformation of Arabidopsis plants with the binary T-DNA vector pROK2, harboring kanamycin resistance to allow the selection of mutants in Col-8 background (Alonso *et al*., 2003). One *MRG1* T-DNA line was also found in the Syngenta T-DNA population, which was created by Arabidopsis transformation with the pCSA110 vector (basta resistance) in Col-3 background (McElver *et al*., 2001; Sessions *et al*., 2002). Information about the lines used in this work is summarized inTable 4.

Table 4. Arabidopsis knockout mutants.
Gene name, mutant name, original designation and plasmid used for TDNA mutant generation, are given.

Gene	Mutant name	Line name	Plasmid
MYB101	*myb101-1*	SALK_061355	pROK2
MYB101	*myb101-2*	SALK_149918	pROK2
MRG1	*mrg1-1*	SAIL_299_A02	pCSA110

2.8. Overexpression lines

Target validation with 5´RACE is a fast method to confirm a miRNA target. However, this method shows only the cleavage product caused by the RISC complex guided by a certain miRNA, but it lacks information about the real functionality of this post-transcriptional regulation. One way to study the functionality of a miRNA regulation is to analyze, in planta, the effect of the disruption of the miRNA binding site in a target mRNA sequence.

MYB101 was amplified from the clone MYB1010-GFP (2.6) using primers MYB101-056 and T004 (with SacI site). This PCR product was cleaved with BamHI and SacI and cloned into the pMAV5-3'GFP vector, cleaved with the same

enzymes. The clone was sequenced and the integrity of *MYB101* confirmed. This clone was named *35S$_{pro}$:MYB101*. To obtain miRNA binding site mutant of *MYB101*, a PCR-based approach was used: overlap PCR (2.4.2.3). The first primer pair was MYB101-056 and MYB101-310 that amplified a fragment from the start codon of *MYB101* to the miR159 binding site. The second amplicon was amplified with primers MYB101-57 and T004, which were used to amplify a fragment from the miR159 binding site to the stop codon of *MYB101*. The third PCR was done with MYB101-056 and T004 using both previous amplicons as template, resulting in the amplification of a full length *MYB101* cDNA with eight mutations in the miR159 binding site that do not change the protein sequence. This fragment was cloned in the same way as described above and the clone was sequenced to confirm the introduction of only the eight desired mutations. This clone was named *35S$_{pro}$:MYB101mutBS*.

MRG1 was amplified from the clone MRG1-GFP (2.6) using primers At2g34010-51 and At2g34010-31 (with SacI site). The amplicon was digested with BamHI and SacI and cloned in the pMAV5-3'GFP vector cleaved with the same enzymes. The clone was sequenced and the integrity of *MRG1* was confirmed. This clone was named *35S$_{pro}$:MRG1*. Overlapping PCR was also used for introduce point mutations in the miR159 binding site of *MRG1*. The first primer pair was At2g34010-51 and At2g34010-33, which amplified a fragment from the start codon of *MRG1* to the miR159 binding site. The second amplicon was amplified with At2g34010-53 and At2g34010-31, which was used to amplify a fragment from the miR159 binding site to the stop codon of *MRG1*. The third PCR was done with At2g34010-51 and At2g34010-31, using both previous obtained amplicons as template, resulting in the amplification of a full length *MRG1* cDNA with seven point mutations in the miR159 binding site that do not change the protein sequence. This fragment was cloned in the same way as above and, the clone was sequenced to confirm the introduction of only the seven desired mutations. This clone was named *35S$_{pro}$:MRG1mutBS*.

In the pMAV5-3'GFP vector, the expression cassette composed of CaMV *35S$_p$ro:GFP:nosT* is surrounded by HindIII and EcoRI. Using this cleavage sites, the expression cassettes of *35S$_{pro}$:MYB101*, *35S$_{pro}$:MYB101mutBS*, *35S$_{pro}$:MRG1* and *35S$_{pro}$:MRG1mutBS* were subcloned tino a binary vector, pGPTV-BAR, for

transformation of Arabidopsis. Analysis of overexpression plants were done in the T2 generation.

2.9. Promoter GUS lines

Promoter GUS lines were generated to investigate the promoter activity of *MYB101*, *MRG1*, *MIR159A*, *MIR159B* and *MIR161*. All promoter sequences were cloned into the pANGUS vector in transcriptional fusion with the beta-glucoronidase gene (uidA). All promoter sequences were amplified from genomic DNA of Arabidopsis ecotype Col-0 using a proof reading DNA polymerase. Primers used for *MYB101* promoter were L011 (with EcoRI site) and L012 (with NcoI site) and for *MRG1* promoter were L013 (with EcoRI site) and L014 (with NcoI site). For the miRNA promoters the following primers were used: for the *MIR159A* promoter, L003 (with EcoRI site) and L004 (with NcoI site); for the *MIR159B* promoter, L005 (with EcoRI site) and L006 (with NcoI site); and, for the *MIR161* promoter, L009 (with EcoRI site) and L010 (with NcoI site). Amplicons were cleaved with EcoRI and NcoI and cloned into the pANGUS vector cleaved with the same enzymes. Isolated clones were sequenced and denominated as follows: $MYB101_{pro}$*:GUS*, $MRG1_{pro}$*:GUS*, $MIR159A_{pro}$*:GUS*, $MIR159B_{pro}$*:GUS* and $MIR161_{pro}$*:GUS*.

2.9.1. Promoter GUS Analysis

Analysis of promoter GUS lines were done in the T2 generation. Seedlings and different tissues of adult plants were used. Seedlings, which were either 8 or 13 days old, were grown on MS plates in long day cycles. Adult tissues, rosette leaves, cauline leaves, stem sections, flower in diverse stages, as well as siliques, were taken from plants growing in soil. Such plants were grown under, which were under short day conditions for eight weeks followed by two weeks in long day.

Plant materials were harvested and incubated in GUS fixing solution for at least 45 minutes at room temperature. Then, fixed plant samples were washed twice with NaPi buffer for 45 minutes to remove the fixing solution. X-Gluc solution was added in such amount to cover completely the sample. After vacuum infiltration, samples were incubated overnight at 37^{o}C. On the following day, X-Gluc solution was discarded and samples were washed twice with NaPi buffer for 45 minutes.

Then, samples were incubated in 100% ethanol for two to five hours, until the chlorophyll was completely removed. Meanwhile, the ethanol was changed two or three times. A final step was to remove the 100% ethanol and to add 60% ethanol. Then, samples were kept in the dark at 4°C until the microscopy analysis. About two hours prior to the analysis, samples were submerged into a 30% glycerol solution, to facilitate the slide preparations. the samples were analyzed under stereomicroscope (Carl Zeiss) and optical microscope (Leica DM5500B). Images were captured with CCD camera and DISKUS 4.50 software.

GUS fixing solution

0.3% (v/v) formaldehyde
10 mM MES-KOH pH 5.6
300 mM mannitol

NaPi buffer

50 mM Na_2HPO_4
pH 7.0 adjusted with phosphoric acid

X-Glus solution

0,5 mg/ml X-Gluc (Roth) in NaPi buffer

2.10. Generation of transgenic plants

2.10.1. Transformation of *A. tumefaciens*

Electro competent *Agrobacterium tumefaciens* cells were prepared according to Clough *et al*., (1998). Therefore, 5 ml of YEP medium supplemented with antibiotics inoculated with A. tumefaciens were grown to early saturation stage (overnight) at 28°C with shaking at 200 rpm. Then, 2 ml of the culture were transferred into 500 ml YEP medium with antibiotics and incubated overnight as above. The culture was harvested by centrifugation at 3,750g for 15 minutes at 4°C. The bacterial pellet was resuspended in 500 ml of ice-cold sterilized water. These steps were done twice and then after another harvesting by centrifugation, the bacterial pellet was resuspended in 50 ml of ice-cold 10% glycerol. After another centrifugation, the pellet was resuspended in 2 ml of ice-cold 10% glycerol. Competent *A. tumefaciens* were aliquoted (25 µl), frozen in liquid N_2 and stored at – 80°C. For transformation, 500 ng of plasmid DNA was pipette on top of

25 µl frozen competent agrobacteria and after 5 minutes incubation on ice, the cells were transferred to a 1 mm gap electroporation cuvette. The transformation was made in a BioRAD Micro Puser electroporator with the pre-programmed settings for *A. tumefaciens* (2.20 kV, one pulse). After transformation, 1 ml of YEP medium was added to the cells and they were placed on an incubator for 3-4 hours at 28°C with shaking at 200 rpm. Then, the *A. tumefaciens* was pelleted for 2 minutes at 2500g, 800 µl of medium were removed, and the pellet was resuspended in the remaining medium. Aliquots of 20 and 100 µl were plated on YEP plates with antibiotics and grown at 28°C for 3 days. To verify the presence of the binary vector, colony PCR (2.4.2.2) was used to genotype positive agrobacteria colonies. Glycerol stocks from the positive clones were prepared and used for inoculation of cultures for transformation of Arabidopsis plants.

2.10.2. Transformation of Arabidopsis

The transformed *A. tumefaciens* cells harboring the constructs of interest were grown at 28°C with 180 rpm shaking in YEP media with appropriate antibiotics. A 5 ml pre-culture was prepared by adding 50 µl of culture in glycerol stock (2.10) and was grown overnight. The main-culture was prepared by adding the whole amount of pre-culture into 500 ml of YPE media. The main-culture was incubated until an OD_{600} value of 1.2 –1.5 was reached. Then, sucrose and Silwet L-77® surfactant (GE Silicones, USA) were added to the culture to a final concentration of 5.0% and 0.05%, respectively. After Arabidopsis plants were grown for four to six weeks in short-day cycles, they were moved to long day conditions. The emerging first bolt was cut to induce the growth of secondary bolts. One week after the clipping, the plants possessing numerous unopened floral buds were submerged into inoculation medium of *A. tumefaciens*, containing a vector with a construct of interest. The plants were then placed on their side and kept at high humidity under plastic wrap for two days then, they were uncovered and set upright. Selections of harvested seeds were done according to the resistant marker of the construct. For plants transformed with pGPTV-BAR, the selection of transformants was done in plants growing in soil. Plants with four to six leaves were sprayed with BASTA solution and seeds of resistant plants were collected. For plants transformed with pANGUS construct, seeds were grown on kanamycin (50 µg/ml) containing MS

plates to select transformants. The presence of the desired construct in selected transgenic plants was confirmed by PCR.

BASTA solution:

240 µg/ml BASTA (Hoechst Schering AgrEvo, Düsseldorf)
0,005% Silwet L-77® surfactant (GE Silicones, USA)

2.11. Serial deletions on miRNA promoters

Deletions in the promoter sequence of two miRNAs were prepared to investigate portions of promoters that render change in activity, measured through a GUS enzymatic assay. Deletion constructs were derived from the full-length promoter construct of *MIR159A* and *MIR161*, described in the section 2.9, via PCR-derived fragments. Reverse primers were the same as ones used to clone the whole promoter. Forward primers were positioned in order to amplify portions from the whole promoter with deletions in the 5' end. All constructs were cloned into the pBT10 vector using EcoRI and NcoI sites. Promoter deletions in the MIR159A promoter were done with primers L094 to L100, and, for deletions in the MIR161 promoter, primers L065 to L071 were used.

Protoplast isolation, transfection and GUS enzymatic assays were performed as described by Hartmann *et al*. (1998). The effects of deletions were analyzed by co-transfecting AT7 protoplasts with 10 µg of a promoter construct and with 5µg of a standardization construct pBT10-UBI_{pro}:LUC that expresses luciferase gene under the control of the ubiquitin promoter, as well as, 10 µg of a promoterless luciferase construct pBT10-LUC. Two constructs were used as controls: pBT10-$35S_{pro}$:GUS and promoterless pBT10 (Sprenger-Haussels and Weisshaar, 2000).

2.12. AT7 protoplast system

2.12.1. Protoplasts preparations from AT7 cells

Arabidopsis 5 days-old AT7 cells were harvested by centrifugation at 800g for 5 minutes at room temperature. Cells were washed with 40 ml of 240 mM $CaCl_2$

solution and centrifuged as described above. The supernatant was discarded and cells were resuspended in 60 ml cellulase solution. The cell suspension was divided into two Petri's dishes and incubated for 20 hours at 26°C in the dark shaking at20 rpm. Before harvesting, the protoplasts were shaking 40 rpm for 20 minutes. They were transferred to a 50ml tube and centrifuged at 800g for 6 minutes at room temperature. The supernatant was discarded and protoplasts were resuspended in 25 ml of 240 mM $CaCl_2$ solution and centrifuged at 800g for 6 minutes at room temperature. The protoplast pellet was resuspended with B5-sucrose solution and centrifuged at 800g for 6 minutes at room temperature. After this centrifugation step, the living protoplasts were floating in the solution, whereas dead protoplasts were positioned in the bottom of the tube. Floating protoplasts, which were ready for transfection, were collected to a new tube (modified from Dangl *et al*., 1987).

B5-sucrose solution

3.2 g Gamborg's B5 medium (Sigma) for 1 liter
1 mg 2,4-Dichlorophenoxyacetic acid pH 7.50.
0.4 M Sucrose
pH 5.7 adjusted with 0.1 M KOH

Celullase solution

0.7g Cellulase (1.2 U/mg)
1625 g Mazerase (0.55 U/mg)
60 ml 240 mM $CaCl_2$
Filter sterilized

2.12.2. Transfection of AT7 protoplasts

Plasmid DNA was transfected to protoplasts mediated by polyethylene glycol (PEG). In a 10 ml centrifuge tube, 200 µl of protoplast were mixed with 25µg of plasmid DNA (10 µg of a promoter construct and 5 µg of a standardization construct pBT10-UBI_{pro}:LUC and 10µ g of a promoterless luciferase construct pBT10-LUC). To this mixture, 200 µl of PEG solution were added and incubated 15 minutes at room temperature. The incubation was stopped by adding 5 ml of 275 mM $Ca(NO_3)_2$ solution (pH 6.0) and protoplasts were centrifuged at 400g for 8 minutes at room temperature. The supernatant was discarded and protoplasts were resuspended in 7ml of B5-sucrose solution. The protoplasts were incubated at 26°C in the dark for 20 hours. For transient expression of miRNA precursors, protoplasts were transfected with 12.5 µg of a miRNA precursor construct and 12.5 µg of the pBT10 empty vector. For transient expression of miRNA precursor

and its putative target, 12.5 μg of each construct were transfected to protoplast (modified from Krens *et al*., 1982; Hain *et al*., 1985; Lipphardt *et al*., 1988).

PEG solution

25% PEG_{6000}
100mM $Ca(NO_3)_2$
450mM Manitol

2.12.3. Harvesting protoplast

On the day following the transfection, protoplasts were mixed with 20 ml of 240mM $CaCl_2$ solution and centrifuged at 400rpm for 10 minutes at 4°C. The supernatant was removed with the help of a vacuum pump until 1 ml was left. Protoplasts were resuspended and transferred to a 1.5 ml tube. After a brief centrifugation, 13000rpm for 10 seconds, the supernatant was removed and the protoplasts were frozen in liquid N_2. Protoplasts were kept at -80°C until the protein or RNA extraction.

2.12.4. Protein extraction of protoplast

Measurement of promoter activity was done at the protein level. To this aim, protein extracts were prepared from transfected protoplasts. To each tube containing protoplast pellet, 800 μl of luciferase extraction buffer were added and tubes were shaken for 30 seconds. Protoplast debris was separated by centrifugation (10minutes at 4°C at 12000g) and the supernatant was transferred to a new 1.5 ml tube. The protein extract was kept on ice until the measurement of protein concentration, luciferase activity and GUS activity.

Luciferase extraction buffer

100 mM KH_2PO_4, pH 7,5
1 mM DTT

2.12.5. Protein quantification with Bradford

Protein quantification was done by Bradford assay (Bradford, 1976). For the standard curve, freshly prepared bovine serum albumin (BSA) dilutions of 1 μg, 2 μg, 5 μg, 10 μg, 15 μg and 20 μg per μl in Luciferase extraction buffer were used. Protoplast protein extract was diluted to 1:5 in the same buffer. For measurement, 800µl of diluted protein sample was added to 200µl of Protein Assay Dye Reagent (Bio-Rad) and incubated at room temperature for 20 minutes. After incubation time, the protein concentration was measured in a Biophotometer (Eppendorf) at 595nm wavelength. Comparison to a standard curve provided a relative measurement of protein concentration.

2.12.6. Luciferase Assay

For luciferase assay (Wood, 1991), 10 μl of protein extract were transferred to a glass tube and 100 μl of luciferase solution were added. The tube was briefly mixed and the measurement was immediately performed in a luminometer (MiniLum, BioScan, Washington DC, USA). Such measurement provides the relative light units (RLU) of the sample. The RLU value of the sample refers to the luciferase activitity by protein amount (μg) by second (RLU μg^{-1} sec^{-1}).

Luciferase reaction buffer

20 mM Tricine
2.67 mM $MgSO_4$
0.1 mM EDTA
33.3 mM DTT
270 μM CoA
470 μM D-Luciferin
530 μM ATP

2.12.7. GUS activity

Beta-glucoronidase fluorimetrical assay (Jefferson *et al*., 1986) is based upon the conversion of 4-methylumbelliferyl-beta-D-glucuronide (4MUG) into the fluorescent product 4-methylumbelliferyl (4MU) by beta-glucoronidase. To measure the GUS activity in protein extracts, 100 μl of protein extract were mixed with 100 μl of GUS-

solution in a MicroWell Black™ plate. Measurement was made in a fluorimeter (Fluoristar Optima, BMG LABTECH, Offenburg, Germany). The micro plate was incubated at 37°C and fluorescence was measured with excitation at 365 nm and emmision at 460 nm at three time points: 20, 40 and 60 minutes. The fluorimeter was calibrated with freshly prepared 4MU standard at different concentrations, ranging from zero to 4000 pMol of 4MU. The difference in fluorescence between time points (60'-40 and 40'-20') was calculated (ΔE_{460}/20minutes). The protein amount in the extract was calculated as described in 2.12.5 and the obtained values were used for the calculation of specific GUS activity [E_a(GUS)] according to this formula:

$$(1) \qquad E_a(GUS) = \frac{\Delta E_{460} * 1000\mu g / mg *}{20min * \mathbf{m}/pMol * \mu g\ Protein}$$

where:

m is the slope according to 4MU standard curve

The normalization of the GUS activity was done dividing the E_a(GUS) of a given sample by the Luciferase normalization factor, which was calculated by dividing the Luciferase activity of the sample by the average of the luciferase activity of all samples. With the normalized GUS values, the average and standard deviation were calculated for each construct and controls.

2.13. BY-2 protoplast system

Tobacco BY-2 protoplasts were prepared and mainteined according to Merkle *et al*., (1996).

2.13.1. Protoplasts preparations from Tobacco BY-2 cells

Tobacco BY-2 protoplast was a second culture system utilized to evaluate the overexpression of miRNAs from introduced constructs containing a miRNA precursor. This system was also used for cellular localization of MRG1-GFP fused

proteins. For preparation of BY-2 protoplasts, 20ml of three-days old cultures were centrifuged at 400g for 5 minutes at room temperature. Cells were resuspended in wash solution and centrifuged as above. Wash solution was discarded and cells were resuspended in 13 ml of digestion solution. Cells were then transferred to a Petri dish, sealed and incubated overnight at 26^{o}C in the dark.

On the following day, protoplasts were transferred to a 50 ml tube and collected by centrifugation at 100g for five minutes at room temperature. Protoplasts were washed with 10 ml of W5 solution and centrifuged at 100g for 5 minutes at room temperature. Supernatant was discarded and protoplasts were resuspended in 10 ml of W5 solution. Then, the protoplasts were incubated for 30 minutes at 4^{o}C in dark. After incubation, W5 solution was discarded, protoplasts were washed twice with 10 ml of MMM solution and centrifuged as above. Protoplast pellet was resuspended in 4ml of MMM solution. At this step, protoplasts were ready for DNA transfection.

Wash Solution

0.5 % (w/v) BSA
0.01 % (w/v) 2-Mercaptoethanol
50 mM $CaCl_2$
10 mM Sodium Acetate
0.25 M Mannitol
Sterilized by filtration

Digestion solution

same as wash solution with
1 % (w/v) Cellulase Onuzuka RS
0.5 % (w/v) Macerozyme Onuzuka RS
0.1 % (w/v) Pectinase
Sterilized by filtration

W5 Solution

154 mM NaCl
125 mM $CaCl_2$
5 mM KCl
5 mM Glucose
pH 5.8-6.0 adjusted with KOH
Sterilized by filtration

MMM solution

0.1 % (w/v) MES-KOH pH 5.8
15 mM $MgCl_2$
0.5 mM Mannitol
Sterilized by filtration

2.13.2. Transfection of BY-2 protoplasts

Plasmids DNA were transfected to protoplasts mediated by PEG. In a 10 ml centrifuge tube, 300 μl of protoplast were mixed with 30 μg of plasmid DNA (when two constructs were co-transfected, 20 μg of each plasmid were used). To this

mixture, 300 µl of PEG solution were added and incubated for 10 minutes at room temperature. This incubation was stopped by adding 10 ml of W5 solution and protoplasts were centrifuged at 100g for five minutes at room temperature. The supernatant was discarded and protoplasts resuspended in 0.7ml of MS-sucrose solution. The protoplasts were incubated at 26°C in the dark for 20 hours. Prior to the RNA extraction, protoplasts were harvested as described in 2.12.3. For microscopy, protoplasts were gently resuspended and 20µl were transferred to a glass slide for visualization in a confocal laser-scanner microscopy DM RBE TCS4D Microscope (Leica, Bensheim).

PEG solution
25 % (w/v) PEG_{4000}
100 mM $Ca(NO_3)_2$
400 mM Mannitol
pH 8-9 adjusted with KOH
Sterilized by autoclavation

MS+Sucrose solution
0.4 M Saccharose
in MS cell culture medium (Merkle *et al*., 1996)
Sterilized by filtration

3. Results

3.1. Prediction and validation of miRNA targets

3.1.1. Prediction of novel miRNA targets

Prediction of miRNA targets is an important method to find valuable information about miRNA functions. In plants, miRNAs show nearly perfect sequence complementarity to their targets. Due to this fact, the prediction of miRNA targets in plants is easier than in animals (Jones-Rhoades *et al*., 2006). In an attempt to identify novel miRNA targets, the RNAhybrid program (Rehmsmeier *et al*., 2004) was applied to search for miRNA targets in the whole Arabidopsis transcriptome, e.g. sequences from all predicted and validated CDS, 3'UTR and 5'UTR. The program was set up in a way that considers four basic assumptions concerning the hybridization pattern between the miRNA and the respective miRNA binding site. First, counting from the 5´end of the miRNA, the duplex must show perfect base pairing from nucleotides 8 to 12, a pattern that will be referred to as "seed". Second, internal loops were allowed only with a maximum of two nucleotides in each strand. Third, bulges with no more than one nucleotide were permitted and fourth, the MFE (minimum free energy) between putative target and miRNA must be at least 75% of the MFE calculated for a hybrid between the same miRNA and its perfect counterpart (following DNA-DNA base pairing).

The percentage of the MFE of a perfect match was used as a cutoff in this prediction. It was defined after analysis of the signal-to-noise ratio. To estimate the signal-to-noise ratio in this prediction, the total number of predicted miRNA targets per miRNA for the set authentic miRNAs was divided by the number of predicted targets per miRNA for the set of random miRNAs (10 cohorts for each miRNA). The set of authentic miRNA used in this analysis contain of 55 mature miRNA sequences, that is, one member of each miRNA family. The sequence of miRNA cohorts were randomly generated maintaining the di-nucleotide frequency observed in each of the 55 authentic miRNAs.

Table 5. Analysis of false-positive ratio and sensitivity.
Ratios of false positives and sensitivity are listed for four different MFE cutoffs based on the MFE of the perfect match (see text above). The ratio of false positives was inferred by dividing the number of predicted targets per miRNA of a set of authentic miRNA by the number of miRNA per target for a set of random miRNAs (10 cohorts for each authentic miRNA). Sensitivity represents the percentage of experimentally validated miRNA targets found in the prediction.

cutoff	*signal-to-noise*	*sensitivity*
70%	1.7	100%
72%	2	95.9%
75%	2.6	93.1%
77%	3.1	82.2%
80%	5.4	72.6%
85%	14.6	61.6%

In Table 5, the result of the estimation of false positives (signal-to-noise ratio) and sensibility of this prediction is summarized. The cutoff value of 75% percent of the MFE of a perfect match was chosen due to sensitivity (93.1%) and an estimated signal-to-noise ratio of 2.6:1 (Table 5). Using this approach, the number of putative miRNA targets was increased by over 2-fold, with 281 predicted novel miRNA targets. A list including miRNA:target structures of all novel miRNA targets is presented in Appendix 2. Examples of four structures are shown in Figure 8.

Several miRNAs are involved in the regulation of plant development, signal transduction, protein degradation, response to environmental stress, pathogen invasion, and regulation of their own biogenesis. miRNAs regulate the expression of many important genes, and the majority of these genes are transcription factors (Jones-Rhoades *et al*., 2006). In order to gain more information about predicted novel miRNA targets, the annotated biological functions using gene ontology (GO) were taken into account. GO terms for 254 targets were found in the molecular function class. A comparative analysis of GO annotations from predicted novel targets and targets against GO annotations from the whole genome categorization showed that some classes are underrepresented or overrepresented in both novel predicted and previously predicted/validated group of targets. Three classes are overrepresented in previously predicted/validated targets: transferases, transcription factors and DNA/RNA binding proteins. Several classes are underrepresented: transporters, proteins with structural functions, protein-binding proteins, nucleic acid binding proteins, kinases and hydrolases (Figure 9).

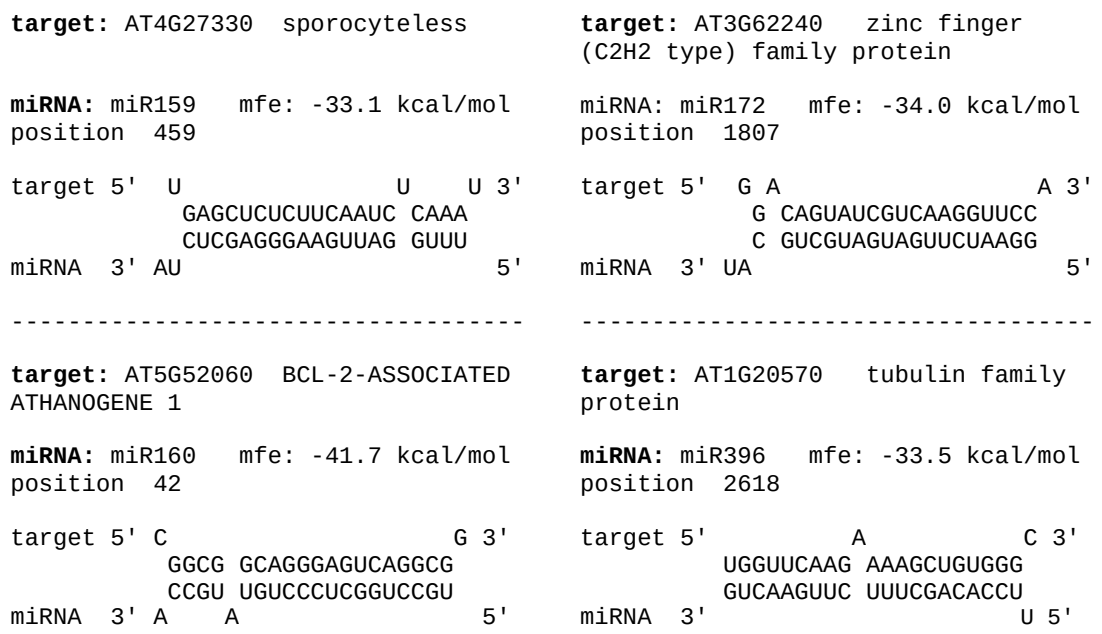

Figure 8. Predicted structures of novel miRNA targets.
Examples of four predicted structures of miRNA:target hybrids are shown. In this example, all targets were taken from the CDS dataset. For each target, the AGI code, a small description, the calculated MFE of the hybrid and the start position of the hybrid in the target sequence are given.

From the set of novel putative targets, there are no major differences from the whole genome categorization, but some classes are underrepresented. These include structural proteins, proteins with receptor binding or receptor activity. Again, some are also overrepresented: nucleotide binding proteins and hydrolases. Comparing classes from newly predicted with previously predicted/validated targets also show several differences in these two groups of genes. Transcription factors are 4-fold increased in previous predicted/validated targets, whereas they are not increased in the new prediction. The same can be pointed out for transferases, receptor binding/activity and DNA/RNA binding classes. Hydrolases, kinases, nucleic acid binding, protein binding and transporters are classes with proportionally more targets in the new prediction than in the previously predicted/validated group (Figure 9).

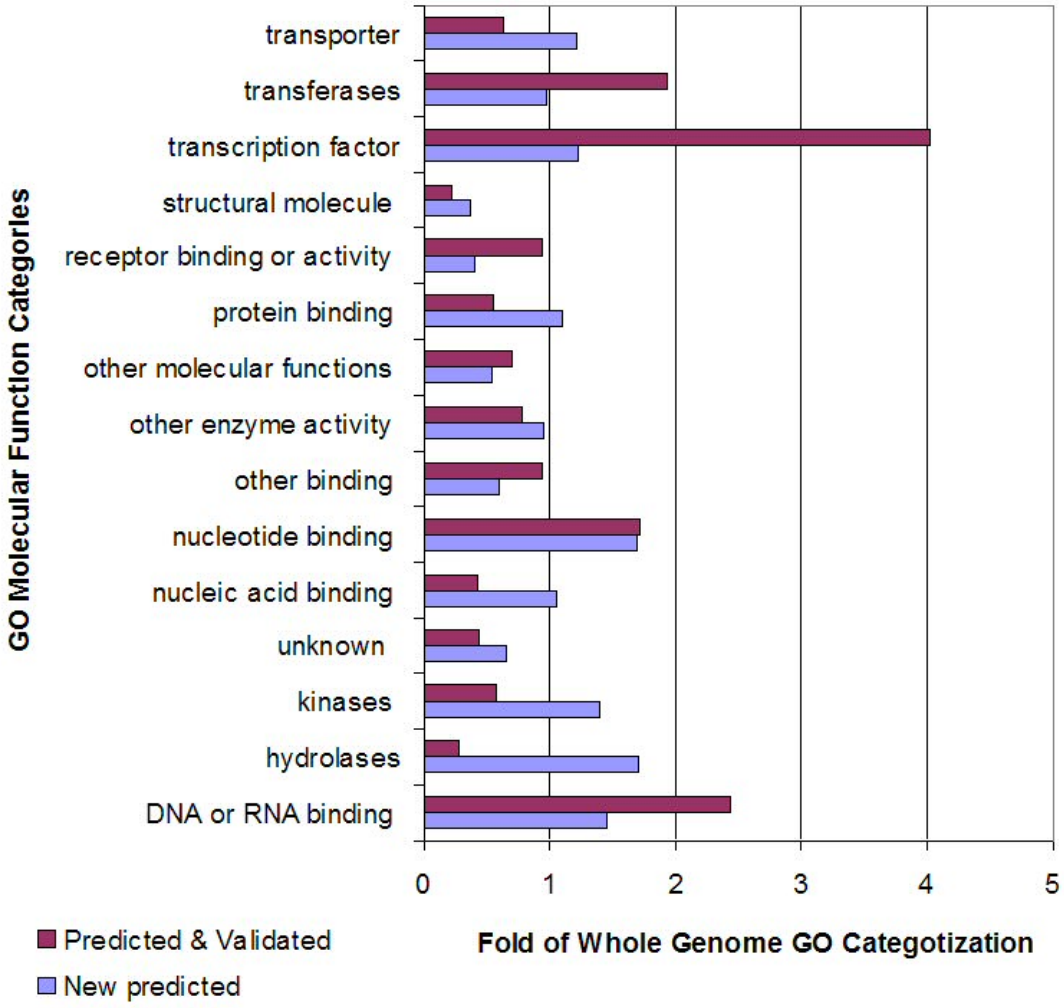

Figure 9. Analysis of GO annotation terms for molecular function category.
The percentage of GO annotation terms for each category was divided by the percentage of GO annotations of the whole Arabidopsis genome.

A set of 58 miRNA families was used for prediction of miRNA targets using RNAhybrid with the parameters described above. Novel putative miRNA targets for 48 miRNA families were found, and for nine families, no novel miRNA target was predicted. For one miRNA family, miR414, 383 novel miRNA targets were predicted, However, these candidates are not included in the results because miR414 may not be a miRNA but an endogenous siRNA (Xie *et al*., 2005). Over 47% of the predicted targets belong to from five miRNA families, miR396 (23), miR413 (34), miR773 (36), miR779 (16) and miR783 (23).

3.1.2. Novel putative miRNA targets for conserved miRNA families

There are 22 miRNA families in the Arabidopsis genome that are conserved in others plant genomes. For these miRNA families, miRNA targets had already been predicted and many of them had also been validated (Rhoades *et al*., 2002; Jones-Rhoades and Bartel, 2004; Wang *et al*., 2004b; Adai *et al*., 2005; Xie *et al*., 2005). Some miRNA families target a group of similar genes, for example, miR156/157, whose targets comprise transcription factors of the group Squamosa promoter-binding protein-like (SPL) or miR159, whose predicted and validated targets are genes that encode MYB transcription factors (Rhoades *et al*., 2002; Jones-Rhoades and Bartel, 2004). Among novel targets for this group of miRNAs, only a few are related to previously predicted targets. Only two out of five novel miR156 targets and none out of six novel miR157 targets are *SPL* genes. One of the novel targets is a tyrosine-specific phosphatase (AtEYA) predicted to be target of miR157. AtEYA is only the second protein of tyrosine-specific phosphatases to be described in plants (Rayapureddi *et al*., 2005).

miR159 is known to regulate a group of genes that encodes MYB transcription factors. We found ten novel targets for miR159. Among these is *SPOROCYTELESS*, which encodes a putative transcription factor that is required for the initiation of both micro- and megagametogenesis (Yang *et al*., 1999). The only predicted novel target of miR160 is *BAG1*, which belongs to a family of proteins that function in cell protection under stress and inhibit a programmed cell death that shares features associated with apoptosis (Doukhanina *et al*., 2006). Two auxin-responsive factors are regulated by miR167; six novel genes were predicted as targets, including a topoisomerase II (AtTOPII), which accumulates at a higher level in young seedlings in correlation with the proliferative state of this particular tissue (Xie and Lam, 1994).

BREVIS RADIX (BRX) is a novel nuclear-localized regulatory factor of plant development that controls the extent of cell proliferation and elongation in the growth zone of the root tip (Mouchel *et al*., 2004). The observed phenotype in plants that do not express *BRX* results from a decreased level of brassinosteroid in root tissues due to a down-regulation of a rate-limiting enzyme of the brassinosteroid pathway. The low level of brassinosteroids affects auxin-

responsive gene expression. The expression of *BRX* is affected by auxin, which induces *BRX* expression and is slightly repressed by brassinolide. Therefore, *BRX* acts in a feedback loop that maintains brassinosteroid levels leading to an optimal auxin action (Mouchel *et al*., 2006). *BRX* is a novel putative target of miR319.

MiR396 is one of the miRNA families with the highest number of novel targets. It is known that miR396 regulates the expression of Growth Regulating Factors (GRF). Among the novel targets, there are genes that encode of members of the tubulin family (At1g20570 and At1g80260), a WRKY21 transcription factor and a mitochondrial transcription terminator factor (At5g55580). This miRNA family may also be involved in the regulation of *ASA1*, which encodes the alpha subunit of anthranilate synthase. This enzyme participates in the first steps in the tryptophan biosynthetic pathway (Niyogi and Fink, 1992).

A predicted novel target of miR397 is *DPA*, a dimerization partner of E2F transcription factor, which is involved in stimulating the transcription of genes needed for G1-to-S and S phase progression in cell cycles (Vandepoele *et al*., 2002; Magyar *et al*., 2005).

MiR408 seems to be a new regulator of the flavonol and anthocyanin biosinthesis. One of the novel targets is *F3H*, which encodes flavone 3-hydroxylase, an enzyme that catalyzes an early step in flavonoid metabolism, the formation of dihydrokaempferol from naringenin, and therefore provides precursors for many classes of flavonoids and anthocyanins compounds (Pelletier and Shirley, 1996). Another predicted target of miR408 is *PAA2*, which encodes a P-Type ATPase that mediates copper transport to the chloroplast thylakoid lumen. PAA2 is required for the accumulation of copper-containing plastocyanin in the thylakoid lumen and for effective photosynthetic electron transport (Abdel-Ghany *et al*., 2005).

3.1.3. Novel putative miRNA targets for nonconserved miRNA families

Many miRNA families are found exclusively in Arabidopsis; they are referred as nonconserved miRNA families. In Arabidopsis there are 35 nonconserved miRNA families (Sunkar and Zhu, 2004; Wang *et al*., 2004b; Xie *et al*., 2005; Lu *et al*.,

2006). This count dos not include 49 additional nonconserved miRNAs have that been recently described (Arteaga-Vazquez *et al*., 2006; Rajagopalan *et al*., 2006; Fahlgren *et al*., 2007) but did not appear in the release 9.0 of MIRBASE (http://microrna.sanger.ac.uk/). Here, only data of 35 nonconserved miRNA families that are present in the last release of MIRBASE are described.

There are several members of Pentatricopeptide repeat-containing (PPR) protein targets of miR161 (Allen *et al*., 2004). An additional PPR is the only predicted novel target of miR161. Another miRNA, miR400, is predicted to have eleven PPRs as targets. Four more PPRs were predicted as targets for this miRNA (Figure 10). In addition, five PPRs were predicted yet as target of yet four more miRNA families: miR167, miR394, miR396 and miR413 (two targets). Another target of miR400 is gene encoding an auxin-responsive factor (ARF1), ARFs are transcription factors that mediate responses to the plant hormone auxin. ARFs encoding genes are targets of miR160 (*ARF17* and *ARF10*) and miR168 (*ARF8*). ARF1 is a transcriptional repressor (Ulmasov *et al*., 1999; Tiwari *et al*., 2003) and *arf1* mutations enhance the phenotypes observed in *arf2* mutant plants. They are delayed in several processes related to plant aging, including initiation of flowering, rosette leaf senescence, floral organ abscission and silique ripening (Ellis *et al*., 2005).

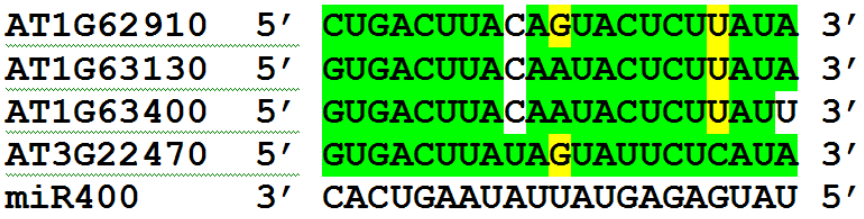

Figure 10. Pentatricopeptide (PPR) genes predicted as targets of miR400.
Four *PPR*s genes are putative novel targets of miR400. Other 11 *PPR* genes were previously predicted as miR400 targets (Sunkar and Zhu, 2004). Nucleotides with green background are those that show Watson-Crick complementarity to the miRNA. Yellow background indicates nucleotides that show G:U pairing. Mismatches have no background color.

MiR413 also constitutes a miRNA family with a high number of predicted targets (34). Among these there are four GTPases genes, two from the Rab family and

two from the Rho family. Other targets are two genes involved in flowering time control. *Early Flowering 8* (*ELF8*) is required (together with *ELF7*) for the enhancement of histone 3 trimethylation at Lys 4 in *Flowering Locus C* (*FLC*) chromatin (He *et al*., 2004). Another novel target of miR413 also affects *FLC* expression. Mutation in the *AtMBD9* leads to a markedly decrease in the expression of *FLC*. Such reduction was associated with a significant decrease in the acetylation level of histones H3 and H4 in the *FLC* chromatin of *atmbd9* mutants (Peng *et al*., 2006).

Mir415 could be involved in the siRNA silencing pathway, since its predicted target is a gene encoding the largest subunit of RNA polymerase IV (Pol IV). Pol IV is involved in the production of small RNAs of 24 nt that are required for de novo cytosine methylation (Herr *et al*., 2005; Kanno *et al*., 2005).

MiR773 is the miRNA family with the highest number of predicted targets (36 putative targets). This includes genes encoding: a member of the WAVE complex, ITB1-SCAR2; an acyl-activating enzyme (AAE7); a Catalase 2 (CAT2); HMA1, a metal-transporting P1B-type ATPase that was recently characterized as an additional way of importing copper in the chloroplast (Seigneurin-Berny *et al*., 2006); Arabidopsis H^+-ATPase 3 (AHA3); two B3 transcription factors; a defensin-like protein (DEFL) and tubulin alpha-3/alpha-5 chain (TUA5). MiR774 is known to target two members of the F-box gene family (Lu *et al*., 2006). No other F-box genes were found among seven putative novel targets. Interestingly, five putative targets are members of the S-locus protein kinase gene family (Figure 11A). Another family with several members predicted to be target of one miRNA is the Ulp1 protease gene family. Seven genes were predicted to be targets of miR781 (Figure 11B).

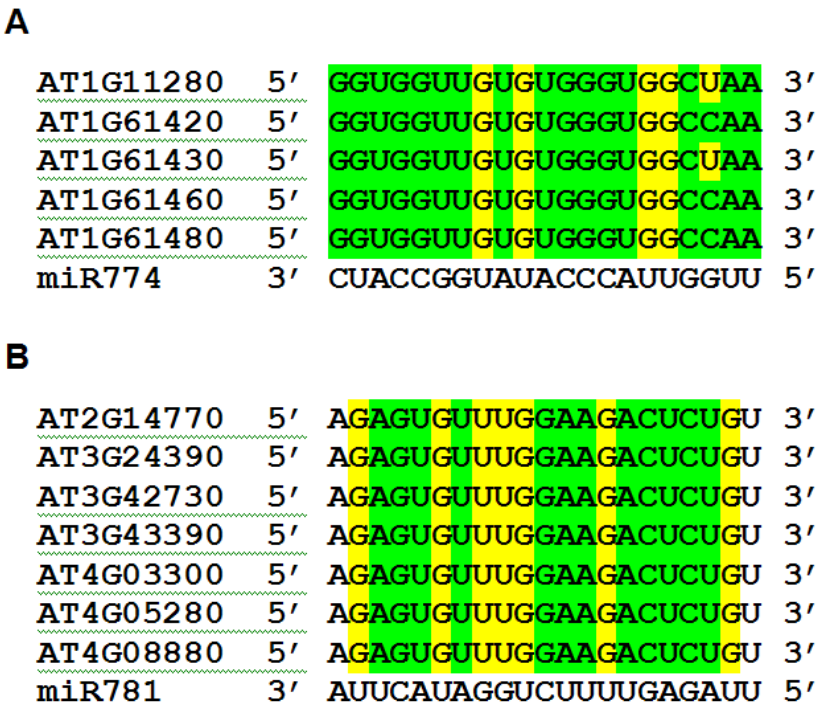

Figure 11. Alignment of miRNAs and predicted binding site.
A, members of the S-locus protein kinase gene family predicted to be targets of miR774. B. predicted targets of miR781, members of the Ulp1 protease gene family. Nucleotides marked with green background are those that show Watson-Crick complementary to the miRNA, yellow indicates G:U pairing. Mismatches have no background color.

3.1.4. Validation of miRNA targets

Some miRNA targets were chosen for validation experiments. The targets were selected based on the gene family they belong to, namely the MYB gene family. Other targets were selected because they were predicted to be targets of miRNAs that were already being subject of validation experiments. In order to validate miRNA targets, both target DNAs and miRNA precursors were cloned. Then, both constructs were co-transfected to Arabidopsis AT7 protoplasts. RNA from protoplasts was extracted and the mapping of the cleavage site was done with the method RNA ligation mediated – rapid amplification of cDNA 5' ends (5'RACE). Before the validation experiments, northern blots were prepared to detect the miRNAs that were going to be used in the validation experiments.

3.1.4.1. Detection of mature miRNAs

Northern blots were employed to detect whether the mature miRNA was produced after transfection of AT7 protoplasts with the precursor of this miRNA. For experiments involving miR161 and miR414, tobacco BY-2 protoplasts were also used. Precursors of miRNAs miR156h, miR159a, miR161, miR172a, miR395d and miR414 were cloned into pMAV5-3'GFG vector. In these constructs, the GFP was replaced by the miRNA precursor and CaMV 35S promoter drives its expression. Arabidopsis AT7 protoplasts were transfected with a construct harboring either the miRNA precursor or the empty vector. RNA was extracted, separated in polyacrylamide gels and blots to detect small RNA were prepared (Figure 12).

Four of the miRNAs tested could be detected in the northern blot: miR161 in both protoplast systems (Figure 12A), miR159, miR156 and miR395 in the AT7 protoplast system (Figure 12B, D and F, respectively). For miR161 and miR395 a markedly difference was observed in the expression level between protoplasts transfected with the miRNA precursor or protoplasts transfected with the empty vector. In fact, miR395 was not detected in protoplasts transfected only with the empty vector. The expression levels of miR156 and miR159 did not show differences between different transfections. Two miRNAs were not detected with northern blots, miR414 and miR172 (Figure 12C and E, respectively). In all blots, there was a positive control for the hybridization, which is a DNA oligonucleotide with the same sequence of the mature miRNA, shown only for blots of miR161, miR414 and miR172. Those miRNAs that could be detected by northern blots, were further used for miRNA target validation experiments.

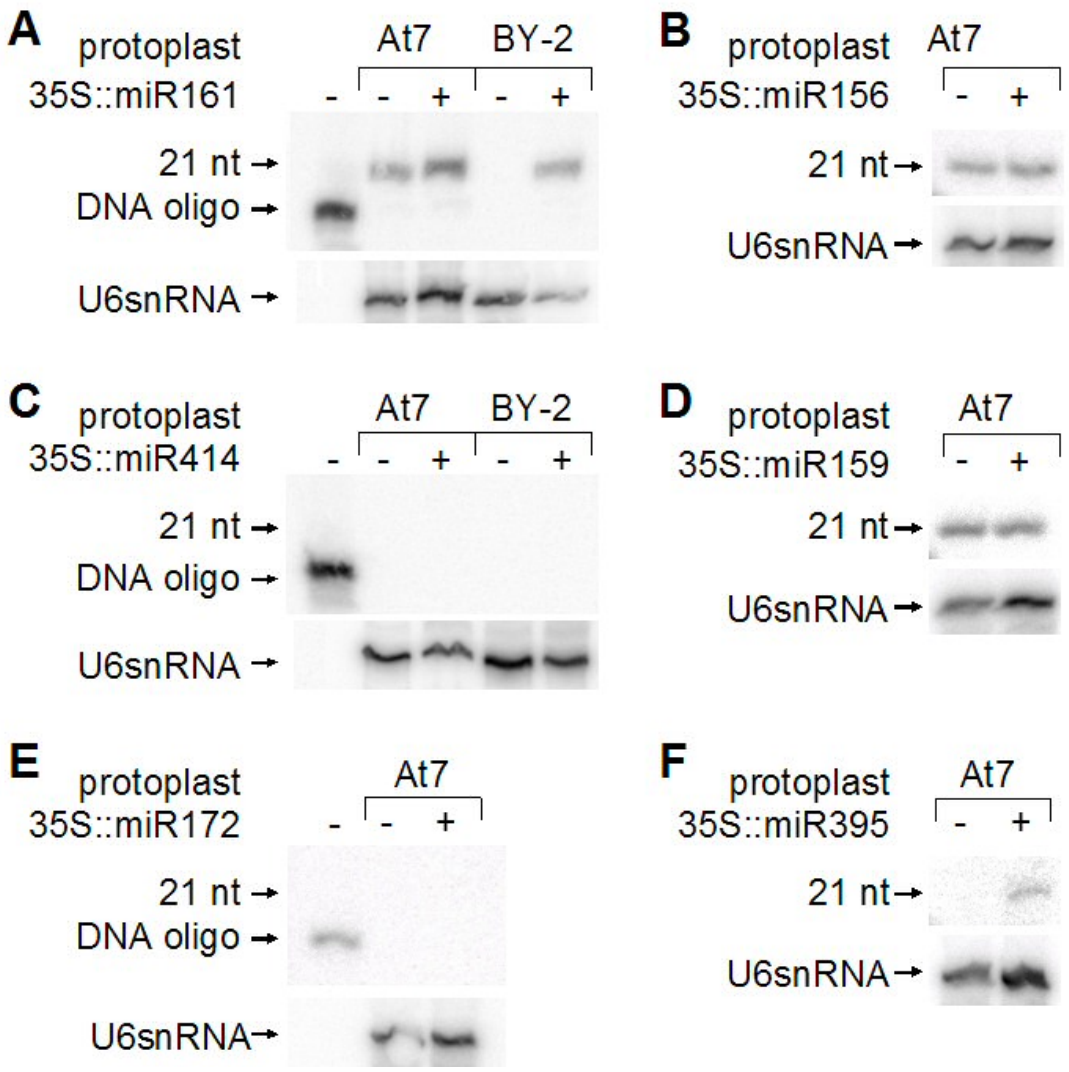

Figure 12. Detection of mature miRNAs expressed in protoplasts.
Northern blots to detect mature miRNAs were prepared from denaturating polyacrylamide gels. In each lane, 20 μg of total RNA was loaded. A positive control, consisting of a DNA oligonucleotide with the same sequence as the corresponding mature miRNA was also included on all blots, but is shown for miR161 (A), miR414 (C) and miRNA172 (E). U6snRNA was used as loading control. An RNA oligonucleotide of 21 nucleotides in length was used as size marker. The position corresponding to 21 nucleotides is indicated.

3.1.4.2. Validation of miRNA targets

Validation of miRNA targets takes advantage of a modified RNA ligase-mediated rapid amplification of cDNAs 5'ends (5´RACE) approach, which is used to precisely map the position of the cleavage induced by the RISC complex (Llave *et al*., 2002a). Normally, the source RNA for 5´RACE is total RNA from any plant

organ (Palatnik *et al*., 2003; Xie *et al*., 2003; Allen *et al*., 2004; Jones-Rhoades and Bartel, 2004; Mallory *et al*., 2004a; Mallory *et al*., 2004b). Transient co-expression of pre-miRNA and the miRNA target in tobacco leaves was also used for miRNA target validation. In these experiments, RNA was extracted and used for 5´RACE (Llave *et al*., 2002b; Palatnik *et al*., 2003) or for northern blot experiments to show the presence of cleavage products (Achard *et al*., 2004). In this work, 5´RACE was used to validate miRNA targets. RNA samples used in these experiments were extracted from AT7 (Arabidopsis) protoplasts that were transfected to overexpress both a precursor miRNA and a putative miRNA target. All putative targets were cloned in fusion with 3´GFP, in order to avoid short 5´RACE products, originated when the position of the miRNA binding site is close to the stop codon of the cDNA, therefore primers annealing to the GFP sequence could be used in the PCR (Table 6).

Table 6. Validations experiments of predicted miRNA targets.
All putative miRNA targets were cloned into pMAV5-3'GFP in translational fusion with GFP. Targets that were predicted previously, the reference is given. (*) denotes targets that were also predicted using the strategy showed in this work. (**) denotes targets found with RNAhybrid program, that do not comply with the perfect match percentage rule.

miRNA	Target name	AGI code	Prediction reference
miR156	*MYB94*	At3g47600	This work**
miR159	*MRG1*	At2g34010	This work
miR159	*ACS8*	At4g37770	Schwab *et al*., (2005)*
miR159	*MYB101*	At2g32460	Rhoades *et al*., (2002)*
miR159	*MYB125*	At3g60460	Rhoades *et al*., (2002)
miR159	*CKL6*	At4g28540	This work**
miR161	*GAE1*	At4g30440	This work**
miR161	*PRF2*	At4g29350	This work**
miR395	*MYB58*	At1g16490	This work**

Two MYB transcription factor genes were validated as miR159 targets. Phylogenetic analysis grouped *MYB101* in the clade of MYB genes called GAMYB. GAMYBs have been suggested to be involved in the gibberellin (GA)-mediated promotion of flowering by activation of the floral meristem identity gene *LEAFY* (Gocal *et al*., 2001) and in the regulation of anther development (Achard *et al*., 2004). All AtGAMYB genes were predicted as mir159 targets (Rhoades *et al*., 2002; Jones-Rhoades and Bartel, 2004). Moreover, for *MYB33*, *MYB65* (Palatnik

et al., 2003) and *MYB101* (Reyes and Chua, 2007) the cleavage products recovered by 5'RACE precisely mapped the cleavage of these two transcripts in the miRNA binding site motif. Using the 5'RACE strategy, the cleavage of *MYB101* by miR159 could also be confirmed (Figure 13).

Figure 13. Experimental validation of predicted miRNA targets.
Each top strand depicts a target mRNA sequence and each bottom strand depicts the miRNA. Matches (Watson-Crick pairing) are indicated with vertical dashes, mismatches are unmarked and G-U wobbles are indicated with a colon. Arrows indicate cleavage sites verified by 5' RACE, with the number of cloned RACE products shown above.

A second validated miR159 target is *MYB125*, also known as *DUO1* (Figure 13). *MYB125/DUO1* control male gamete formation in Arabidopsis. The expression of *MYB125/DUO1* occurs specifically in the male germ line. Mutations in *MYB125/DUO1* produce a single larger diploid sperm cell unable to perform fertilization (Durbarry *et al*., 2005; Rotman *et al*., 2005). A third miR159 target gene is MRG1, which stands for *MICRORNA-REGULATED GENE1* (*MRG1*). *MRG1* is annotated as an expressed protein (The Arabidopsis Genome Initiative, 2000). *MRG1* and *MYB101* were chosen for additional experiments in order to understand the function of these genes. *ACS8* is another target that was successfully validated. *ACS8* is a member of a gene family and codes for 1-

aminocyclopropane-1-carboxylic acid synthase, a key regulatory enzyme in the biosynthetic pathway of the plant hormone ethylene (Vandenbussche *et al*., 2003).

Only one target of miR161 could be validated. This gene encodes an enzyme that acts as a nucleotide sugar UDP-4-epimerase interconverting UDP-D-glucuronate and UDP-D-galacturonate (Molhoj *et al*., 2004).

No other targets could be validated as miRNA targets using the approach described here. For *MYB94* and *PRF2*, no PCR fragments in any 5'RACE library were recovered. A second class of putative targets, which were also not validated, comprises *MYB58*, *MYB97* and *CKL6*. PCR fragments were cloned and sequenced. However, it was not possible to detect a specific cleavage site because no single clone matches to the same nucleotide position (Figure 14).

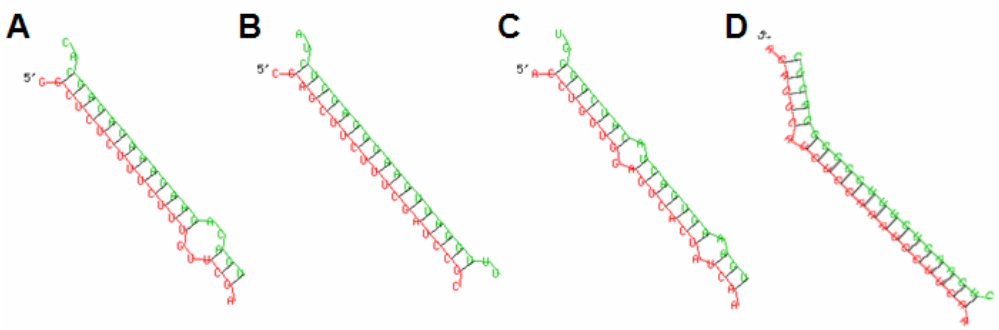

Figure 14. miRNA/targets duplexes of non validated targets.
Hybrid structure between and miRNA and putative targets are shown. These genes were not confirmed as miRNA targets using 5'RACE. A, miR156:*MYB94*; B, miR159:*CKL6*; C, miR161-*PRF2*; D, miR395-*MYB58*. miRNA sequence are shown in green.

3.2. Functional analysis of miR159 targets - MYB101

3.2.1. Isolation of transgenic plants to overexpress *MYB101 and MYB101mutBS*

Besides the mapping of the mRNA cleavage by RISC, another approach to study the regulation of a miRNA target is to express (or overexpress) a miRNA target with point mutations at the miRNA binding site. These point mutations change the nucleotide sequence but the amino acid sequence of the protein remains

unaltered (Palatnik *et al*., 2003; Mallory *et al*., 2004a; Fujii *et al*., 2005; Mallory *et al*., 2005). The *MYB101* cDNA was cloned into pMAV5-3'GFP, replacing the GFP gene. A mutant variant of this cDNA was then generated using a PCR-based site-directed mutagenesis to introduce point mutations in the *MYB101* cDNA. These point mutations do not alter the deduced amino acid sequence of the *MYB101* protein (Figure 15). For each of these constructs, the cassette consisting of CaMV 35S promoter, *MYB101* and Tnos terminator was sub-cloned into a binary vector, pGPTV-BAR. Using *Agrobacterium tumefaciens*, *Arabidopsis thaliana* Col-0 plants were transformed and transgenic plants were selected using BASTA. After selection in the T1 generation, BASTA resistant plants were genotyped using primers P35S and L018. A total of five *35S$_{pro}$:MYB101mutBS* and seven *35S$_{pro}$:MYB101* T1 lines were isolated.

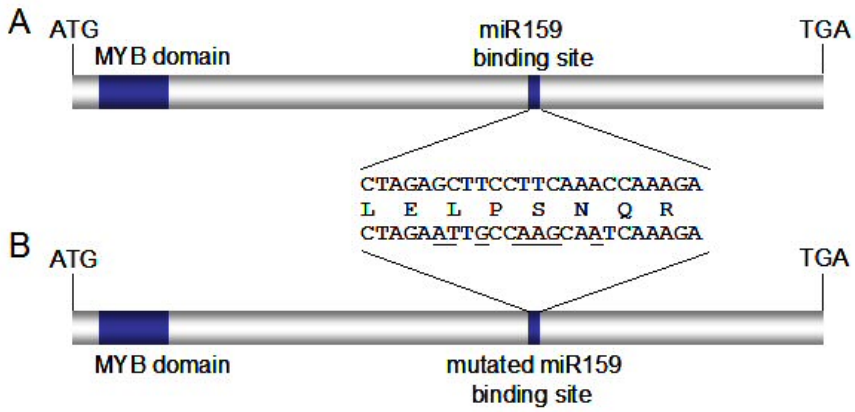

Figure 15. *MYB101* overexpressor constructs.
A, wild-type *MYB101* cDNA was cloned between the 35S promoter and the Tnos terminator in the pMAV5-3'GFP vector, replacing the GFP cDNA. The sequence of the miR159 binding site is shown. B, *MYB101mutBS* was generated by site-directed mutagenesis and cloned as described above. The alteration to the nucleotide sequence in the miRNA target motif is shown, and the nucleotides underlined are those differing from the wild-type sequence. The deduced amino acid sequence is shown in the middle.

3.2.2. Effects of ectopic expression of *MYB101 and MYB101mutBS*

All overexpressing lines were further analyzed in the T2 generation, concerning expression level of the *MYB101* and phenotypic abnormalities due to *MYB101* ectopic expression. The expression level of *MYB101* transcript in T2 lines was investigated using RT-PCR. Were used five lines, two plants from each line,

transformed with *35S$_{pro}$:MYB101mutBS* and seven lines with *35S$_{pro}$:MYB101* constructs. Plants were first genotyped for the presence of the corresponding construct. Most of *35S$_{pro}$:MYB101mutBS* lines show a constitutive expression of *MYB101*. The RNA samples for this experiment were isolated from adult leaves, a tissue where *MYB101* normally is expressed in very low levels. In contrast, most lines carrying a normal version of *MYB101* do not show a detectable expression of this gene (Figure 16).

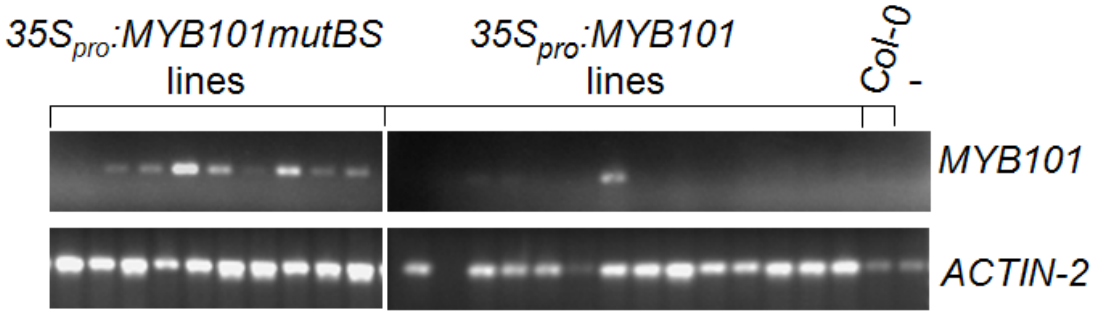

Figure 16. Gene expression analyses in *MYB101* overexpressing plants.
RT-PCR from RNA of leaves of positive T2 plants transformed with either *35S$_{pro}$:MYB101* or *35S$_{pro}$:MYB101mutBS*. Each line was analyzed in duplicate.

Plants show phenotypes that differ from Col-0 wild-type. Transgenic plants growing under long-day conditions show smaller leaves as compared to the Col-0 plants (Figure 17B-G). This phenotype is evident in plants that carry both types of constructs. In *35S$_{pro}$:MYB101mutBS* plants, however, the effect is much more evident (Figure 17D). Plants grown under short-day conditions also show differences in phenotype (Figure 17E-G). After 10 weeks, *35S$_{pro}$:MYB101* plants (Figure 17F) did not differ from Col-0 wild-type (Figure 17E). On the contrary, *35S$_{pro}$:MYB101mutBS* plants (Figure 17G) were smaller as compared to the wild-type plants.

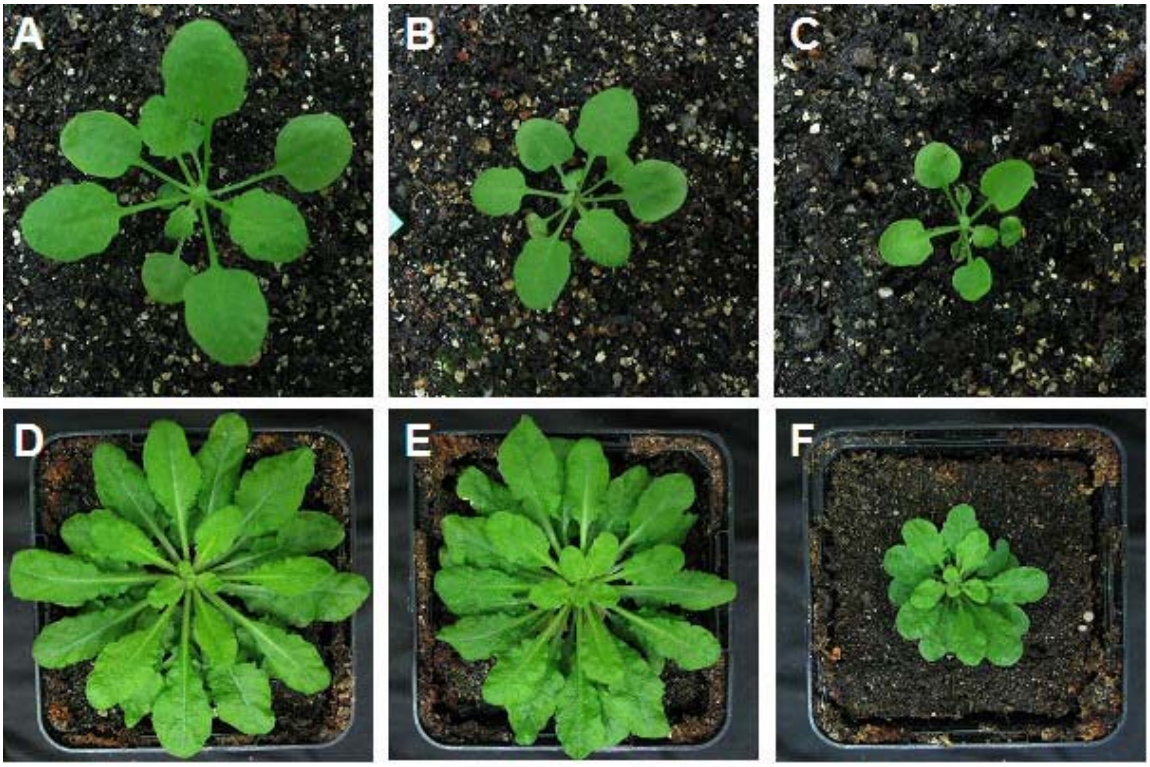

Figure 17. Effects of ectopic expression of *MYB101*.
Effects of the overexpression of *MYB101* were observed in seedlings and in adult plants. A-C, two-week-old seedlings under long-day conditions (16h light-8h dark). From left to right: Col-0, *$35S_{pro}$:MYB101* and *$35S_{pro}$:MYB101mutBS*. E-G, thirteen-week-old plants growing under short-day conditions (8h light-16h dark). From left to right: Col-0, *$35S_{pro}$:MYB101* and *$35S_{pro}$:MYB101mutBS*.

3.2.3. Gene expression pattern of *MYB101*

The gene expression pattern of *MYB101* was investigated using promoter GUS lines and data from microarray experiments from the AtGenExpress project (Schmid *et al*., 2005).

3.2.3.1. MYB101 expression analysis from AtGenExpress

The AtGenExpress project was designed in order to create an atlas of gene expression of Arabidopsis (Schmid *et al*., 2005). *MYB101* expression pattern data was retrieved from the home-page (http://jsp.weigelworld.org/expviz/expviz.jsp) using the AtGenExpress Visualiation Tool. The data presented here were taken from the developmental data set, which includes RNA samples from different tissues. The experiments that were used to create Figure 18 are listed in

Appendix 3. According to these data, the expression of *MYB101* is observed in stamen and, to a greater extent, in pollen.

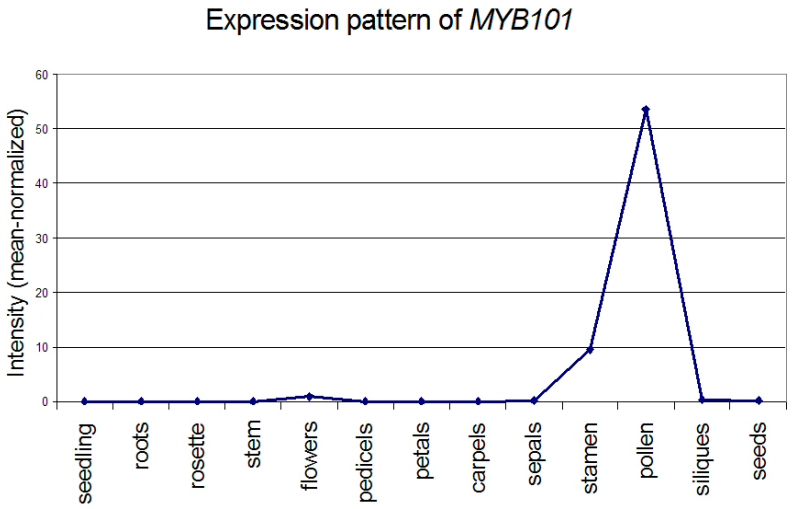

Figure 18. *MYB101* expression pattern in wild-type Col-0
Expression estimates by gcRMA were taken from the AtGenExpress Arabidopsis expression atlas, based on Affymetrix ATH1 analyses. Normalized values were obtained by normalizing absolute values to median, for each gene, across all samples (Schmid *et al*., 2005).

3.2.3.2. Promoter-GUS analysis of *MYB101*

The expression pattern and functional role of the *MYB101* promoter was examined. For this purpose, a promoter fragment of 1748 bp, from the start codon upstream to the next gene, was fused to the beta-glucuronidase (GUS) reporter gene *uidA* in the pANGUS vector. Plasmid DNA was then transferred to Arabidopsis plants via floral dip infiltration, mediated by Agrobacterium tumefaciens to allow expression of the GUS gene under the control of the *MYB101* promoter.

Histochemical staining of five independent transgenic Arabidopsis lines of the T2 progeny harboring the $MYB101_{pro}$*:GUS* construct showed blue staining in different organs of the plant at different developmental stages (Figure 19). Seedlings stained 13 days after germination grown on MS plates long-days showed GUS expression in cotyledons, in young leaves (Figure 19A-B) and in the primary root,

specifically in the root tip (Figure 19D). In flowers, GUS expression was detected in the sepals and petals, moreover, marked expression could be observed only in pollens grains and stamen (Figure 19C). No GUS expression was observed in secondary roots, adult and cauline leaves, stem and siliques.

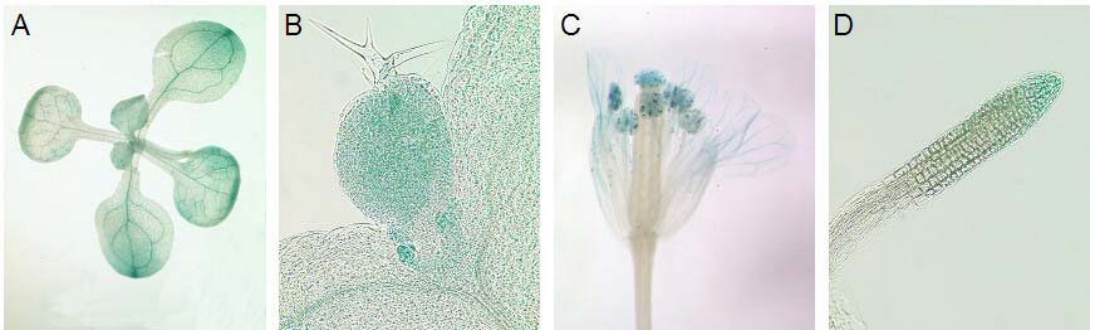

Figure 19. GUS staining of Arabidopsis harboring *MYB101$_{pro}$:GUS* constructs.
Seedlings were grown on MS plates and plants were cultivated in short days for 8 weeks and then two more weeks in long-day conditions. A, 13-days-old seedlings. B, detail of developing leaf in seedlings. C, detail of staining in flower. D, detail of root tip of 13-days-old seedling.

3.2.4. T-DNA insertion lines in *MYB101*

Five T-DNA insertion lines were found in the MYB101 gene using a tool from the T-DNA Express database (http://signal.salk.edu/cgi-bin/tdnaexpress). Two of them were ordered and named *myb101-1* and *myb101-2*, both were from the SALK T-DNA population. Primers for genotyping of these T-DNA lines were designed using the T-DNA Primer Design tool (http://signal.salk.edu/tdnaprimers.2.html). This tool specifically designs primers to be used with T-DNA left border or right border of almost any available T-DNA population. Plants from both lines were grown in soil, and then, DNA was extracted and genotyped for the presence of the T-DNA using PCR with gene-specific primers, L048 and L050 (Figure 20), and the SALK T-DNA left border primer. PCR fragments were sequenced to confirm the presence of the T-DNA in each allele. Then, PCR with gene specific primers was done to identify

homozygous plants homozygous for each allele. In order to confirm the right border of the T-DNA insertion, PCR was used to amplify fragments from each allele using other gene specific primers, L047 and L049 (Figure 20), and SALK T-DNA right border primer. In case of *myb101-1*, it was possible to amplify a fragment. Sequencing of this fragment revealed that the T-DNA insertion event resulted in a deletion of three nucleotides in *MYB101* (Figure 20). For *myb101-2*, a fragment could be amplified using L050 and the SALK T-DNA left border primer. Sequencing of this fragment confirmed that there are at least two T-DNA insertions in the allele *myb101-2*. In addition, a deletion of ten nucleotides was also observed (Figure 20).

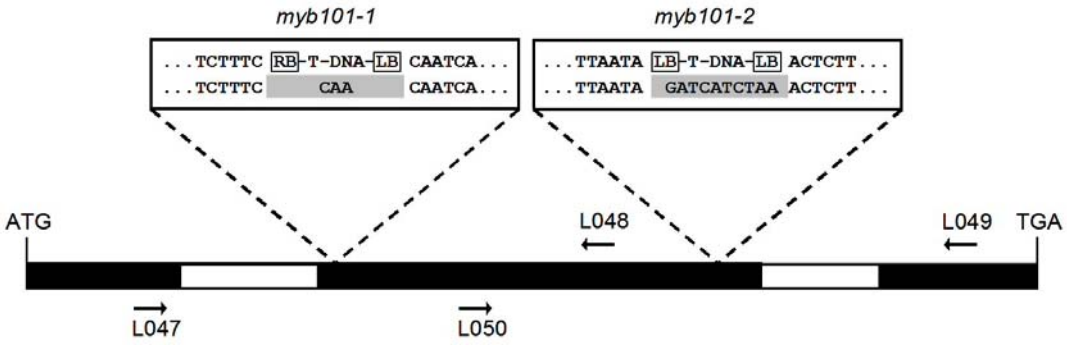

Figure 20. Schematic diagram of *MYB101* T-DNA insertion lines.
The genomic structure of *MYB101* is shown. Exons are represented as solid boxes and introns as open boxes. For each T-DNA insertion line the mutant allele in the upper sequence and the wild-type allele in the lower sequence are shown. The gray box indicates the nucleotides deleted in the mutant alleles; L047, L048, L049 and L050 are primers used for genotyping of these T-DNA lines.

Flowers of wild-type and of homozygous plants from two T-DNA insertion lines were collected and their RNA was extracted, in order to verify if these lines are true knockouts. RT-PCR as performed with primers to amplify the whole *MYB101* transcript. *ACTIN2* was used as reference. A fragment corresponding to the size of the full length transcript of *MYB101* was recovered only in the wild-type sample. However, no detectable expression was observed in any of the T-DNA lines (Figure 21). Homozygous plants of *myb101-1* and *myb101-2* grown in soil did not show any morphological difference from control plants (Col-0 ecotype).

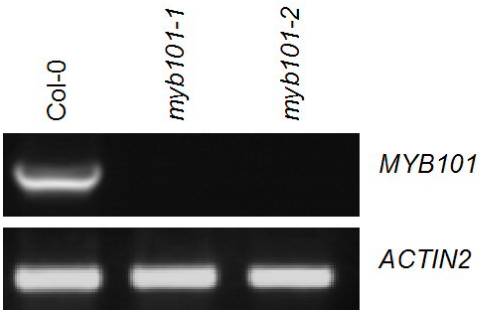

Figure 21. Detection of *MYB101* transcript in T-DNA insertion lines.
RT-PCR analysis to detect the whole transcript of *MYB101* was done with total RNA extracted from flowers of Col-0, *myb101-1* and *myb101-2* plants. For *MYB101*, 35 PCR cycles and for *ACTIN2*, 30 PCR cycles were performed.

3.3. Functional analysis of miR159 targets - *MRG1*

MRG1 is a gene for which no information is available in any database. The nucleotide and peptide sequences do not match to any other sequence found in any database, apart from another putative gene present in the genome of Arabidopsis, At1g29010. In contrast to *MRG1*, the expression of At1g29010 could not be detected by RT-PCR (data not shown). However, this similarity is very low. As *MRG1*, At1g20910 is also annotated as an expressed protein. What these two genes share is a miR159 binding site. *MRG1* does not have any know motif and information about *MRG1* expression was not available.

3.3.1. Gene expression pattern of *MRG1*

The gene expression pattern of *MRG1* was investigated using promoter GUS lines and analysis of *MRG1* transcript levels in different tissues of Arabidopsis Col-0.

3.3.1.1. Expression pattern of MRG1

The expression pattern of *MRG1* was investigated by RT-PCR with RNA samples from different tissues of Arabidopsis Col-0. RNA was extracted from seedlings grown on MS plates for 13 days under long-day conditions. Roots were used from seedlings grown for 18 days on MS plates. A mix of flower and flower buds in different stages (referred as flower), cauline leaves, adult leaves stem and siliques were harvested from adult plants that were grown in soil in short days for six weeks and then three more weeks in long days. With the *MRG1* primers used in

this experiment anneal to sites that surround the miR159 binding site. For *ACTIN2*, the PCR was done with 30 cycles. For *MRG1*, each sample was split into two halves after 30 cycles, and one half of each sample was submitted to 10 more cycles. *MRG1* was detected in seedlings, flowers and leaves after 30 cycles. After 40 cycles, expression was detected also in roots and stems. No expression was detected in cauline leaves and siliques (Figure 22).

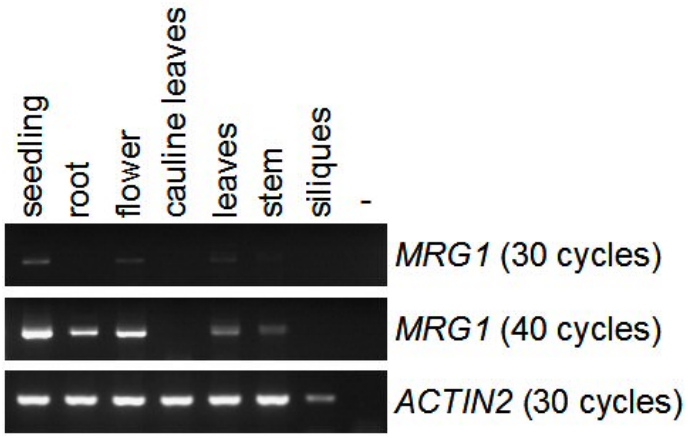

Figure 22. Expression pattern of *MRG1* in Arabidopsis Col-0 wild-type.
Total RNA was extracted from different tissues of Arabidopsis ecotype Col-0. The set of primers for the *MRG1* transcript was designed to amplify a fragment that contains in the miR159a binding. The negative control corresponds to RNA not subjected to reverse transcription reaction. For *MRG1*, aliquots of the reactions were taken after 30 cycles, the remaining samples were submitted to 10 more cycles. *ACTIN2* is the RNA loading control.

3.3.1.2. Promoter-GUS analysis of MRG1

To characterize the temporal and spatial activity of the promoter *MRG1*, an $MRG1_{pro}$*:GUS* reporter gene construct was generated. A fragment of 1800 nucleotides, from the start codon of *MRG1* upstream to the next gene, was cloned into pANGUS. This binary vector was transferred into Agrobacterium tumefaciens. Transgenic lines were generated via floral dip infiltration. After selection of transformants, five independent lines from T2 generation were used for hystochemical staining. Seedlings grown on MS plates in long-days and plants grown in soil maintained for six weeks under short day conditions followed by 3 weeks in long days were analyzed. Promoter activity was detected in almost all Arabidopsis tissues. In 8 and 13-days old GUS staining was observed in

cotyledons, young leaves, primary and secondary roots (Figure 23A-D). In adult plants, GUS staining was detected in rosette leaves, in flower organs (sepals, petals, filaments, stamen and pollen; Figure 23E-F). Siliques were not stained. However, seeds showed a positive stain (Figure 23G).

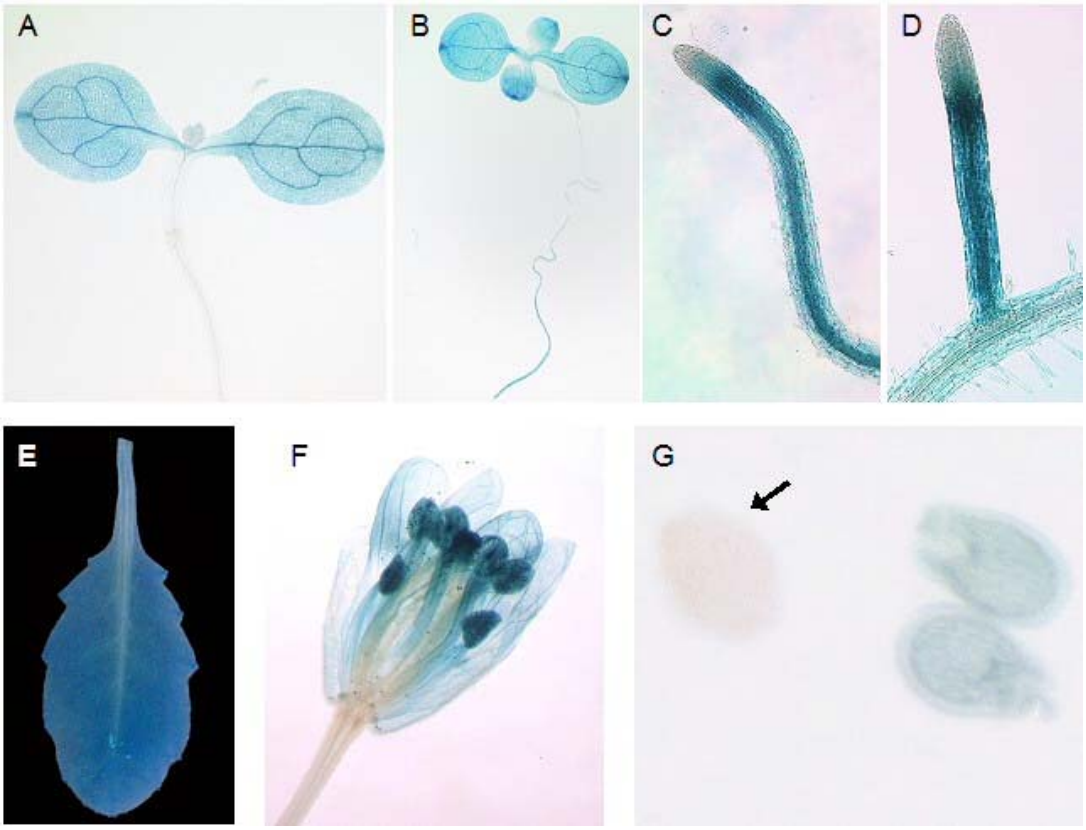

Figure 23. GUS staining of Arabidopsis harboring *MRG1$_{pro}$:GUS* constructs.
Seedlings were grown on MS plates and plants cultivated in short-days for 8 weeks and two more weeks in long-days. A and B, overview of Arabidopsis seedlings that were 8 and 13 days old, respectively. C-D, details of primary root and secondary root from 13-days-old seedligs. E-G, different tissues from adult plant. Rosette leaf, flower and seeds, respectively. A wild-type Col-0 seed is indicated by an arrow.

3.3.2. Cellular localization of MRG1:GFP fusion protein

In order to gain more information about MRG1, a translational fusion of MRG1 and GFP was constrcuted. The cDNA of *MRG1* was cloned into the pMAV5-3'GFP vector. This construct was used for transient transfection of BY-2 tobacco protoplasts. Using confocal laser-scanning microscopy, the MRG1:GFP fusion

protein was observed in the nucleus of BY-2 protoplasts (Figure 24A). GFP alone is distributed between the nucleus and the cytoplasm (Figure 24B).

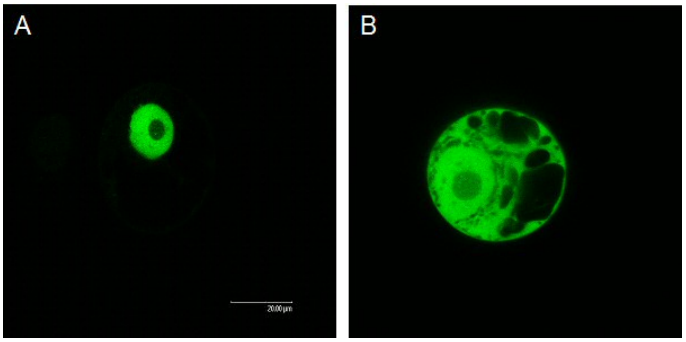

Figure 24. *In vivo* localization of MRG1:GFP fusion protein.
BY-2 protoplasts were transfected with plasmids in order to express MRG1:GFP (A) or GFP alone (B). Protoplasts were anlyzed by confocal laser-scanning microscopy.

3.3.3. Isolation of transgenic plants overexpressing *MRG1 and MRG1mutBS*

Similar to the analysis of *MYB101*, the effect of overexpressing *MRG1* in Arabidopsis was investigated. The cDNA sequence of *MRG1* was cloned into the pMAV5-3'GFP vector, replacing *GFP* ORF, to create the construct *35S$_{pro}$:MRG1:Tnos*. A mutated form of this gene was also created, *35S$_{pro}$:MRG1mutBS:Tnos*. In this construct, the sequence of *MRG1* has seven silencing point mutations in the miR159 binding site, leaving the protein sequence unchanged (Figure 25). Both cassettes, *35S$_{pro}$:MRG1:Tnos* or *35S$_{pro}$:MBRG1mutBS:Tnos*, were sub-cloned into a binary vector, pGPTV-BAR. Using *A. tumefaciens*, Arabidopsis Col-0 plants were transformed and, positive transgenic plants were selected using BASTA.

After selection in the T1 generation, BASTA resistant plants were genotyped using primers P35S and L015. For each construct, five lines independent were isolated.

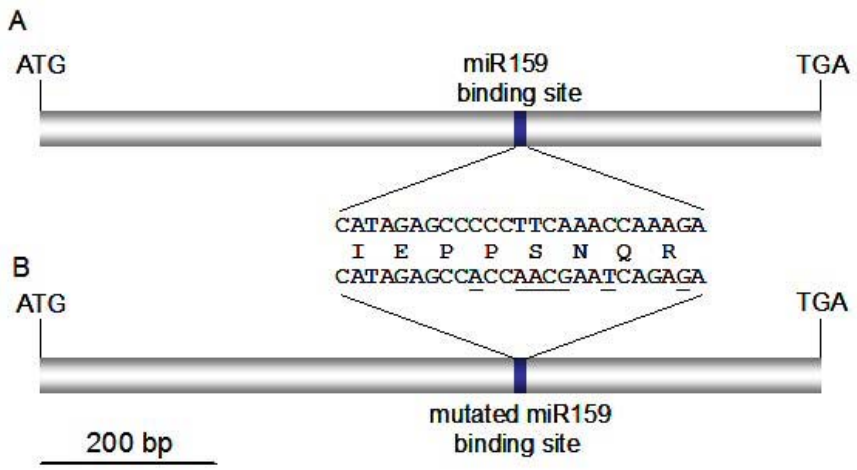

Figure 25. *MRG1* overexpressor constructs.
A, wild-type *MRG1* cDNA was cloned between the 35S promoter and the Tnos terminator in the pMAV5-3'GFP vector replacing the GFP cDNA. The sequence of the miR159 binding site is shown. B, *MRG1mutBS* was generated by site directed mutagenesis and cloned as described above. The altered nucleotides in the miR159 binding site are underlined. The deduced amino acid sequence is shown in the middle.

3.3.4. Effects of ectopic expression of *MRG1 and MRG1mutBS*

Plants carrying *$35S_{pro}$:MRG1* and *$35S_{pro}$:MRG1mutBS* were analyzed in the T2 generation. The expression level of *MRG1* and the phenotypical abnormalities were investigated. The expression level of *MRG1* was investigated by RT-PCR. All T2 lines were used and, samples were collected from two plants per line. The genotype of each plant was confirmed by PCR and RNA was isolated from rosette leaves. In most *$35S_{pro}$:MRG1* plants, the *MRG1* transcript was not observed. *MRG1* transcript was detected only in two samples from two different lines (Figure 26A). In *$35S_{pro}$:MRG1mutBS* plants, the *MRG1* transcript accumulated at detectable levels (in all investigated lines and in all samples). The *MRG1* transcript was not observed in Col-0 leaves (Figure 26B).

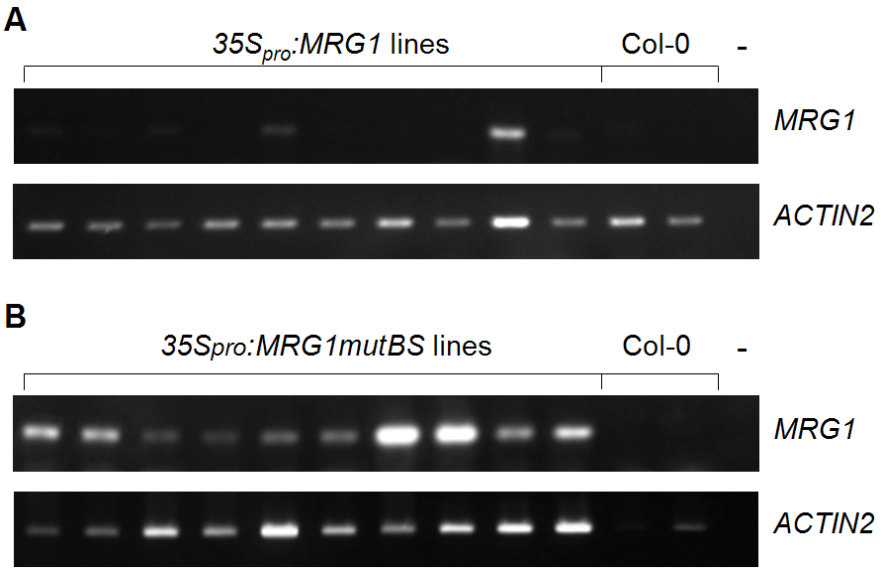

Figure 26. *MRG1* expression in transgenic lines
RT-PCR was done to analyze the *MRG1* expression level in plants transformed in with either *35S$_{pro}$:MRG1* or *35S$_{pro}$:MRG1mutBS*. Leaves of T2 plants genotyped for the presence of constructs were used and lines were analyzed in duplicates. A, RNA sample from plants harboring *35S$_{pro}$:MRG1* construct. B, RNA samples from *35S$_{pro}$:MRG1mutBS* plants. Reactions without cDNA served as negative controls. The number of cycles is 35 for *MRG1* and 30 for *ACTIN2*.

Phenotypical differences were observed in plants harboring both constructs to overexpress *MRG1*. In plants growing under short day conditions in a phytochamber (e.g. under artificial light), an up-curling of leaf blades and elongated petioles were observed in three-week-old plants (Figure 27A-E). At this stage, no differences were observed between *35S$_{pro}$:MRG1* and *35S$_{pro}$:MRG1mutBS* plants. In ten-week-old plants there were more differences among different lines and constructs. Plants expressing *35S$_{pro}$:MRG1mutBS* exhibited a more severe phenotype. They were darker green and smaller than their wild-type counterparts (Figure 27F-J). In addition, they displayed an undulated pattern of the leaf border. In four *35S$_{pro}$:MRG1* lines, the plants display darker pigmentation and leaves that differ slightly from the wild-type (Figure 27I). In one *35S$_{pro}$:MRG1* line, plants show up-curling and serrated leaves (Figure 27J). Plants that were kept in short days for six weeks and then transferred to long-day conditions for two more weeks showed additional phenotypes that differ from the wild-type (Figure 27K). Compared to the wild-type, overexpression of *MRG1*

seems to diminish apical dominance, which was more evident in lines carrying the mutated version of the gene.

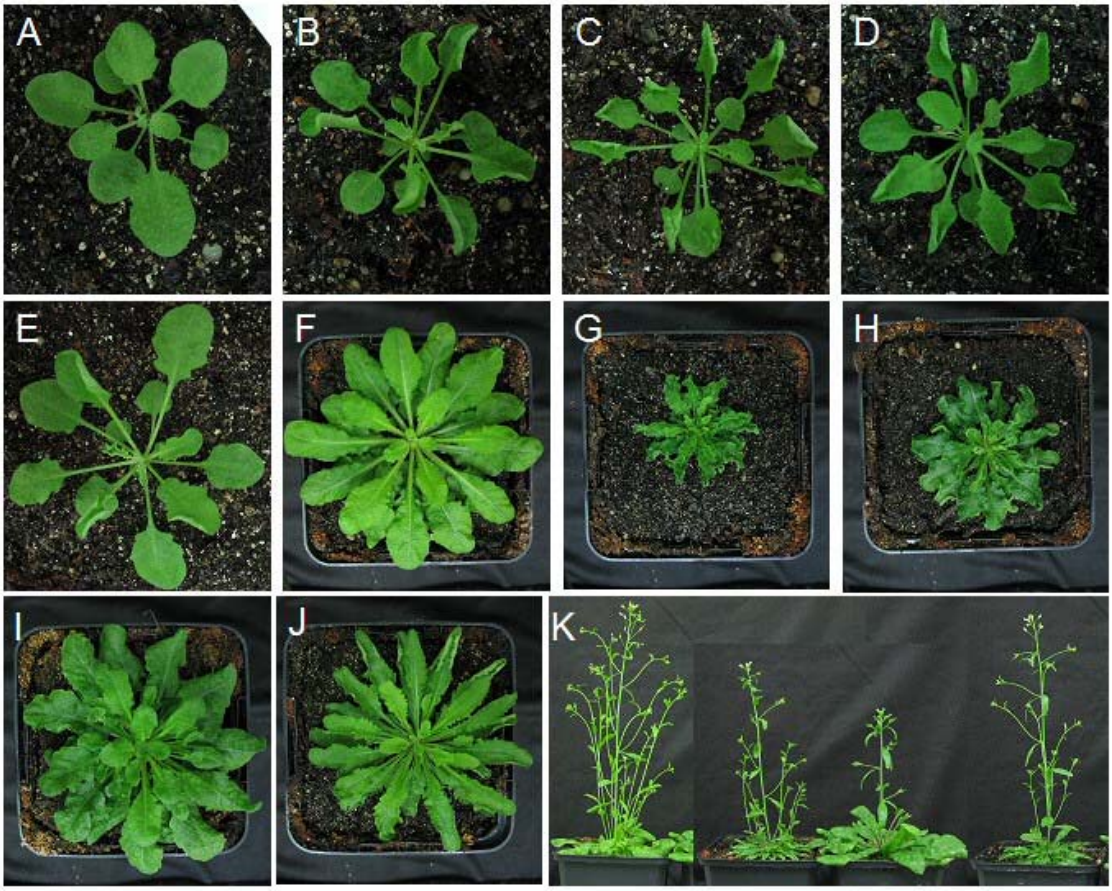

Figure 27. Effects of ectopic expression of *MRG1*
Overexpression of *MRG1* caused an up-curling leaf phenotype and elongated petioles in three-week-old seedlings maintained in short-day. Adult plants (before bolting) were ten weeks old, maintained in short-day. Plants from pictures A and F are Col-0; from pictures B, C, G and H are *$35S_{pro}$:MRG1mutBS* plants; from pictures D,E,I, and J were *$35S_{pro}$:MRG1* plants. Plants overexpressing *$35S_{pro}$:MRG1mutBS* exhibited a more severe phenotype. They were darker and smaller than the wild-type plants (G and H) and showed serrated leaves (G) or an undulated leaf border (H). *$35S_{pro}$:MRG* plants were darker and showed leaves that differ slightly from wild-type (I and J). Besides, in one line up-curling and serrated leaves were observed (J). Adult plants with inflorescence (K) were nine weeks old. They were kept in short days for six weeks and then, transferred to long-day conditions. In these plants, more secondary bolts were observed in plants that harbor both overexpressor constructs. In K, from the left to right: *$35S_{pro}$:MRG1mutBS* (same line as C and H), *35:MRG1mutBS* (same line as B and G), Col-0 and *$35S_{pro}$:MRG1* (same line as E and J). Plants from D and I were also from the same line. These plants were grown in a phytochamber.

Plants that were maintained at the greenhouse under short day conditions showed additional phenotypes. *$35S_{pro}$:MRG1mutBS* plants showed a bush appearance

due to a higher number of leaves (Figure 28A-B). In these plants, the rosette leaf morphology was also altered, the petiole was elongated and, the leaf blade size was reduced and up-curled. In addition, leaf blades were slightly serrated in the region proximal to the petiole (Figure 28C-E). The cauline leaves showed up-curling and undulated leaf margins (Figure 28F). At this stage and conditions, *35S$_{pro}$:MRG1* plants did not differ from the wild-type.

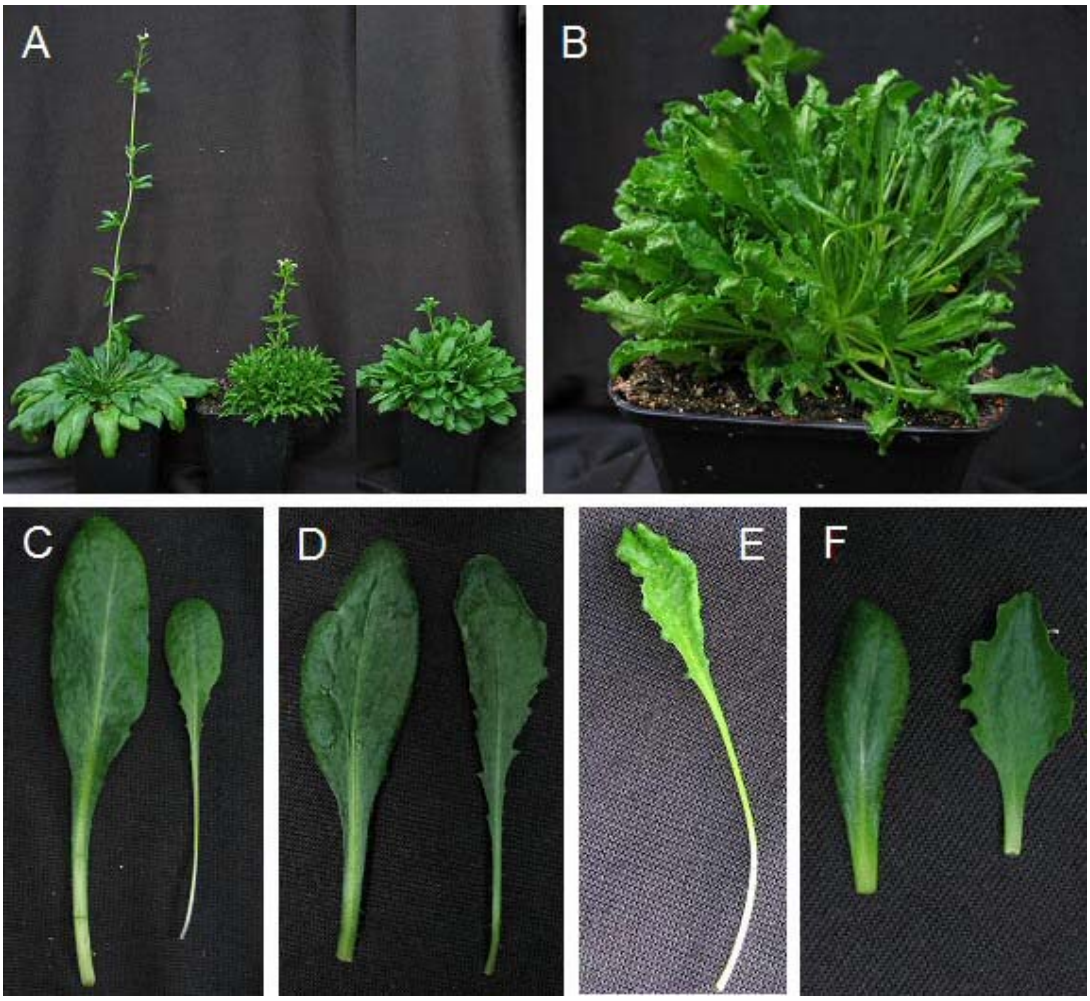

Figure 28. Additional phenotypes in *35S$_{pro}$:MRG1mutBS* plants
Plants kept in a greenhouse in short days showed an increased number of leaves (A, from left to right, Col-0 and two *35S$_{pro}$:MRG1mutBS* plants). A detailed view of the plant in the middle of picture A is shown in B. Leal morphology was also altered in *35S$_{pro}$:MRG1mutBS* plants (C, D, E and F). Rosette leaves had elongated petioles, small leaf blade areas and were often up-curled (C, D and E). Cauline leaves also show altered morphology, with up-curled and undulated leaf blade border (F). In C, D and F, leaves on the left are from Col-0 and those from on the right are *35S$_{pro}$:MRG1mutBS*.

3.4. Promoter analysis of miRNA genes

Promoters of three miRNA genes were investigated for spatial and temporal expression patterns. In addition, in two of them, the effect of serial deletions of the promoter sequence was also analyzed.

3.4.1. Promoter GUS lines

Promoter GUS lines were generated for *MIR159A*, *MIR159B* and *MIR161*. A fragment of *MIR159A* consisting of 1735 bp, from the beginning of the predicted stem loop sequence up to the next gene, was cloned in to the pCR2 vector (Invitrogen). In the same manner, a fragment of 2017 bp upstream of the predicted *MIR159B* precursor sequence was also isolated. Both promoter sequences were sub-cloned into pANGUS binary vector. The promoter of *MIR161*, starting at the precursor of *MIR161* and ending 2004 bp upstream, was cloned directly into the pANGUS vector. Promoter clones were transferred to Agrobacteria and transgenic plants were generated. After selection in the T1 generation, several lines for each construct were recovered and promoter activities were investigated in five lines of the T2 generation. By the time that these promoters were cloned, Xie *et al*., (2005) described the transcription start site for several miRNA promoters, including *MIR159A*, *MIR159B* and *MIR161*. The schematic representations of cloned miRNA promoters are presented in Figure 29. Transcription start sites are denoted as position +1. Positions +325, +481 and +138 represent the end of the cloned sequences, corresponding to the beginning of each miRNA precursor.

Figure 29. Schematic diagram of miRNA promoter GUS constructs.
Promoter of *MIR159A* (A), *MIR159B* (B) and *MIR161* (C) were cloned in front of the beta-glucuronidase (GUS) reporter gene *uidA* in the pANGUS vector.

The expression pattern of *MIR159A* using promoter GUS lines revealed that *MIR159A* is a gene active in many Arabidopsis tissues and, at different developmental stages (Figure 30). In seedlings grown on MS plates, GUS staining was observed in all parts, e.g. cotyledons, young leaves, primary root, secondary roots and roots hairs (Figure 30A-C). In adult plants, staining was detected in rosette leaves, in all flower organs and in the developing seedling (Figure 30A-C). No staining was observed in stems and cauline leaves.

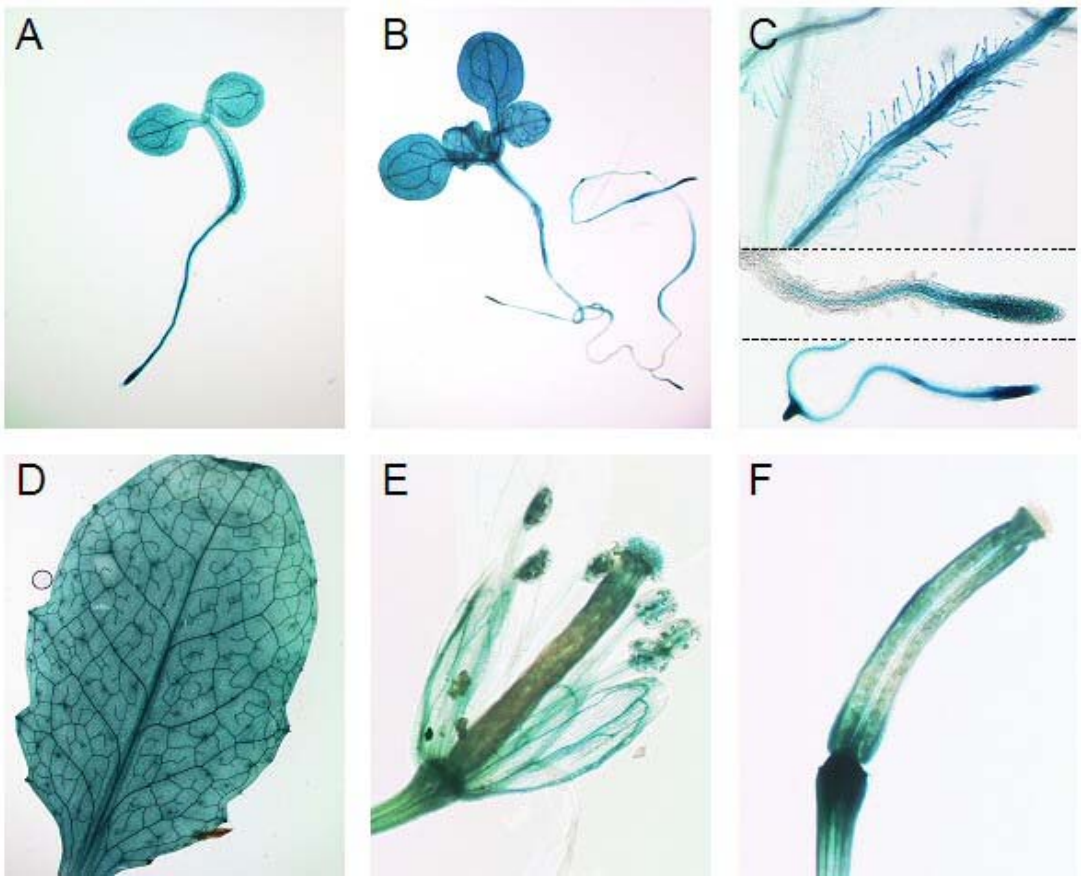

Figure 30. GUS staining of Arabidopsis harboring *MIR159A*$_{pro}$*:GUS* construct.
Seedlings were grown on MS plates. Plants were cultivated in short days for 8 weeks, and then three more weeks in long days. A and B, overview of Arabidopsis seedlings with 8 and 13-days-old, respectively. C, from above to bottom, Details of root hairs, primary root and secondary root. D-F, different tissues from adult plants. Rosette leaf, flower and silique in an early developmental stage, respectively.

The activity of promoter *MIR159B* showed a pattern overlapping with that of *MIR159A*. However, GUS staining of *MIR159Bpro:GUS* plants was generally much weaker. In seedlings, GUS staining was detected in cotyledons, in young leaves and in roots (Figure 31A-C). In roots, the GUS staining concentrated near to the root tip (Figure 31C).

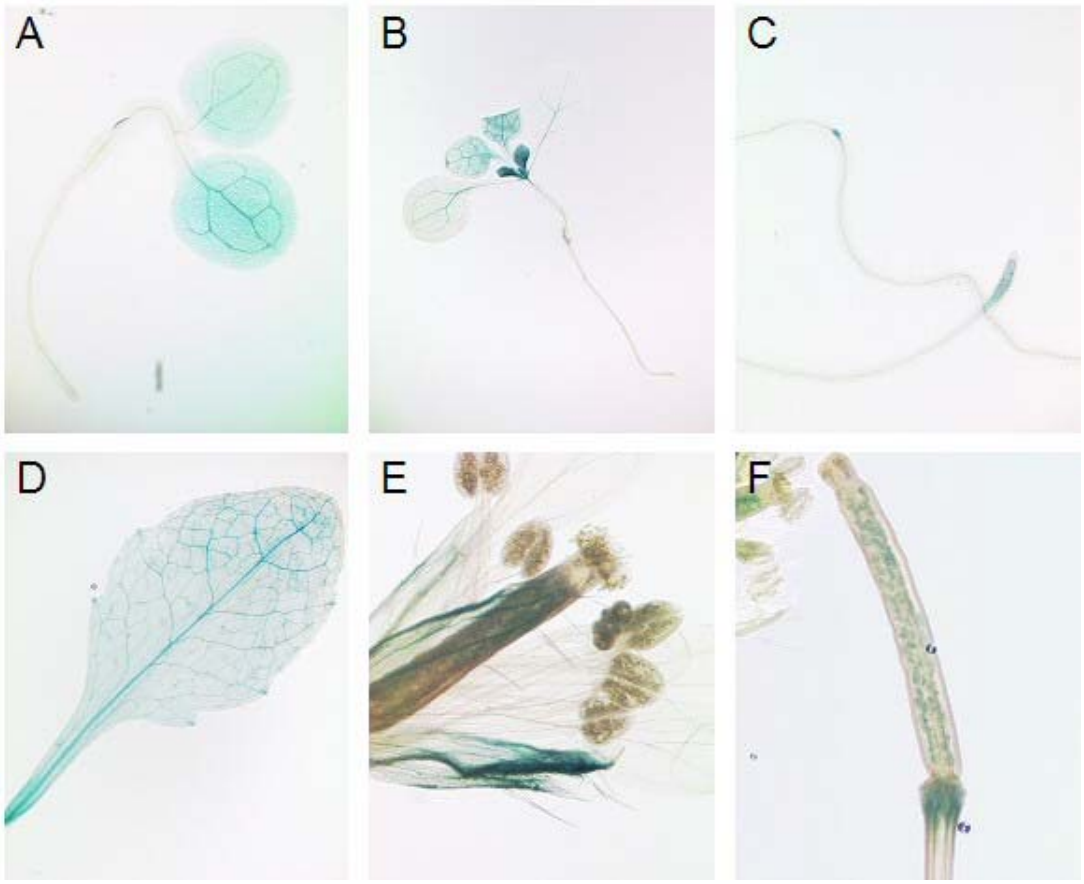

Figure 31. GUS staining of Arabidopsis harboring *MIR159b*$_{pro}$*:GUS* construct. Seedlings were grown on MS plates. Plants cultivated in short days for 8 weeks and three more weeks in long days. A and B, overview of Arabidopsis seedlings with 8 and 13-days-old, respectively. C, details of staining in roots. D-F, different tissues from adult plant. Rosette leaf, flower and silique in early developmental stage, respectively.

A fragment of 2004 nucleotides from the stem-loop of *MIR161* upstream to the next gene was used to analyze the promoter activity of *MIR161*. This gene seems to be expressed in a broad range of tissues (Figure 32). This promoter showed a strong activity in seedlings where GUS staining was detected in cotyledons, hypocotyls, roots, root hairs, secondary roots and emerging leaves (Figure 32A-

D). Activity of this promoter was also observed in adult leaves, restricted to leaf veins, and in cauline leaves (Figure 32F and G). In flowers, promoter activity was observed in sepals, petals, pistils and pollen (Figure 32H-I). No staining was observed in stem and seeds inside siliques, but the siliques themselves showed GUS staining as well as the petioles (Figure 32E).

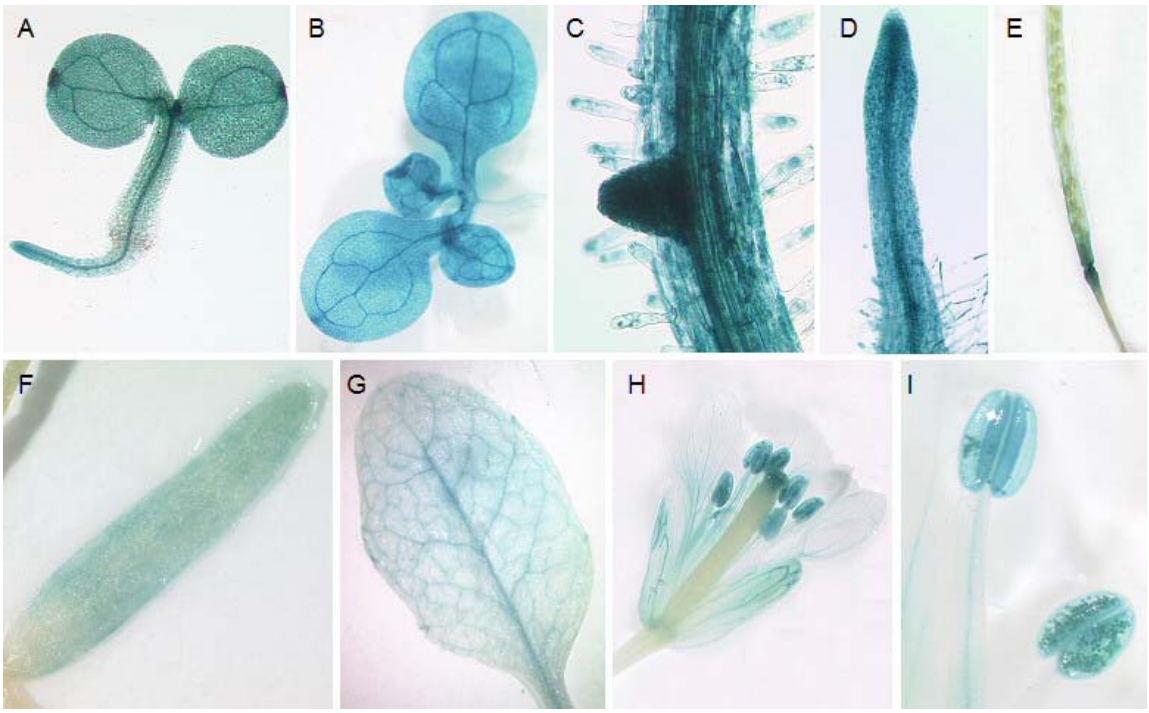

Figure 32. GUS staining of Arabidopsis harboring *MIR161*$_{pro}$*:GUS* construct.
Seedlings were grown on MS plates. Plants were cultivated in short days for 8 weeks and three more weeks in long days. A and B, overview of Arabidopsis seedlings with 8 and 13days-old, respectively. C-D, details of secondary roots and primary roots, respectively. E-I, different tissues from adult plants. Silique, cauline leaf, flower, rosette leaf and stamen, respectively.

3.4.2. Analysis of effect of serial deletions of miRNA promoters

Having analyzed the expression pattern of miRNA genes and miRNA target genes, it would also be important to investigate regulatory units of miRNA promoters. To elucidate this question, a series of promoter deletions fused with the GUS reporter were generated for analyzing the presence of regulatory units in *MIR159A* and *MIR161* promoters. Fragments with different lengths of *MIR159A* and *MIR161* promoters cloned into the pBT10 vector were transfected into AT7 protoplasts. After 24 hours, proteins were extracted and GUS activity was

measured. A promoterless pBT10 vector was used as a negative control and *35S$_{pro}$:GUS* was used as positive control.

The *MIR159A* promoter fragment that comprehends the portion from -802 to +1 showed the highest GUS activity, comparing with either the promoterless construct or the construct +1 to +325. The deletion of portions from -1136 to -802 and -552 to -244 increased the GUS activity, whereas deletion of the portions -802 to -552 and -416 to -244 caused a decrease in the GUS activity (Figure 33A).

The GUS activity from protoplasts transfected with promoter constructs whose sequence covering -1866 to +138, -1387 to +138, -1050 to +138, -810 to +138, -406 to +138 and -206 to +138 were approximately 120 to 150-fold higher compared to the promoterless construct or with the construct containing the portion from +1 to +138. A specific region, ranging from -618 to +138, showed higher gene expression than others *MIR161* promoter constructs and the core promoter of *MIR161* may consist of a region from -618 to +1. (Figure 33B).

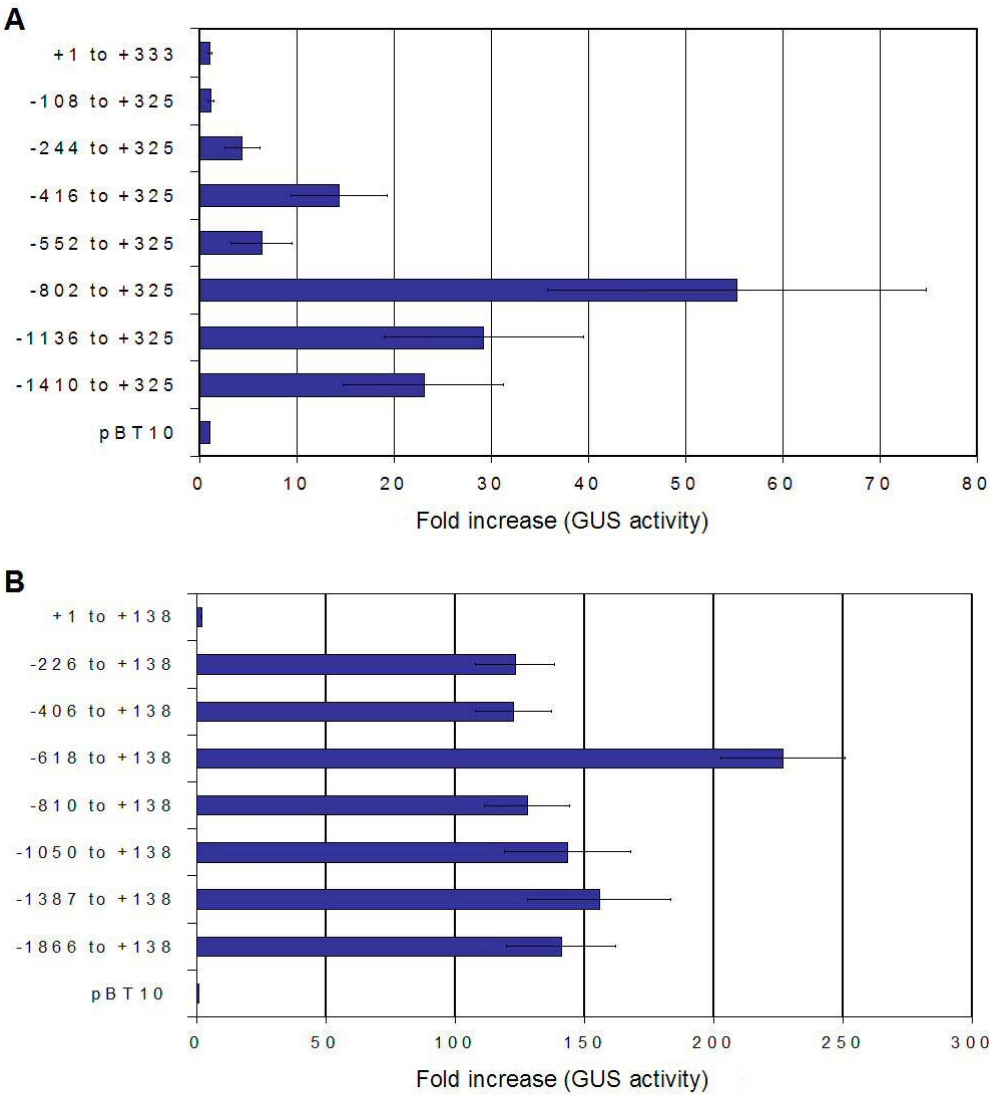

Figure 33. Analysis of deletions in miRNA promoters.
GUS activity in protein extracts of AT7 protoplasts transfected with constructs bearing different deletion constructs of *MIR159A* (A) and *MIR161* (B) of promoters.

4. Discussion

4.1. Prediction and validation of miRNA targets

After the discovery of miRNAs in plants, the next question to be answered was which genes are actually regulated by miRNAs. Bioinformatics predictions of miRNA targets were successfully applied for identification of many miRNA targets (Park *et al*., 2002; Reinhart *et al*., 2002; Rhoades *et al*., 2002; Jones-Rhoades and Bartel, 2004; Sunkar and Zhu, 2004; Wang *et al*., 2004b; Adai *et al*., 2005; Rusinov *et al*., 2005; Schwab *et al*., 2005). Rhoades *et al*. (2002) applied a pattern search technique in order to identify only putative miRNA targets that show complementarity to the miRNA higher than 85%. However, one of the filters they applied in their prediction prevented the prediction of miR163 targets, simply because of the fact that there is a bulge in the hybrid between miR163 and its targets, for a better alignment. In other words, a small change in the algorithm would allow confident prediction of more novel targets. However, when such assumptions are integrated into a bioinformatic prediction pipeline, a drawback is also introduced. The number of wrongly predicted targets is most probably increased. To cope with this problem of high numbers of false-positives, an approach based on comparative genomics was employed (Jones-Rhoades and Bartel, 2004).

The comparative genomic approach consists in the search for a miRNA target in more than one species. The predicted targets are compared to find those that are homologous and predicted as targets for the same miRNA. Thus, miRNA targets with a slightly lower complemetarity than 85% were predicted if any of its homolog also possesses a miRNA binding site for the same miRNA. A miRNA target that is found in only one of the analyzed species would not be considered as a target candidate then, unless the complementarity between the miRNA and its target was high enough. The use of comparative genomics contributed to the prediction of many novel miRNA targets (Jones-Rhoades and Bartel, 2004; Sunkar and Zhu, 2004; Wang *et al*., 2004b; Adai *et al*., 2005).

On the basis of the analysis of genes that were downregulated in transgenic Arabidopsis lines overexpressing miRNA genes, Schwab *et al*. (2005) proposed

some rules to define a miRNA binding site in plants that can be applied as an alternative to avoid the comparative genomics approach (see Figure 4). In the proposed model, there would be no mismatch in the presumptive cleavage site, no more than one mismatch in the positions 2 to 12, and no more than two consecutive mismatches downstream of position 12 (counting from the 5'end of the miRNA). Finally, the MFE of the miRNA:target duplex should be equal or smaller than -30 kcal/mol and at least 72% as compared to a perfectly complementary miRNA:target duplex (Schwab *et al*., 2005).

The approach described in this work to predict miRNA targets in Arabidopsis exploited the program RNAhybrid. RNAhybrid searches for the energetically most favorable hybridization between two sequences based on RNA:RNA hybridization rules (Rehmsmeier *et al*., 2004). The assumptions used in this work are very similar to those proposed by Schwab *et al*. (2005), with slight differences. Even though there are examples that a miRNA binding site can have a mismatch close to the possible cleavage site (Figure 13;Vazquez *et al*., 2004), a mismatch near or in the presumptive cleavage site would decrease the efficiency of the RISC cleavage (Laufs *et al*., 2004; Mallory *et al*., 2004b; Parizotto *et al*., 2004; Vaucheret *et al*., 2004). This characteristic is also true for animal miRNAs (Lewis *et al*., 2003; Doench and Sharp, 2004; Brennecke *et al*., 2005), although most of the animal miRNAs do not lead to cleavage of mRNAs. Therefore, no mismatches were allowed at the nucleotides 8 to 12 of the miRNA. The second and third rules are base on miRNA:mRNA hybrids of validated targets. In these interactions, a mismatch loop should not contain more than two nucleotides in each strand and bulge loops (nucleotide(s) unpaired in either of the strands) were not allowed with more than one nucleotide. The main difference of this approach is that G:U base pairings are not always considered as a mismatch in the RNA:RNA hybridization (see Figure 6).

In RNA:RNA hybridization, base pairing can occur not only according to canonical Watson-Crick rules (A:U and G:C), but also by wobble pairing (G:U), although a G:U base pair cannot be considered as a full substitute for a canonical base pair. Structural studies of RNA have shown that the G:U base pair causes some distortions in the helical regions of dsRNA (Wohnert *et al*., 1999). In the prediction of miRNA targets with RNA hybrid, the G:U base pairing was not considered as a

mismatch. However, when the MFE of a miRNA:target duplex was calculated, a duplex with a perfect match results in a smaller MFE than a duplex that contains one or more G:U base pairing. This is because G:U base pairings lead to a less stable duplex, and, therefore, to a greater MFE value during the RNA structure assessment with RNAhybrid (Rehmsmeier *et al*., 2004).

RNAhybrid was used to predict Arabidopsis miRNA targets, and to sort them according to the calculated MFE of the hybrid duplexes. According to those assumptions described in this work, hybrid structures with four mismatch loops, each loop having two nucleotides, could be predicted as putative targets. To eliminate such kind of output, an interesting solution would be the use of comparative genomics to find the miRNA binding site in homologous sequences from other species (Jones-Rhoades and Bartel, 2004; Sunkar and Zhu, 2004; Wang *et al*., 2004b). In this work, a different approach was employed. The MFE of the hybrids was used as a cutoff in order to shorten the list of possible candidates, to maximize the number of true positives and to eliminate most of the true negatives. Therefore, the number of predicted targets of a set of 55 authentic miRNAs was compared with the number of predicted targets of a set of randomly generated miRNA sequences. For each miRNA sequence, ten cohorts were created and used to predict miRNA targets with RNAhybrid, applying the same Arabidopsis dataset and the same assumptions. The number of targets per miRNA was calculated for each set of miRNA, authentic and cohort, and the false-positive ratio was calculated by dividing the number of predicted targets per miRNA of the authentic set by the number of predicted targets per miRNA of the set of randomized miRNAs. In the data presented in Table 5, the signal-to-noise ratio refers to the number of targets per miRNA in the authentic dataset compared to the number of targets per miRNA predicted with the random dataset. For example, using an MEF cutoff of 70%, there are 1.7 targets per miRNA in the authentic dataset compared to 1.0 target per miRNA in the random dataset.

As expected, the higher the MFE cutoff the better is the signal-to-noise ratio. However, the sensibility, e.g. the number of experimentally validated targets, decreases with a higher MFE cutoff. In other words, more positives may be lost. The best situation would be to have a sensibility of 100%, which is reached when the 70% cutoff is applied, but the number of false positives would then be too high.

An MFE cutoff of 75% provides an acceptable ratio of signal-to-noise that does not result in a sensibility that is too low. 93.1% of the validated targets were recovered using this setting, leading to 2.6 times more authentic targets as expected by chance. A similar result was found by Rajagopalan *et al*. (2006) when predicting targets of newly identified Arabidopsis miRNAs that were not found in other plant species, achieving a sensibility of 86% and a signal-to-noise ratio of 3:1, which was calculated in the same way as in the present work.

Most of the predicted and validated miRNA targets are genes that encode transcription factors (Dugas and Bartel, 2004; Jones-Rhoades *et al*., 2006). However, the high number of transcriptions factors may reflect just the occurrence of many transcription factors in the Arabidopsis genome. To evaluate this hypothesis, the GO annotation of the whole genome of Arabidopsis was assessed. The percentage of each category was used to normalize the GO annotation results from previously predicted/validated and novel putative targets predicted in this work (Figure 9). The percentage of transcription factors in the previous predicted/validated group was 4 times the percentage of transcription factors in the whole genome categorization. The high number of transcription factors among miRNA targets reflects the key role of miRNAs in gene regulatory networks (Jones-Rhoades *et al*., 2006). For the putative targets presented here, no major GO category was overrepresented. In addition, this work contributed to identify novel putative targets among GO categories that were underrepresented in the previously predicted/validated group. Putative targets within GO categories like protein binding, transporter, nucleic acid binding, kinases, hydrolases and DNA/RNA binding had similar hit frequency as compared their occurrence in the whole genome categorization (Figure 9). Thus, the spectrum of miRNA regulation may be broader than considered before.

For four miRNA families miR396, miR413, miR774, and miR783 more than 20 miRNA targets were predicted, along with some already predicted targets. This may constitute a group of miRNAs with many distinctive functions. In plants, the number of targets per miRNA family is much smaller than in metazoan (Mallory and Vaucheret, 2006; Zhang *et al*., 2007). In humans, for example, miR1 and miR124 seem to downregulate a far greater number of targets than previously predicted, by reducing the levels of many of their target transcripts, not just the

amount of protein that derive from these transcripts (Lim *et al*., 2005). In plants, miR159 is an example of a miRNA with diverse functions. Among its eleven predicted targets there are genes that encode seven MYB transcription factors of the group 7 (GAMYBs), as well as MYB125, OPT1, ACS8 and At1g29010 (Rhoades *et al*., 2002; Jones-Rhoades and Bartel, 2004; Schwab *et al*., 2005). This work contributed six candidate targets. Seven miR159 targets were experimentally validated: *MYB33*, *MYB65* (Palatnik *et al*., 2003; Jones-Rhoades and Bartel, 2004), *OPT1* (Schwab *et al*., 2005)*, MYB101* (this work and Reyes and Chua, 2007), *MYB125, ACS8* and *MRG1* (this work). Therefore, miR159 is involved in many different biological processes, ranging from GA signaling and flowering transition to oligonucleotide transport, control of the male gamete formation, regulation of the biosynthetic pathway of the plant hormone ethylene, ABA signaling, and leaf morphogenesis (Rhoades *et al*., 2002; Jones-Rhoades and Bartel, 2004; Schwab *et al*., 2005; Reyes and Chua, 2007).

Among novel predicted miRNA targets of conserved miRNA genes are AtEYA (miR157), which encodes a tyrosine-specific phosphatase that participates in regulating cellular tyrosine phosphorylation levels (Rayapureddi *et al*., 2005). One predicted target of miR160, BAG1, along with other members of the BAG gene family, has functional roles in cell protection under stress and inhibition of programmed cell death (Doukhanina *et al*., 2006). One of the predicted targets of miR167 is a gene that encodes the topoisomerase AtTOPII, which is involved in DNA replication and chromatin condensation. In Arabidopsis, the levels of *AtTPOII* are higher in seedlings than in mature plants, correlating with high cell proliferation observed in developing seedlings (Xie and Lam, 1994). Thus, miR167 may also control cell cycle by reducing the levels of *AtTOPII*.

SPOROCYTELESS encodes a putative transcription factor that is involved in both micro- and megagametogenesis. In *sporocyteless* plants, a perturbed sporocyte formation was observed leading to complete sterility plants (Yang *et al*., 1999). Along with *MYB33* and *MYB65*, *SPOROCYTELESS* is another target of miR159 that is involved in male fertility. In double mutant plants *myb33 myb65*, the male gametogenesis is arrested, resulting in no pollen production owing to an overwhelming growth of tapetum cells and consequently degradation of microsporocytes (Millar and Gubler, 2005). The *sporocyteless* mutation blocks the

differentiation of primary sporogenous cells into microsporocytes and anther wall formation resulting in anthers that are composed of highly vacuolated parenchyma cells (Yang *et al*., 1999). miR159 overexpressing plants were male sterile, showed increased size and darkening of anthers. Siliques were smaller that wild-type and contained no seeds. The downregulation of *MYB33* by miR159 was the explanation for these phenotypes (Achard *et al*., 2004). Thus, miR159 seems to be an important regulator of the male gametogenesis.

miR397, for which three genes encoding laccases were validated as targets (Jones-Rhoades and Bartel, 2004), may participate in the regulatory network that controls cell cycle. E2F is a transcription factor that stimulates the transcription of genes necessary for G1-to-S and S phase progression during cell cycle. For E2F function, the presence of the dimerization partner A (DPA) is necessary (Vandepoele *et al*., 2002; Magyar *et al*., 2005). DPA is encoded by a gene predicted to be a target of miR397.

miR319 regulates the expression of a few *TCP* transcription factor genes, whose downregulation cause abnormalities in leaf development (Palatnik *et al*., 2003). Leaves of miR319 overexpressing plants can not be flattened without cutting leaf margins, because of a crinkled phenotype. This phenotype is caused by a delay in cell division and differentiation arrest, leading to accumulation of excess cells in the leaf periphery margin. miR319 may also regulate a gene involved in cell division and elongation in the growth zone of the root tip, *BREVIS RADIX* (*BRX*). The lack of *BRX* expression causes reduction in root size, due to a decrease in cell number and cell length. The reporter protein GFP was not detected in plants carrying a reporter construct containing the *BRX* promoter and *GPF*, yet a construct with PRO_{BRX}*:BRX:GFP* could rescue the *BRX* phenotype, although the level of BRX protein detected by western blot with GFP antibody was very low (Mouchel *et al*., 2004; Mouchel *et al*., 2006). Interestingly, the predicted binding site of miR319 is located in the *BRX* promoter, and miR319 may act to keep *BRX* transcript at a low level, but high enough for the function of the BRX protein.

Recently, the involvement of miRNAs, as well ta-siRNAs, in the flavonol and anthocyanin biosynthesis was described. Two MYB transcription factor genes, *MYB75/PAP1* and *MYB90/PAP2*, are targets of TAS4-siR81. The production of

TAS4 siRNAs is mediated by the recently described mi828 (Rajagopalan *et al*., 2006). miR408 may also regulate other step of the flavonol and anthocyanin biosynthesis. A predicted target of miR408 is a gene that encodes flavone-3-hydroxilase (F3H), which catalyzes the conversion of naringenin in dihydrokaempferol. Another interesting example of a miRNA possibly regulating the level of an enzyme that acts in a biosynthetic pathway is miR396, whose predicted target, *ASA1*, encodes an alpha subunit of anthranilate synthase, the enzyme in the first step of the biosynthetic pathway of the amino acid tryptophan (Niyogi and Fink, 1992).

Copper is transported into chloroplasts by two mechanisms in Arabidopsis (Abdel-Ghany *et al*., 2005; Seigneurin-Berny *et al*., 2006). PAA1 and PAA2 sequentially mediate copper transport to the chloroplast envelope and tylakoids, respectively (Abdel-Ghany *et al*., 2005). An additional mechanism for copper uptake into chloroplasts was recently discovered, involving HMA1, a P1B-type ATPase. Like PAA1, HMA1 is localized in the chloroplast envelope (Seigneurin-Berny *et al*., 2006). Two miRNAs possibly regulate the copper level in the chloroplast; PAA2 and HMA1 are predicted targets of miR408 and miR773, respectively. These two miRNAs would participate together with miR398 in the regulation of copper homeostasis. In plants growing in MS medium with the standard amount of copper, miR398 was detected in northern blots. On the contrary, miR398 targets, *CSD1* and *CSD2* are detected at very low levels. In plants growing on MS medium supplemented with copper, decreased levels of miR398 and increased levels of CDS1 and CDS2 were detected (Yamasaki *et al*., 2007).

The Pentatricopeptide repeat (PPR) family of proteins represents one of the biggest protein families in Arabidopsis with over 450 members, most of which are predicted to localize in the plastids or the mitochondria. The biological functions of PPRs are not known. Only a few members of the PPR family have been characterized. They have been implicated in RNA metabolism, acting in a sequence-specific manner in both mitochondria and plastids (see Shikanai, 2006). *PPR*s are among predicted and validated targets of miR161 and miR400 (Rhoades *et al*., 2002; Sunkar and Zhu, 2004; Allen *et al*., 2005). In this work we found another *PPR* gene as putative target of miR161 and four *PPR* genes as novel candidate targets of miR400 (Figure 10). In addition, four other miRNAs may

be implicated in the regulation of *PPR*s; miR167, miR394, miR396 with one putative target each, and miR773 with two target candidates. The PPR proteins are encoded by genes that were either predicted or validated as miRNA targets, but have not been functionally characterized, as it is the case for most PPR proteins. However, in Arabidopsis, the functionally characterized PPRs act in RNA editing, RNA cleavage, RNA stabilization during translation and RNA cleavage during splicing (Hashimoto *et al*., 2003; Meierhoff *et al*., 2003; Yamazaki *et al*., 2004; Kotera *et al*., 2005). Therefore, miRNAs may have specific functions regulating RNA maturation, editing and stabilization.

The involvement of miRNAs in flower development was described for miR156, miR159, mir164 and miR172. They influence flower development because they control the expression of genes involved in floral organ identity, flowering time control, *LFY* expression and the number of petals. miR413 is possibly another miRNA involved in flower development. Two of its predicted targets affect the expression of *Flowering Locus C* (*FLC*) by means of chromatin modifications. FLC is a repressor protein that acts inhibiting the floral transition (Michaels and Amasino, 1999). Mutants in genes that participate in the activation of *FLC* have in common an early-flowering phenotype. One of the predicted miR413 targets, *Early Flowering 8* (*ELF8*) is a gene encoding a protein that is required for histone 3 trimethylation at Lys 4 in the *FLC* chromatin. The reduced level of *FLC* chromatin methylation observed on *elf8* plants resulted in low expression of *FLC* and early flowering in both short and long-day conditions (He *et al*., 2004). The second putative target of miR413 that affects the *FLC* expression is *AtMBD9*, one among 13 Arabidopsis proteins that contain a methyl-CpG-binding domain. In *atmbd9* plants, the early flowering phenotype was explained by the reduced, yet still detectable, level of *FLC* as a consequence of a decreased level of acetylation in histones 3 and 4 of *FLC* chromatin (Peng *et al*., 2006). Thus, miR413 may regulate the level of *FLC* by two distinct mechanisms, although both mechanisms modify the state of *FLC* chromatin.

The influence of miRNAs on their own biogenesis and functional mechanism of action were described by the role of miR162 and miR168 in the regulation of *DCL1* and *AGO1*, respectively (Xie *et al*., 2003; Vaucheret *et al*., 2004). Moreover, miRNAs are involved in the biogenesis of ta-siRNAs by initiating the phasing

process that results in the production of ta-siRNAs (Peragine *et al*., 2004; Vazquez *et al*., 2004b; Allen *et al*., 2005; Chen *et al*., 2007). The gene silencing induced by DNA methylation mediated by siRNAs may also be subject to regulation by miRNAs. The gene that encodes the largest subunit of RNA polymerase IV (RNPD1A) was predicted as a miR415 target. In *rdr2*, *dcl3* and *rnpd1a* mutant plants, siRNAs of 24 nucleotides were not detected. Therefore the proposed model for origin of these siRNAs was summarized as follows: transcription by RNPD1A, synthesis of RNA double strand by RDR2 and the double-stranded RNA would be processed into siRNA by DCL3 (Hamilton *et al*., 2002; Herr *et al*., 2005).

Many of the previously predicted and validated targets of a given miRNA belong to a gene family (Jones-Rhoades *et al*., 2006). The novel putative targets found in this work, in general, do not fall in the same miRNA family of previously predicted or validated targets. However, for two miRNA families, most of the novel predicted targets belong to the same gene family. Five predicted targets of miR774 are members of the S-locus protein kinase gene family (Figure 11A), whereas Ulp1 protease gene family has seven members predicted as miR781 target (Figure 11B).

The simplest way to experimentally validate a miRNA target is by use of a modified version of 5'RACE. This approach was widely applied to experimentally validate plant miRNAs because of the main mode of action of miRNAs in this kingdom (Chen, 2005; Jover-Gil *et al*., 2005). Plant miRNAs show a high degree of complementarity to theirs targets and they act like endogenous siRNAs that cleave the mRNA molecule that is complementary to them. The recovery of cleavage products using 5'RACE allows the identification of the precise point where the cleavage happened (Llave *et al*., 2002a). This experimental validation proves whether the mRNA of the target can be cleaved *in vivo.* However, it does not reveal the functionality of this cleavage event and the effects on target mRNA accumulation. In addition, 5'RACE can be used only for targets that are regulated by miRNAs that act like siRNAs, therefore targets that are regulated by a mechanism that inhibits the mRNA translation without changing in the mRNA level cannot be validated with such an approach.

For 5'RACE target validation, co-expression of the miRNA and its target must exist. In this work, the 5'RACE experiments were performed with RNA samples extracted from Arabidopsis AT7 protoplasts co-transfected with constructs that overexpress both miRNA and its putative target. Before 5'RACE experiments, the capability of the cloned pre-miRNA, corresponding to the smaller sequence that can be folded into a stem-loop, in expresses a mature miRNA was tested. Constructs harboring a pre-miRNA sequence were transfected in AT7 protoplasts, RNA was extracted and analyzed by northern blots. The presence of mature miRNAs was observed in constructs that lead to the overexpression of pre-miRNA of miR156, miR159, miR161 and miR395. However, only miR161 and miR395 showed higher expression of the mature miRNA in protoplasts transfected with the pre-miRNA construct compared to the control, for which protoplasts were transfected with the empty vector only. The overexpression of several miRNAs was not changed when genomic fragments that contained the pre-miRNAs were as large as 1.5 kb or was limited to the size of the predicted pre-miRNA (Schwab *et al*., 2005). The *35S*$_{pro}$:pre-miR172 construct is made up with the sequence of the pre-miR172a. It may be possible that to overexpress miR172 a sequence that contains not only the pre-miRNA (the stem-loop) but the complete transcript is needed. Two different cDNAs of the *MIR172* were found in the Genbank database (BX820161 and AK118705), both cDNAs are bigger than the pre-miR172a.

The same explanation may be valid to explain the failure of miR414 overexpression. A cDNA (DR368538) corresponding to the *MIR414* is much bigger than the predicted pre-miR414. However, different groups (Xie *et al*., 2005 174; Rajagopalan *et al*., 2006 351) questioned the classification of miR414 as authentic miRNA, based on expression level and the repetitive nature of its sequence. It is worth to mention that miR414 was first predicted as a miRNA, but was not cloned. The only evidence of expression is its detection in a northern blot experiment (Wang *et al*., 2004b). The presence of miR414 was not detected in northern blots with samples from different tissues of Arabidopsis (data not show). In addition, deep sequencing of small RNA samples, performed by three different groups, did not find any evidence of miR414 expression (Lu *et al*., 2005a; Rajagopalan *et al*., 2006; Fahlgren *et al*., 2007). Therefore, either miR414 is expressed under very specific conditions, or it may a represent non-miRNA locus (Xie *et al*., 2005;

Rajagopalan *et al*., 2006). The miRNA target prediction presented here could find more than 300 putative targets of miR414, many of them having miRNA binding sites with perfect complementarity to miR414. Thus, it is conceivable to assume that a high expression of miR414 would lead to a collapse because of many potential targets that would be downregulated at the same time. The miR414 putative targets are, therefore, not included in this work. The other computationally predicted miRNAs that were also not cloned or found in the deep sequencing studies, may also not be authentic miRNA genes. They are miR413, and miR415 to miR420 and miR426 (all described in the same study as miR414; Wang *et al*., 2004). However, unlike miR414, the overexpression was not assayed in this work and the predicted targets are listed in the Appendix 2.

In the 5'RACE experiments described in this work to validate miRNA targets, the source for total RNA were Arabidopsis AT7 protoplasts co-transfected with both the pre-miRNA and the target cDNA constructs. Five miRNA targets were validated, four targets of miR159 (*MYB101*, *MRG1*, *MYB125*, *ACS8*); and *GAE1*, which is a target of miR161 (Figure 13).

Along with *MYB33* and *MYB65*, *MYB101* was the third GAMYB encoding gene validated as miR159 target. The cleavage of *MYB101* mediated by miR159 was demonstrated by 5'RACE, as it was recently showed by Reyes and Chua (2007). The expression of *MYB101* was reduced in plants overexpressing miR159 indicating the regulatory role of miR159 over *MYB101*, although the expression level of *MYB33* and *MYB65*, which were already validated by 5'RACE as miR159 targets, were not reduced in the same plants, (Schwab *et al*., 2005). Another gene encoding a MYB transcription factor was validated as miR159 target, *MYB125/DUO1*. Interestingly, *MYB125/DUO1* is another example of a miR159 target involved with pollen development. *myb125/duo1* plants are male sterile owing to a formation of a large diploid sperm cell that is unable to fertilize an ovule (Durbarry *et al*., 2005; Rotman *et al*., 2005). So far, three validated targets of miR159 are involved in proper pollen formation, null mutants of *MYB33 MYB65*, *MYB125* displayed male sterility. Plants lacking *SPOROCYTELESS* are also male sterile, and the expression pattern of *MYB101* also indicated a possible role of this gene in gametogenesis (Figure 18 and Figure 19).

Two other targets of miR159 validated in this work are not involved in gametogenesis. *ASC8* encodes 1-aminocyclopropane-1-carboxylic acid synthase, which is a key enzyme in the biosynthesis of the plant hormone ethylene (Vandenbussche *et al*., 2003). In Arabidopsis, the ACS family contains 11 genes and one pseudogene. The functional genes form eight functional (ACS2, ACS4-9, and ACS11) homodimers, and 17 functional heterodimers. It has been postulated that the presence of ACS isozymes may reflect tissue-specific expression that is required by the biochemical environment of the cells or tissues in which each isozyme is expressed (Yamagami *et al*., 2003; Tsuchisaka and Theologis, 2004a, b). *ACS8* transcript level was greatly reduced in miR159 overexpressing plants (Schwab *et al*., 2005). This was the first evidence that miRNA may regulate the production of the hormone ethylene, and here the functional cleavage of ACS8 mediated by miR159 was demonstrated. However, it is not clear if miR159 really influences ethylene biosynthesis because of the high redundancy of ACS isozymes that can perform the same catalytic step in the ethylene biosynthesis. The cleavage point mapped in the *ACS8* sequence did not match to the middle of the miRNA binding site, as normally is the case for RISC mediated-cleavage. However, examples of miRNA-mediated cleavage mapped downstream to the miRNA binding site have also been shown for several miRNAs and ta-siRNAs targets (Jones-Rhoades and Bartel, 2004; Allen *et al*., 2005; Lauter *et al*., 2005; Chen *et al*., 2007). The last validated target of miR159 is *MRG1*, which encodes a small protein of 301 amino-acid residues. The miR159 binding site is the only known motive found in both nucleotide and amino-acid sequences.

The cleavage characteristic of miRNA-mediated cleavage was demonstrated for *GAE1*, which encodes a UDP-4-epimerase. GAE1 convert UDP-D-glucoronate into UDP-D-galacturonate, which is responsible for the negative charge in pectic cell wall (Molhoj *et al*., 2004).

Four putative targets were not validated experimentally as miRNA target: *MYB94* (miR156), *CKL6* (miR159), *PRF2* (miR161) and *MYB58* (miR395). These putative targets are not present in the list in the Appendix 2 because the MFE of the duplex is smaller than 75% of the hybrid with perfect match. However, one of the validated targets, *GAE1*, also does not satisfy this assumption. In addition, the miR161:PRF2 hybrid has a mismatch in the position 12. Nonetheless they were

chosen for validation experiments because their hybrids structure showed less than five mismatches (Figure 14). The failure in the validation of most of the targets with less than 75% of the MFE of the perfect match hybrid indicates that this cutoff is a good value to differentiate between most of the true miRNA targets. However, using this cutoff, the achieved sensibility was 93.1%, and the validation of *GAE1* confirms that some true miRNA targets are among the candidates eliminated by the 75% rule.

4.2. MYB101

The MYB101 is a transcription factor that is classified into the group of GAMYBs because MYB101 activate transcription by binding to a gibberellin-responsive element (GARE) in the alfa-amylase promoter in barley (Blazquez and Weigel, 2000). Together with all others Arabidopsis *GAMYBs* genes, *MYB101* was predicted as a miR159 target (Rhoades *et al*., 2002; Jones-Rhoades and Bartel, 2004). Evidence that miR159 would affect *MYB101* expression was found by Schwab *et al*. (2005). Analyzing miR159 overexpressing plants, they observed that the expression level of *MYB101* was greatly reduced, and the miR159-mediated cleavage of *MYB101* was demonstrated (this work and Reyes and Chua, 2007). The temporal and spatial expression pattern of *MYB101* was analyzed in the present work by means of promoter-GUS lines. In Arabidopsis, the promoter of the *MYB101* was active in seedlings, flowers and in root tips (Figure 19). The activity of the *MYB101* promoter in flowers was markedly intense in pollens grains, but was also observed in sepals, petals and stamen. The observed promoter expression pattern does not match to the expression pattern of *MYB101* analyzed with microarray data (Figure 18). The *MYB101* expression pattern according to AtGenExpress data, clearly show a specific expression in pollen. Northern blot analysis detected *MYB101* in flowers. In addition, *in situ* hybridization experiments localized *MYB101* transcripts in the hypocotyl hooks in germinating seeds (Gocal *et al*., 2001). The *MYB101* promoter is active in tissues where *MYB101* transcript is not found. The different expression pattern observed between microarray data and promoter-GUS lines suggest the importance of the regulatory role of miR159 over *MYB101*. The expression pattern of *MYB33* analyzed with promoter-GUS lines also showed evidence of constrained expression of this gene by miR159. In

proMYB33:GUS lines promoter activity in flowers (sepals, style, receptacle, and anther filaments), shoot apices, and root tips were observed. By contrast, analysis of *proMYB33MYB33:GUS* lines revealed that the reporter protein was detected solely in young anthers, and no staining was seen in shoot meristems or root tips (Millar and Gubler, 2005). The analysis of promoter activity defines the spatial and temporal expression pattern of *MYB101* based only in the promoter sequence. However, since *MYB101* is post-transcriptionaly regulated by miR159, this expression pattern does not reflect where the MYB101 protein accumulates. Experiments to characterize the *MYB101* accumulation pattern are under way.

The functionality of the miR159 binding site found in the *MYB101* gene was tested clarified by the use of transgenic plants that express both *MYB101* and *MYB101mutBS* under the control of the strong 35S promoter (Figure 15). The observation that in several lines of $35S_{pro}$*:MYB101* plants the *MYB101* transcript was not detected in leaves by RT-PCR, whereas *it* was detected in $35S_{pro}$*:MYB101mutBS* plants, supports the functional role of miR159-based regulation of *MYB101* (Figure 16). This confirms that *MYB101* expression in many tissues is constrained by miR159. However, according to promoter-GUS lines *MIR159A* is also expressed in pollens (Figure 30). Thus, it could be feasible that, in pollens, either *MYB101* expression is too high for a complete downregulation by miR159/RISC or the mature miR159 is not present in pollen. The two explanations are equally possible, however, control of the maturation of the miRNA was shown only in mammals to date. As an example, the pre-miR138 can be detected by northern blot in several cell lines, but the mature miRNA ca be detected only in specific cell lines (Obernosterer *et al*., 2006). Support for the second possible explanation comes from the observation that some validated miRNA targets did not show a strong decrease in mRNA levels in miRNA overexpressing lines (Schwab *et al*., 2005). Thus, the miRNA would not only act completely in downregulating a gene, but also providing a fine-tuning in the level of an mRNA. According to this model, called micromanager model, targets could be downregulated to levels that cannot be detected anymore, which is the case for most of plant miRNA:targets interactions. Other miRNA targets would suffer only slight downregulation, and the miRNA would act to keep the optimal level of the target mRNA transcript (Bartel and Chen, 2004; Mello and Czech, 2004).

Effects of ectopic expression of *MYB101* were observed in seedlings and in adult leaves (Figure 17). Seedlings that carry a construct to express both *MYB101* and *MYB101mutBS*, are smaller than wild-type. However, *MYB101mutBS* seedlings were much smaller than *MYB101* seedlings. Adult plants overexpressing *MYB101* did not differ from wild-type, whereas *MYB101mutBS* plants developed a phenotype similar to dwarfism, as adult plants were smaller than wild-type. Trying to understand the effect of the overexpression of *MYB101*, knockout lines were analyzed. Two T-DNA insertion lines for *MYB101* were found and in both lines the insertion event resulted in deletions of a few nucleotides (Figure 20). The deletions alone would result in a truncated *MYB101* protein. In addition, the full-length *MYB101* transcript was not detected by RT-PCR in both lines, confirming the efficient knockout of *MYB101* (Figure 21). However, no phenotypical changes were observed in any of these lines growing under short-day conditions. Overexpression of *MYB33* caused a very similar phenotype as overexpression of *MYB101* in seedlings (Palatnik *et al*., 2003), suggesting that these genes may share some overlapping functions. Recently, ABA hyposensibility was described for *myb33* and *myb101* single mutants (Reyes and Chua, 2007), but *myb33*, *myb65* or *myb101* plants do not differ in any other characteristic to wild-type plants (Millar and Gubler, 2005; Reyes and Chua, 2007), but a double mutant *myb33 myb65* displayed male sterility (Millar and Gubler, 2005).

Although data from this work extended the knowledge about *MYB101*, still many things have to be done for a deep understanding of *MYB101* function. Some experiments are currently being done, for example, analysis of double mutants (*myb33 myb101* and *myb65 myb101*) and the triple mutant *myb33 myb65 myb101*. The MYB101 protein contains a nuclear localization signal (NLS) and three nuclear export signal (NES), thus the cellular localization of MYB101 is not restricted to the nucleus. The MYB101 protein localized more to the nucleus but can also be found in the cytoplasm (Julia Starmann, personal communication). Another interesting analysis is the overexpression of *MYB101* with mutations in both miR159 binding site and NES. It may be possible that the uncoupling of MYB101 from these two different regulatory mechanisms, post-transcriptional regulation by miR159 and nucleo-cytoplasmatic partitioning (Merkle, 2003), may lead to a better understanding of the role of MYB101.

4.3. MRG1

The prediction and validation of *MRG1* as miR159 target was the initial step of the study of this gene. Because not much information about *MRG1* was available, the investigation of this gene started with the analysis of *MRG1* expression. The expression pattern of *MRG1* analyzed by RT-PCR revealed that *MRG1* transcripts can be detected, although to different levels, in most of the analyzed tissues (Figure 22). The expression pattern of *MRG1* in promoter-GUS lines also showed that *MRG1* could be found in many Arabidopsis organs, including seedlings (cotyledons, young leaves and root), flowers, adult leaves, roots and developing seeds (Figure 23). Evidence for *MRG1* expression in tissues where miR159 can be found may lead to the conclusion that *MRG1* may not be regulated by miR159. However, it was found that the level of *MRG1* transcript is very low in most of the tissues, as PCR products after 30 cycles were very faint. In additions, for many tissues, PCR products where observed only after 40 cycles. Thus, miR159 might be responsible for the low expression level of *MRG1*.

The functional regulation of *MRG1* by miR159 was also shown in transgenic lines that harbor the constructs *$35S_{pro}$:MRG1* or *$35S_{pro}$:MRG1mutBS* (Figure 25). The overexpression of *MRG1* was observed in all *$35S_{pro}$:MRG1mutBS* lines, whereas in most of *$35S_{pro}$:MRG1* lines the transcript was not detected (Figure 26). In addition, the main effect of the overexpression of *MRG1*, an altered leaf form observed during seedling stage and in adult rosette leaves, is much more severe in *$35S_{pro}$:MRG1mutBS* plants (Figure 27). The regulation of *MRG1* by miR159 could be an example that a miRNA does not necessarily need to completely eliminate an mRNA, but only keep it to a certain level for proper plant development. The relationship between miR159 and *MRG1* could be an example of the micromanager model of gene expression proposed for miRNA function (Bartel and Chen, 2004). Overexpression of *MRG1* also altered the plant appearance. In plants carrying both constructs there were more secondary bolts than in the wild type, thus showing a reduced apical dominance. These phenotypes were observed in plants growing in a phytochamber under controlled environmental conditions.

They were even more characteristic in *35S$_{pro}$:MRG1mutBS* plants grown in the green house, which is supplemented with artificial light but also receives natural light. Under these conditions, *35S$_{pro}$:MRG1mutBS* plants in short-days developed with a highly altered leaf appearance, as evident by the high number of adult rosette leaves observed, conferring a bushy phenotype due to the high number of leaves probably growing form axillary meristems (Figure 27). Leaves of these plants have longer petioles and smaller leaf-blade areas than wild-type plants (Figure 28). Overexpression of several transcription factor genes that are miRNA targets also caused many pleiotropic effects (Jones-Rhoades *et al*., 2006). There is no evidence that *MRG1* encodes a transcription factor. However, like many transcription factors, an MRG1:GPF fusion protein was localized in the nucleus compartment (Figure 24), although no conserved domain was found in the MRG1 sequence. To better understand the observed gain-of-function in *35S$_{pro}$:MRG1mutBS,* one *MRG1* T-DNA line was identified (data not show), but was not phenotypically analyzed yet.

Important aspects of leaf morphogenesis are conserved among distantly related plant species, for example the expression of class III HD-zip genes *REVOLUTA* (*REV*), *PHV* and *PHB*. They are responsible for the adaxialization of leaves and are controlled by miR166/165, which is conserved among all land plants including angiosperms, gymnosperms, ferns, lycopods and mosses (Floyd and Bowman, 2004). This is contradicting to the general model of leaf evolution that suggested that this organ may have evolved independently in these groups (Tsukaya, 2005). The leaf phenotypes observed in *MRG1* overexpressing plants are a mixture of several characteristics found in loss- or gain-of-function mutations of different genes involved in leaf morphogenesis. The high number of leaves growing from axiliary meristems resembled loss-of-function mutants of *BRANCHED1* (Aguilar-Martinez *et al*., 2007). Defects in leaf blade observed in *35S$_{pro}$:KNAT6* (Dean *et al*., 2004), *serrate, assymetric1* (Ori *et al*., 2000) and *angustifolia* (Folkers *et al*., 2002; Kim *et al*., 2002) mutant plants are not the same as observed in *35S$_{pro}$:MRG1mutBS* plants, but they are pretty much similar. However, overexpression of *MRG1* affected only the leaf development, where as most of these mutations have pleiotropic effects in the whole plant development (Tsukaya, 2003). All these mutant genes also have conserved homologs in different species.

MRG1, however, does not have any homolog in any other species, thus it may constitute a novel important gene involved leaf development and axillary bud development. Nonetheless, the control mechanism via miR159 is conserved in many plant species (Lu *et al*., 2005b; Zhang *et al*., 2005; Dezulian *et al*., 2006; Talmor-Neiman *et al*., 2006; Tuskan *et al*., 2006; Xie *et al*., 2007). In order to address the question of which are the genes whose expression levels are changed in *35S$_{pro}$:MRG1mutBS* plants, a microarray experiment for analysis of the global expression profile is currently being carried out.

4.4. Expression of miRNA genes

The evidence that miRNA genes are transcribed by RNA polymerase II (Aukerman and Sakai, 2003; Lee *et al*., 2004) and the analysis of primary transcripts from several miRNA genes (Xie *et al*., 2005) indicated that sequences upstream of the transcription start site could function as promoter, regulating miRNA expression. Furthermore, an insertional mutation in the promoter of *MIR164C* caused an aberrant phenotype due to the reduced level of miR164 (Baker *et al*., 2005). In addition to transcriptional regulation of the miRNA gene, the accumulation of a mature miRNA may be subject to regulation through any step of the miRNA biogenesis (Vaucheret, 2006).

The expression of miRNA genes was analyzed by the use of promoter-GUS lines of three miRNA genes: *MIR159A*, *MIR159B* and *MIR161*. Although this approach does not confirm the presence of the mature miRNA, it can be used to analyze the expression pattern of individual genes. Expression analysis of miR159 by northern blot detected a strong signal in seedlings and flowers and a less intense signal in rosette leaves, cauline leaves and siliques. No signal was detected in roots (Achard *et al*., 2004). The promoters of *MIR159A* and *MIR159B* were shown to be active in seedlings, roots, rosette leaves, flowers and siliques. Differential results were observed in roots and cauline leaves (Figure 30 and 29). It may be possible that both promoters are active in cauline leaves but not at a level to be analyzed by promoter-GUS lines. Because the three *MIR159* genes do not produce the same mature miRNA (Figure 5A), deep sequencing of small RNA samples can also discriminate *MIR159* transcripts, resulting in a quantitative profile of small RNA expression. Analysis of small RNA samples with a the new 454 sequencing

technology produced evidence for the expression of both *MIR159A* and *MIR159B* in flowers, roots, rosette leaves, seedlings and siliques (Lu *et al*., 2006; Rajagopalan *et al*., 2006; Fahlgren *et al*., 2007). Comparing the expression pattern of *MIR159A* and *MIR159B*, it is clear that *MIR159A* is the most important gene that produces the mature miR159, although, the expression pattern of both genes are very similar (Figure 30 and 29). This observation was also confirmed by data from small RNA expression profiles. The number of reads of *MIR159A* was always much greater that for the other two *MIR159* genes in all analyzed libraries. The expression of *MIR159C* is extremely small, as little as 4 transcripts per quarter million (TPQ), for *MIR159B* and *MIR159A*, 48 and 205 TPQ were found, respectively (Lu *et al*., 2006). Taking all miR159 transcripts into account, *MIR159A* counts for 82.7 to 87.6% of the total *MIR159* transcripts observed in different libraries, whereas *MIR159B* transcripts correspond to 9.9-16% and *MIR159C* for 0.1 to 2.4% of the total *MIR159* transcripts (Lu *et al*., 2006; Rajagopalan *et al*., 2006; Fahlgren *et al*., 2007).

The promoter of *MIR159A* was further analyzed in detail for the characterization of elements that may be important for the regulation of *MIR159A* expression. The sequence used for miR159 promoter-GUS lines was serially shortened from -1410 upstream down to the transcription start site. The expression of cloned promoters fragments was measured in the AT7 protoplast system. The core promoter of *MIR159A* seems to consist of the portion from -802 to +1, as the highest GUS activity was observed with this promoter fragment. Two regions in the *MIR159A* promoter seem to contain repressor properties. The difference observed in the GUS activity of the fragment -1136 to +1 to the fragment -802 to +1, and the fragment -416 to +1 compared to the fragment -552 to +1, revealed that transcription factors may recognize elements within the regions -1136 to -802 and -552 to -416 to affect *MIR159A* gene expression. In the same way, positive elements may be present in the regions -802 to -552 and -416 to -244 (Figure 30A). In the regions that were identified to be important for promoter activity, many putative transcription factor binding sites were predicted, a for example LEAFY consensus binding motive, a MYB binding site, a bZIP binding site, a RAV1-b binding site motive (Megraw *et al*., 2006), TATAbox motif (Xie *et al*., 2005), ABA responsive elements (Reyes and Chua, 2007) and potential GA responsive

elements (Achard *et al*., 2004). Using this information experiments are going to be done to identify which proteins bind to these specific regions of the *MIR159A* promoter. The presence of ABA and GA responsive elements on *MIR159A* promoter are in agreement with the role of these two hormones in over-accumulation of miR159 (Achard *et al*., 2004; Reyes and Chua, 2007). In addition, the observation that *MIR159A* and not *MIR159B* is induced by GA in seedlings (Niemeier, 2006) defined which member of the gene family is responsible to GA. Interestingly, the signal transduction of both hormones may be mediated by the product of two miR159 targets. MYB101 and MYB33 may mediate the effects of ABA in seedlings (Reyes and Chua, 2007) and MYB33 may act in the GA activation of LFY for promoting flowering (Gocal *et al*., 2001) and specifically in the anther development (Achard *et al*., 2004).

The expression of *MIR161* was initially analyzed by northern blots. The mature miR161 was detected in seedlings, leaves, stems, flowers and siliques (Reinhart *et al*., 2002). Reads of miR161 were also sequenced in samples of small RNA from flowers, roots, seedlings siliques, inflorescences and leaves (Lu *et al*., 2006; Rajagopalan *et al*., 2006; Fahlgren *et al*., 2007). In these studies, which are able to quantify the expression of miRNAs, *MIR161* was appointed to one of the most highly expressed miRNA genes. In this work, the expression of *MIR161* was analyzed using promoter-GUS lines (Figure 32). The signals of the reporter protein were very strong in all positive tissues. Interestingly, promoter activity was not found in stems. In pumpkin (*Cucurbita maxima*), several miRNAs were isolated from the phloem sap, but it is still unkown where they are produced (Yoo *et al*., 2004).

The serial deletions of the promoter of *MIR161* also demonstrated the high expression level of *MIR161* (Figure 33). For the 35S promoter, which is a known strong promoter, the GUS activity was 300-fold the GUS activity of the promoter-less construct (data not shown). Even the smallest promoter fragment,-226 to +1, was enough to set a high expression of the reporter gene, this portion may consist of the core *MIR161* promoter. In the *MIR161* promoter there are also two regions, to which transcription factors may bind and either suppress (-810 to -618) or activate (-618 to -406) the expression. Promoter motifs, such as T-Box, SORLREP3, DPBF1, DPBF2, MYB, SORLIP2, CATAbox (Megraw *et al*., 2006)

and TATAbox (Xie *et al*., 2005; Megraw *et al*., 2006), were found the *MIR161* promoter by in silico analysis.

4.5. Conclusions and outlook

In this work, different points concerning miRNA biology were addressed. Novel putative miRNA genes were predicted with RNAhybrid using additional assumptions to better discriminate between true and false miRNA targets. A total of 281 novel miRNA targets candidates were predicted, and many of them have predicted functions in biological processes to which only a few of the previously predicted or validated miRNA targets were assigned. This implies that possibly most of the miRNA targets are still transcriptions factors genes. However, the spectrum of miRNA regulation was broadened by many more processes. Some miRNA targets were experimentally validated using modified 5'RACE. Interestingly, many of the targets that were not experimentally validated also failed in pass the MFE cutoff proposed in this work, confirming that this cutoff can be used confidently for a miRNA target prediction.

Two miR159 targets were studied in more detail: *MYB101* and *MRG1*. Although both genes were investigated by means of overexpression lines, promoter-GUS lines, miRNA-resistant overexpressing lines, T-DNA insertion lines (*MYB101* only), expression pattern and cellular localization (*MRG1* only), the biological functions of these two genes are still unknown. According to the expression pattern, *MYB101* may participate, together with *MYB33* and *MYB65,* in pollen development. These three genes may act together because single null mutants did not show any defects in pollen nor were they infertile. Only the double mutant *myb33 myb65* showed a certain degree of male infertility.

For the future, genetic analyses with triple mutants of these genes are planned. In addition, overexpression lines of *MYB101* with mutations in the miRNA binding site and in the nuclear export signal are ready for analysis (Julia Starmann, personal communication). Depending on the results of these experiments, a further search for genes that are regulated by *MYB101* can be performed, for example, a microarray experiment using any of above mentioned lines.

In the case of *MRG1*, this work contributed with novel information about the pattern of expression, the effects of overexpression, the prediction and validation as miR159 target and the cellular localization. Still, no conclusion can be drawn, but it is clear that *MRG1* and miR159 (because its regulatory role over *MRG1*), influence leaf development and auxillary meristems. Whether these effects are caused directly by *MRG1* or whether they are indirect via unknown genes whose expression levels were altered by *MRG1* is still not known. However, experiments are actually underway to analyze the expression profile in *MRG1mutBS* overexpression lines.

The expression patterns of three miRNA genes were examined using promoter-GUS lines. This approach was particularly interesting for *MIR159A* and *MIR159B* because previous indications that *MIR159A* counts for the majority of the accumulation of mature miR159 was confirmed, although the promoter activity of one gene of the miR159 family was not analyzed yet. Furthermore, by a reporter assay, regulatory units within the *MIR159A* promoter were identified, two regions seem to be the place where proteins bind and repress *MIR159A* expression, whereas two other specific regions of the *MIR159A* promoter seem to be the place for binding of proteins that activate *MIR159A* expression. Similar serial deletions of the promoter of *MIR159B* will be performed. The expression pattern of *MIR161* was also analyzed using promoter-GUS lines and revealed that this is a broadly expressed miRNA. This was supported by the analysis of serial deletions in the *MIR161* promoter, given that even the smallest tested part of the promoter conferred high signal of the reporter gene. Within the *MIR161* promoter, regulatory units were also found, one that may act by suppression (thought not completely) and one that clearly acts by activation, conferring the highest *MIR161* expression. These regulatory units found in these two promoters can be used to identify proteins that bind and regulate the expression levels of these two miRNA genes.

5. References

Abdel-Ghany, S.E., Muller-Moule, P., Niyogi, K.K., Pilon, M., and Shikanai, T. (2005). Two P-type ATPases are required for copper delivery in Arabidopsis thaliana chloroplasts. Plant Cell **17,** 1233-1251.

Achard, P., Herr, A., Baulcombe, D.C., and Harberd, N.P. (2004). Modulation of floral development by a gibberellin-regulated microRNA. Development **131,** 3357-3365.

Adai, A., Johnson, C., Mlotshwa, S., Archer-Evans, S., Manocha, V., Vance, V., and Sundaresan, V. (2005). Computational prediction of miRNAs in Arabidopsis thaliana. Genome Res **15,** 78-91.

Aguilar-Martinez, J.A., Poza-Carrion, C., and Cubas, P. (2007). Arabidopsis BRANCHED1 acts as an integrator of branching signals within axillary buds. Plant Cell **19,** 458-472.

Aida, M., Ishida, T., Fukaki, H., Fujisawa, H., and Tasaka, M. (1997). Genes involved in organ separation in Arabidopsis: an analysis of the cup-shaped cotyledon mutant. Plant Cell **9,** 841-857.

Allen, E., Xie, Z., Gustafson, A.M., and Carrington, J.C. (2005). microRNA-directed phasing during trans-acting siRNA biogenesis in plants. Cell **121,** 207-221.

Allen, E., Xie, Z., Gustafson, A.M., Sung, G.H., Spatafora, J.W., and Carrington, J.C. (2004). Evolution of microRNA genes by inverted duplication of target gene sequences in Arabidopsis thaliana. Nat Genet **36,** 1282-1290.

Alonso, J.M., Stepanova, A.N., Leisse, T.J., Kim, C.J., Chen, H., Shinn, P., Stevenson, D.K., Zimmerman, J., Barajas, P., Cheuk, R., Gadrinab, C., Heller, C., Jeske, A., Koesema, E., Meyers, C.C., Parker, H., Prednis, L., Ansari, Y., Choy, N., Deen, H., Geralt, M., Hazari, N., Hom, E., Karnes, M., Mulholland, C., Ndubaku, R., Schmidt, I., Guzman, P., Aguilar-Henonin, L., Schmid, M., Weigel, D., Carter, D.E., Marchand, T., Risseeuw, E., Brogden, D., Zeko, A., Crosby, W.L., Berry, C.C., and Ecker, J.R. (2003). Genome-wide insertional mutagenesis of Arabidopsis thaliana. Science **301,** 653-657.

Alvarez, J.P., Pekker, I., Goldshmidt, A., Blum, E., Amsellem, Z., and Eshed, Y. (2006). Endogenous and synthetic microRNAs stimulate simultaneous, efficient, and localized regulation of multiple targets in diverse species. Plant Cell **18,** 1134-1151.

Ambros, V., Bartel, B., Bartel, D.P., Burge, C.B., Carrington, J.C., Chen, X., Dreyfuss, G., Eddy, S.R., Griffiths-Jones, S., Marshall, M., Matzke, M., Ruvkun, G., and Tuschl, T. (2003). A uniform system for microRNA annotation. Rna **9,** 277-279.

Arazi, T., Talmor-Neiman, M., Stav, R., Riese, M., Huijser, P., and Baulcombe, D.C. (2005). Cloning and characterization of micro-RNAs from moss. Plant J **43,** 837-848.

Arteaga-Vazquez, M., Caballero-Perez, J., and Vielle-Calzada, J.P. (2006). A Family of MicroRNAs Present in Plants and Animals. Plant Cell **18,** 3355-3369.

Aukerman, M.J., and Sakai, H. (2003). Regulation of flowering time and floral organ identity by a MicroRNA and its APETALA2-like target genes. Plant Cell **15,** 2730-2741.

Aung, K., Lin, S.I., Wu, C.C., Huang, Y.T., Su, C.L., and Chiou, T.J. (2006). pho2, a phosphate overaccumulator, is caused by a nonsense mutation in a microRNA399 target gene. Plant Physiol **141,** 1000-1011.

Axtell, M.J., and Bartel, D.P. (2005). Antiquity of microRNAs and their targets in land plants. Plant Cell **17,** 1658-1673.

Baker, C.C., Sieber, P., Wellmer, F., and Meyerowitz, E.M. (2005). The early extra petals1 mutant uncovers a role for microRNA miR164c in regulating petal number in Arabidopsis. Curr Biol **15,** 303-315.

Bao, N., Lye, K.W., and Barton, M.K. (2004). MicroRNA binding sites in Arabidopsis class III HD-ZIP mRNAs are required for methylation of the template chromosome. Dev Cell **7,** 653-662.

Bartel, D.P. (2004). MicroRNAs: genomics, biogenesis, mechanism, and function. Cell **116,** 281-297.

Bartel, D.P., and Chen, C.Z. (2004). Micromanagers of gene expression: the potentially widespread influence of metazoan microRNAs. Nat Rev Genet **5,** 396-400.

Baumberger, N., and Baulcombe, D.C. (2005). Arabidopsis ARGONAUTE1 is an RNA Slicer that selectively recruits microRNAs and short interfering RNAs. Proc Natl Acad Sci U S A **102,** 11928-11933.

Becker, D., Kemper, E., Schell, J., and Masterson, R. (1992). New plant binary vectors with selectable markers located proximal to the left T-DNA border. Plant Mol Biol **20,** 1195-1197.

Bedell, J.A., Budiman, M.A., Nunberg, A., Citek, R.W., Robbins, D., Jones, J., Flick, E., Rholfing, T., Fries, J., Bradford, K., McMenamy, J., Smith, M., Holeman, H., Roe, B.A., Wiley, G., Korf, I.F., Rabinowicz, P.D., Lakey, N., McCombie, W.R., Jeddeloh, J.A., and Martienssen, R.A. (2005). Sorghum genome sequencing by methylation filtration. PLoS Biol **3,** e13.

Blazquez, M.A., and Weigel, D. (2000). Integration of floral inductive signals in Arabidopsis. Nature **404,** 889-892.

Blazquez, M.A., Soowal, L.N., Lee, I., and Weigel, D. (1997). LEAFY expression and flower initiation in Arabidopsis. Development **124,** 3835-3844.

Blazquez, M.A., Green, R., Nilsson, O., Sussman, M.R., and Weigel, D. (1998). Gibberellins promote flowering of arabidopsis by activating the LEAFY promoter. Plant Cell **10,** 791-800.

Bonnet, E., Wuyts, J., Rouze, P., and Van de Peer, Y. (2004). Detection of 91 potential conserved plant microRNAs in Arabidopsis thaliana and Oryza sativa identifies important target genes. Proc Natl Acad Sci U S A **101,** 11511-11516.

Borsani, O., Zhu, J., Verslues, P.E., Sunkar, R., and Zhu, J.K. (2005). Endogenous siRNAs derived from a pair of natural cis-antisense transcripts regulate salt tolerance in Arabidopsis. Cell **123,** 1279-1291.

Bradford, M.M. (1976). A rapid and sensitive method for the quantitation of microgram quantities of protein utilizing the principle of protein-dye binding. Anal Biochem **72,** 248-254.

Brennecke, J., Stark, A., Russell, R.B., and Cohen, S.M. (2005). Principles of microRNA-target recognition. PLoS Biol **3,** e85.

Chen, H.M., Li, Y.H., and Wu, S.H. (2007). Bioinformatic prediction and experimental validation of a microRNA-directed tandem trans-acting siRNA cascade in Arabidopsis. Proc Natl Acad Sci U S A **104,** 3318-3323.

Chen, J., Li, W.X., Xie, D., Peng, J.R., and Ding, S.W. (2004). Viral virulence protein suppresses RNA silencing-mediated defense but upregulates the role of microrna in host gene expression. Plant Cell **16,** 1302-1313.

Chen, X. (2004). A microRNA as a translational repressor of APETALA2 in Arabidopsis flower development. Science **303,** 2022-2025.

Chen, X. (2005). MicroRNA biogenesis and function in plants. FEBS Lett **579,** 5923-5931.

Chiou, T.J. (2007). The role of microRNAs in sensing nutrient stress. Plant Cell Environ **30,** 323-332.

Chiou, T.J., Aung, K., Lin, S.I., Wu, C.C., Chiang, S.F., and Su, C.L. (2006). Regulation of phosphate homeostasis by MicroRNA in Arabidopsis. Plant Cell **18,** 412-421.

Chu, C.Y., and Rana, T.M. (2006). Translation repression in human cells by microRNA-induced gene silencing requires RCK/p54. PLoS Biol **4,** e210.

Clough, S.J., and Bent, A.F. (1998). Floral dip: a simplified method for Agrobacterium-mediated transformation of Arabidopsis thaliana. Plant J **16,** 735-743.

Dangl, J.L., Hauffe, K.D., Lipphardt, S., Hahlbrock, K., and Scheel, D. (1987). Parsley protoplasts retain differential responsiveness to u.v. light and fungal elicitor. Embo J **6,** 2551-2556.

Dean, G., Casson, S., and Lindsey, K. (2004). KNAT6 gene of Arabidopsis is expressed in roots and is required for correct lateral root formation. Plant Mol Biol **54,** 71-84.

Dezulian, T., Remmert, M., Palatnik, J.F., Weigel, D., and Huson, D.H. (2006). Identification of plant microRNA homologs. Bioinformatics **22,** 359-360.

Doench, J.G., and Sharp, P.A. (2004). Specificity of microRNA target selection in translational repression. Genes Dev **18,** 504-511.

Doukhanina, E.V., Chen, S., van der Zalm, E., Godzik, A., Reed, J., and Dickman, M.B. (2006). Identification and functional characterization of the BAG protein family in Arabidopsis thaliana. J Biol Chem **281,** 18793-18801.

Dugas, D.V., and Bartel, B. (2004). MicroRNA regulation of gene expression in plants. Curr Opin Plant Biol **7,** 512-520.

Durbarry, A., Vizir, I., and Twell, D. (2005). Male germ line development in Arabidopsis. duo pollen mutants reveal gametophytic regulators of generative cell cycle progression. Plant Physiol **137,** 297-307.

Edwards, K., Johnstone, C., and Thompson, C. (1991). A simple and rapid method for the preparation of plant genomic DNA for PCR analysis. Nucleic Acids Res **19,** 1349.

Ellis, C.M., Nagpal, P., Young, J.C., Hagen, G., Guilfoyle, T.J., and Reed, J.W. (2005). AUXIN RESPONSE FACTOR1 and AUXIN RESPONSE FACTOR2 regulate senescence and floral organ abscission in Arabidopsis thaliana. Development **132,** 4563-4574.

Emery, J.F., Floyd, S.K., Alvarez, J., Eshed, Y., Hawker, N.P., Izhaki, A., Baum, S.F., and Bowman, J.L. (2003). Radial patterning of Arabidopsis shoots by class III HD-ZIP and KANADI genes. Curr Biol **13,** 1768-1774.

Fahlgren, N., Howell, M.D., Kasschau, K.D., Chapman, E.J., Sullivan, C.M., Cumbie, J.S., Givan, S.A., Law, T.F., Grant, S.R., Dangl, J.L., and Carrington, J.C. (2007). High-Throughput Sequencing of Arabidopsis microRNAs: Evidence for Frequent Birth and Death of MIRNA Genes. PLoS ONE **2,** e219.

Floyd, S.K., and Bowman, J.L. (2004). Gene regulation: ancient microRNA target sequences in plants. Nature **428,** 485-486.

Folkers, U., Kirik, V., Schobinger, U., Falk, S., Krishnakumar, S., Pollock, M.A., Oppenheimer, D.G., Day, I., Reddy, A.S., Jurgens, G., and Hulskamp, M. (2002). The cell morphogenesis gene ANGUSTIFOLIA encodes a CtBP/BARS-like protein and is involved in the control of the microtubule cytoskeleton. Embo J **21,** 1280-1288.

Fujii, H., Chiou, T.J., Lin, S.I., Aung, K., and Zhu, J.K. (2005). A miRNA involved in phosphate-starvation response in Arabidopsis. Curr Biol **15,** 2038-2043.

Gandikota, M., Birkenbihl, R.P., Hohmann, S., Cardon, G.H., Saedler, H., and Huijser, P. (2007). The miRNA156/157 recognition element in the 3' UTR of the Arabidopsis SBP box gene SPL3 prevents early flowering by translational inhibition in seedlings. Plant J.

Gocal, G.F., Sheldon, C.C., Gubler, F., Moritz, T., Bagnall, D.J., MacMillan, C.P., Li, S.F., Parish, R.W., Dennis, E.S., Weigel, D., and King, R.W. (2001). GAMYB-like genes, flowering, and gibberellin signaling in Arabidopsis. Plant Physiol **127,** 1682-1693.

Griffiths-Jones, S. (2004). The microRNA Registry. Nucleic Acids Res **32,** D109-111.

Griffiths-Jones, S., Grocock, R.J., van Dongen, S., Bateman, A., and Enright, A.J. (2006). miRBase: microRNA sequences, targets and gene nomenclature. Nucleic Acids Res **34,** D140-144.

Grigg, S.P., Canales, C., Hay, A., and Tsiantis, M. (2005). SERRATE coordinates shoot meristem function and leaf axial patterning in Arabidopsis. Nature **437,** 1022-1026.

Gubler, F., Kalla, R., Roberts, J.K., and Jacobsen, J.V. (1995). Gibberellin-regulated expression of a myb gene in barley aleurone cells: evidence for Myb transactivation of a high-pI alpha-amylase gene promoter. Plant Cell **7,** 1879-1891.

Guddeti, S., Zhang, D.C., Li, A.L., Leseberg, C.H., Kang, H., Li, X.G., Zhai, W.X., Johns, M.A., and Mao, L. (2005). Molecular evolution of the rice miR395 gene family. Cell Res **15,** 631-638.

Guo, H.S., Xie, Q., Fei, J.F., and Chua, N.H. (2005). MicroRNA directs mRNA cleavage of the transcription factor NAC1 to downregulate auxin signals for arabidopsis lateral root development. Plant Cell **17,** 1376-1386.

Hain, R., Stabel, P., Czernilofsky, A.P., Steinbiß, H.H., Herrera-Estrella, L., and Schell, J. (1985). Uptake, integration, expression and genetic transmission of a selectable chimeric gene by plant protoplasts. Molecular General Genetics **199,** 161-168.

Hamilton, A., Voinnet, O., Chappell, L., and Baulcombe, D. (2002). Two classes of short interfering RNA in RNA silencing. Embo J **21,** 4671-4679.

Hamilton, A.J., and Baulcombe, D.C. (1999). A species of small antisense RNA in posttranscriptional gene silencing in plants. Science **286,** 950-952.

Han, M.H., Goud, S., Song, L., and Fedoroff, N. (2004). The Arabidopsis double-stranded RNA-binding protein HYL1 plays a role in microRNA-mediated gene regulation. Proc Natl Acad Sci U S A **101,** 1093-1098.

Hartmann, U., Valentine, W.J., Christie, J.M., Hays, J., Jenkins, G.I., and Weisshaar, B. (1998). Identification of UV/blue light-response elements in the Arabidopsis thaliana chalcone synthase promoter using a homologous protoplast transient expression system. Plant Mol Biol **36,** 741-754.

Hashimoto, M., Endo, T., Peltier, G., Tasaka, M., and Shikanai, T. (2003). A nucleus-encoded factor, CRR2, is essential for the expression of chloroplast ndhB in Arabidopsis. Plant J **36,** 541-549.

He, Y., Doyle, M.R., and Amasino, R.M. (2004). PAF1-complex-mediated histone methylation of FLOWERING LOCUS C chromatin is required for the vernalization-responsive, winter-annual habit in Arabidopsis. Genes Dev **18,** 2774-2784.

Herr, A.J., Jensen, M.B., Dalmay, T., and Baulcombe, D.C. (2005). RNA polymerase IV directs silencing of endogenous DNA. Science **308,** 118-120.

Hofacker, I.L. (2003). Vienna RNA secondary structure server. Nucleic Acids Res **31,** 3429-3431.

Initiative, T.A.G. (2000). Analysis of the genome sequence of the flowering plant Arabidopsis thaliana. Nature **408,** 796-815.

Jacobsen, S.E., Running, M.P., and Meyerowitz, E.M. (1999). Disruption of an RNA helicase/RNAse III gene in Arabidopsis causes unregulated cell division in floral meristems. Development **126,** 5231-5243.

Jefferson, R.A., Burgess, S.M., and Hirsh, D. (1986). beta-Glucuronidase from Escherichia coli as a gene-fusion marker. Proc Natl Acad Sci U S A **83,** 8447-8451.

Jones-Rhoades, M.W., and Bartel, D.P. (2004). Computational identification of plant microRNAs and their targets, including a stress-induced miRNA. Mol Cell **14,** 787-799.

Jones-Rhoades, M.W., Bartel, D.P., and Bartel, B. (2006). MicroRNAS and their regulatory roles in plants. Annu Rev Plant Biol **57,** 19-53.

Jover-Gil, S., Candela, H., and Ponce, M.R. (2005). Plant microRNAs and development. Int J Dev Biol **49,** 733-744.

Juarez, M.T., Kui, J.S., Thomas, J., Heller, B.A., and Timmermans, M.C. (2004). microRNA-mediated repression of rolled leaf1 specifies maize leaf polarity. Nature **428,** 84-88.

Kanno, T., Huettel, B., Mette, M.F., Aufsatz, W., Jaligot, E., Daxinger, L., Kreil, D.P., Matzke, M., and Matzke, A.J. (2005). Atypical RNA polymerase subunits required for RNA-directed DNA methylation. Nat Genet **37,** 761-765.

Kasschau, K.D., Xie, Z., Allen, E., Llave, C., Chapman, E.J., Krizan, K.A., and Carrington, J.C. (2003). P1/HC-Pro, a viral suppressor of RNA silencing, interferes with Arabidopsis development and miRNA unction. Dev Cell **4,** 205-217.

Khvorova, A., Reynolds, A., and Jayasena, S.D. (2003). Functional siRNAs and miRNAs exhibit strand bias. Cell **115,** 209-216.

Kidner, C.A., and Martienssen, R.A. (2004). Spatially restricted microRNA directs leaf polarity through ARGONAUTE1. Nature **428,** 81-84.

Kim, G.T., Shoda, K., Tsuge, T., Cho, K.H., Uchimiya, H., Yokoyama, R., Nishitani, K., and Tsukaya, H. (2002). The ANGUSTIFOLIA gene of Arabidopsis, a plant CtBP gene, regulates leaf-cell expansion, the arrangement of cortical microtubules in leaf cells and expression of a gene involved in cell-wall formation. Embo J **21,** 1267-1279.

Kim, J., Jung, J.H., Reyes, J.L., Kim, Y.S., Kim, S.Y., Chung, K.S., Kim, J.A., Lee, M., Lee, Y., Narry Kim, V., Chua, N.H., and Park, C.M. (2005). microRNA-directed cleavage of ATHB15 mRNA regulates vascular development in Arabidopsis inflorescence stems. Plant J **42,** 84-94.

Koncz, C., and Schell, J. (1986). The promoter of TL-DNA gene 5 controls

the tissue specific expression of chimeric genes carried by a

novel type of Agrobacterium binary vector. Mol Gen Genet **204,** 383-396.

Kotera, E., Tasaka, M., and Shikanai, T. (2005). A pentatricopeptide repeat protein is essential for RNA editing in chloroplasts. Nature **433,** 326-330.

Krens, F.A., Molendijk, L., Wullems, G.J., and Schilperoort, R.A. (1982). *In vitro* transformation of plant protoplasts with Ti-plasmid DNA. Nature **296,** 72-74.

Kurihara, Y., Takashi, Y., and Watanabe, Y. (2006). The interaction between DCL1 and HYL1 is important for efficient and precise processing of pri-miRNA in plant microRNA biogenesis. Rna **12,** 206-212.

Lagos-Quintana, M., Rauhut, R., Lendeckel, W., and Tuschl, T. (2001). Identification of novel genes coding for small expressed RNAs. Science **294,** 853-858.

Lau, N.C., Lim, L.P., Weinstein, E.G., and Bartel, D.P. (2001). An abundant class of tiny RNAs with probable regulatory roles in Caenorhabditis elegans. Science **294,** 858-862.

Laufs, P., Peaucelle, A., Morin, H., and Traas, J. (2004). MicroRNA regulation of the CUC genes is required for boundary size control in Arabidopsis meristems. Development **131,** 4311-4322.

Lauter, N., Kampani, A., Carlson, S., Goebel, M., and Moose, S.P. (2005). microRNA172 down-regulates glossy15 to promote vegetative phase change in maize. Proc Natl Acad Sci U S A **102,** 9412-9417.

Lee, R.C., and Ambros, V. (2001). An extensive class of small RNAs in Caenorhabditis elegans. Science **294,** 862-864.

Lee, R.C., Feinbaum, R.L., and Ambros, V. (1993). The C. elegans heterochronic gene lin-4 encodes small RNAs with antisense complementarity to lin-14. Cell **75,** 843-854.

Lee, Y., Kim, M., Han, J., Yeom, K.H., Lee, S., Baek, S.H., and Kim, V.N. (2004). MicroRNA genes are transcribed by RNA polymerase II. Embo J **23,** 4051-4060.

Lee, Y., Ahn, C., Han, J., Choi, H., Kim, J., Yim, J., Lee, J., Provost, P., Radmark, O., Kim, S., and Kim, V.N. (2003). The nuclear RNase III Drosha initiates microRNA processing. Nature **425,** 415-419.

Lewis, B.P., Shih, I.H., Jones-Rhoades, M.W., Bartel, D.P., and Burge, C.B. (2003). Prediction of mammalian microRNA targets. Cell **115,** 787-798.

Li, J., Yang, Z., Yu, B., Liu, J., and Chen, X. (2005a). Methylation protects miRNAs and siRNAs from a 3'-end uridylation activity in Arabidopsis. Curr Biol **15,** 1501-1507.

Li, Y., Li, W., and Jin, Y.X. (2005b). Computational identification of novel family members of microRNA genes in Arabidopsis thaliana and Oryza sativa. Acta Biochim Biophys Sin (Shanghai) **37,** 75-87.

Lim, L.P., Lau, N.C., Garrett-Engele, P., Grimson, A., Schelter, J.M., Castle, J., Bartel, D.P., Linsley, P.S., and Johnson, J.M. (2005). Microarray analysis shows that some microRNAs downregulate large numbers of target mRNAs. Nature **433,** 769-773.

Lipphardt, S., Brettschneider, R., Kreuzaler, F., Schell, J., and Dangl, J.L. (1988). UV-inducible transient expression in parsley protoplasts identifies regulatory cis-elements of a chimeric Antirrhinum majus chalcone synthase gene. Embo J **7,** 4027-4033.

Liu, B., Li, P., Li, X., Liu, C., Cao, S., Chu, C., and Cao, X. (2005a). Loss of function of OsDCL1 affects microRNA accumulation and causes developmental defects in rice. Plant Physiol **139,** 296-305.

Liu, J., Valencia-Sanchez, M.A., Hannon, G.J., and Parker, R. (2005b). MicroRNA-dependent localization of targeted mRNAs to mammalian P-bodies. Nat Cell Biol **7,** 719-723.

Llave, C., Xie, Z., Kasschau, K.D., and Carrington, J.C. (2002a). Cleavage of Scarecrow-like mRNA targets directed by a class of Arabidopsis miRNA. Science **297,** 2053-2056.

Llave, C., Kasschau, K.D., Rector, M.A., and Carrington, J.C. (2002b). Endogenous and silencing-associated small RNAs in plants. Plant Cell **14,** 1605-1619.

Lobbes, D., Rallapalli, G., Schmidt, D.D., Martin, C., and Clarke, J. (2006). SERRATE: a new player on the plant microRNA scene. EMBO Rep **7,** 1052-1058.

Lu, C., and Fedoroff, N. (2000). A mutation in the Arabidopsis HYL1 gene encoding a dsRNA binding protein affects responses to abscisic acid, auxin, and cytokinin. Plant Cell **12,** 2351-2366.

Lu, C., Tej, S.S., Luo, S., Haudenschild, C.D., Meyers, B.C., and Green, P.J. (2005a). Elucidation of the small RNA component of the transcriptome. Science **309,** 1567-1569.

Lu, C., Kulkarni, K., Souret, F.F., MuthuValliappan, R., Tej, S.S., Poethig, R.S., Henderson, I.R., Jacobsen, S.E., Wang, W., Green, P.J., and Meyers, B.C. (2006). MicroRNAs and other small RNAs enriched in the Arabidopsis RNA-dependent RNA polymerase-2 mutant. Genome Res **16,** 1276-1288.

Lu, S., Sun, Y.H., Shi, R., Clark, C., Li, L., and Chiang, V.L. (2005b). Novel and mechanical stress-responsive MicroRNAs in Populus trichocarpa that are absent from Arabidopsis. Plant Cell **17,** 2186-2203.

Luo, Y.C., Zhou, H., Li, Y., Chen, J.Y., Yang, J.H., Chen, Y.Q., and Qu, L.H. (2006). Rice embryogenic calli express a unique set of microRNAs, suggesting regulatory roles of microRNAs in plant post-embryogenic development. FEBS Lett **580,** 5111-5116.

Magyar, Z., De Veylder, L., Atanassova, A., Bako, L., Inze, D., and Bogre, L. (2005). The role of the Arabidopsis E2FB transcription factor in regulating auxin-dependent cell division. Plant Cell **17,** 2527-2541.

Mallory, A.C., and Vaucheret, H. (2006). Functions of microRNAs and related small RNAs in plants. Nat Genet **38 Suppl 1,** S31-36.

Mallory, A.C., Bartel, D.P., and Bartel, B. (2005). MicroRNA-directed regulation of Arabidopsis AUXIN RESPONSE FACTOR17 is essential for proper development and modulates expression of early auxin response genes. Plant Cell **17,** 1360-1375.

Mallory, A.C., Dugas, D.V., Bartel, D.P., and Bartel, B. (2004a). MicroRNA regulation of NAC-domain targets is required for proper formation and separation of adjacent embryonic, vegetative, and floral organs. Curr Biol **14,** 1035-1046.

Mallory, A.C., Reinhart, B.J., Jones-Rhoades, M.W., Tang, G., Zamore, P.D., Barton, M.K., and Bartel, D.P. (2004b). MicroRNA control of PHABULOSA in leaf development: importance of pairing to the microRNA 5' region. Embo J **23,** 3356-3364.

McElver, J., Tzafrir, I., Aux, G., Rogers, R., Ashby, C., Smith, K., Thomas, C., Schetter, A., Zhou, Q., Cushman, M.A., Tossberg, J., Nickle, T., Levin, J.Z., Law, M., Meinke, D., and Patton, D. (2001). Insertional mutagenesis of genes required for seed development in Arabidopsis thaliana. Genetics **159,** 1751-1763.

Megraw, M., Baev, V., Rusinov, V., Jensen, S.T., Kalantidis, K., and Hatzigeorgiou, A.G. (2006). MicroRNA promoter element discovery in Arabidopsis. Rna.

Meierhoff, K., Felder, S., Nakamura, T., Bechtold, N., and Schuster, G. (2003). HCF152, an Arabidopsis RNA binding pentatricopeptide repeat protein involved in the processing of chloroplast psbB-psbT-psbH-petB-petD RNAs. Plant Cell **15,** 1480-1495.

Mello, C.C., and Czech, M.P. (2004). Micromanaging insulin secretion. Nat Med **10,** 1297-1298.

Merkle, T. (2003). Nucleo-cytoplasmic partitioning of proteins in plants: implications for the regulation of environmental and developmental signalling. Curr Genet **44,** 231-260.

Merkle, T., Leclerc, D., Marshallsay, C., and Nagy, F. (1996). A plant in vitro system for the nuclear import of proteins. Plant J **10,** 1177-1186.

Mette, M.F., van der Winden, J., Matzke, M., and Matzke, A.J. (2002). Short RNAs can identify new candidate transposable element families in Arabidopsis. Plant Physiol **130,** 6-9.

Michaels, S.D., and Amasino, R.M. (1999). FLOWERING LOCUS C encodes a novel MADS domain protein that acts as a repressor of flowering. Plant Cell **11,** 949-956.

Millar, A.A., and Gubler, F. (2005). The Arabidopsis GAMYB-like genes, MYB33 and MYB65, are microRNA-regulated genes that redundantly facilitate anther development. Plant Cell **17,** 705-721.

Molhoj, M., Verma, R., and Reiter, W.D. (2004). The biosynthesis of D-Galacturonate in plants. functional cloning and characterization of a membrane-anchored UDP-D-Glucuronate 4-epimerase from Arabidopsis. Plant Physiol **135,** 1221-1230.

Mouchel, C.F., Briggs, G.C., and Hardtke, C.S. (2004). Natural genetic variation in Arabidopsis identifies BREVIS RADIX, a novel regulator of cell proliferation and elongation in the root. Genes Dev **18,** 700-714.

Mouchel, C.F., Osmont, K.S., and Hardtke, C.S. (2006). BRX mediates feedback between brassinosteroid levels and auxin signalling in root growth. Nature **443,** 458-461.

Niemeier, S. (2006). Synthetische microRNAs als Mittel zur Erzeugung stabiler knock-downs für Genfamilien in Arabidopsis thaliana. In Universitaet Bielefeld, Fakultät für Biologie, pp. 188.

Niyogi, K.K., and Fink, G.R. (1992). Two anthranilate synthase genes in Arabidopsis: defense-related regulation of the tryptophan pathway. Plant Cell **4,** 721-733.

Obernosterer, G., Leuschner, P.J., Alenius, M., and Martinez, J. (2006). Post-transcriptional regulation of microRNA expression. Rna **12,** 1161-1167.

Ori, N., Eshed, Y., Chuck, G., Bowman, J.L., and Hake, S. (2000). Mechanisms that control knox gene expression in the Arabidopsis shoot. Development **127,** 5523-5532.

Palatnik, J.F., Allen, E., Wu, X., Schommer, C., Schwab, R., Carrington, J.C., and Weigel, D. (2003). Control of leaf morphogenesis by microRNAs. Nature **425,** 257-263.

Papp, I., Mette, M.F., Aufsatz, W., Daxinger, L., Schauer, S.E., Ray, A., van der Winden, J., Matzke, M., and Matzke, A.J. (2003). Evidence for nuclear processing of plant micro RNA and short interfering RNA precursors. Plant Physiol **132,** 1382-1390.

Parizotto, E.A., Dunoyer, P., Rahm, N., Himber, C., and Voinnet, O. (2004). In vivo investigation of the transcription, processing, endonucleolytic activity, and functional relevance of the spatial distribution of a plant miRNA. Genes Dev **18,** 2237-2242.

Park, M.Y., Wu, G., Gonzalez-Sulser, A., Vaucheret, H., and Poethig, R.S. (2005). Nuclear processing and export of microRNAs in Arabidopsis. Proc Natl Acad Sci U S A **102,** 3691-3696.

Park, W., Li, J., Song, R., Messing, J., and Chen, X. (2002). CARPEL FACTORY, a Dicer homolog, and HEN1, a novel protein, act in microRNA metabolism in Arabidopsis thaliana. Curr Biol **12,** 1484-1495.

Pasquinelli, A.E., Reinhart, B.J., Slack, F., Martindale, M.Q., Kuroda, M.I., Maller, B., Hayward, D.C., Ball, E.E., Degnan, B., Muller, P., Spring, J., Srinivasan, A., Fishman, M., Finnerty, J., Corbo, J., Levine, M., Leahy, P., Davidson, E., and

Ruvkun, G. (2000). Conservation of the sequence and temporal expression of let-7 heterochronic regulatory RNA. Nature **408,** 86-89.

Pelletier, M.K., and Shirley, B.W. (1996). Analysis of flavanone 3-hydroxylase in Arabidopsis seedlings. Coordinate regulation with chalcone synthase and chalcone isomerase. Plant Physiol **111,** 339-345.

Peng, M., Cui, Y., Bi, Y.M., and Rothstein, S.J. (2006). AtMBD9: a protein with a methyl-CpG-binding domain regulates flowering time and shoot branching in Arabidopsis. Plant J **46,** 282-296.

Peragine, A., Yoshikawa, M., Wu, G., Albrecht, H.L., and Poethig, R.S. (2004). SGS3 and SGS2/SDE1/RDR6 are required for juvenile development and the production of trans-acting siRNAs in Arabidopsis. Genes Dev **18,** 2368-2379.

Pfeffer, S., Zavolan, M., Grasser, F.A., Chien, M., Russo, J.J., Ju, J., John, B., Enright, A.J., Marks, D., Sander, C., and Tuschl, T. (2004). Identification of virus-encoded microRNAs. Science **304,** 734-736.

Rajagopalan, R., Vaucheret, H., Trejo, J., and Bartel, D.P. (2006). A diverse and evolutionarily fluid set of microRNAs in Arabidopsis thaliana. Genes Dev **20,** 3407-3425.

Rayapureddi, J.P., Kattamuri, C., Chan, F.H., and Hegde, R.S. (2005). Characterization of a plant, tyrosine-specific phosphatase of the aspartyl class. Biochemistry **44,** 751-758.

Rehmsmeier, M., Steffen, P., Hochsmann, M., and Giegerich, R. (2004). Fast and effective prediction of microRNA/target duplexes. RNA **10,** 1507-1517.

Reinhart, B.J., Weinstein, E.G., Rhoades, M.W., Bartel, B., and Bartel, D.P. (2002). MicroRNAs in plants. Genes Dev **16,** 1616-1626.

Reinhart, B.J., Slack, F.J., Basson, M., Pasquinelli, A.E., Bettinger, J.C., Rougvie, A.E., Horvitz, H.R., and Ruvkun, G. (2000). The 21-nucleotide let-7 RNA regulates developmental timing in Caenorhabditis elegans. Nature **403,** 901-906.

Reyes, J.L., and Chua, N.H. (2007). ABA induction of miR159 controls transcript levels of two MYB factors during Arabidopsis seed germination. Plant J.

Rhoades, M.W., Reinhart, B.J., Lim, L.P., Burge, C.B., Bartel, B., and Bartel, D.P. (2002). Prediction of plant microRNA targets. Cell **110,** 513-520.

Rotman, N., Durbarry, A., Wardle, A., Yang, W.C., Chaboud, A., Faure, J.E., Berger, F., and Twell, D. (2005). A novel class of MYB factors controls sperm-cell formation in plants. Curr Biol **15,** 244-248.

Rusinov, V., Baev, V., Minkov, I.N., and Tabler, M. (2005). MicroInspector: a web tool for detection of miRNA binding sites in an RNA sequence. Nucleic Acids Res **33,** W696-700.

Sambrook, J., and Russel, D.W. (2001). Molecular cloning: a laboratory manual. (Cold Spring Harbor, New York: Cold Spring Harbor Laboratory Press).

Schmid, M., Davison, T.S., Henz, S.R., Pape, U.J., Demar, M., Vingron, M., Scholkopf, B., Weigel, D., and Lohmann, J.U. (2005). A gene expression map of Arabidopsis thaliana development. Nat Genet **37,** 501-506.

Schwab, R., Ossowski, S., Riester, M., Warthmann, N., and Weigel, D. (2006). Highly specific gene silencing by artificial microRNAs in Arabidopsis. Plant Cell **18,** 1121-1133.

Schwab, R., Palatnik, J.F., Riester, M., Schommer, C., Schmid, M., and Weigel, D. (2005). Specific effects of microRNAs on the plant transcriptome. Dev Cell **8,** 517-527.

Schwarz, D.S., Hutvagner, G., Du, T., Xu, Z., Aronin, N., and Zamore, P.D. (2003). Asymmetry in the assembly of the RNAi enzyme complex. Cell **115,** 199-208.

Seigneurin-Berny, D., Gravot, A., Auroy, P., Mazard, C., Kraut, A., Finazzi, G., Grunwald, D., Rappaport, F., Vavasseur, A., Joyard, J., Richaud, P., and Rolland, N. (2006). HMA1, a new Cu-ATPase of the chloroplast envelope, is essential for growth under adverse light conditions. J Biol Chem **281,** 2882-2892.

Sen, G.L., and Blau, H.M. (2005). Argonaute 2/RISC resides in sites of mammalian mRNA decay known as cytoplasmic bodies. Nat Cell Biol **7,** 633-636.

Sessions, A., Burke, E., Presting, G., Aux, G., McElver, J., Patton, D., Dietrich, B., Ho, P., Bacwaden, J., Ko, C., Clarke, J.D., Cotton, D., Bullis, D., Snell, J., Miguel, T., Hutchison, D., Kimmerly, B., Mitzel, T., Katagiri, F., Glazebrook, J., Law, M., and Goff, S.A. (2002). A high-throughput Arabidopsis reverse genetics system. Plant Cell **14,** 2985-2994.

Shikanai, T. (2006). RNA editing in plant organelles: machinery, physiological function and evolution. Cell Mol Life Sci **63,** 698-708.

Sprenger-Haussels, M., and Weisshaar, B. (2000). Transactivation properties of parsley proline-rich bZIP transcription factors. Plant J **22,** 1-8.

Stracke, R., Werber, M., and Weisshaar, B. (2001). The R2R3-MYB gene family in Arabidopsis thaliana. Curr Opin Plant Biol **4,** 447-456.

Sunkar, R., and Zhu, J.K. (2004). Novel and stress-regulated microRNAs and other small RNAs from Arabidopsis. Plant Cell **16,** 2001-2019.

Sunkar, R., Kapoor, A., and Zhu, J.K. (2006). Posttranscriptional induction of two Cu/Zn superoxide dismutase genes in Arabidopsis is mediated by downregulation of miR398 and important for oxidative stress tolerance. Plant Cell **18,** 2051-2065.

Sunkar, R., Girke, T., Jain, P.K., and Zhu, J.K. (2005). Cloning and characterization of microRNAs from rice. Plant Cell **17,** 1397-1411.

Talmor-Neiman, M., Stav, R., Frank, W., Voss, B., and Arazi, T. (2006). Novel micro-RNAs and intermediates of micro-RNA biogenesis from moss. Plant J **47,** 25-37.

Tang, G., Reinhart, B.J., Bartel, D.P., and Zamore, P.D. (2003). A biochemical framework for RNA silencing in plants. Genes Dev **17,** 49-63.

Tiwari, S.B., Hagen, G., and Guilfoyle, T. (2003). The roles of auxin response factor domains in auxin-responsive transcription. Plant Cell **15,** 533-543.

Tsuchisaka, A., and Theologis, A. (2004a). Unique and overlapping expression patterns among the Arabidopsis 1-amino-cyclopropane-1-carboxylate synthase gene family members. Plant Physiol **136,** 2982-3000.

Tsuchisaka, A., and Theologis, A. (2004b). Heterodimeric interactions among the 1-amino-cyclopropane-1-carboxylate synthase polypeptides encoded by the Arabidopsis gene family. Proc Natl Acad Sci U S A **101,** 2275-2280.

Tsukaya, H. (2003). Organ shape and size: a lesson from studies of leaf morphogenesis. Curr Opin Plant Biol **6,** 57-62.

Tsukaya, H. (2005). Leaf shape: genetic controls and environmental factors. Int J Dev Biol **49,** 547-555.

Tuskan, G.A., Difazio, S., Jansson, S., Bohlmann, J., Grigoriev, I., Hellsten, U., Putnam, N., Ralph, S., Rombauts, S., Salamov, A., Schein, J., Sterck, L., Aerts, A., Bhalerao, R.R., Bhalerao, R.P., Blaudez, D., Boerjan, W., Brun, A., Brunner, A., Busov, V., Campbell, M., Carlson, J., Chalot, M., Chapman, J., Chen, G.L., Cooper, D., Coutinho, P.M., Couturier, J., Covert, S., Cronk, Q., Cunningham, R., Davis, J., Degroeve, S., Dejardin, A., Depamphilis, C., Detter, J., Dirks, B.,

Dubchak, I., Duplessis, S., Ehlting, J., Ellis, B., Gendler, K., Goodstein, D., Gribskov, M., Grimwood, J., Groover, A., Gunter, L., Hamberger, B., Heinze, B., Helariutta, Y., Henrissat, B., Holligan, D., Holt, R., Huang, W., Islam-Faridi, N., Jones, S., Jones-Rhoades, M., Jorgensen, R., Joshi, C., Kangasjarvi, J., Karlsson, J., Kelleher, C., Kirkpatrick, R., Kirst, M., Kohler, A., Kalluri, U., Larimer, F., Leebens-Mack, J., Leple, J.C., Locascio, P., Lou, Y., Lucas, S., Martin, F., Montanini, B., Napoli, C., Nelson, D.R., Nelson, C., Nieminen, K., Nilsson, O., Pereda, V., Peter, G., Philippe, R., Pilate, G., Poliakov, A., Razumovskaya, J., Richardson, P., Rinaldi, C., Ritland, K., Rouze, P., Ryaboy, D., Schmutz, J., Schrader, J., Segerman, B., Shin, H., Siddiqui, A., Sterky, F., Terry, A., Tsai, C.J., Uberbacher, E., Unneberg, P., Vahala, J., Wall, K., Wessler, S., Yang, G., Yin, T., Douglas, C., Marra, M., Sandberg, G., Van de Peer, Y., and Rokhsar, D. (2006). The genome of black cottonwood, Populus trichocarpa (Torr. & Gray). Science **313,** 1596-1604.

Ulmasov, T., Hagen, G., and Guilfoyle, T.J. (1999). Dimerization and DNA binding of auxin response factors. Plant J **19,** 309-319.

Vandenbussche, F., Vriezen, W.H., Smalle, J., Laarhoven, L.J., Harren, F.J., and Van Der Straeten, D. (2003). Ethylene and auxin control the Arabidopsis response to decreased light intensity. Plant Physiol **133,** 517-527.

Vandepoele, K., Raes, J., De Veylder, L., Rouze, P., Rombauts, S., and Inze, D. (2002). Genome-wide analysis of core cell cycle genes in Arabidopsis. Plant Cell **14,** 903-916.

Vaucheret, H. (2006). Post-transcriptional small RNA pathways in plants: mechanisms and regulations. Genes Dev **20,** 759-771.

Vaucheret, H., Vazquez, F., Crete, P., and Bartel, D.P. (2004). The action of ARGONAUTE1 in the miRNA pathway and its regulation by the miRNA pathway are crucial for plant development. Genes Dev **18,** 1187-1197.

Vazquez, F., Gasciolli, V., Crete, P., and Vaucheret, H. (2004a). The nuclear dsRNA binding protein HYL1 is required for microRNA accumulation and plant development, but not posttranscriptional transgene silencing. Curr Biol **14,** 346-351.

Vazquez, F., Vaucheret, H., Rajagopalan, R., Lepers, C., Gasciolli, V., Mallory, A.C., Hilbert, J.L., Bartel, D.P., and Crete, P. (2004b). Endogenous trans-acting siRNAs regulate the accumulation of Arabidopsis mRNAs. Mol Cell **16,** 69-79.

Wang, J.F., Zhou, H., Chen, Y.Q., Luo, Q.J., and Qu, L.H. (2004a). Identification of 20 microRNAs from Oryza sativa. Nucleic Acids Res **32,** 1688-1695.

Wang, J.W., Wang, L.J., Mao, Y.B., Cai, W.J., Xue, H.W., and Chen, X.Y. (2005). Control of root cap formation by MicroRNA-targeted auxin response factors in Arabidopsis. Plant Cell **17,** 2204-2216.

Wang, X.J., Reyes, J.L., Chua, N.H., and Gaasterland, T. (2004b). Prediction and identification of Arabidopsis thaliana microRNAs and their mRNA targets. Genome Biol **5,** R65.

Wightman, B., Ha, I., and Ruvkun, G. (1993). Posttranscriptional regulation of the heterochronic gene lin-14 by lin-4 mediates temporal pattern formation in C. elegans. Cell **75,** 855-862.

Williams, L., Grigg, S.P., Xie, M., Christensen, S., and Fletcher, J.C. (2005). Regulation of Arabidopsis shoot apical meristem and lateral organ formation by microRNA miR166g and its AtHD-ZIP target genes. Development **132,** 3657-3668.

Wohnert, J., Dingley, A.J., Stoldt, M., Gorlach, M., Grzesiek, S., and Brown, L.R. (1999). Direct identification of NH...N hydrogen bonds in non-canonical base pairs of RNA by NMR spectroscopy. Nucleic Acids Res **27,** 3104-3110.

Wood, K.V. (1991). The origin of beetle luciferases. Bioluminescence and Chemiluminescence: current status. Stanley P., Kricka L., Wiley J. and sons (eds.), Chichester **1**.

Wu, M.F., Tian, Q., and Reed, J.W. (2006). Arabidopsis microRNA167 controls patterns of ARF6 and ARF8 expression, and regulates both female and male reproduction. Development **133,** 4211-4218.

Xie, F.L., Huang, S.Q., Guo, K., Xiang, A.L., Zhu, Y.Y., Nie, L., and Yang, Z.M. (2007). Computational identification of novel microRNAs and targets in Brassica napus. FEBS Lett **581,** 1464-1474.

Xie, Q., Guo, H.S., Dallman, G., Fang, S., Weissman, A.M., and Chua, N.H. (2002). SINAT5 promotes ubiquitin-related degradation of NAC1 to attenuate auxin signals. Nature **419,** 167-170.

Xie, S., and Lam, E. (1994). Abundance of nuclear DNA topoisomerase II is correlated with proliferation in Arabidopsis thaliana. Nucleic Acids Res **22,** 5729-5736.

Xie, Z., Kasschau, K.D., and Carrington, J.C. (2003). Negative feedback regulation of Dicer-Like1 in Arabidopsis by microRNA-guided mRNA degradation. Curr Biol **13,** 784-789.

Xie, Z., Allen, E., Fahlgren, N., Calamar, A., Givan, S.A., and Carrington, J.C. (2005). Expression of Arabidopsis MIRNA genes. Plant Physiol **138,** 2145-2154.

Yamagami, T., Tsuchisaka, A., Yamada, K., Haddon, W.F., Harden, L.A., and Theologis, A. (2003). Biochemical diversity among the 1-amino-cyclopropane-1-carboxylate synthase isozymes encoded by the Arabidopsis gene family. J Biol Chem **278,** 49102-49112.

Yamasaki, H., Abdel-Ghany, S.E., Cohu, C.M., Kobayashi, Y., Shikanai, T., and Pilon, M. (2007). Regulation of copper homeostasis by microRNA in Arabidopsis. J Biol Chem.

Yamazaki, H., Tasaka, M., and Shikanai, T. (2004). PPR motifs of the nucleus-encoded factor, PGR3, function in the selective and distinct steps of chloroplast gene expression in Arabidopsis. Plant J **38,** 152-163.

Yang, L., Liu, Z., Lu, F., Dong, A., and Huang, H. (2006). SERRATE is a novel nuclear regulator in primary microRNA processing in Arabidopsis. Plant J.

Yang, W.C., Ye, D., Xu, J., and Sundaresan, V. (1999). The SPOROCYTELESS gene of Arabidopsis is required for initiation of sporogenesis and encodes a novel nuclear protein. Genes Dev **13,** 2108-2117.

Yekta, S., Shih, I.H., and Bartel, D.P. (2004). MicroRNA-directed cleavage of HOXB8 mRNA. Science **304,** 594-596.

Yoo, B.C., Kragler, F., Varkonyi-Gasic, E., Haywood, V., Archer-Evans, S., Lee, Y.M., Lough, T.J., and Lucas, W.J. (2004). A systemic small RNA signaling system in plants. Plant Cell **16,** 1979-2000.

Zhang, B., Wang, Q., and Pan, X. (2007). MicroRNAs and their regulatory roles in animals and plants. J Cell Physiol **210,** 279-289.

Zhang, B.H., Pan, X.P., Wang, Q.L., Cobb, G.P., and Anderson, T.A. (2005). Identification and characterization of new plant microRNAs using EST analysis. Cell Res **15,** 336-360.

6. Appendices

Appendix I List of oligonucleotides used in this work.

Oligonucleotide	SEQUENCE 5′ → 3′
Amplification of miRNA targets	
At2g34010-31	CTCGAGCTCCTATAACTTAAGGTTGAGATCAATTCCATGATCAGC
At2g34010-32	ACTCCCGGGTAACTTAAGGTTGAGATCAATTCCATGATCAGC
At2g34010-51	CTAGGATCCAACAATGTGTAGTAACAACAACACAAGTAGTGGA
L077-MYB125-51	GGAATCTAGATGGAAGCGAAGAAGGAAGAGATAAAGAAAGG
L078-MYB125-31	GCTACCCGGGAGGACTTGGGATTGGATCAACCTGATCAAAC
L079-MYB58-51	GGAATCTAGATGGGCAAAGGAAGAGCACCATGTTGTGAC
L080-MYB58-31	GCTACCCGGGATGTATGAGGAGCTCGTAACTCTCCAAGAG
L081-MYB94-51	GGAATCTAGATGGGAAGACCACCATGCTGTGACAAGATTG
L091-MYB94-31	GCTACCCGGGGAACAACACTTCCTGACCCTCTAGTGACATG
L126-ACS8-51	GGAAGGATCCAACAATGGGTCTCTTGTCAAAGAAAGCTAGTTGC
L127-ACS8-31	GCTACCCGGGTCGTTCCTCGGGTTCACGGTCGTG
L128-CKL6-51	GGAAGGATCCAACAATGGACTTGAAAATGGATAATGTTATTGGG
L129-CKL6-31	GCTACCCGGGTTTGCGGATCGAAAGAAGCTCGAAGCT
L143-GAE1-51	GGAAGGATCCAACAATGCCTTCAATAGAAGATGAGCTGTTTCCG
L144-GAE1-31	GCTACCCGGGGGCTAAATCGACCCGGTTTTTGCC
MYB101-39	GCTACCCGGGACAGATGCTAGGCATGTTGCTCCA
MYB101-56	ATCGGATCCAACAATGGATGGTGGTGGAGAGACGA
T004-MYB101-311	CTCGAGCTCCTAACAGATGCTAGGCATGTTGCTC
PFL-31	ACTCCCGGGGAGACCAGACTCGATAAGGATATCGCCGA
PFL-51	AGAGGATCCAACAATGTCGTGGCAATCATACGTCGATGACC
Amplification of pre-miRNA	
L031-miR414-51	GGAATCTAGAGATGGTGGTGAGGATGAGACTAGGAAAG
L032-miR414-31	CTCGAGCTCCTTGAAGTGGGAGAGTCAGCAATTTGAAGGG
L073-miR156h-51	GGAATCTAGAGTCACAGAGCCACCGTCACTGCTTACTTAC
L074-miR156h-31	CTCGAGCTCATACGCTCATGACACGATCACACAACATGG
L075-miR395c-51	GGAATCTAGAATATATAAATAGGCATGCAGTGTTAGTGTT
L076-miR395c-31	CTCGAGCTCGATTTAAAAGATAATAGAAAACCGCAGCAA
miR172-31	CTCGAGCTCACCCGGGGCTTGTGGATCTATTAATGTCTTGATAAAG
miR172-51	GGTTTCTAGATGGTTAGGTTCCAACTAAGTATACGAG

Oligonucleotide	**SEQUENCE 5′ → 3′**
mir161-31	CTCGAGCTCACAATCGGATCATATCCATCTCCTTACAC
mir161-51	GACTCTAGACTGCCGAAGCTTTGATCAGTACTTCTC
159a-01-F	ATATTCTAGACAAGATACTTTGTTTTTCGATAGATC
159a-02-R	CCAAGGATCTTCTCATCTACCCGAGGCAGTTGC
Amplification of miRNA binding site mutant	
MYB101-57	CCTAGAATTGCCAAGCAATCAAAGACCGACCCATTCGTTCAG
MYB101-310	GGTCTTTGATTGCTTGGCAATTCTAGGACGCTATTGTCTAGTCCT
At2g34010-33	CTCTGATTGCTTGGTGGCTCTATGAATTGATAAAATCTTCCTGCTCCT
At2g34010-53	CATAGAGCCACCAAGCAATCAGAGATCTTGCGTCGATTCTGTGTC
Amplification miRNAs and targets promoter sequence	
L003-pro-miR159a-01F	AGAGAATTCTCTCCGGAACTCTCTAATCGGATCACAAGC
L004-pro-miR159a-02R	CTCCCATGGCCCTGCTCAACTCATGTTTGAACTTTAAGGAGC
L094-pro159a03F	AGAGAATTCCTCAACATTGACTCGTCAATTATTCTTCGG
L095-pro159a04F	AGAGAATTCAATGGGCTCATAAGAAAGAGATGCAGCCCA
L096-pro159a05F	AGAGAATTCGCCATTGAATTGTGAAAGAGACGAGACTCG
L097-pro159a06F	AGAGAATTCGACCGTACATCAACCTATTTCACTATTTCG
L098-pro159a07F	AGAGAATTCACTAGTAGTTGGCAGGAACGATAATAATTG
L099-pro159a08F	AGAGAATTCCATGTCTTTTCAGATGCACCCACCTGTTCC
L100-pro159a09F	AGAGAATTCAAAACATGACGTGGCCTCTTCTCTCTCTC
L005-pro-miR159b-01F	AGAGAATTCTAACGTCCTGCCAAACCCGTCCCGCCAAC
L006-pro-miR159b-02R	CTCCCATGGGGCTTATGGGATCCATAGCTTAGCAGC
L009-pro-miR161-01F	AGAGAATTCGTGTCGTGAATGTGAGCACCGCCGTCAATG
L010-pro-miR161-02R	CTCCCATGGCGGAACCCCGATGTAGTCACTTTCAATGCA
L065-pro161-1387	AGAGAATTCGGCAACATCATGGGGGCTTATAACCTAGTG
L066-pro161-1050	AGAGAATTCGCTTGAAGTTAGCGTAACGATCAGATAGGG
L067-pro161-810	AGAGAATTCGCATGTGGGTATTCGGGTCGGGTTTTTCG
L068-pro161-618	AGAGAATTCACCCGAAAAATCCACAATTATAACAAGT
L069-pro161-406	AGAGAATTCTCGGTTCGGGTAATACCCGATACCCACAGT
L070-pro161-226	AGAGAATTCTACGAGGACGAGCCTTGTTGTAGTTGCAAC
L071-pro161-	AGAGAATTCAACTCATCCTTCTCTTCTATGAAAATTCCA

Oligonucleotide	**SEQUENCE 5′ → 3′**
start	
L011-pro-MYB101-01F	AGAGAATTCGGTGGGACTTAGATCAATCTCTCTATCATAATC
L012-pro-MYB101-02R	CTCCCATGGTTTTCAACACGGCGACCCTCCGATCAAGGAGA
L013-proAT2g34010-1F	GTAGAATTCAACCTCATGACTGTTCCTTGTTTTCTC
L014-proAT2g34010-2R	GTGTTGTTGTTACTACCCATGGTTCTCAAGTGCAGAG
Used as probe or positive control in northern blot	
L072-U6snRNA	TCATCCTTGCGCAGGGGCCA
L055-miR159a	TTTGGATTGAAGGGAGCTCTA
L056-miR159a-star	TAGAGCTCCCTTCAATCCAAA
L057-miR161	TTGAAAGTGACTACATCGGGG
L058-miR161-star	CCCCGATGTAGTCACTTTCAA
L059-miR414	TCATCTTCATCATCATCGTCA
L060-miR414-star	TGACGATGATGATGAAGATGA
L180-ath-miR172a	AGAATCTTGATGATGCTGCAT
L181-miR172a-star	ATGCAGCATCATCAAGATTCT
L178-ath-miR395b	CTGAAGTGTTTGGGGGGACTC
L179-miR395b-star	GAGTCCCCCCAAACACTTCAG
L176-ath-miR156h	TTGACAGAAGAAAGAGAGCAC
L177-miR156h-star	GTGCTCTCTTTCTTCTGTCAA
RNA marker	TGGCCCCTGCGCAAGGATGA
Used for T-DNA genotyping	
J504-Salk_LB	GCGTGGACCGCTTGCTGCAACTCTCTCAGG
L046-LB2r-Salk	AATCAGCTGTTGCCCGTCTCA
J507-SALK-RB	CTCCGCTCATGATCAGATTGTCGTTTCCCG
L064-LB1-SAIL	GCCTTTTCAGAAATGGATAAATAGCCTTGCTTCC
L157-SAIL-RB1	CAAACTAGGATAAATTATCGCGCGCGGTGTCA
L047-LPSalk061355	CATCTCCGGCCAAATCTAAAG
L048-RP-Salk061355	TTGAAGGAAGCTCTAGGACGC
L049-LP-Salk149918	GGATCTACACTGGACGAAGGC

Oligonucleotide	**SEQUENCE 5’ → 3’**
L050-RP-Salk149918	CCGATTCTTCGATGGATTTTC
L062-LP-SAIL_299_A02	TTTTCATAAAGGCCCCTACTC
L063-RP-SAIL_299_A02	CCATTAGAGAATGTTGGCTCC
Sequencing primers	
35S-PromoterPr	ACAATCCCACTATCCTTC
BTtG	GAGTCAGTGAGCGAGGAAGCG
GFPseq5	CAAGAATTGGGACAACTCCAGTG
GUSu	CGCGATCCAGACTGAATGCCCA
nosTerm-Primer	GCAAGACCGGCAACAGGATT
To2f	AACAGCTATGACCATGATTACGCC
To2r	GACGTTGTAAAACGACGGCCAGTG
Used for 5’RACE target validation	
RNA adaptor	GCUGAUGGCGAUGAAUGAACACUGCGUUUGCUGGCUUUGAUGAAA
L001-5RACE-OUTER	GCTGATGGCGATGAATGAACACTG
L002-5RACE-Inner	GAACACTGCGTTTGCTGGCTTTGATG
L051-GFP-GSP1	ACTTGTGGCCGAGGATGTTTC
L052-GFP-GSP2	TCTCCTGCACGTATCCCTCAG
L015-At2g340105RaceI	CAATGGCGATGGGGTTGCTAG
L016-At2g340105RaceO	GGTCACATGGTCGTTGTTCTTGG
L023-At2g34010-GSP3	CTTGCGTCGATTCTGTGTCTCAG
L017-MYB101-5RACE-in	GGGAAGTTGTTGAGAAGGCTCGTC
L018-MYB101-5RACE-ou	ATCTACACTGGACGAAGGCGGCAC
L030-MYB101-GSP3	GGTGTCCATCTTGAGCCACCTTC
L029-PFL-GSP3	GACTACTCAAGCTCTAGTCTTTGG
L083-GSP1-MYB58	TGAGGAGCTCGTAACTCTCCAAGA
L084-GSP2-MYB58	CTAACCCGAGTTCGCTTTCCAGGT
L085-GSP3-MYB58	TGCTGGTTCCAACATTTCAAGCAA
L086-GSP1-MYB125	CTTAACACCCAAATCCGGCAACCT
L087-GSP2-MYB125	CGTTTTTGCCCTTGAGTCGATGAG
L088-GSP3-MYB125	CAACGCACCGGCAAATCCTGT
L089-GSP3-MYB94	GAGCAAAGCCACGATATGATC

Oligonucleotide	**SEQUENCE 5′ → 3′**
L145-ACS8-GSP1	GTTTTCGAGCTTTCTGTCTTTGAG
L146-ACS8-GSP2	GAGATGAAGTCCAAGAGATGGTTT
L147-ACS8-GSP3	GCTAACGAGACTCTCATGTTTTGT
L148-GAE1-GSP1	TCCAGAGATCCTAAACATCCTTTC
L149-GAE-GSP2	GGTAATGGCAAGACCGTAAATATG
L150-GAE-GSP3	GGTGTTAGATACGCTTTGGAGAAT

Appendix II Hybrid structure of novel predicted miRNA targets.

Hybrid structures of novel predicted miRNA targets. When the position of the miRNA binding site is not in the coding sequence, the reference “3’UTR” or “5’UTR” after the AGI number is given. When a target was predicted for several members of a miRNA gene family, only the structure from the smallest MFE is shown. Structures are listed numerically according to miRNA families.

```
target: AT3G15270.1 3'UTR  squamosa
promoter-binding protein-like 5 (SPL5)
miRNA : ath-miR156a    mfe: -35.4 kcal/mol
target 5'  C    U             U 3'
            GCUC CUCUCUUCUGUCA
            CGAG GAGAGAAGACAGU
miRNA  3' CA    U              5'

target: AT2G42200.1  squamosa promoter-
binding protein-like 9 (SPL9)
miRNA : ath-miR156g    mfe: -39.2 kcal/mol
position  741
target 5' C       U            A 3'
           UGUGCUC CUCUCUUCUGUC
           ACACGAG GAGAGAAGACAG
miRNA  3'         U            C 5'

target: AT3G25540.1 5'UTR  LAG1 family
protein
miRNA : ath-miR156h    mfe: -31.6 kcal/mol
position  84
target 5' U      G         G     C 3'
           UGCUCU CUUUCUUCU GUCAA
           ACGAGA GAAAGAAGA CAGUU
miRNA  3' C                      5'

target: AT3G11960.1  cleavage and
polyadenylation specificity factor (CPSF)
A subunit C-terminal domain-containing
protein
miRNA : ath-miR156h    mfe: -32.4 kcal/mol
position  496
target 5' A   G          G       U 3'
           GUG UCUCUUUCUU CUGUCAG
           CAC AGAGAAAGAA GACAGUU
miRNA  3'     G                  5'

target: AT5G38610.1  invertase/pectin
methylesterase inhibitor family protein
miRNA : ath-miR156h    mfe: -33.9 kcal/mol
position  565
target 5' A                   C 3'
           UGCUCUC UUCUUCUGUCA
           ACGAGAG AAGAAGACAGU
miRNA  3' C       A           U 5'

target: AT2G35320.1 5'UTR  tyrosine-
specific phosphatase (atEYA)
miRNA : ath-miR157a    mfe: -31.9 kcal/mol
position  52
target 5'  A             G    U 3'
            GCUCUCUAUCUUU GUCA
            CGAGAGAUAGAAG CAGU
miRNA  3' CA             A    U 5'

target: AT1G30450.1  cation-chloride
cotransporter(CCC1) Family Member
miRNA : ath-miR157a    mfe: -34.2 kcal/mol
position  916
target 5' U                   U 3'
           UGCUCUCUAUCUUCUG CA
           ACGAGAGAUAGAAGAC GU
miRNA  3' C                A  U 5'

target: AT2G34960.1  cationic amino acid
transportr 5 (CAT5)
miRNA : ath-miR157a    mfe: -32.6 kcal/mol
position  340
target 5' A                  U  3'
           UGCUCUCUGUCUUCUG C
           ACGAGAGAUAGAAGAC G
miRNA  3' C               A UU 5'
```

```
target: AT5G53540.1  MSP1 protein putative
miRNA : ath-miR157a    mfe: -32.1 kcal/mol
position  1054
target 5'  A      A          U  3'
            GCUCUC AUCUUCUGUC
            CGAGAG UAGAAGACAG
miRNA  3' CA      A          UU 5'

target: AT3G19553.1 5'UTR  amino acid
permease family protein
miRNA : ath-miR157d    mfe: -33.8 kcal/mol
position  95
target 5'  A           C       G 3'
            GCUCUCUGUCU UCUGUCG
            CGAGAGAUAGA AGACAGU
miRNA  3' CA                    5'

target: AT2G45990.1  expressed protein
miRNA : ath-miR157d    mfe: -31.7 kcal/mol
position  58
target 5'  A           G      A 3'
            GCUCUCUAUCU CUGUUA
            CGAGAGAUAGA GACAGU
miRNA  3' CA           A        5'

target: AT3G07400.1 3'UTR  lipase class 3
family protein
miRNA : ath-miR158b    mfe: -31.9 kcal/mol
position  406
target 5' G               U  C 3'
           GCUUUGUCUACAUUUG GG
           CGAAACAGAUGUAAAC CC
miRNA  3' A                  C 5'

target: AT2G34010.1  expressed protein
miRNA : ath-miR159a    mfe: -33.1 kcal/mol
position  424
target 5' A      C        A     G 3'
           UAGAGC CCCUUCAA CCAAA
           AUCUCG GGGAAGUU GGUUU
miRNA  3'        A        A       5'

target: AT2G41440.1  expressed protein
miRNA : ath-miR159a    mfe: -32.4 kcal/mol
position  999
target 5'  U                  U 3'
            GGGUUUCCUUCGAUCCGA
            CUCGAGGGAAGUUAGGUU
miRNA  3' AU                  U 5'

target: AT4G27330.1  sporocyteless (SPL)
miRNA : ath-miR159a    mfe: -33.1 kcal/mol
position  459
target 5'  U              U    U 3'
            GAGCUCUCUUCAAUC CAAA
            CUCGAGGGAAGUUAG GUUU
miRNA  3' AU                    5'

target: AT2G16750.1  protein kinase family
protein
miRNA : ath-miR159b    mfe: -32.3 kcal/mol
position  373
target 5' A                  C  3'
           AAGAGCUUCCUUCAA CCA
           UUCUCGAGGGAAGUU GGU
miRNA  3'                A   UU 5'

target: AT4G15530.2  pyruvate
orthophosphate dikinase
miRNA : ath-miR159b    mfe: -33.1 kcal/mol
position  586
target 5' C             G       G 3'
           AAGAGUUUCCUUCA AUCCAAA
           UUCUCGAGGGAAGU UAGGUUU
miRNA  3'                         5'

target: AT5G67090.1  subtilase family
protein
miRNA : ath-miR159b    mfe: -35.4 kcal/mol
position  1084
target 5' G                    U 3'
           GAGAGUUCCCUUCGGUUCAG
           UUCUCGAGGGAAGUUAGGUU
miRNA  3'                      U 5'

target: AT5G52060.1  BCL-2-ASSOCIATED
ATHANOGENE 1 (BAG1)
miRNA : ath-miR160a    mfe: -41.7 kcal/mol
position  42
target 5' C                    G 3'
           GGCG GCAGGGAGUCAGGCG
           CCGU UGUCCCUCGGUCCGU
miRNA  3' A    A                5'

target: AT2G16880.1   pentatricopeptide
(PPR) repeat-containing protein
miRNA : ath-miR161    mfe: -33.6 kcal/mol
position  1026
target 5' G                A   U 3'
           CCCGAUGUGGGUUACUU CAA
           GGGCUACAUCAGUGAA GUU
miRNA  3' G                A     5'



target: AT5G17930.1   similar to MIF4G
domain-containing protein
miRNA : ath-miR162a    mfe: -35.1 kcal/mol
position  1687
target 5' A                    G 3'
           UGGAUGCAGAGGUU GUUGA
           ACCUACGUCUCCAA UAGCU
miRNA  3' G              A       5'

target: AT4G24160.1 3'UTR  hydrolase,
alpha/beta fold family protein
miRNA : ath-miR163    mfe: -36.9 kcal/mol
position  113
target 5' U                      C  3'
           AUUGGAGUUUCAAGUCCUCUUU
           UAGCUUCAAGGUUCAGGAGAAG
miRNA  3'                        UU 5'

target: AT3G23890.1   DNA topoisomerase
II(TOP2)
miRNA : ath-miR167a    mfe: -33.9 kcal/mol
position  2893
target 5' G   A                G 3'
           AGA CAUGCUGGCGGCU CG
           UCU GUACGACCGUCGA GU
miRNA  3' A   A             A    5'

target: AT3G21810.1   zinc finger (CCCH-
type) family protein
miRNA : ath-miR167c    mfe: -32.5 kcal/mol
position  354
target 5'  U                   A 3'
            GAUUAUGCUGGUGGUUUGA
            CUAGUACGACCGUCGAAUU
miRNA  3' UU                   5'

target: AT4G08340.1   Ulp1 protease family
protein
miRNA : ath-miR167c    mfe: -35.1 kcal/mol
position  1282
target 5'  C                   G 3'
            GAUC UGCUGGCGGCUUGA
            CUAG ACGACCGUCGAAUU
miRNA  3' UU    U              5'
```

```
target: AT5G16860.1   pentatricopeptide
(PPR) repeat-containing protein
miRNA : ath-miR167c    mfe: -31.4 kcal/mol
position  1874
target 5' U             C G    A 3'
           AGGUCGUGCUGGC G UUGA
           UCUAGUACGACCG C AAUU
miRNA  3' U             U G      5'

target: AT3G07810.1   heterogeneous
nuclear ribonucleoprotein putative / hnRNP
miRNA : ath-miR167d    mfe: -37.0 kcal/mol
position  1422
target 5' U                   A  G 3'
           CCAGGUUAUGUUGGCAGUU CA
           GGUCUAGUACGACCGUCGA GU
miRNA  3'                     A    5'

target: AT5G42120.1   lectin protein
kinase family protein
miRNA : ath-miR169b    mfe: -37.1 kcal/mol
position  1051
target 5' C    A               A 3'
           CUGG AGGUUAUCCUUGGCUG
           GGCC UUCAGUAGGAACCGAC

miRNA  3'      G                 5'

target: AT3G47170.1   transferase family
protein
miRNA : ath-miR170    mfe: -34.1 kcal/mol
position  531
target 5' U                     U 3'
           GGUAUUGGCAUGGCUCAGUU
           CUAUAACUGUGCCGAGUUAG
miRNA  3'                       U 5'

target: AT4G01910.1   DC1 domain-
containing protein
miRNA : ath-miR171a    mfe: -34.9 kcal/mol
position  1410
target 5' C      G              U 3'
           GAUGUU GGUGCGGUUCAAUC
           CUAUAA CCGCGCCGAGUUAG
miRNA  3'                       U 5'

target: AT1G01420.1   UDP-
glucoronosyl/UDP-glucosyl transferase
family protein
miRNA : ath-miR171b    mfe: -34.7 kcal/mol
position  1187
target 5' U    G               U  3'
           CGUG AUGUUGGUGCGGCUC
           GCAC UAUAACCGUGCCGAG
miRNA  3'                      UU 5'

target: AT3G47170.1   transferase family
protein
miRNA : ath-miR171b    mfe: -37.3 kcal/mol
position  530
target 5'  A                   U 3'
            UGGUAUUGGCAUGGCUCAG
            ACUAUAACCGUGCCGAGUU
miRNA  3' GC                    5'

target: AT4G29430.1 5'UTR  RPS15aE
ribosomal protein S15aE
miRNA : ath-miR172a    mfe: -31.9 kcal/mol
position  5
target 5' U                    U 3'
           GUGUAGUAUCGUCGGGAUUUU
           UACGUCGUAGUAGUUCUAAGA
miRNA  3'                       5'

target: AT3G07770.1   heat shock protein-
related
miRNA : ath-miR172a    mfe: -30.8 kcal/mol
position  238
target 5' A        G            U 3'
           GUGCAGCA CAUCA GAUUCU
           UACGUCGU GUAGU CUAAGA
miRNA  3'          A     U        5'

target: AT4G24630.1   zinc finger (DHHC
type) family protein
miRNA : ath-miR172a    mfe: -32.1 kcal/mol
position  597
target 5'  G       A            G 3'
            GCGGUAU CAUCAAGAUUCU
            CGUCGUA GUAGUUCUAAGA
miRNA  3' UA                     5'

target: AT5G27840.1 3'UTR
serine/threonine protein phosphatase PP1
isozyme 8 (TOPP8)
miRNA : ath-miR172e    mfe: -32.6 kcal/mol
position  357
target 5' U                   A 3'
           UGCA UAUCGUCAAGAUUCC
           ACGU GUAGUAGUUCUAAGG
miRNA  3' U    C                5'

target: AT2G37670.1   WD-40 repeat family
protein
miRNA : ath-miR172e    mfe: -31.3 kcal/mol
position  2495
target 5'  A      U            G 3'
            GCAGCA UCAUCGAGGUUU
            CGUCGU AGUAGUUCUAAG
miRNA  3' UA                   G 5'

target: AT2G47410.1   WD-40 repeat family
miRNA : ath-miR172e    mfe: -32.5 kcal/mol
position  3731
target 5'  A    G          G    U 3'
            GCAG GUCAUCAAGA UUCC
            CGUC UAGUAGUUCU AAGG
miRNA  3' UA    G                5'

target: AT3G54350.1   forkhead-associated
domain-containing protein
miRNA : ath-miR172e    mfe: -32.1 kcal/mol
position  604
target 5' G                    G 3'
           AUGUGGU UCAUCAAGAUUCC
           UACGUCG AGUAGUUCUAAGG
miRNA  3'         U               5'

target: AT3G62240.1   zinc finger (C2H2
type) family protein
miRNA : ath-miR172e    mfe: -34.0 kcal/mol
position  1807
target 5'  G A                 A 3'
            G CAGUAUCGUCAAGGUUCC
            C GUCGUAGUAGUUCUAAGG
miRNA  3' UA                    5'

target: AT5G42060.1 5'UTR  expressed
protein
miRNA : ath-miR173    mfe: -35.6 kcal/mol
position  3
target 5' U              C      A 3'
           UGGUUUCUCUCUGU GGCGAG
           ACUAAAGAGAGACG UCGCUU
miRNA  3' C              U        5'
```

```
target: AT5G67090.1   subtilase family
protein
miRNA : ath-miR319a    mfe: -36.6 kcal/mol
position  1083
target 5' U  A                  U 3'
          GG GAGUUCCCUUCGGUUCAG
          CC CUCGAGGGAAGUCAGGUU
miRNA  3'                        5'

target: AT1G31880.1 5'UTR  BREVIS RADIX
(BRX)
miRNA : ath-miR319c    mfe: -36.9 kcal/mol
position  17
target 5' C                 U  3'
          GGAGCUCCUUUCAGUUC
          CCUCGAGGGAAGUCAGG
miRNA  3' U                 UU 5'

target: AT3G66658.2   betaine-aldehyde
dehydrogenase putative
miRNA : ath-miR319c    mfe: -35.9 kcal/mol
position  963
target 5' A      A             C 3'
          AGGGGC CUCUUCAGUCCAG
          UCCUCG GGGAAGUCAGGUU
miRNA  3'        A               5'

target: AT1G06440.1   expressed protein
miRNA : ath-miR391    mfe: -37.9 kcal/mol
position  260
target 5' G        C U            A 3'
          UGGCGCUG U CUUUCCUGCGAA
          ACCGCGAU A GAGAGGACGCUU
miRNA  3'                          5'

target: AT1G10700.1   ribose-phosphate
pyrophosphokinase 3 (PRS3)
miRNA : ath-miR391    mfe: -37.5 kcal/mol
position  1
target 5' A    G           G     U 3'
          UGGC GCUAUUUCUCC GCGAA
          ACCG CGAUAGAGAGG CGCUU
miRNA  3'                  A       5'

target: AT1G50990.1   protein kinase-
related
miRNA : ath-miR391    mfe: -37.5 kcal/mol
position  1337
target 5'  U                  C 3'
            GUGCUAUCUCUUCUGCGA
            CGCGAUAGAGAGGACGCU
miRNA  3' AC                  U 5'

target: AT3G55950.1   protein kinase
family protein
miRNA : ath-miR391    mfe: -37.1 kcal/mol
position  492
target 5' C       G            C 3'
          GGCGUUG UUUCUCCUGCGG
          CCGCGAU AGAGAGGACGCU
miRNA  3' A                    U 5'

target: AT3G59220.1   pirin putative
miRNA : ath-miR393a    mfe: -33.7 kcal/mol
position  764
target 5'  U                 U  U 3'
            UCAGUGUGGUCCCUUUG GA
            AGUUACGCUAGGGAAAC CU
miRNA  3' CU                     5'

target: AT1G10920.1   disease resistance
protein (CC-NBS-LRR class)
miRNA : ath-miR394a    mfe: -34.1 kcal/mol
position  122
target 5' U        A            A 3'
          GGGGGUGG ACAGAGUGUUGA
          CCUCCACC UGUCUUACGGUU
miRNA  3'                         5'

target: AT3G04980.1   DNAJ heat shock N-
terminal domain-containing protein
miRNA : ath-miR394a    mfe: -34.0 kcal/mol
position  548
target 5' U      U            C 3'
          GAGGUG GAUGGAGUGCCA
          CUCCAC CUGUCUUACGGU
miRNA  3' C                   U 5'

target: AT4G14850.1   similar to
pentatricopeptide (PPR) repeat-containing)
miRNA : ath-miR394a    mfe: -38.0 kcal/mol
position  1585
target 5' G                    C 3'
          GGAGGUGGGCGGAA GCCAA
          CCUCCACCUGUCUU CGGUU
miRNA  3'                A       5'

target: AT5G09670.2   loricrin-related
miRNA : ath-miR394a    mfe: -35.6 kcal/mol
position  525
target 5' U     A       G       A 3'
          GGAGG GGACAGA AUGCCAA
          CCUCC CCUGUCU UACGGUU
miRNA  3'       A                5'


target: AT5G13630.1   magnesium-chelatase
subunit chlH
miRNA : ath-miR395a    mfe: -35.6 kcal/mol
position  3421
target 5' A                     G 3'
          GAGUUUUCUCAAACGCUUCAG
          CUCAAGGGGGUUUGUGAAGUC
miRNA  3'                        5'

target: AT1G20570.1   tubulin family
protein
miRNA : ath-miR396a    mfe: -33.5 kcal/mol
position  2618
target 5'          A           C 3'
         UGGUUCAAG AAAGCUGUGGG
         GUCAAGUUC UUUCGACACCU
miRNA  3'                     U 5'

target: AT1G80260.1   similar to tubulin
family protein
miRNA : ath-miR396a    mfe: -33.5 kcal/mol
position  2531
target 5' U        A           C 3'

          GGUUCAAG AAAGCUGUGGG
          UCAAGUUC UUUCGACACCU
miRNA  3' G                   U 5'

target: AT2G15630.1   pentatricopeptide
(PPR) repeat-containing protein
miRNA : ath-miR396a    mfe: -31.4 kcal/mol
position  1361
target 5'  U                  A 3'
            GUUUGAGAAAGUUGUGGGA
            CAAGUUCUUUCGACACCUU
miRNA  3' GU                    5'
```

```
target: AT2G30590.1   WRKY family
transcription factor
miRNA : ath-miR396a    mfe: -31.7 kcal/mol
position  139
target 5' A                    U 3'
           GGUUCAAGAGAGUUG GGAG
           UCAAGUUCUUUCGAC CCUU
miRNA  3' G               A      5'

target: AT3G14880.1   DNA-binding protein-
related
miRNA : ath-miR396a    mfe: -31.9 kcal/mol
position  132
target 5' A     A              C 3'
           CGGUU AGGGAGGCUGUGGA
           GUCAA UUCUUUCGACACCU
miRNA  3'       G              U 5'

target: AT3G44830.1   LACT family protein
miRNA : ath-miR396a    mfe: -31.4 kcal/mol
position  679
target 5' G                  U  3'
           GGUUUAAGAAAGUUGUGG
           UCAAGUUCUUUCGACACC
miRNA  3' G                  UU 5'

target: AT4G12050.1   DNA-binding protein-
related
miRNA : ath-miR396a    mfe: -35.5 kcal/mol
position  826
target 5' C              G      G 3'
           CAGUUCAAGGAGGC GUGGAG
           GUCAAGUUCUUUCG CACCUU
miRNA  3'                A        5'

target: AT5G01370.1   expressed protein
miRNA : ath-miR396a    mfe: -36.3 kcal/mol
position  580
target 5' A                    G 3'
           GGUUCGAGAAGGUUGUGGAA
           UCAAGUUCUUUCGACACCUU
miRNA  3' G                      5'

target: AT5G30510.1   30S ribosomal
protein S1 putative
miRNA : ath-miR396a    mfe: -31.4 kcal/mol
position  1043
target 5'  U              A    A 3'
            GUUCGAGAAGGCUG GGAG
            CAAGUUCUUUCGAC CCUU
miRNA  3' GU              A      5'

target: AT5G53440.1   expressed protein
miRNA : ath-miR396a    mfe: -31.1 kcal/mol
position  3153
target 5' A     U             C  3'
           GGUUC GAGGAAGCUGUGG
           UCAAG UUCUUUCGACACC
miRNA  3' G                  UU 5'

target: AT5G58980.1   ceramidase family
protein
miRNA : ath-miR396a    mfe: -34.7 kcal/mol
position  1068
target 5' G                C   U 3'
           CAGUUCAAGAAGGCUG GGA
           GUCAAGUUCUUUCGAC CCU
miRNA  3'                  A   U 5'

target: AT1G46696.1   expressed protein
miRNA : ath-miR396b    mfe: -31.9 kcal/mol
position  870
target 5' G     G               G 3'
           AAGUU AAGGGAGUUGUGGAG
           UUCAA UUCUUUCGACACCUU
miRNA  3'       G                 5'

target: AT2G34530.1   expressed protein
miRNA : ath-miR396b    mfe: -31.2 kcal/mol
position  744
target 5' U               A     U 3'
           GAGUUCAAGAAAGUU UGGAA
           UUCAAGUUCUUUCGA ACCUU
miRNA  3'                 C       5'

target: AT2G44770.1   phagocytosis and
cell motility protein ELMO1-related
miRNA : ath-miR396b    mfe: -30.7 kcal/mol
position  265
target 5' G   C  U              A 3'
           AAG UC AAGGGAGCUGUGGAA
           UUC AG UUCUUUCGACACCUU
miRNA  3'     A                   5'

target: AT5G05730.1   anthranilate
synthase alpha subunit component I-1
(ASA1)
miRNA : ath-miR396b    mfe: -31.3 kcal/mol
position  921
target 5' A    A              U  3'
           GAGU CAAGGAGGCUGUGG
           UUCA GUUCUUUCGACACC
miRNA  3'      A              UU 5'



target: AT5G13655.1   hypothetical protein
miRNA : ath-miR396b    mfe: -31.4 kcal/mol
position  272
target 5' C               C     U 3'
           AAGUUCGAGAGGGU GUGGA
           UUCAAGUUCUUUCG CACCU
miRNA  3'                A     U 5'

target: AT5G24660.1   expressed protein
miRNA : ath-miR396b    mfe: -31.7 kcal/mol
position  69
target 5' A   A G               G 3'
           GAG U GAGAAAGCUGUGGAG
           UUC A UUCUUUCGACACCUU
miRNA  3'     A G                 5'

target: AT5G43060.1   cysteine proteinase
putative
miRNA : ath-miR396b    mfe: -34.3 kcal/mol
position  460
target 5' A   A                 G 3'
           AAG UCAAGGAAGCUGUGGGA
           UUC AGUUCUUUCGACACCUU
miRNA  3'     A                   5'

target: AT5G51310.1   gibberellin 20-
oxidase-related
miRNA : ath-miR396b    mfe: -31.0 kcal/mol
position  942

target 5' G                     C 3'
           AAGUUCGAGAAGGUUG GGGA
           UUCAAGUUCUUUCGAC CCUU
miRNA  3'                  A      5'
```

```
target: AT5G55580.1   mitochondrial
transcription termination factor (mTERF)
family protein
miRNA : ath-miR396b    mfe: -32.5 kcal/mol
position  482
target 5' U             A       A 3'
          GAGUUCGAGGAAGU UGUGGAG
          UUCAAGUUCUUUCG ACACCUU
miRNA  3'                         5'

target: AT5G57590.1   aminotransferase
class III family protein
miRNA : ath-miR396b    mfe: -30.6 kcal/mol
position  1271
target 5' A  C                  C 3'
          AA UUUAAGAGAGCUGUGGGA
          UU AAGUUCUUUCGACACCUU
miRNA  3'    C                   5'

target: AT5G60360.1   cysteine proteinase
putative
miRNA : ath-miR396b    mfe: -30.9 kcal/mol
position  469
target 5' A   A               U 3'
          AAG UCAGGGAGGUUGUGGA
          UUC AGUUCUUUCGACACCU
miRNA  3'     A               U 5'

target: AT5G66420.1   expressed protein
miRNA : ath-miR396b    mfe: -31.4 kcal/mol
position  1233
target 5' A               G      U 3'
          AAGUUUGAGGAAGCU GUGGGA
          UUCAAGUUCUUUCGA CACCUU
miRNA  3'                         5'

target: AT3G06470.1   GNS1/SUR4 membrane
family protein
miRNA : ath-miR397a    mfe: -32.8 kcal/mol
position  733
target 5'  U                  C 3'
            UCAACGCUGCAUUUAAUG
            AGUUGCGACGUGAGUUAC
miRNA  3' GU                  U 5'

target: AT3G17880.1   tetratricoredoxin
(TDX)
miRNA : ath-miR397a    mfe: -33.0 kcal/mol
position  788
target 5'  C                   C 3'
            UCAG GCUGCACUCAAUGA
            AGUU CGACGUGAGUUACU
miRNA  3' GU    G               5'

target: AT3G59100.1   glycosyl transferase
family 48 protein
miRNA : ath-miR397a    mfe: -33.1 kcal/mol
position  624
target 5' G     G             C 3'
          GUCAA GCUGCAUUCAGUG
          UAGUU CGACGUGAGUUAC
miRNA  3' G     G             U 5'

target: AT4G33230.1   pectinesterase
family protein
miRNA : ath-miR397a    mfe: -33.5 kcal/mol
position  926
target 5' C                  A C 3'
          CAUCAACGCUGCACUUAA G
          GUAGUUGCGACGUGAGUU C
miRNA  3'                    A U 5'

target: AT1G19500.1   expressed protein
miRNA : ath-miR397b    mfe: -33.0 kcal/mol
position  123
target 5' U    C               A 3'
           GUCA CGAUGCAUUCAAUGA
           UAGU GCUACGUGAGUUACU
miRNA  3' G    U                 5'

target: AT1G21160.1   eukaryotic
translation initiation factor 2 (eIF-2)
family protein
miRNA : ath-miR397b    mfe: -33.3 kcal/mol
position  2211
target 5' G               C    A 3'
          GUCAACGGUGUACUC GUGA
          UAGUUGCUACGUGAG UACU
miRNA  3' G               U      5'

target: AT1G49530.1   geranylgeranyl
pyrophosphate synthase (GGPS6)
miRNA : ath-miR397b    mfe: -31.6 kcal/mol
position  780
target 5' G  G                 G 3'
          AU GAUGAUGUACUCGAUGA
          UA UUGCUACGUGAGUUACU
miRNA  3' G  G                   5'

target: AT3G57870.1   ubiquitin-
conjugating enzyme putative
miRNA : ath-miR397b    mfe: -34.7 kcal/mol
position  178
target 5' C              U       G 3'
          CAUUAACGAUGCAC UCAGUGA
          GUAGUUGCUACGUG AGUUACU
miRNA  3'                          5'

target: AT4G01050.1   hydroxyproline-rich
glycoprotein family protein
miRNA : ath-miR397b    mfe: -32.1 kcal/mol
position  794
target 5' G                     G 3'
          CAUCAGCGGUGUAUUUGGUGA
          GUAGUUGCUACGUGAGUUACU
miRNA  3'                          5'

target: AT5G02470.1   DP-2 transcription
factor putative (DPA)
miRNA : ath-miR397b    mfe: -32.6 kcal/mol
position  324
target 5' A   U               U 3'
          GUC ACGAUGCGCUCAAUG
          UAG UGCUACGUGAGUUAC
miRNA  3' G   U               U 5'

target: AT5G58870.1   FtsH
miRNA : ath-miR397b    mfe: -31.9 kcal/mol
position  2008
target 5' A       A             U 3'
          UAUCAAC GGUGCACUUGAUGA
          GUAGUUG CUACGUGAGUUACU
miRNA  3'                          5'

target: AT3G06370.1 3'UTR   member of
Sodium proton exchanger family (NHX4)
miRNA : ath-miR398b    mfe: -37.8 kcal/mol
position  315
target 5' A               U    C 3'
          UAGGGGUGACUUGAG ACAC
          GUCCCCACUGGACUC UGUG
miRNA  3'                 U    U 5'
```

```
target: AT1G08050.1   zinc finger (C3HC4-
type RING finger) family protein
miRNA : ath-miR398b    mfe: -37.8 kcal/mol
position  1569
target 5' U              C  G   G 3'
           GGGGGUGACCUGAG GG GCA
           UCCCCACUGGACUC UU UGU
miRNA  3' G                 G     5'

target: AT2G37790.1   aldo/keto reductase
family protein
miRNA : ath-miR399b    mfe: -35.9 kcal/mol
position  610
target 5' U                   G  3'
           CAGGGU ACUCUCCUUUGG
           GUCCCG UGAGAGGAAACC
miRNA  3'        U            GU 5'

target: AT3G43790.3   transporter-related
protein
miRNA : ath-miR399b    mfe: -36.5 kcal/mol
position  1113
target 5' U             A      G 3'
           GGGGUGACUCUCC UUUGGU
           UCCCGUUGAGAGG AAACCG
miRNA  3' G                    U 5'

target: AT2G23840.1   HNH endonuclease
domain-containing protein
miRNA : ath-miR399d    mfe: -36.2 kcal/mol
position  101
target 5' C   U                U 3'
           CGG GGUGGAUCUCCUUUGGU
           GCC CCGUUUAGAGGAAACCG
miRNA  3'                      U 5'

target: AT4G09730.1   DEAD/DEAH box
helicase putative
miRNA : ath-miR399d    mfe: -39.8 kcal/mol
position  1833
target 5' C               C    A 3'
           CGGGGCAAGUCUUCUU GGCA
           GCCCCGUUUAGAGGAA CCGU
miRNA  3'                 A      5'

target: AT5G43280.1   Encodes the
peroxisomal delta-3-5-delta2-4-dienoyl-CoA
isomerase
miRNA : ath-miR399e    mfe: -35.5 kcal/mol
position  652
target 5' G               A  U 3'
           GAGGCAAGUCUCCUUU GC
           CUCCGUUUAGAGGAAA CG
miRNA  3' G               C  U 5'

target: AT1G59750.1   auxin-responsive
factor (ARF1)
miRNA : ath-miR400    mfe: -28.7 kcal/mol
position  606
target 5' A      G             U 3'
           GUGGCU GUGAUGCUUUCAUA
           CACUGA UAUUAUGAGAGUAU
miRNA  3'        A               5'

target: AT1G62910.1   pentatricopeptide
(PPR) repeat-containing protein
miRNA : ath-miR400    mfe: -29.3 kcal/mol
position  1194
target 5' A        C           A 3'
           GUGACUUA AGUACUCUUAUA
           CACUGAAU UUAUGAGAGUAU
miRNA  3'          A             5'

target: AT1G63130.1   pentatricopeptide
(PPR) repeat-containing protein
miRNA : ath-miR400    mfe: -29.3 kcal/mol
position  1188
target 5' A        C            A 3'
           GUGACUUA AAUACUCUUAUA
           CACUGAAU UUAUGAGAGUAU
miRNA  3'          A              5'

target: AT1G63400.1   pentatricopeptide
(PPR) repeat-containing protein
miRNA : ath-miR400    mfe: -27.5 kcal/mol
position  1200
target 5' A        C           U 3'
           GUGACUUA AAUACUCUUAU
           CACUGAAU UUAUGAGAGUA
miRNA  3'          A           U 5'

target: AT3G22470.1   pentatricopeptide
(PPR) repeat-containing protein
miRNA : ath-miR400    mfe: -33.4 kcal/mol
position  1155
target 5' C                     A 3'
           GUGACUUAUAGUAUUCUCAUA
           CACUGAAUAUUAUGAGAGUAU
miRNA  3'                       5'

target: AT3G49990.1   expressed protein
miRNA : ath-miR400    mfe: -27.8 kcal/mol
position  410
target 5'  A            G       U 3'
            GGCUUAUGAUGC UCUCGUG
            CUGAAUAUUAUG AGAGUAU
miRNA  3' CA                    5'

target: AT5G36905.1   RNase H domain-
containing protein
miRNA : ath-miR402    mfe: -34.6 kcal/mol
position  1183
target 5' A   U              G   A 3'
           UAG GGUUUGGUGGGCCU GAA
           GUC CCAAAUUAUCCGGA CUU
miRNA  3'     U              G     5'

target: AT4G21510.1   F-box family protein
miRNA : ath-miR403    mfe: -32.9 kcal/mol
position  229
target 5' U      G             C  3'
           CGAGUU UGUGCGUGAAUCU
           GCUCAA ACACGCACUUAGA
miRNA  3'                      UU 5'

target: AT2G01480.1 5'UTR   expressed
protein
miRNA : ath-miR404    mfe: -42.1 kcal/mol
position  177
target 5' C       C          A   G 3'
           CUGCCGC ACCGCCGGCG UAG
           GACGGCG UGGCGGUCGC AUU
miRNA  3' C       U          A   A 5'

target: AT1G03660.1   expressed protein
miRNA : ath-miR406    mfe: -29.3 kcal/mol
position  90
target 5' U    U              C  3'
           CUGG UUGCAAUAGCAUUC
           GACC AAUGUUAUCGUAAG
miRNA  3'      U              AU 5'
```

```
target: AT1G06410.1   trehalose-
phosphatase family protein
miRNA : ath-miR406    mfe: -28.8 kcal/mol
position  1768
target 5' U               C    A 3'
           UGGAUUAUGAUGGCA UCUG
           ACCUAAUGUUAUCGU AGAU
miRNA  3' G               A      5'

target: AT3G06710.1   expressed protein
miRNA : ath-miR406    mfe: -29.3 kcal/mol
position  500
target 5' G               A   G  G 3'
           CUGGAUUGCAAUAGC AUU UA
           GACCUAAUGUUAUCG UAA AU
miRNA  3'                    G    5'

target: AT4G23510.1   disease resistance
protein (TIR class)
miRNA : ath-miR406    mfe: -29.1 kcal/mol
position  1159
target 5'  G                  U 3'
            GGGUUGCAGUAGUGUUCU
            CCUAAUGUUAUCGUAAGA
miRNA  3' GA                  U 5'

target: AT5G40340.1   PWWP domain-
containing protein
miRNA : ath-miR406    mfe: -30.3 kcal/mol
position  1004
target 5' A               G   A 3'
           UGGGUUACAAUGGCGU CUA
           ACCUAAUGUUAUCGUA GAU
miRNA  3' G               A     5'

target: AT3G10070.1 3'UTR  TBP-associated
58 kDa subunit protein (TAFII58)
miRNA : ath-miR407    mfe: -27.3 kcal/mol
position  206
target 5' G               A     U 3'
           GCCAAAAGUGUAUGA UUGAG
           UGGUUUUCAUAUACU AAUUU
miRNA  3'                 A       5'

target: AT1G77760.1   nitrate reductase 1
(NR1)
miRNA : ath-miR407    mfe: -24.5 kcal/mol
position  2445
target 5' A       U            C  3'
           ACCGAGA GUAUGUGGUUUA
           UGGUUUU CAUAUACUAAAU
miRNA  3'                      UU 5'

target: AT2G42180.1  expressed protein
miRNA : ath-miR408    mfe: -37.7 kcal/mol
position  43
target 5' A               U   A 3'
           UUAGGGAGGGGGCAGU GCA
           GGUCCCUUCUCCGUCA CGU
miRNA  3' C                   A 5'

target: AT1G15830.1   expressed protein
miRNA : ath-miR408    mfe: -42.6 kcal/mol
position  1147
target 5' G                   U  3'
           GCUGGGGAGGAGGCGGUGC
           CGGUCCCUUCUCCGUCACG
miRNA  3'                     UA 5'

target: AT1G15830.1   expressed protein
miRNA : ath-miR408    mfe: -35.6 kcal/mol
position  1057
target 5' G                U C  3'
           GCUGGGGAGGAGGCGGU C
           CGGUCCCUUCUCCGUCA G
miRNA  3'                  C UA 5'

target: AT3G02200.1   proteasome family
protein
miRNA : ath-miR408    mfe: -39.0 kcal/mol
position  654
target 5' A    A         U      G 3'
           GCCA GGAGGAGGC GUGCGU
           CGGU CCUUCUCCG CACGUA
miRNA  3'      C         U        5'

target: AT3G51240.1   flavanone 3-
hydroxylase (F3H)
miRNA : ath-miR408    mfe: -37.7 kcal/mol
position  356
target 5' U             U     A 3'
           CCAGGG AGAGGC GUGCA
           GGUCCC UCUCCG CACGU
miRNA  3' C      U      U     A 5'

target: AT5G21930.1   ATPase E1-E2 type
family protein /
miRNA : ath-miR408    mfe: -39.6 kcal/mol
position  2144
target 5'  A               G   A 3'
            CAGGGAAGGGGCAGU GCA
            GUCCCUUCUCCGUCA CGU
miRNA  3' CG                   A 5'

target: AT1G10320.1   U2 snRNP auxiliary
factor-related
miRNA : ath-miR413    mfe: -31.8 kcal/mol
position  207
target 5'  G                  A 3'
            GCGGAACAGGAGAGAUUG
            CGUCUUGUUCUCUUUGAU
miRNA  3' CA                  A 5'

target: AT1G10910.1   pentatricopeptide
(PPR) repeat-containing protein
miRNA : ath-miR413    mfe: -30.3 kcal/mol
position  1266
target 5' U                 G A 3'
           UGCAGAGCAGGAGAGAU G
           ACGUCUUGUUCUCUUUG U
miRNA  3' C                 A A 5'

target: AT1G77030.1   glycine-rich protein
miRNA : ath-miR413    mfe: -31.4 kcal/mol
position  598
target 5' C                 G A 3'
           UGCAGAGCAAGAGAGGC G
           ACGUCUUGUUCUCUUUG U
miRNA  3' C                 A A 5'

target: AT1G79540.1   pentatricopeptide
(PPR) repeat-containing protein
miRNA : ath-miR413    mfe: -29.9 kcal/mol
position  1581
target 5' C               C    A 3'
           UGCAGAGCAGGAGA AUUG
           ACGUCUUGUUCUCU UGAU
miRNA  3' C               U    A 5'

target: AT2G05160.1   zinc finger (CCCH-
type) family protein
miRNA : ath-miR413    mfe: -30.8 kcal/mol
position  1409
target 5' A                 A G 3'
           UGCGGAGCAAGAGGAAC A
           ACGUCUUGUUCUCUUUG U
miRNA  3' C                 A A 5'
```

```
target: AT2G06210.1   phosphoprotein-
related
miRNA : ath-miR413    mfe: -31.0 kcal/mol
position  2510
target 5' C   U               C 3'
           UGC GAGCAGGAGGAGCUG
           ACG CUUGUUCUCUUUGAU
miRNA  3' C   U               A 5'

target: AT2G12875.1   hypothetical protein
miRNA : ath-miR413    mfe: -30.9 kcal/mol
position  751
target 5'  A  C               G 3'
            GC GAGCAAGAGAGACUA
            CG CUUGUUCUCUUUGAU
miRNA  3' CA  U               A 5'

target: AT2G19090.1   expressed protein
miRNA : ath-miR413    mfe: -31.1 kcal/mol
position  1025
target 5' U        G           C 3'
           GUGUAGAG AGGAGAAGCUA
           CACGUCUU UUCUCUUUGAU
miRNA  3'          G           A 5'

target: AT2G30960.1   expressed protein
miRNA : ath-miR413    mfe: -30.2 kcal/mol
position  725
target 5'  A                  G 3'
            GCAGAACGAGAG AGCUG
            CGUCUUGUUCUC UUGAU
miRNA  3' CA            U     A 5'

target: AT2G30960.1   expressed protein
miRNA : ath-miR413    mfe: -27.2 kcal/mol
position  198
target 5'  A      G         G   G 3'
            GCGGAG AGGAGAAGC UAU
            CGUCUU UUCUCUUUG AUA
miRNA  3' CA      G              5'

target: AT2G32780.1   ubiquitin-specific
protease 1 putative (UBP1)
miRNA : ath-miR413    mfe: -29.8 kcal/mol
position  214
target 5' G    U  U              G 3'
           GUGC AG AACAGGAGAGACUG
           CACG UC UUGUUCUCUUUGAU
miRNA  3'                        A 5'

target: AT2G42760.1   expressed protein
miRNA : ath-miR413    mfe: -29.9 kcal/mol
position  347
target 5' U       A           C 3'
           UGCGGAA GAGAGAGACUA
           ACGUCUU UUCUCUUUGAU
miRNA  3' C       G           A 5'

target: AT3G01460.1   PHD finger family
protein
miRNA : ath-miR413    mfe: -34.5 kcal/mol
position  5351
target 5' U                    G 3'
           UGCAGAGCGAGAGAAAUUGU
           ACGUCUUGUUCUCUUUGAUA
miRNA  3' C                    5'

target: AT3G10030.1
aspartate/glutamate/uridylate kinase
family protein
miRNA : ath-miR413    mfe: -30.7 kcal/mol
position  353
target 5'  G      U            A 3'
            GCAGAG CAGGAGGAGCUA
            CGUCUU GUUCUCUUUGAU
miRNA  3' CA                   A 5'

target: AT3G18010.1   homeobox-leucine
zipper transcription factor family protein
miRNA : ath-miR413    mfe: -30.9 kcal/mol
position  26
target 5'  A            G      A 3'
            GCAGAACAAGAG GAGCUG
            CGUCUUGUUCUC UUUGAU
miRNA  3' CA                   A 5'

target: AT3G19650.1   cyclin-related
miRNA : ath-miR413    mfe: -30.6 kcal/mol
position  616
target 5'  A A                 G 3'
            G CAGAACGAGAGGAACUG
            C GUCUUGUUCUCUUUGAU
miRNA  3' CA                   A 5'
target: AT3G50200.1   expressed protein
miRNA : ath-miR413    mfe: -29.8 kcal/mol
position  555
target 5' C   A      U           G 3'
           GUG CAGAGC AAGAGGAGCUG
           CAC GUCUUG UUCUCUUUGAU
miRNA  3'                        A 5'

target: AT3G60590.2   expressed protein
miRNA : ath-miR413    mfe: -30.0 kcal/mol
position  256
target 5' A        G        G  G 3'

           GUGCAGAG AAGAGAAA UA
           CACGUCUU UUCUCUUU AU
miRNA  3'          G        G  A 5'

target: AT4G00440.1   expressed protein
miRNA : ath-miR413    mfe: -32.0 kcal/mol
position  970
target 5' U                A  U 3'
           UGCAGAACGAGAGAAAC GU
           ACGUCUUGUUCUCUUUG UA
miRNA  3' C                A    5'

target: AT4G00450.1   expressed protein
miRNA : ath-miR413    mfe: -29.9 kcal/mol
position  6192

target 5'  A    C             A 3'
            GCAG ACAAGGGAAGCUG
            CGUC UGUUCUCUUUGAU
miRNA  3' CA    U             A 5'

target: AT4G08580.1   microfibrillar-
associated protein-related
miRNA : ath-miR413    mfe: -33.6 kcal/mol
position  581
target 5' U                  U  3'
           UGCAGAGCGAGAGAGGCU
           ACGUCUUGUUCUCUUUGA
miRNA  3' C                  UA 5'

target: AT4G08580.1   microfibrillar-
associated protein-related
miRNA : ath-miR413    mfe: -28.3 kcal/mol
position  893
target 5'  A      G           G 3'
            GCAGGA AGGAGAGAUUG
            CGUCUU UUCUCUUUGAU
miRNA  3' CA      G           A 5'

target: AT4G14410.1   basic helix-loop-
helix (bHLH) family protein
miRNA : ath-miR413    mfe: -30.5 kcal/mol
position  385
target 5'  A      G           A 3'
            GCAGAG AGGAGGAACUA
            CGUCUU UUCUCUUUGAU
miRNA  3' CA      G           A 5'
```

```
target: AT4G16970.1   protein kinase
family protein
miRNA : ath-miR413    mfe: -35.3 kcal/mol
position  401
target 5' A                   G 3'
           UGCGGAACAAGAGGAGCUA
           ACGUCUUGUUCUCUUUGAU
miRNA  3' C                   A 5'

target: AT4G20450.1   leucine-rich repeat
protein kinase
miRNA : ath-miR413    mfe: -30.4 kcal/mol
position  1725
target 5'  G                   A 3'
            GC GAACAAGAGAAGCUAU
            CG CUUGUUCUCUUUGAUA
miRNA  3' CA  U                  5'

target: AT4G26750.1   hydroxyproline-rich
glycoprotein family protein
miRNA : ath-miR413    mfe: -30.6 kcal/mol
position  131
target 5'  C                   A 3'
            GCAGAGCGAGAG AACUA
            CGUCUUGUUCUC UUGAU
miRNA  3' CA            U     A 5'

target: AT4G29000.1   tesmin/TSO1-like CXC
domain-containing protein
miRNA : ath-miR413    mfe: -35.1 kcal/mol
position  1488
target 5'  C                  G 3'
            GCAGAGCAGGAGAGACUG
            CGUCUUGUUCUCUUUGAU
miRNA  3' CA                  A 5'

target: AT4G35020.1   Rho-like GTP binding
protein.
miRNA : ath-miR413    mfe: -29.8 kcal/mol
position  182
target 5' C                   C 3'
           UGCAGGGCAAGAG GACUA
           ACGUCUUGUUCUC UUGAU
miRNA  3' C             U     A 5'

target: AT4G35950.1   rac-like GTP binding
protein Arac6
miRNA : ath-miR413    mfe: -30.8 kcal/mol
position  182
target 5' C                    A 3'
           UGCAGGGCAAGAG GACUAU
           ACGUCUUGUUCUC UUGAUA
miRNA  3' C             U        5'

target: AT4G36060.1   basic helix-loop-
helix (bHLH) family protein
miRNA : ath-miR413    mfe: -33.1 kcal/mol
position  147
target 5'  A                  U  3'
            GCAGAGCGAGAGAAGCU
            CGUCUUGUUCUCUUUGA
miRNA  3' CA                  UA 5'

target: AT4G37100.1   expressed protein
miRNA : ath-miR413    mfe: -30.1 kcal/mol
position  1742
target 5'  C                  C  3'
            GCGGAAUAGGAGGAGCU
            CGUCUUGUUCUCUUUGA
miRNA  3' CA                  UA 5'

target: AT5G08440.1   expressed protein
miRNA : ath-miR413    mfe: -30.0 kcal/mol
position  896
target 5' C                U  C  3'
           UGCAGAGCAAGAGAGG CU
           ACGUCUUGUUCUCUUU GA
miRNA  3' C                   UA 5'

target: AT5G10260.1   Ras-related GTP-
binding protein
miRNA : ath-miR413    mfe: -31.2 kcal/mol
position  107
target 5' C                   U  3'
           UGCAGGACAGGAGAGAUU
           ACGUCUUGUUCUCUUUGA
miRNA  3' C                   UA 5'

target: AT5G17900.1   expressed protein
miRNA : ath-miR413    mfe: -33.6 kcal/mol
position  581
target 5' U                   U  3'
           UGCAGAGCGAGAGAGGCU
           ACGUCUUGUUCUCUUUGA
miRNA  3' C                   UA 5'

target: AT5G17900.1   expressed protein
miRNA : ath-miR413    mfe: -28.3 kcal/mol
position  893
target 5'  A      G           G 3'
            GCAGGA AGGAGAGAUUG
            CGUCUU UUCUCUUUGAU
miRNA  3' CA      G           A 5'

target: AT5G64990.1   Ras-related GTP-
binding protein
miRNA : ath-miR413    mfe: -31.5 kcal/mol
position  188
target 5' C                   U  3'
           UGCAGGACAAGAGAGAUU
           ACGUCUUGUUCUCUUUGA
miRNA  3' C                   UA 5'

target: AT5G65495.1   expressed protein
miRNA : ath-miR413    mfe: -30.1 kcal/mol
position  132
target 5'  A  A                A 3'
            GC AGGGCGAGAGAAGCUG
            CG UCUUGUUCUCUUUGAU
miRNA  3' CA                   A 5'

target: AT1G17180.1 3'UTR   glutathione S-
transferase ATGSTU25
miRNA : ath-miR415    mfe: -35.5 kcal/mol
position  33
target 5' U     G                U 3'
           GUGUU CUGUUUCUGCUCUGUU
           UACAA GACAAAGACGAGACAA
miRNA  3'                          5'

target: AT1G63020.1 3'UTR   putative
plant-specific RNA polymerase IV (NRPD1A)
miRNA : ath-miR415    mfe: -32.2 kcal/mol
position  242
target 5' C             U      A 3'
           UGUUCUGUUUCUG UUCUGU
           ACAAGACAAAGAC GAGACA
miRNA  3' U                    A 5'

target: AT3G29075.1 3'UTR  glycine-rich
protein
miRNA : ath-miR415    mfe: -30.7 kcal/mol
position  92
target 5' U                   G 3'
           UGUUUUGUUUUUGCUUUGU
           ACAAGACAAAGACGAGACA
miRNA  3' U                   A 5'
```

```
target: AT4G09670.1 3'UTR  oxidoreductase
family protein
miRNA : ath-miR415    mfe: -30.5 kcal/mol
position  104
target 5' U         C       G   C 3'
           AUGUUCUGU UUCUGCU UGU
           UACAAGACA AAGACGA ACA
miRNA  3'                   G   A 5'

target: AT4G10390.1 5'UTR  protein kinase
family protein
miRNA : ath-miR415    mfe: -31.6 kcal/mol
position  202
target 5' C  C                 U 3'
           UG UCUGUUUUUGCUCUGUU
           AC AGACAAAGACGAGACAA
miRNA  3' U  A                  5'

target: AT1G53530.1 5'UTR  signal
peptidase I family protein
miRNA : ath-miR417    mfe: -31.4 kcal/mol
position  3
target 5' C    C               G 3'
           UGGA CGAGUUCGCUACCUUC
           GCUU GUUUAAGUGAUGGAAG
miRNA  3' A                     5'

target: AT2G22570.2   isochorismatase
hydrolase family protein
miRNA : ath-miR417    mfe: -30.0 kcal/mol
position  505
target 5' G                    A 3'
           UUGAACAAGUUUACUGCUUUU
           AGCUUGUUUAAGUGAUGGAAG
miRNA  3'                       5'

target: AT5G49680.1   cell expansion
protein putative
miRNA : ath-miR417    mfe: -32.5 kcal/mol
position  1109
target 5' G                  G  3'
           UCGAACAAGUUCACUAUCU
           AGCUUGUUUAAGUGAUGGA
miRNA  3'                    AG 5'

target: AT1G75910.1   family II
extracellular lipase 4 (EXL4)
miRNA : ath-miR418    mfe: -32.4 kcal/mol
position  690
target 5' U   G               G  3'
           GGU GGUUCGUCAUCACGU
           CCA UCAAGUAGUAGUGUA
miRNA  3'     G              AU 5'

target: AT2G36290.1 3'UTR   hydrolase,
alpha/beta fold family protein
miRNA : ath-miR419    mfe: -32.2 kcal/mol
position  162
target 5' A                  C  3'
           AACAUUCUCAGCAUUCAU
           UUGUAGGAGUCGUAAGUA
miRNA  3' G                 UU 5'

target: AT3G46240.1   protein kinase-
related
miRNA : ath-miR419    mfe: -31.0 kcal/mol
position  316
target 5' U                  A C 3'
           CGAUAUCCUCAGCAUUCG A
           GUUGUAGGAGUCGUAAGU U
miRNA  3'                    A U 5'

target: AT4G31200.2   SWAP (Suppressor-of-
White-APricot)/surp domain-containing
protein
miRNA : ath-miR419    mfe: -30.0 kcal/mol
position  117
target 5' G               C   C  3'
           CAACAUCCUCAGUAU CAU
           GUUGUAGGAGUCGUA GUA
miRNA  3'                 A   UU 5'

target: AT5G61580.1   phosphofructokinase
family protein
miRNA : ath-miR419    mfe: -30.0 kcal/mol
position  524
target 5' A                  G  A 3'
           UAACAUUCUCGGCAUUCA GG
           GUUGUAGGAGUCGUAAGU UU
miRNA  3'                    A    5'

target: AT1G03030.1
phosphoribulokinase/uridine kinase family
protein
miRNA : ath-miR447a    mfe: -35.2 kcal/mol
position  233
target 5' U                    C 3'
           GGCGGAACGUCUUGUCCCUA
           UUGUUUUGUAGAGCAGGGGU
miRNA  3' G                    U 5'

target: AT1G68140.1   expressed protein
miRNA : ath-miR447c    mfe: -35.4 kcal/mol
position  219
target 5' U                    C 3'
           GACAAGGGAUGUCGUCCUUA
           UUGUUUUCUACAGCAGGGGU
miRNA  3' G                    U 5'

target: AT2G02820.1   MYB88
miRNA : ath-miR447c    mfe: -34.5 kcal/mol
position  446
target 5' A          C            A 3'
           CAACAAGAGA UGUUGUUCCCAG
           GUUGUUUUCU ACAGCAGGGGUU
miRNA  3'                         5'

target: AT2G30280.1   expressed protein
miRNA : ath-miR772    mfe: -33.0 kcal/mol
position  436
target 5' A                    A 3'
           UAUGG CGGAGUAGGAAGGG
           AUACC GCCUCAUCCUUUUU
miRNA  3' C     C                5'

target: AT3G26820.1
esterase/lipase/thioesterase family
protein
miRNA : ath-miR772    mfe: -35.1 kcal/mol
position  711
target 5'  A              U    G 3'
            AUGGGCGGAGUGGG GGAG
            UACCCGCCUCAUCC UUUU
miRNA  3' CA              U      5'

target: AT3G26840.1
esterase/lipase/thioesterase family
protein
miRNA : ath-miR772    mfe: -35.4 kcal/mol
position  816
target 5'  A              U    G 3'
            AUGGGCGGAGUAGG GGAG
            UACCCGCCUCAUCC UUUU
miRNA  3' CA              U      5'
```

```
target: AT1G03720.1   cathepsin-related
miRNA : ath-miR773    mfe: -31.8 kcal/mol
position  436
target 5' A  U               U 3'
          AG CGAAGGCUGGGAGCGA
          UC GUUUUCGACCUUCGUU
miRNA  3' C  U               U 5'


target: AT1G15340.1   methyl-CpG-binding
domain-containing protein
miRNA : ath-miR773    mfe: -30.7 kcal/mol
position  666
target 5' G    A               G 3'
          GAGA GAAGGCUGGGAGUGGA
          CUCU UUUUCGACCUUCGUUU
miRNA  3'      G                 5'

target: AT1G35660.1   expressed protein
miRNA : ath-miR773    mfe: -30.7 kcal/mol
position  1354
target 5'  C   C              U 3'
           GAC AAAGUUGGAAGCAAA
           CUG UUUCGACCUUCGUUU
miRNA  3' CU   U                5'

target: AT1G50770.1   hypothetical protein
miRNA : ath-miR773    mfe: -31.3 kcal/mol
position  1316
target 5' A                   G 3'
          AGA AGAAGCUGGAAGCAAA
          UCU UUUUCGACCUUCGUUU
miRNA  3' C   G                 5'

target: AT1G59980.1   DNAJ heat shock N-
terminal domain-containing protein
miRNA : ath-miR773    mfe: -30.7 kcal/mol
position  1103
target 5' A                     A 3'
          GAG CAGAAGCUGGA GCAAG
          CUC GUUUUCGACCU CGUUU
miRNA  3'     U           U       5'

target: AT1G74260.1   AIR synthase-related
family protein
miRNA : ath-miR773    mfe: -31.0 kcal/mol
position  1164
target 5' U        U        U    U 3'
          GAGACAGG GCUGGAGG CGAA
          CUCUGUUU CGACCUUC GUUU
miRNA  3'          U              5'

target: AT1G79830.1   expressed protein
miRNA : ath-miR773    mfe: -31.3 kcal/mol
position  2629
target 5' A                 C  3'
          AGGC AGAGCUGGAAGCA
          UCUG UUUCGACCUUCGU
miRNA  3' C    U            UU 5'

target: AT2G01340.1   expressed protein
miRNA : ath-miR773    mfe: -31.6 kcal/mol
position  176
target 5' C  A                G 3'
          GA GCAGAGGUUGGAGGCGAA
          CU UGUUUUCGACCUUCGUUU
miRNA  3'    C                  5'

target: AT2G24650.1   transcriptional
factor B3 family protein

miRNA : ath-miR773    mfe: -30.8 kcal/mol
position  3768
target 5' U    U              U  3'
          GGAC AAGAGCUGGAAGUA
          UCUG UUUUCGACCUUCGU
miRNA  3' C                   UU 5'

target: AT2G38440.1   Encodes a subunit of
the WAVE complex.
miRNA : ath-miR773    mfe: -31.7 kcal/mol
position  4145
target 5'  U     U            C 3'
           GGCAA GGCUGGAAGCGA
           CUGUU UCGACCUUCGUU
miRNA  3' CU     U            U 5'

target: AT2G38440.1   Encodes a subunit of
the WAVE complex.
miRNA : ath-miR773    mfe: -26.9 kcal/mol
position  234
target 5'  U U    C             G 3'
           G GCAA AGUUGGAAGCAGA
           C UGUU UCGACCUUCGUUU
miRNA  3' CU      U               5'

target: AT2G43520.1   Encodes a defensin-
like (DEFL) family protein.
miRNA : ath-miR773    mfe: -30.7 kcal/mol
position  216
target 5' A              U    U  3'
          GGGGCAGGAGCUGG AGUA
          CUCUGUUUUCGACC UCGU
miRNA  3'                U    UU 5'

target: AT3G04420.1   no apical meristem
(NAM) family protein
miRNA : ath-miR773    mfe: -30.7 kcal/mol
position  900
target 5' A     U         G      A 3'
          GGGAC GGGGCUGGA GGCAAA
          CUCUG UUUCGACCU UCGUUU
miRNA  3'       U                  5'

target: AT3G15680.1   zinc finger (Ran-
binding) family protein
miRNA : ath-miR773    mfe: -31.1 kcal/mol
position  273
target 5' C     C  C            G 3'
          GAGAC GG GCUGGAGGCGGA
          CUCUG UU CGACCUUCGUUU
miRNA  3'       U  U             5'

target: AT3G16910.1   Encodes a
peroxisomal protein with acetyl-CoA
synthetase activity
miRNA : ath-miR773    mfe: -30.6 kcal/mol
position  420
target 5' G    A               C 3'
          GAGG GAAAGCUGGAAGUAG
          CUCU UUUUCGACCUUCGUU
miRNA  3'      G               U 5'

target: AT3G18750.1   protein kinase
family protein
miRNA : ath-miR773    mfe: -31.2 kcal/mol
position  1584
target 5' A                   U 3'
          AGACAAGAGCUGGAGG AGA
          UCUGUUUUCGACCUUC UUU
miRNA  3' C               G     5'
```

```
target: AT3G19420.1   expressed protein
miRNA : ath-miR773    mfe: -31.0 kcal/mol
position  84
target 5'  U                 U 3'
            G CAGAAGCUGGAAGCGA
            C GUUUUCGACCUUCGUU
miRNA  3' CU U               U 5'
```

```
target: AT3G43300.1   guanine nucleotide
exchange family protein
miRNA : ath-miR773    mfe: -31.4 kcal/mol
position  4873
target 5'  C              G  C 3'
            GGCAAGAGCUGGAAG AA
            CUGUUUUCGACCUUC UU
miRNA  3' CU              G  U 5'
```

```
target: AT4G00260.1   transcriptional
factor B3 family protein
miRNA : ath-miR773    mfe: -30.8 kcal/mol
position  1047
target 5' U    U             U  3'
           GGAC AAGAGCUGGAAGUA
           UCUG UUUUCGACCUUCGU
miRNA  3' C                  UU 5'
```

```
target: AT4G03070.1   2-oxoglutarate-
dependent dioxygenase (AOP1.2)
miRNA : ath-miR773    mfe: -30.6 kcal/mol
position  913
target 5' C              C   U  3'
           AGACAGAAGCUGGA GUA
           UCUGUUUUCGACCU CGU
miRNA  3' C              U   UU 5'
```

```
target: AT4G11730.1   ATPase
miRNA : ath-miR773    mfe: -31.9 kcal/mol
position  1164
target 5' A                U    G 3'
           GAGGCAAGAGCUGGAA UAGA
           CUCUGUUUUCGACCUU GUUU
miRNA  3'                  C      5'
```

```
target: AT4G14920.1   PHD finger
transcription factor
miRNA : ath-miR773    mfe: -30.8 kcal/mol
position  1794
target 5' U      C U           U 3'
           GAGAUA A GCUGGAAGCAAA
           CUCUGU U CGACCUUCGUUU
miRNA  3'        U U             5'
```

```
target: AT4G26180.1   mitochondrial
substrate carrier family protein
miRNA : ath-miR773    mfe: -31.3 kcal/mol
position  799
target 5' A    A              C 3'
           GAGA GAAGGUUGGAAGCAA
           CUCU UUUUCGACCUUCGUU
miRNA  3'      G              U 5'
```

```
target: AT4G33330.1   similar to
glycogenin glucosyltransferase
(glycogenin)-related
miRNA : ath-miR773    mfe: -30.8 kcal/mol
position  265
target 5' C                 C  3'
           AGACA AAGCUGGAGGCG
           UCUGU UUCGACCUUCGU
miRNA  3' C     U           UU 5'
```

```
target: AT4G35090.1   catalase 2
miRNA : ath-miR773    mfe: -30.8 kcal/mol
position  1433
target 5' U              C    C U 3'
           GGGACAGAAGCUGG AAGC G
           CUCUGUUUUCGACC UUCG U
miRNA  3'                    U U 5'
```

```
target: AT4G37270.1   cadmium/zinc-
transporting ATPase putative (HMA1)
miRNA : ath-miR773    mfe: -31.3 kcal/mol
position  918
target 5' G               A    G 3'
           GAGGCAAAAGCUGGAG UAGA
           CUCUGUUUUCGACCUU GUUU
miRNA  3'                 C      5'
```

```
target: AT5G06680.1   tubulin family
protein
miRNA : ath-miR773    mfe: -32.1 kcal/mol
position  1717
target 5' G               U   U  3'
           GAGACAGAGGCUGGGA GUA
           CUCUGUUUUCGACCUU CGU
miRNA  3'                   UU 5'
```

```
target: AT5G09660.1   microbody NAD-
dependent malate dehydrogenase
miRNA : ath-miR773    mfe: -30.4 kcal/mol
position  768
target 5' G                 U  U 3'
           GAGGCAAAAGCUGG AGC GG
           CUCUGUUUUCGACC UCG UU
miRNA  3'               U   U    5'
```

```
target: AT5G14270.1   DNA-binding
bromodomain-containing protein
miRNA : ath-miR773    mfe: -31.2 kcal/mol
position  207
target 5' A                  U 3'
           AGACAAGAGCUGGAA CAAA
           UCUGUUUUCGACCUU GUUU
miRNA  3' C              C      5'
```

```
target: AT5G16960.1   NADP-dependent
oxidoreductase
miRNA : ath-miR773    mfe: -30.9 kcal/mol
position  703
target 5' G         U      U    U 3'
           GAGGCAAGA GCUGGA GCAG
           CUCUGUUUU CGACCU CGUU
miRNA  3'                  U    U 5'
```

```
target: AT5G19780.1   tubulin alpha-
3/alpha-5 chain (TUA5)
miRNA : ath-miR773    mfe: -31.0 kcal/mol
position  162
target 5' C     U        G     U  3'
           GAGAC GGAGCUGG AAGCA
           CUCUG UUUCGACC UUCGU
miRNA  3'       U              UU 5'
```

```
target: AT5G42860.1   expressed protein
miRNA : ath-miR773    mfe: -30.5 kcal/mol
position  459
target 5' U        U          U  3'
           GGACAAGA GCUGGAGGUA
           UCUGUUUU CGACCUUCGU
miRNA  3' C                  UU 5'
```

```
target: AT5G51210.1   glycine-rich protein
/ oleosin
miRNA : ath-miR773    mfe: -33.0 kcal/mol
position  346
target 5' C                    G 3'
          GGAUGAAGGUUGGAAGCAGA
          UCUGUUUUCGACCUUCGUUU
miRNA  3' C                     5'

target: AT5G57010.1   calmodulin-binding
family protein
miRNA : ath-miR773    mfe: -30.7 kcal/mol
position  559
target 5' U                   A 3'
          GGGCAAGAGCUGGAA CAAA
          UCUGUUUUCGACCUU GUUU
miRNA  3' C               C      5'

target: AT5G57350.1   ATPase 3
miRNA : ath-miR773    mfe: -33.6 kcal/mol
position  1161
target 5' A               U    G 3'
          GAGGCAAGAGCUGGAA CAGA
          CUCUGUUUUCGACCUU GUUU
miRNA  3'                 C      5'

target: AT5G58000.1   phosphatase-related
miRNA : ath-miR773    mfe: -31.7 kcal/mol
position  1865
target 5' A                  U  3'
          GAGACAAAAGUUGGA GCA
          CUCUGUUUUCGACCU CGU
miRNA  3'                U   UU 5'

target: AT5G64550.1   loricrin-related
miRNA : ath-miR773    mfe: -31.5 kcal/mol
position  1490
target 5' A                   G 3'
          AGAUA AAGCUGGAAGCAAG
          UCUGU UUCGACCUUCGUUU
miRNA  3' C     U               5'

target: AT1G61460.1 5'UTR   S-locus
protein kinase family protein
miRNA : ath-miR774    mfe: -36.6 kcal/mol
position  477
target 5' G                     U 3'
          GGUGGUUGUGUGGGUGGCCAA
          CUACCGGUAUACCCAUUGGUU
miRNA  3'                        5'

target: AT1G11280.1   S-locus protein
kinase family protein
miRNA : ath-miR774    mfe: -34.2 kcal/mol
position  251
target 5' G                    C 3'
          GGUGGUUGUGUGGGUGGCUAA
          CUACCGGUAUACCCAUUGGUU
miRNA  3'                        5'

target: AT1G61420.1   S-locus protein
kinase family protein
miRNA : ath-miR774    mfe: -36.6 kcal/mol
position  209
target 5' G                     U 3'
          GGUGGUUGUGUGGGUGGCCAA
          CUACCGGUAUACCCAUUGGUU
miRNA  3'                        5'

target: AT1G61430.1   S-locus protein
kinase family protein
miRNA : ath-miR774    mfe: -34.5 kcal/mol
position  209
target 5' A                    U 3'
          GGUGGUUGUGUGGGUGGCUAA
          CUACCGGUAUACCCAUUGGUU
miRNA  3'                       5'


target: AT1G61480.1   S-locus protein
kinase family protein
miRNA : ath-miR774    mfe: -36.6 kcal/mol
position  209
target 5' G                     U 3'
          GGUGGUUGUGUGGGUGGCCAA
          CUACCGGUAUACCCAUUGGUU
miRNA  3'                        5'

target: AT4G29690.1   type I
phosphodiesterase/nucleotide
pyrophosphatase family protein
miRNA : ath-miR774    mfe: -33.6 kcal/mol
position  426
target 5' A    A    U            C 3'
          GGUG GCCG UGUGGGUGACCG
          CUAC CGGU AUACCCAUUGGU
miRNA  3'                       U 5'

target: AT4G29700.1   type I
phosphodiesterase/nucleotide
pyrophosphatase family protein
miRNA : ath-miR774    mfe: -33.5 kcal/mol
position  435
target 5' A    A    C            C 3'
          GGUG GCCG UGUGGGUAACCG
          CUAC CGGU AUACCCAUUGGU
miRNA  3'                       U 5'

target: AT1G20780.1   armadillo/beta-
catenin repeat protein-related / U-box
domain-containing protein
miRNA : ath-miR775    mfe: -35.5 kcal/mol
position  1457
target 5' G              A C     A 3'
          UGGCACUGCUGGAC A UCGGA
          ACCGUGACGAUCUG U AGCUU
miRNA  3' A                      5'

target: AT2G23980.1   cyclic nucleotide-
regulated ion channel / cyclic nucleotide-
gated channel (CNGC6)
miRNA : ath-miR776    mfe: -28.6 kcal/mol
position  1937
target 5' C   G               C 3'
          ACA CAAUGGAGGACUUGGG
          UGU GUUAUCUUCUGAAUCU
miRNA  3' U   A                 5'

target: AT2G28260.1   cyclic nucleotide-
regulated ion channel putative (CNGC15)
miRNA : ath-miR776    mfe: -33.5 kcal/mol
position  1808
target 5' C                   C 3'
          GCAUCAAUGGAGGACUUGGG
          UGUAGUUAUCUUCUGAAUCU
miRNA  3' U                     5'
```

```
target: AT2G29800.1   F-box family protein
miRNA : ath-miR776    mfe: -28.3 kcal/mol
position  835
target 5' C     A               G 3'
           GACGU GAUGGGAGACUUGGG
           UUGUA UUAUCUUCUGAAUCU
miRNA  3'       G                5'

target: AT2G37710.1   lectin protein
kinase
miRNA : ath-miR776    mfe: -29.3 kcal/mol
position  1447
target 5' G                    G 3'
           AGC UCAAUGGGAGACUUGGG
           UUG AGUUAUCUUCUGAAUCU
miRNA  3'     U                 5'

target: AT3G44240.1   CCR4-NOT
transcription complex protein
miRNA : ath-miR776    mfe: -28.0 kcal/mol
position  171
target 5' C              A     G 3'
           GAUAUCAAUGGAAGA UUGGA
           UUGUAGUUAUCUUCU AAUCU
miRNA  3'                G       5'

target: AT3G55620.1   eukaryotic
translation initiation factor 6 putative /
eIF-6
miRNA : ath-miR776    mfe: -30.4 kcal/mol
position  492
target 5' C  C                A 3'
           AC UCAGUGGAAGACUUGGA
           UG AGUUAUCUUCUGAAUCU
miRNA  3' U  U                 5'

target: AT4G32717.1   S-locus cysteine-
rich protein related
miRNA : ath-miR776    mfe: -29.2 kcal/mol
position  90
target 5' U   A               C 3'
           ACA CGAUAGGAGACUUGGA
           UGU GUUAUCUUCUGAAUCU
miRNA  3' U   A                5'

target: AT5G24820.1   aspartyl protease
family protein
miRNA : ath-miR776    mfe: -28.1 kcal/mol
position  558
target 5' U        C           U 3'
           GGCGUCGA GGGAGACUUAG
           UUGUAGUU UCUUCUGAAUC
miRNA  3'          A           U 5'

target: AT5G53130.1   cyclic nucleotide-
gated channel (CNGC1)
miRNA : ath-miR776    mfe: -28.9 kcal/mol
position  1853
target 5' C   A               C 3'
           ACA CAAUGGAAGACUUGGG
           UGU GUUAUCUUCUGAAUCU
miRNA  3' U   A                5'

target: AT2G24710.1   plant glutamate
receptor family protein (GLR2.3)
miRNA : ath-miR777    mfe: -32.5 kcal/mol
position  2375
target 5' A                    C 3'
           GGCAAUGGAGCUCGA GCGUG
           UCGUUGCUUUGAGUU CGCAU
miRNA  3'                A       5'

target: AT2G39500.1   expressed protein
miRNA : ath-miR777    mfe: -33.1 kcal/mol
position  2
target 5' U                   A  3'
           GGCGACGAGAUUCGAUGUG
           UCGUUGCUUUGAGUUACGC
miRNA  3'                    AU 5'

target: AT1G73840.1   hydroxyproline-rich
glycoprotein family protein
miRNA : ath-miR778    mfe: -32.9 kcal/mol
position  322
target 5'  A                   A 3'
            GUGUACAUGAGCC AGCCA
            CACAUGUAUUUGG UCGGU
miRNA  3' GC             U       5'

target: AT1G22060.1   expressed protein
miRNA : ath-miR779    mfe: -32.2 kcal/mol
position  806
target 5' U                U   G 3'
           UGGGUGGCAACAUGGC GGG
           ACUCGUCGUUGUAUCG CUU
miRNA  3' U                U     5'

target: AT1G50830.1   expressed protein
miRNA : ath-miR779    mfe: -32.1 kcal/mol
position  2017
target 5' G               A    U 3'
           AUGAGCAGCAACAUA UGGA
           UACUCGUCGUUGUAU GUCU
miRNA  3'                 C    U 5'

target: AT1G76260.1   WD-40 repeat family
protein
miRNA : ath-miR779    mfe: -37.6 kcal/mol
position  274
target 5'  G                  U 3'
            GAGCAGCAAUAUGGCAGA
            CUCGUCGUUGUAUCGUCU
miRNA  3' UA                  U 5'

target: AT2G30080.1   metal transporter
putative (ZIP6)
miRNA : ath-miR779    mfe: -32.7 kcal/mol
position  37
target 5'  A                   A 3'
            GAGCAGCGGCAU GUAGAG
            CUCGUCGUUGUA CGUCUU
miRNA  3' UA            U        5'

target: AT2G36660.1   polyadenylate-
binding protein putative / PABP
miRNA : ath-miR779    mfe: -36.9 kcal/mol
position  1487
target 5'  C A                  C 3'
            G AGCAGCAGCAUAGCAGAA
            C UCGUCGUUGUAUCGUCUU
miRNA  3' UA                     5'

target: AT2G41050.1   PQ-loop repeat
family protein / transmembrane family
protein
miRNA : ath-miR779    mfe: -34.1 kcal/mol
position  761
target 5' C                    C 3'
           U AGCAGCAACGUAGCAGAA
           A UCGUCGUUGUAUCGUCUU
miRNA  3' U C                   5'
```

```
target: AT2G43140.1   basic helix-loop-
helix (bHLH) family protein
miRNA : ath-miR779    mfe: -32.9 kcal/mol
position  143
target 5'  G C           C       U 3'
            G AGCAGCAGCAU AGCAGAA
            C UCGUCGUUGUA UCGUCUU
miRNA  3' UA                      5'

target: AT3G20310.1   Ethylene Response
Factor, subfamily B-1 of ERF/AP2
transcription factor family (ATERF-7).
miRNA : ath-miR779    mfe: -31.6 kcal/mol
position  419
target 5'  C            G     C  3'
            GAGUAGCAGCAU AGCAG
            CUCGUCGUUGUA UCGUC
miRNA  3' UA                 UU 5'

target: AT3G28770.1   expressed protein
miRNA : ath-miR779    mfe: -34.2 kcal/mol
position  617
target 5'  C                   A 3'
            GGGCAGUAACAUGGUGGAG
            CUCGUCGUUGUAUCGUCUU
miRNA  3' UA                     5'

target: AT3G58560.1
endonuclease/exonuclease/phosphatase
family protein
miRNA : ath-miR779    mfe: -33.8 kcal/mol
position  1550
target 5' C               A   C 3'
           UGAGCAGCAACGUAG AGA
           ACUCGUCGUUGUAUC UCU
miRNA  3' U              G   U 5'

target: AT3G58560.1
endonuclease/exonuclease/phosphatase
family protein
miRNA : ath-miR779    mfe: -28.6 kcal/mol
position  210
target 5'  C   A         U    U  3'
            GAG CGGCAACAU GCAG
            CUC GUCGUUGUA CGUC
miRNA  3' UA             U    UU 5'

target: AT3G62900.1   expressed protein
miRNA : ath-miR779    mfe: -31.6 kcal/mol
position  3269
target 5'  A   G              U 3'
            GAG AGUAAUAUAGCAGA
            CUC UCGUUGUAUCGUCU
miRNA  3' UA   G              U 5'

target: AT4G08730.1   expressed protein
miRNA : ath-miR779    mfe: -31.8 kcal/mol
position  382
target 5' A                    A 3'
           AUG GUAGUGACAUGGCAGGA
           UAC CGUCGUUGUAUCGUCUU
miRNA  3'     U                  5'

target: AT4G14010.1   rapid alkalinization
factor (RALF) family protein
miRNA : ath-miR779    mfe: -33.2 kcal/mol
position  119
target 5'  A U                 A 3'
            G GCAGCAGCAUGGUGGAG
            C CGUCGUUGUAUCGUCUU
miRNA  3' UA U                   5'

target: AT4G38190.1   cellulose synthase
family protein
miRNA : ath-miR779    mfe: -31.6 kcal/mol
position  723
target 5' G     A               A 3'
           AUGAG GGCGGCAUGGUGGAA
           UACUC UCGUUGUAUCGUCUU
miRNA  3'       G                5'

target: AT5G06220.1   expressed protein
miRNA : ath-miR779    mfe: -34.5 kcal/mol
position  946
target 5'  C                   U 3'
            GGGCAGCAGCAU GCAGAG
            CUCGUCGUUGUA CGUCUU
miRNA  3' UA            U        5'

target: AT5G50350.1   expressed protein
miRNA : ath-miR779    mfe: -33.2 kcal/mol
position  1101
target 5'  G   G               A 3'
            GAG AGCAGCGUGGUAGAG
            CUC UCGUUGUAUCGUCUU
miRNA  3' UA   G                 5'

target: AT5G64240.1 3'UTR   latex-abundant
family protein (AMC3)
miRNA : ath-miR780    mfe: -30.5 kcal/mol
position  20
target 5'  U                   A 3'
            UCAGGUGUUCACGGGGAAG
            GGUCUAUAAGUGCUUCUUU
miRNA  3' AC                     5'

target: AT2G37810.1   CHP-rich zinc finger
protein
miRNA : ath-miR780    mfe: -30.7 kcal/mol
position  463
target 5' A              U    U 3'
           UGCUGGAUGUUCACG GGAA
           ACGGUCUAUAAGUGC UCUU
miRNA  3'                U    U 5'

target: AT2G46100.1   expressed protein
miRNA : ath-miR780    mfe: -30.5 kcal/mol
position  371
target 5' C      G             A 3'
           GCCGGA GUUUAUGAGGAGA
           CGGUCU UAAGUGCUUCUUU
miRNA  3' A      A               5'

target: AT4G02330.1   pectinesterase
family protein
miRNA : ath-miR780    mfe: -31.6 kcal/mol
position  884
target 5' C                    A 3'
           GUCAGGUGUUUAUGAGGAAA
           CGGUCUAUAAGUGCUUCUUU
miRNA  3' A                      5'

target: AT4G14810.1   expressed protein
miRNA : ath-miR780    mfe: -39.3 kcal/mol
position  1
target 5' A                     C 3'
           UGCCAGAUAUUCACGAAGAAA
           ACGGUCUAUAAGUGCUUCUUU
miRNA  3'                        5'

target: AT5G23480.1 5'UTR   expressed
protein
miRNA : ath-miR781    mfe: -33.5 kcal/mol
position  154
target 5'  U                   A 3'
            AGUAUCCAGAAAACUCUAG
            UCAUAGGUCUUUUGAGAUU
miRNA  3' AU                     5'
```

```
target: AT5G57050.1 5'UTR  abscisic acid-
insensitive 2 (ABI2)
miRNA : ath-miR781    mfe: -28.7 kcal/mol
position  83
target 5'  C  A                U 3'
            AG AUCCAGGAAACUCUGA
            UC UAGGUCUUUUGAGAUU
miRNA  3' AU  A                  5'

target: AT1G34740.1   Ulp1 protease family
protein
miRNA : ath-miR781    mfe: -28.4 kcal/mol
position  542

target 5' A                    U 3'
           GAGUGUUUGGAAGACUCUG
           UUCAUAGGUCUUUUGAGAU
miRNA  3' A                    U 5'

target: AT1G44900.1   DNA replication
licensing factor putative
miRNA : ath-miR781    mfe: -33.9 kcal/mol
position  2475
target 5'  U                   G 3'
            GGUGUCCAGAGAACUCUAA
            UCAUAGGUCUUUUGAGAUU
miRNA  3' AU                     5'

target: AT1G52820.1   2-oxoglutarate-
dependent dioxygenase putative
miRNA : ath-miR781    mfe: -27.9 kcal/mol
position  101
target 5' C                    C 3'
           UGA UGUCCAGAAAGCUCUA
           AUU AUAGGUCUUUUGAGAU
miRNA  3'     C                U 5'

target: AT1G69490.1   no apical meristem
(NAM) family protein
miRNA : ath-miR781    mfe: -28.6 kcal/mol
position  316
target 5' G        A            U 3'
           UAGGUGUC AGAAAGCUCUAG
           AUUCAUAG UCUUUUGAGAUU
miRNA  3'          G              5'

target: AT1G72300.1   leucine-rich repeat
transmembrane protein kinase
miRNA : ath-miR781    mfe: -27.9 kcal/mol
position  2233
target 5' A    A A               G 3'
           GAGU A UCCAGGAGACUCUGA
           UUCA U AGGUCUUUUGAGAUU
miRNA  3' A                       5'

target: AT1G76490.1   HMG-CoA reductase 2
(HMGR2)
miRNA : ath-miR781    mfe: -28.7 kcal/mol
position  1095
target 5' G   A                U 3'
           GAG AUCCAGAGAACUUUGA
           UUC UAGGUCUUUUGAGAUU
miRNA  3' A   A                  5'

target: AT2G14770.1   Ulp1 protease family
protein
miRNA : ath-miR781    mfe: -28.4 kcal/mol
position  542
target 5' A                    U 3'
           GAGUGUUUGGAAGACUCUG
           UUCAUAGGUCUUUUGAGAU
miRNA  3' A                    U 5'

target: AT2G40085.1   expressed protein
miRNA : ath-miR781    mfe: -30.2 kcal/mol
position  256
target 5' G                    U 3'
           AAG AUCCAGAGGACUCUGA
           UUC UAGGUCUUUUGAGAUU
miRNA  3' A   A                  5'

target: AT3G09780.1   protein kinase
family protein
miRNA : ath-miR781    mfe: -29.2 kcal/mol
position  854
target 5' U        G            U 3'
           UGAGUGUU GGGAAACUCUAA
           AUUCAUAG UCUUUUGAGAUU
miRNA  3'          G              5'

target: AT3G24390.1   Ulp1 protease family
protein
miRNA : ath-miR781    mfe: -28.4 kcal/mol
position  542
target 5' A                    U 3'
           GAGUGUUUGGAAGACUCUG
           UUCAUAGGUCUUUUGAGAU
miRNA  3' A                    U 5'

target: AT3G28380.1   P-glycoprotein
putative
miRNA : ath-miR781    mfe: -32.5 kcal/mol
position  3698
target 5' C                  C  3'
           AGGUAUCCAGAGAACUCU
           UUCAUAGGUCUUUUGAGA
miRNA  3' A                  UU 5'

target: AT3G42730.1   Ulp1 protease family
protein
miRNA : ath-miR781    mfe: -28.4 kcal/mol
position  542
target 5' A                    U 3'
           GAGUGUUUGGAAGACUCUG
           UUCAUAGGUCUUUUGAGAU
miRNA  3' A                    U 5'

target: AT3G43390.1   expressed protein
miRNA : ath-miR781    mfe: -28.4 kcal/mol
position  542
target 5' A                    U 3'
           GAGUGUUUGGAAGACUCUG
           UUCAUAGGUCUUUUGAGAU
miRNA  3' A                    U 5'

target: AT4G00020.1   BRCA2 repeat-
containing protein
miRNA : ath-miR781    mfe: -28.5 kcal/mol
position  1488
target 5' A              G   C  3'
           AGGUAUCCAGAAAA UCU
           UUCAUAGGUCUUUU AGA
miRNA  3' A              G   UU 5'

target: AT4G03300.1   Ulp1 protease family
protein
miRNA : ath-miR781    mfe: -28.4 kcal/mol
position  998
target 5' A                    U 3'
           GAGUGUUUGGAAGACUCUG

           UUCAUAGGUCUUUUGAGAU
miRNA  3' A                    U 5'
```

```
target: AT4G05280.1   Ulp1 protease family
protein
miRNA : ath-miR781    mfe: -28.4 kcal/mol
position  542
target 5' A                   U 3'
           GAGUGUUUGGAAGACUCUG
           UUCAUAGGUCUUUUGAGAU
miRNA  3' A                   U 5'

target: AT4G08880.1   Ulp1 protease family
protein
miRNA : ath-miR781    mfe: -28.4 kcal/mol
position  134
target 5' A                   U 3'
           GAGUGUUUGGAAGACUCUG
           UUCAUAGGUCUUUUGAGAU
miRNA  3' A                   U 5'

target: AT4G28890.1   zinc finger (C3HC4-
type RING finger) family protein
miRNA : ath-miR781    mfe: -28.8 kcal/mol
position  536
target 5' A    U               A 3'
           GAGU UCCGGAAGAUUCUGA
           UUCA AGGUCUUUUGAGAUU
miRNA  3' A    U                 5'

target: AT5G17920.1   ATCIMS cytosolic
methionine synthase
miRNA : ath-miR781    mfe: -29.5 kcal/mol
position  1187
target 5' A               G   C 3'
           GGGUGUCCAGAAGGCU CUG
           UUCAUAGGUCUUUUGA GAU
miRNA  3' A                   U 5'

target: AT5G27030.1   WD-40 repeat family
protein
miRNA : ath-miR781    mfe: -28.5 kcal/mol
position  2322
target 5'  U                  A 3'
            GGUAUCCAGAGA CUCUGG
            UCAUAGGUCUUU GAGAUU
miRNA  3' AU            U       5'

target: AT5G41570.1   WRKY family
transcription factor
miRNA : ath-miR781    mfe: -28.5 kcal/mol
position  145
target 5'  U                C  3'
            GGUAUCCAGAAAGCUUU
            UCAUAGGUCUUUUGAGA
miRNA  3' AU                UU 5'

target: AT1G64890.1   integral membrane
transporter family protein
miRNA : ath-miR782    mfe: -31.7 kcal/mol
position  818
target 5' U      C            G 3'
           AGGGAU UCCAAGGUGUUUG
           UUCUUG AGGUUCCACAAAC
miRNA  3'        U            A 5'

target: AT2G26960.1   MYB81
miRNA : ath-miR783    mfe: -30.7 kcal/mol
position  723
target 5' U C               C  3'
           A CAUGAACGAGCAAAGC
           U GUACUUGCUCGUUUCG
miRNA  3' C U               AA 5'

target: AT3G03830.1   auxin-responsive
protein
miRNA : ath-miR783    mfe: -31.5 kcal/mol
position  53
target 5' U    A            A  3'
           AGCA GAACGAGCAAAGC
           UUGU CUUGCUCGUUUCG
miRNA  3' C    A            AA 5'

target: AT3G09070.1   glycine-rich protein
miRNA : ath-miR783    mfe: -32.7 kcal/mol
position  1436
target 5' C              C       U 3'
           GGAUAUGGACGAGC AAAGCUU
           CUUGUACUUGCUCG UUUCGAA
miRNA  3'                          5'

target: AT4G01090.1   extra-large G-
protein-related
miRNA : ath-miR783    mfe: -35.6 kcal/mol
position  216
target 5' A              U      U 3'
           GAGCAUGAACGAGC GAGCUU
           CUUGUACUUGCUCG UUCGAA
miRNA  3'                U        5'

target: AT4G38530.1   similar to
phosphoinositide-specific phospholipase C
(PLC1)
miRNA : ath-miR783    mfe: -32.1 kcal/mol
position  972
target 5' C               U    A 3'
           AGCAUGGACGAGCAG GGCU
           UUGUACUUGCUCGUU UCGA
miRNA  3' C                    A 5'
```

Appendix III AtGenExpress experiments.

The AtGenExpress data was retrieved from the internet site (http://jsp.weigelworld.org/expviz/expviz.jsp). Flowers and floral organs are form stage 15 flowers.

AtGenExpress Experiment code	*Tissue*	*Genotype*	*Growth conditions*
ATGE_7	seedling	Col-0	7 days continuous light on soil
ATGE_9	roots	Col-0	17 days continuous light on soil
ATGE_16	rosette	Col-0	17 days continuous light on soil
ATGE_27	stem	Col-0	21 days continuous light on soil
ATGE_39	flower	Col-0	21 days continuous light on soil
ATGE_40	pedicel	Col-0	21 days continuous light on soil
ATGE_42	petal	Col-0	21 days continuous light on soil
ATGE_45	carpel	Col-0	21 days continuous light on soil
ATGE_41	sepals	Col-0	21 days continuous light on soil
ATGE_43	stamen	Col-0	21 days continuous light on soil
ATGE_73	pollen	Col-0	6 weeks continuous light on soil
ATGE_78	silique	Col-0	8 weeks continuous light on soil
ATGE_81	seeds	Col-0	8 weeks continuous light on soil